

Universal few-body physics and cluster formation

Chris H. Greene,^{*} P. Giannakeas,[†] and J. Pérez-Ríos[‡]*Department of Physics and Astronomy, Purdue University, West Lafayette, Indiana 47907-2036, USA*

(published 28 August 2017)

A recent rejuvenation of experimental and theoretical interest in the physics of few-body systems has provided deep, fundamental insights into a broad range of problems. Few-body physics is a cross-cutting discipline not restricted to conventional subject areas such as nuclear physics or atomic or molecular physics. To a large degree, the recent explosion of interest in this subject has been sparked by dramatic enhancements of experimental capabilities in ultracold atomic systems over the past decade, which now permit atoms and molecules to be explored deep in the quantum mechanical limit with controllable two-body interactions. This control, typically enabled by magnetic or electromagnetically dressed Fano-Feshbach resonances, allows, in particular, access to the range of universal few-body physics, where two-body scattering lengths far exceed all other length scales in the problem. The Efimov effect, where three particles experiencing short-range interactions can counterintuitively exhibit an infinite number of bound or quasibound energy levels, is the most famous example of universality. Tremendous progress in the field of universal Efimov physics has taken off, driven particularly by a combination of experimental and theoretical studies in the past decade, and prior to the first observation in 2006, by an extensive set of theoretical studies dating back to 1970. Because experimental observations of Efimov physics have usually relied on resonances or interference phenomena in three-body recombination, this connects naturally with the processes of molecule formation in a low-temperature gas of atoms or nucleons, and more generally with N -body recombination processes. Some other topics not closely related to the Efimov effect are also reviewed in this article, including confinement-induced resonances for explorations of lower-dimensionality systems, and some chemically interesting systems with longer-range forces such as the ion-atom-atom recombination problem.

DOI: [10.1103/RevModPhys.89.035006](https://doi.org/10.1103/RevModPhys.89.035006)

CONTENTS

I. Introduction and Overview	2	1. ⁶ Li	18
A. Systems with finite-range interactions	2	2. ⁷ Li	19
B. Coulomb systems	3	3. ³⁹ K	19
C. Chemical physics	5	4. ⁸⁵ Rb	20
D. Fragmentation, recombination, and molecule formation	6	5. ¹³³ Cs	20
E. Recombination processes involving cluster resonances with more than three particles	8	G. Four-body and five-body bound states and recombination resonances	20
II. Adiabatic Hyperspherical Treatment	8	H. Efimov states in heteronuclear mass-imbalanced systems	21
A. Recombination cross sections and rate coefficients	11	I. Efimov and universal bound states for fermionic systems	23
III. The Birth of Few-body Physics: The Effects of Thomas and Efimov	13	J. Naturally occurring Efimov physics in the helium trimer	24
A. The Thomas collapse	13	IV. Few-body Perspectives on Many-body Systems	25
B. Efimov physics and universality in ultracold gases	13	A. Polaron physics attacked from a few-body viewpoint	26
C. Faddeev equations for three identical bosons: Bound states	13	B. Bose-Einstein condensates viewed in hyperspherical coordinates	26
1. Hamiltonian and Faddeev operator equations	13	C. The unitary Bose gas	27
2. Faddeev equations in momentum representation	14	D. Two-component Fermi gases and the BCS-BEC crossover problem	28
3. Separable potential approximation: Two-body transition elements and the reduced Faddeev equation	15	E. A step beyond independent particles: The Tan contact	28
D. Separable potentials for van der Waals pairwise interactions	16	F. Toward many-body theory with realistic interactions	29
E. The Efimov spectrum and its universal aspects	17	V. Ultracold Atoms in Low-dimensional Traps	30
F. Efimov states in homonuclear systems	18	A. Confinement-induced resonances: An interlude	30
		1. Two-body collisions in a cigar-shaped trap	31
		2. Fermions in a cigar-shaped trap	34
		B. Confinement-induced resonances: Delving deeper	38
		C. Synthetic spin-orbit coupled systems	39
		D. Confined dipoles and dynamical CIR	40
		E. Inelastic few-body collisions in 1D	41

^{*}chgreene@purdue.edu[†]pgiannak@purdue.edu[‡]jperezri@purdue.edu

F. 2D, quasi-2D systems, and the super-Efimov effect	41
VI. Few-body Physics in Nuclear and Chemical Systems	42
A. Hyperspherical methods in nuclear physics	42
B. Universality in nuclear systems	43
C. Few-body physics and universality in chemistry	44
1. General classical treatment of few-body collisions	45
2. Classical trajectory calculations in hyperspherical coordinates	46
3. Classical three-body recombination for neutrals and ion-neutral-neutral systems	48
4. Classical threshold law for three-body recombination: Universality in cold chemistry	49
VII. Conclusions	51
Acknowledgments	51
References	52

I. INTRODUCTION AND OVERVIEW

Spectacular recent breakthroughs for the three-body problem with near-resonant two-body interaction, in both experiments and theories, have spawned this review of universal few-body physics, which concentrates on systems with finite-range interactions. Vitaly Efimov's 1970 prediction (Efimov, 1970) that an infinite family of universal three-body states should emerge when two or more two-body scattering lengths are sufficiently large in magnitude first received partial experimental confirmation in 2006 by Rudi Grimm's group in Innsbruck (Kraemer *et al.*, 2006). That development was quickly followed by many subsequent experiments (Ferlandino *et al.*, 2008, 2009, 2011; Ottenstein *et al.*, 2008; Barontini *et al.*, 2009; Gross *et al.*, 2009, 2010, 2011; Knoop *et al.*, 2009, 2010; Pollack, Dries, and Hulet, 2009; Wenz *et al.*, 2009; Zaccanti *et al.*, 2009; Lompe, Ottenstein, Serwane, Viering *et al.*, 2010; Nakajima *et al.*, 2010, 2011; Berninger *et al.*, 2011, 2013; Machtey, Kessler, and Khaykovich, 2012; Machtey *et al.*, 2012; Wild *et al.*, 2012; Bloom *et al.*, 2013; Dyke, Pollack, and Hulet, 2013; Roy *et al.*, 2013; Zenesini *et al.*, 2013; Hu *et al.*, 2014; Huang, O'Hara *et al.*, 2014; Huang, Sidorenkov *et al.*, 2014; Pires, Ulmanis *et al.*, 2014; Tung *et al.*, 2014; Huang, Sidorenkov, and Grimm, 2015; Kunitzki *et al.*, 2015; Maier *et al.*, 2015; Johansen *et al.*, 2016; Ulmanis, Häfner, Pires, Kuhnle *et al.*, 2016; Ulmanis, Häfner, Pires, Werner *et al.*, 2016; Wacker *et al.*, 2016; Wang *et al.*, 2016; Häfner *et al.*, 2017) bearing on various aspects of the Efimov effect and universality; see Fig. 1. This class of phenomena is called *universal* because it can occur for systems with vastly different energy and length scales. While it was originally predicted for few-nucleon systems such as the triton, with energy scales of the order of 10^6 eV and distance scales of the order of 10^{-14} m, all of the convincing demonstrations to date have involved energy and distance scales of order 10^{-12} eV and 10^{-7} m, respectively. Some of the few-body physics topics discussed here have already been reviewed elsewhere, and the interested reader is encouraged to explore a large body of literature (Ohsaki and Nakamura, 1990; Suzuki and Varga, 1998; Nielsen *et al.*, 2001; Jensen *et al.*, 2004b; Braaten and Hammer, 2006; Yurovsky, Olshanii, and Weiss, 2008; Rittenhouse *et al.*, 2011; Baranov *et al.*, 2012; Blume, 2012a; Frederico *et al.*, 2012; Petrov, 2012; Wang,

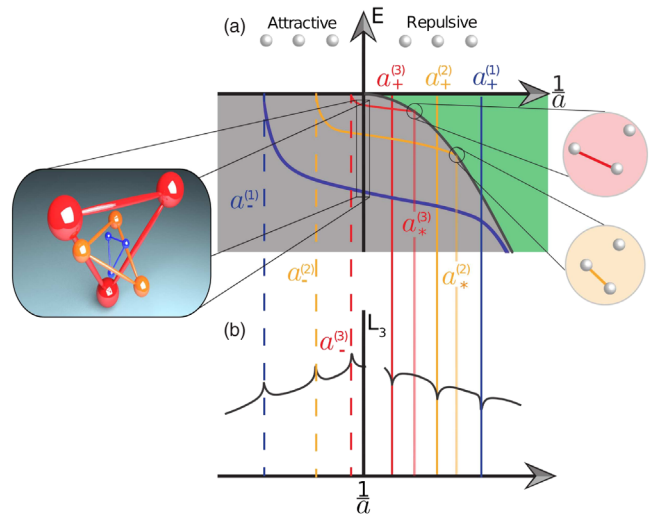


FIG. 1. Characterization of universal Efimov trimers in ultracold gases. (a) The universal trimer energy dependence on the inverse two-body scattering length, i.e., a . In particular, the Efimov trimers cross the three-body continuum at $a_+^{(n)}$, where $n = 1$ denotes the Efimov ground state, $n = 2$ the first excited states, etc. Efimov states intersecting the atom-dimer continuum are characterized by $a_*^{(n)}$ for the positive two-body scattering length. (b) A log-log plot of the recombination rates of three identical bosons at low energies vs the inverse two-body scattering length a . Minima in three-body recombination occur at scattering length values denoted here as $a_+^{(n)}$. The negative values of the atom-atom scattering length marked as $a_-^{(n)}$ indicate positions of the maxima in L_3 at ultracold temperatures, i.e., where Efimov states intersect the atom-atom-atom three-body threshold.

D'Incao, and Esry, 2013; Zinner and Jensen, 2013; Wang, Julienne, and Greene, 2015a; Côté, 2016; Naidon and Endo, 2017).

A. Systems with finite-range interactions

It is reasonable to ask why finding a new family of resonances has generated such excitement in few-body physics, excitement that has translated into an exponentially growing rate of citations for the 1970 Efimov paper during the past 15 years. In fact these resonances are unique and counterintuitive. For every previously known example of a system where infinitely many bound states or resonances exist that converge to a breakup threshold, the forces were infinite in their extent. The best known example of this is of course the asymptotically attractive Coulomb potential $V(r) \rightarrow -1/r$ which has an energy level formula $E_n \propto -1/n^2$, and a second example is the charge-dipole two-body potential $V(r) \rightarrow -(s^2 + 1/4)/2r^2$ at $r > r_0$ which has (for a system of units with reduced mass $\mu = 1$) an energy level formula $E_n = E_0 \exp(-2\pi n/s)$. The presence of a finite versus infinite number of quantized levels below a threshold hinges on the convergence or nonconvergence of the zero-energy Jeffreys-Wentzel-Kramers-Brillouin (JWKB) phase integral with Langer correction included. Morse and Feshbach (1953) present a pedagogical derivation of the Langer correction needed for accurate semiclassical calculations, e.g., when the independent

coordinate domain is semi-infinite or finite as is true for the radial coordinate in three-dimensional problems. That is, one can deduce the energy level formula relevant to a given two-body potential energy function $V(r)$ by evaluating the zero-energy total phase

$$\phi = \int_{r_0}^{\infty} \sqrt{-2\mu V(r)/\hbar^2 - \frac{1}{4r^2}} dr.$$

If this ϕ is infinite, then the number of converging energy levels will also be infinite, whereas if ϕ is finite then their number is also finite. This type of analysis also applies to the recently predicted “super-Efimov effect” (Nishida, Moroz, and Son, 2013; Gridnev, 2014; Moroz and Nishida, 2014; Volosniev *et al.*, 2014; Gao, Wang, and Yu, 2015) which is likewise predicted to yield an infinite sequence of bound (or resonant) levels for a system of three fermions in two dimensions [see also Efremov *et al.* (2013)] with a density of states far smaller than in the original Efimov effect.

A common thread running through this story is the fact that hyperspherical coordinate techniques played a key role in the early theoretical predictions of the Thomas and Efimov effects in the pre-1980 studies, and they have played an equally crucial role in showing later that ultracold quantum gases should provide a powerful way to observe universal Efimov physics, by linking the Efimov effect quantitatively to the loss process of three-body recombination. Hyperspherical studies have shown unusual flexibility, as they have been used, on the one hand, with zero-range regularized pseudopotential interactions to obtain closed-form analytical results (Efimov, 1970, 1971, 1973, 1979; Macek, 1986, 2002; Watanabe and Komine, 1989; Nielsen and Macek, 1999; Nielsen *et al.*, 2001; Kartavtsev and Macek, 2002; Macek, Ovchinnikov, and Gasaneo, 2005; Mehta *et al.*, 2008) and, on the other hand, as the basis for quantitative numerical solutions using finite-range analytical or numerical three-body Hamiltonians (Esry *et al.*, 1996; Esry, Greene, and Burke, 1999; Suno *et al.*, 2002; D’Incao and Esry, 2005; Esry and Greene, 2006; Wang, D’Incao, Esry, and Greene, 2012; Wang, Wang *et al.*, 2012). This flexibility has led to a tremendous deepening of our understanding of three-body recombination and atom-dimer elastic and inelastic scattering over the past two decades, both the quantitative understanding and, equally important, qualitative and semiquantitative ways to understand the main reaction pathways which govern the corresponding physical mechanisms. Despite this headway, there has not been a comprehensive review or monograph that has presented the full hyperspherical methodology, nor has there been one that covered much of the connections with diverse areas of physics from nuclear systems to cold atoms to exotic species and atomic electron states, and one of the goals of the present review is to bridge this gap in the existing literature.

The concepts of the hyperspherical approach are of course far from being a new innovation in few-body theoretical physics. They go back at least as far as the pioneering work of Llewellyn Hillel Thomas (Thomas, 1935) who realized that three nucleons whose ratio of potential range to scattering length becomes arbitrarily small, $r_0/|a| \rightarrow 0$, must have a ground state energy that “collapses” to $E \rightarrow -\infty$. The triton

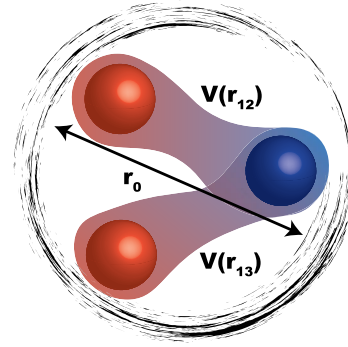


FIG. 2. Tritium nucleus model assumed by Thomas. The neutron-proton interaction is characterized by a finite-range potential $V(r_{ij})$, whose range is given by r_0 , but the neutron-neutron interaction is neglected (which is known nowadays to be far from correct). See text for details.

model considered by Thomas is depicted in Fig. 2. This was demonstrated by showing that the effective potential energy of such a system, as a function of the hyperradius R (Thomas denoted this variable as s), has the form $-1/R^2$, a potential that exhibits the well-known “fall to the center” collapse of its ground state energy, as discussed in quantum mechanics textbooks (Landau and Lifshitz, 1997). Another early application of hyperspherical coordinates framework was developed by Julian Schwinger’s student at Harvard, R. E. Clapp, in his Ph.D. thesis work on the triton binding energy (Clapp, 1949). Fock’s 1958 study of the analytical nature of the electronic helium atom wave function at small hyperradii also utilized hyperspherical coordinates in a fundamental way (Fock, 1958).

Some of the deepest insights into the nature of the three-body problem have emerged from Macek’s adiabatic hyperspherical methodology (Macek, 1968). The latter consists of a comprehensive theoretical framework in which the Hamiltonian of the system is initially diagonalized at fixed values of the hyperradius R , yielding adiabatic curves which represent the energies of the system as functions of R . These give an immediate, dynamics-based representation of the available reaction pathways for any given system and highlight the emerged structure of the bound and quasibound states of the system as well as their excitation and decay mechanisms (Fano, 1976, 1983; Lin, 1986, 1995). Coupling matrix elements can also be computed which permit, as shown in this review article, a systematic solution of the full three-body Schrödinger equation to the accuracy desired for arbitrary bound state problems as well as two-body inelastic and rearrangement collisions ($A + BC$), three-body collisions ($A + B + C$), and photon-assisted collision processes (Fink and Zoller, 1985).

B. Coulomb systems

The three-body problem in quantum mechanics with Coulomb interactions has generated intense effort throughout the past century. Early in the days of the “old quantum theory” it was a major problem to understand the ground and excited states of the helium atom. With Schrödinger’s wave mechanics, in combination with other tools such as the Ritz

variational method, it became possible by the 1930s to calculate properties of such low-lying states in the three-body Coulomb problem to high precision. For higher excited states lying in the two-body or three-body continua, however, progress was much slower. The ability to nonperturbatively calculate the simple process of electron impact ionization of hydrogen at low energies (<1 eV) above the double escape threshold, for instance, did not emerge until the 1990s (Kato and Watanabe, 1995; McCurdy, Rescigno, and Byrum, 1997; Robicheaux, Pindzola, and Plante, 1997; Bartlett *et al.*, 2003; Kadyrov *et al.*, 2009), although important theoretical work prior to that had identified the unusual threshold behavior for two-electron escape (Wannier, 1953; Peterkop, 1971; Klar and Schlecht, 1976; Greene and Rau, 1982, 1983; Fano, 1983; Rau, 1984; Read, 1984; Selles, Mazeau, and Huetz, 1987; Watanabe, 1991). Analogous theoretical headway occurred over that same period for other three-body observables, such as double photoionization of He and H^- (Meyer and Greene, 1994; Meyer, Greene, and Esry, 1997; Robicheaux, Pindzola, and Plante, 1997). Of course long before the quantal version of the three-body problem became topical, the Newtonian version with inverse square forces had acquired paramount importance and was singled out by researchers such as Poincaré and Hilbert as a crucial bottleneck that had to be solved.

Early efforts on systems with Coulomb interactions by Macek, Lin, and Fano demonstrated that significant insight into the qualitative and semiquantitative nature of doubly excited states of He and H^- emerges when an adiabatic hyperspherical approximation is implemented (Macek, 1968; Fano, 1976; Lin, 1986; Lin and Morishita, 2000). Surprisingly high doubly excited states of two-electron atoms can be treated in the adiabatic scheme, as seen for calculations of high states which yielded a simple interpretation of regularities seen in photoabsorption (Sadeghpour and Greene, 1990; Domke *et al.*, 1991; Rau, 1992; Tang *et al.*, 1992). Extensions to other atomic systems such as the alkaline earth atoms (Greene, 1981) and the negative ion of helium (Watanabe, 1982) were also developed, which showed that nonadiabatic couplings often need to be incorporated in order for the results to be even qualitatively useful (Christensen-Dalsgaard, 1984). The exploration of near separability of the two-electron wave function in alternative choices of coordinates, which yields nontrivial insights in some cases, was reviewed by Tanner, Richter, and Rost (2000).

Another arena where three-body Coulombic interactions have been subjected to intensive study has been in the context of muon-catalyzed fusion (Hino and Macek, 1996). Interesting studies of the $d\mu$ reaction of importance for muon-catalyzed fusion were carried out, for instance, using hyperspheroidal coordinates (Hara *et al.*, 1988; Fukuda, Ishihara, and Hara, 1990). Another hyperspheroidal coordinate application was to HD^+ by Macek and Jerjian (1986) and by Hara, Fukuda, and Ishihara (1989). Some of the most suitable systems for an adiabatic representation in hyperspherical coordinates are those with two or more equal mass particles, such as the ion formed from two electrons and one positron, i.e., the positronium negative ion (Botero and Greene, 1985, 1986; Fabre de la Ripelle, 1993). Also, not to be overlooked

is the fact that this approach can be made quantitatively accurate, in some cases with direct solution of the coupled hyperradial equations in the adiabatic representation (Kadomtsev, Vinitsky, and Yukajlovic, 1987).

In fact the adiabatic representation has challenges as the system grows in complexity and in the number of relevant coupled hyperradial equations, and for such systems the clever recasting as a set of diabatic equations, called the “slow-variable discretization” (SVD) method proposed by Tolstikhin, Watanabe, and Matsuzawa (1996), improves the efficiency enormously. When propagation to very large hyperradii is required in order to obtain accurate scattering information, a hybrid method (Wang, D’Incao, and Greene, 2011) has proven to be quite efficient and accurate, which uses SVD at small to intermediate hyperradii but solves the direct coupled adiabatic equations at very large hyperradii. One of the most recent applications of the SVD hyperspherical treatment is an investigation of the famous Hoyle triple- α resonance by Suno, Suzuki, and Descouvemont (2015).

Other exotic examples of three-body Coulombic systems that have been studied include the antiproton + hydrogen atom system, explored by Esry and Sadeghpour (2003), which gives an idea of the prototypical hyperspherical potential curves that emerge from applying the adiabatic hyperspherical method to the $\bar{p}pe$ system, as shown in Fig. 3. A large number of interacting channels are evident, which might initially seem hopelessly daunting in complexity. A closer inspection shows, however, that most of the curve crossings are highly diabatic,

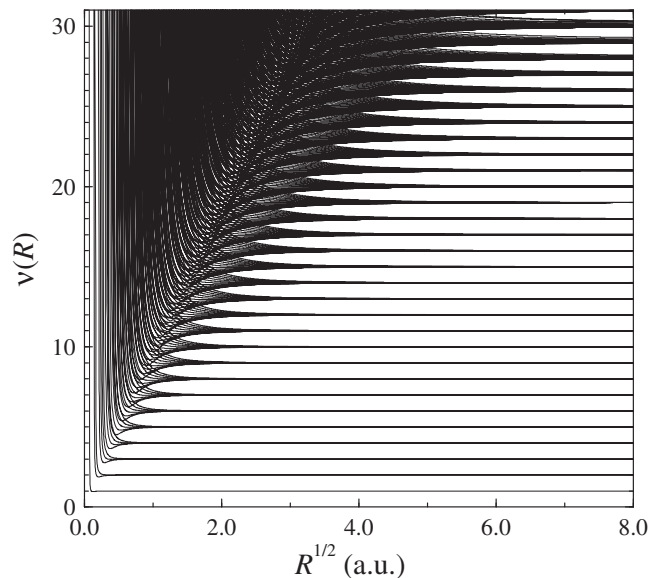


FIG. 3. Hyperspherical potential energy curves for the even-parity, zero angular momentum states of the $\bar{p}pe$ system, showing the rich variety of collision channel pathways that exist in this system. The states shown in the energy range displayed here are mostly of the type of “antihydrogen plus electron.” Note that the energy and hyperradius are displayed, respectively, here on an “effective quantum number scale” $\nu \equiv [-mU(R)]^{-1/2}$ with m the proton mass, and square root hyperradial scale $R^{1/2}$ reflecting the usual scaling in a Coulomb potential. For instance $\nu = 1$ corresponds to the energy of the ground $1s$ state of the hydrogenic $\bar{p}p$ state on this scale. From Esry and Sadeghpour, 2003.

and the diabatic potential curves are remarkably simple, suggesting approximately conserved quantum numbers. Further examples of such simplicity emerging for a seemingly complex system will be demonstrated throughout the present review. Some exciting headway in treating four-body Coulomb systems has also occurred during the last few decades, notably by Morishita *et al.* (1997), Morishita and Lin (1998, 1999), and D’Incao (2003), in a robust improvement over primitive early studies (Clark and Greene, 1980; Greene and Clark, 1984). A small number of treatments have extended adiabatic hyperspherical ideas to more than four particles, although they are still at a relatively primitive state at this time (Bohn, Esry, and Greene, 1998; Blume and Greene, 2000; Kim and Zubarev, 2000; Kushibe *et al.*, 2004; Morishita and Lin, 2005; Sogo *et al.*, 2005; Rittenhouse *et al.*, 2006; Rittenhouse and Greene, 2008; Daily and Greene, 2014; Ding and Greene, 2017). Figure 4 shows an example of the lowest potential energy curves obtained by Daily and Greene (2014) for a system of three electrons and two positrons. These potentials contain bound states of the different symmetries of this five-body system, and they also describe the lowest energy scattering processes.

Early interest in three-body continuum states in Coulombic systems was mainly triggered by a desire to understand electron impact ionization of atoms, especially in the low-energy range, through phenomena such as the Wannier-Rau-Peterkop threshold law for that process derived initially through entirely classical arguments (Wannier, 1953) and later confirmed through quantum mechanical and semiclassical arguments by Peterkop (1971, 1983) and Rau (1971). Experimental confirmations of this unusual irrational threshold law for a process with both electrons escaping from a residual particle of positive charge Ze , namely, $\sigma \propto E^\gamma$, where

$$\gamma = \frac{1}{4} \left[\left(\frac{100Z - 9}{4Z - 1} \right)^{1/2} - 1 \right],$$

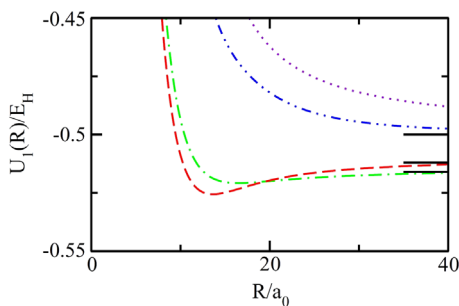


FIG. 4. The lowest several potential energy curves for zero angular momentum and even total parity are shown vs hyper-radius for a five-body Coulomb system, consisting of three electrons and two positrons. Denoting (S_+, S_-) the separate spin quantum numbers of the positrons and the electrons, these potentials shown as dashed, dash-dotted, dash-dot-dotted, and dotted lines correspond to $(S_+, S_-) = (1, \frac{1}{2}), (0, \frac{1}{2}), (1, \frac{3}{2}), (0, \frac{3}{2})$, respectively. The horizontal solid lines ordered from lowest to highest indicate the asymptotic fragmentation threshold energies of $\text{Ps}_2 + e^-$, $\text{Ps} + \text{Ps}^-$, and $2\text{Ps} + e^-$. From Daily and Greene, 2014.

were measured for electron impact ionization of atomic helium by Cvejanovic and Read (1974) and for two-electron photodetachment of H^- (Donahue *et al.*, 1982) (both for $Z = 1, \gamma = 1.127\dots$). Going beyond the double escape threshold law proved to be highly challenging, with some of the first credible absolute cross sections from a theoretical calculation, for the fundamental $e + \text{H} \rightarrow e + e + p$ process, emerging in the numerical “convergent close-coupling” studies by Bray and Stelbovics (1993), Bartlett *et al.* (2003), and Kadyrov *et al.* (2009), performed in ordinary independent electron coordinates. One of the first studies that obtained competitively accurate results within a hyperspherical coordinate framework was that of Kato and Watanabe (1995, 1997), and it was followed by a subsequent detailed study by Kazansky, Selles, and Malegat (2003), Malegat (2003, 2004), and Selles *et al.* (2004). Highly quantitative results have also now been obtained for this two-electron escape process by direct solution of the time-independent (McCurdy, Baertschy, and Rescigno, 2004) or time-dependent (Pindzola and Robicheaux, 1998; Pindzola *et al.*, 2007) Schrödinger equations. Recent years have seen extensive interest in the time-reversed process: three-body recombination. For a low-temperature plasma consisting of electrons and protons, this is the reaction $e + e + p \rightarrow \text{H}(nl) + e$ (Robicheaux, 2007; Pohl, Vranceanu, and Sadeghpour, 2008; Robicheaux *et al.*, 2010) or its antimatter analog with positrons and antiprotons; this mechanism underpins recent exciting progress in the formation of antihydrogen (Andresen *et al.*, 2010, 2011).

C. Chemical physics

Another class of studies that has utilized a three-body hyperspherical solution to solve a challenging problem in chemical physics is the dissociative recombination (DR) of H_3^+ (Kokoouline, Greene, and Esry, 2001; Kokoouline and Greene, 2003; Petrigani *et al.*, 2011). To describe the DR process where an electron collides with H_3^+ and the final state dissociates into $\text{H}_2 + \text{H}$ or $\text{H} + \text{H} + \text{H}$, the use of hyperspherical coordinates has both a practical computational advantage and a qualitative conceptual advantage. For instance, the theory of DR is much better understood for a diatomic target than for a polyatomic target, so the use of an adiabatic hyperspherical representation of the nuclear positions ultimately maps polyatomic DR theory back in terms of more familiar diatomic DR theory. Those studies also showed that a nontrivial rearrangement collision can be controlled by conical intersection dynamics, more specifically in this case the Jahn-Teller effect. Part of that solution was a description of the incident electron channels as well as the energetically closed Rydberg channel pathways using multichannel quantum defect techniques, which will not be discussed in detail here but are summarized elsewhere in the literature (Kokoouline, Douguet, and Greene, 2011).

In chemical physics, some of the most impressive theoretical studies of few-atom reactive scattering have been carried out using a hyperspherical coordinate framework. See for instance an early treatment by Kuppermann and Hipes (1986) of $\text{H} + \text{H}_2$ scattering. In 1985, experimentalists Neumark and co-workers performed a groundbreaking study (Neumark *et al.*, 1985) of the famous $\text{F} + \text{H}_2 \rightarrow \text{FH} + \text{H}$

reaction, which required several years before a converged theoretical treatment using hyperspherical coordinates in a variant of Macek’s adiabatic representation—the diabatic-by-sector method—was developed by Launay and Le Dourneuf (1990). Other studies of importance in hyperspherical treatments of reactive scattering were developed by Pack and Parker (1987, 1989). However, other studies of important rearrangement reactions were carried out using Jacobi or other coordinates, such as the calculation by Neuhauser *et al.* (1991), but our focus in this article is primarily on methodologies that ultimately boil down to solving one or a coupled set of one-dimensional hyperradial Schrödinger equations. A simple and popular method for solving such coupled 1D differential equations is the log-derivative method (Johnson, 1973; Manolopoulos, Jamieson, and Pradhan, 1993), while a more advanced technique frequently utilized when there are many close avoided crossings in the potential curves was developed by Tolstikhin, Watanabe, and Matsuzawa (1996) and implemented in various studies such as Wang, D’Incao, and Greene (2011).

A handful of studies have even gone beyond three-atom processes and computed scattering cross sections for reactions involving four atoms using hyperspherical (Clary, 1991) or other methods (Bohr *et al.*, 2014). These studies can be viewed as solutions to the few-body Schrödinger equation, starting from the Born-Oppenheimer potential energy surface as a function of the internuclear coordinates. Of course a number of important reactive systems have two or more fundamentally coupled potential surfaces, with or without conical intersections, and these require further sophistication even in formulating the basic Born-Oppenheimer Hamiltonian governing the coupled electronic and nuclear degrees of freedom.

D. Fragmentation, recombination, and molecule formation

The general theory of nuclear reactions was formulated in hyperspherical coordinates by Delves (1958, 1960), who showed that the usual unitary scattering matrix can be defined in general by inspecting the asymptotic form of the flux-conserving solution at large hyperradii. Hyperspherical coordinates were picked up by Smirnov and others in the Soviet school of nuclear physics, and that work is reviewed by Smirnov and Shitikova (1977). The work of that school concentrated on the development of noninteracting solutions in the hyperangular degrees of freedom, the so-called hyperspherical harmonics, including a graphical way to construct the solutions, and the analog of fractional parentage coefficients to achieve their antisymmetrization when applied to several fermionic particles such as nucleons (Smirnov and Shitikova, 1977). This was developed further in nuclear collision theory by Barnea and Novoselsky (1997), Barnea (1999), and Nielsen *et al.* (2001). More recently, a model treatment of elastic nucleon scattering of the type $A + A_2$ has shown that there is a significant benefit from adopting adiabatic hyperspherical ideas in the calculation, particularly if the theory is implemented using integral relations for the scattering amplitudes that were developed by Barletta and Kievsky (2008, 2009) and Barletta *et al.* (2009).

The variant of the three-body problem involving short-range forces, particularly relevant in nuclear physics, has served as an

independent but equally important testing ground for theory. Whereas in ultracold atomic physics it is a recombination process such as $A + B + C \rightarrow AB + C$ that is of greatest interest, which can form a diatomic molecule in a gas of free atoms, in nuclear physics it is more typically the time reverse of recombination, i.e., $AB + C \rightarrow A + B + C$ whose reaction rates and scattering amplitudes are of interest in laboratory experiments and in astrophysical contexts. An early study by Thomas (1935) showed that the range r_0 of two-body nuclear forces cannot be made arbitrarily smaller than the nucleon-nucleon scattering lengths $a_{nn}(S=0) = -18.9$, $a_{np}(S=0) = -23.7$, and $a_{np}(S=1) = 5.43$ fm, because the three-nucleon ground state would become *arbitrarily deep* and plummet all the way to $-\infty$ in the limit $r_0 \rightarrow 0$, a behavior never observed experimentally, of course, but which is now referred to as the “Thomas collapse” effect. Interestingly, however, one sees that the scattering lengths are generally much larger in magnitude than the known range $r_0 \sim 1\text{--}2$ fm of the nucleon-nucleon strong force. Another intriguing foray into the behavior of three particles interacting via short-range forces came decades later from Efimov, who predicted an effect that bears some connection with the Thomas collapse effect: Efimov predicted that for a system of three particles having infinite two-body scattering lengths, there must be an infinite number of three-body bound levels that become *arbitrarily weak* in their binding. Efimov’s work went on to predict that in the limit where three equal mass particles have common interparticle scattering lengths a , the number of such universal bound levels becomes finite and is truncated to the approximate value $N \approx (1/\pi) \ln(|a|/r_0)$. These levels are called universal because they depend only on the dimensionless ratio between the scattering length and the distance r_0 beyond which the two-body interactions are negligible, and in some cases an additional parameter is needed, such as the “three-body parameter” discussed in Sec. III.

The recombination process that occurs when three ultracold atoms collide, e.g., $A + A + A \rightarrow A_2 + A$ in a Bose-Einstein condensate (BEC), became a particularly important topic in the field of degenerate quantum gases in the mid-1990s, when it was increasingly realized that this was the dominant loss process in most experiments. The reason was that most of the experimental ingenuity had been directed toward turning off inelastic two-body losses by cleverly designing the quantum states of the trapped atoms. This left little possibility to further turn off inelastic three-body losses, although the gases in real experiments were usually sufficiently dilute that the quantum gas produced could be studied for reasonable periods of time, usually from 0.1 to 100 s. The process of three-body recombination was studied in a perturbative treatment by Verhaar and collaborators for the case of spin-polarized atomic hydrogen (de Goey *et al.*, 1986); the rate coefficient for the process is only of the order of 10^{-38} cm⁶/s, i.e., of extremely low probability because it requires a spin flip via magnetic interactions. For more typical systems such as alkali atoms that recombine in an ultracold gas, an application of the Verhaar approach (Moerdijk, Boesten, and Verhaar, 1996; Moerdijk and Verhaar, 1996) predicted that the recombination rate should scale overall as a^2 , i.e., as the *square* of the atom-atom scattering length a .

In fact the growth of the recombination rate coefficient K_3 with a was eventually shown to be much faster than quadratic. The first promising step toward a deeper understanding of three-body recombination emerged from a study by Fedichev *et al.* (1996) which predicted that the true scaling of K_3 should vary much more strongly with scattering length as a^4 . Sparked by growing interest throughout the ultracold science community in the need for a deeper understanding of three-body recombination, two nonperturbative treatments of this process at large two-body scattering lengths were published in 1999, one by Nielsen and Macek (1999) and the other by Esry, Greene, and Burke (1999). While these 1999 Letters confirmed the (Fedichev, Reynolds, and Shlyapnikov, 1996) prediction of an overall a^4 scaling of the three-body recombination rate coefficient K_3 , they both found an additional Stueckelberg interference modulation with the encouraging potential to cause destructive interference at some very large values of a , potentially beneficial for experiments where loss needs to be minimized. In addition, Esry, Greene, and Burke (1999) predicted that an infinite number of resonances should periodically enhance the recombination rate at large negative a , and that these resonances are Efimov states that have become unbound and merged into the three-body continuum. In the case of homonuclear three-body recombination, those “zero-energy” resonances are predicted to have an approximate geometric scaling in the scattering length, with each successive Efimov resonance occurring at a two-body scattering length that is $e^{\pi/s_0} \approx 22.7$ times larger than the preceding one.

Following these initial predictions, subsequent theoretical studies extended and amplified them, e.g., as reviewed with a focus on the hyperspherical coordinate point of view by several articles (Nielsen *et al.*, 2001; Greene, 2010; Rittenhouse *et al.*, 2011; Wang, D’Incao, and Esry, 2013; Wang, Julienne, and Greene, 2015a, 2015a). Importantly, alternative treatments found largely similar conclusions using methods such as effective field theory (Bedaque, Braaten, and Hammer, 2000; Braaten and Hammer, 2001, 2003, 2006), a separable interaction application of effective field theory (Shepard, 2007), two exactly solvable models (Macek, Yu Ovchinnikov, and Gasaneo, 2006; Gogolin, Mora, and Egger, 2008; Mora, Gogolin, and Egger, 2011), and the treatment by Köhler (2002) and Lee, Köhler, and Julienne (2007) that adopted the early theoretical nuclear physics treatment of Alt, Grassberger, and Sandhas (1967). All of these explorations tremendously added to confidence in the theory community that the Efimov effect should be observable, despite the dearth of experimental confirmation prior to 2006.

Then, however, this field received a tremendous injection of excitement in 2006 when recombination rate measurements for a Cs gas by Grimm’s Innsbruck group (Kraemer *et al.*, 2006) observed the aforementioned Efimov resonance in the three-body rate coefficient K_3 at a large negative scattering length, in agreement with the 1999 prediction (Esry, Greene, and Burke, 1999). That study provided the first experimental confirmation of the Efimov effect. The scattering length dependence of measured recombination rates in that 2006 experiment closely resembled the predicted shape (Esry, Greene, and Burke, 1999) for a three-body Efimov resonance, but a skeptic might argue that observation of one resonance

alone might not be convincing evidence of its Efimov character. However, subsequent observations of three-body recombination in numerous systems have solidified, confirmed, and extended that interpretation beyond any doubt. The most dramatic signature has been observing multiple resonances, separated by the predicted Efimov factor of 22.7 in the scattering length, and multiple predicted interference minima, separated by that same universal factor (Esry, Greene, and Burke, 1999; Nielsen and Macek, 1999; Braaten and Hammer, 2006; Greene, 2010).

A further unexpected level of universality emerged from experimental studies with three-atom recombination. The three-body parameter had been thought by virtually all theorists to occur “randomly” and to vary widely from system to system. The three-body parameter can be viewed as setting the energy E_0 of the lowest Efimov state at $a = \infty$ (unitarity), or alternatively as the smallest scattering length $a_-^{(1)}$ at which a zero-energy Efimov resonance occurs and thus sets the location of all subsequent resonances through the universal scaling formula $a_-^{(n)} = a_-^{(1)} e^{(n-1)\pi/s_0}$. The remarkable surprise was experimental evidence from the Grimm group (Berninger *et al.*, 2011) and several others (Gross *et al.*, 2009, 2010, 2011; Wild *et al.*, 2012; Dyke, Pollack, and Hulet, 2013; Roy *et al.*, 2013) which showed that for homonuclear three-body systems dominated by van der Waals (vdW) $-C_6 r^{-6}$ two-body interactions at long range, an approximate *van der Waals universality* fixes $a_-^{(1)} \approx -10\ell_{\text{vdW}}$ in terms of the characteristic length $\ell_{\text{vdW}} \equiv (mC_6/16\hbar^2)^{1/4}$. As Fig. 5 shows, the three-body parameter is fixed to within approximately 15% by this simple relation. Shortly after this experimental evidence was published, a theoretical interpretation emerged from Wang, D’Incao, Esry, and Greene (2012) which showed that a classical suppression of the two-body probability density whenever two particles approach to within $r < \ell_{\text{vdW}}$ produces an effective hyperradial barrier that restricts three-body motion at $R < 2\ell_{\text{vdW}}$ and sets the three-body parameter. To clarify, there is a classical suppression because the probability of a classical particle having local velocity $v(r)$ to exist in a region of width Δr is proportional to $\Delta r/v(r)$, the time spent by the particle in that region in each traversal. In the presence

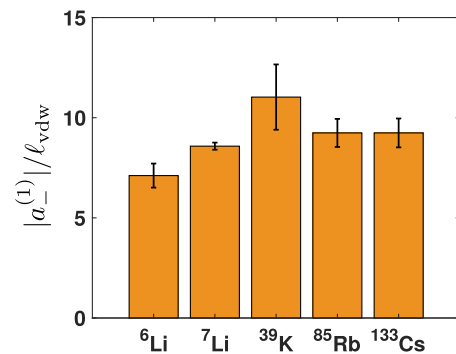


FIG. 5. Three-body parameter scaled by ℓ_{vdW} for three equal mass particles. Specifically, this quantity is the value of the (negative) atom-atom scattering length at which the first universal Efimov resonance is observable in a zero-energy three-body recombination process. The error bars have been calculated as the weighted mean of the experimental results reported in Sec. III.

of an attractive van der Waals force, the velocity increases suddenly and dramatically when the interparticle distance r decreases to less than the van der Waals length, causing this probability density to plummet in such regions. The existence of the hyperradial barrier was subsequently confirmed and extended in further studies by Naidon, Hiyama, and Ueda (2012) and Naidon, Endo, and Ueda (2014a, 2014b) which stressed particularly that a key element of this van der Waals universality is a change from a very floppy equilateral to a roughly linear geometry that occurs near $R \approx 2\ell_{\text{vdW}}$; the geometry change then triggers strong non-Born-Oppenheimer repulsion and suppresses the three-body solution at all smaller hyperradii in the relevant potential curve. An alternative toy model addressing the implications of two-body van der Waals forces on the three-body approximate universality was also published by Chin (2011). Other treatments aimed at this issue of three-body parameter universality that start from a two-channel or narrow two-body resonance point of view are presented by Schmidt, Rath, and Zwerger (2012), Sørensen *et al.* (2012), and Wang and Julienne (2014).

The case of heteronuclear universal Efimov physics appears to be significantly more complicated, e.g., for the particularly interesting case of heavy-heavy-light (HHL) systems that exhibit more favorable Efimov scaling than for the homonuclear three-body systems. But a degree of van der Waals universality has been predicted by Wang, Wang *et al.* (2012) to still be relevant for the “Efimov favored” HHL case. The complexity grows for these heteronuclear systems because more parameters control the universality, namely, two van der Waals lengths and a mass ratio, and the universal energy spectrum now depends on two scattering lengths that are uncorrelated in general. Nevertheless, early experimental evidence from two different experimental groups (Pires, Ulmanis *et al.*, 2014; Tung *et al.*, 2014; Ulmanis, Häfner, Pires, Kuhnle *et al.*, 2016) suggests that this generalized van der Waals universality for HHL systems is at least approximately valid, but still deserves careful study in the future. A recent experimental paper (Johansen *et al.*, 2016) suggests that, for Efimov physics near a narrow two-body Fano-Feshbach resonance in the ${}^6\text{Li} - {}^{133}\text{Cs} - {}^{133}\text{Cs}$ system, the universal van der Waals theoretical predictions developed for Efimov physics in the HHL system near a broad two-body resonance (Wang, Wang *et al.*, 2012) will require substantial modifications by implementing a multichannel model for the two-body interaction Hamiltonian as in Kartavtsev and Macek (2002), Mehta *et al.* (2008), and Wang and Julienne (2014). For light-light-heavy (LLH) three-body systems, Wang, Wang *et al.* (2012) stressed that these are “Efimov unfavored,” and it is unlikely that a true Efimov state will be observable experimentally.

E. Recombination processes involving cluster resonances with more than three particles

A detailed discussion of universal four-boson and five-boson energy levels and recombination resonances is given in Sec. III.G, but here we point out some of the basic issues involved in describing cluster resonances in systems of $N > 3$ identical bosons having short-range interactions. Most of these systems have a pairwise attractive long-range interaction

and a strong short-range repulsion, as in the case of N bosonic helium atoms. Simple counting then shows that in the relative coordinate system the number of positive terms in the kinetic energy operator is proportional to $N - 1$ whereas the number of net attractive terms in the pairwise potential energy is equal to $N(N - 1)/2$. Thus, one expects that if one is in a negative region of the two-body scattering length a where three particles are not quite attracted strongly enough to bind a universal trimer state, there could be a value of the negative scattering length $a = a_{4B}^-$ where four or more particles are able to bind. Similarly, if one goes to a region where four particles are not quite strongly enough to be bound, there should be a negative value of $a = a_{5B}^-$ at which five particles are just bound. One can explore this theoretically either by varying the two-body potential strength to modify the scattering length (Yamashita, Fedorov, and Jensen, 2010; von Stecher, 2010, 2011; Gattobigio, Kievsky, and Viviani, 2012; Nicholson, 2012; Yan and Blume, 2015) or by artificially changing the particle mass in the calculations for a fixed two-body potential, which also modifies the repulsive versus attractive balance in the Hamiltonian (Hanna and Blume, 2006). This concept has been studied in a number of studies, and some universal aspects have already emerged. In particular, the most recent discussion by Yan and Blume (2015) gives evidence that for general short-range two-body interactions, such as Gaussians or other short-range potentials, the N -body cluster energies at unitarity $a \rightarrow \infty$ are not uniquely specified since they depend on the type of “three-body regulator” implemented. However, there does appear to be a quasiuniversality that emerges in the case of van der Waals two-body interactions: the cluster bound state energies at unitarity are then approximately fixed in terms of the van der Waals length scale.

These and other developments will be addressed in the remainder of this review, including a detailed description of the techniques, while stressing methods of interpretive analysis that have been utilized to study these universal phenomena from a hyperspherical coordinate perspective. A recent treatment of universal five-body bound states in a mass-imbalanced fermionic system was developed by Bazak and Petrov (2017) using alternative (integral equation) techniques (Pricoupenko, 2011).

II. ADIABATIC HYPERSPHERICAL TREATMENT

A Schrödinger wave equation for N interacting particles, with masses m_i moving in three dimensions per particle, becomes in the absence of external fields, a $d = 3N - 3$ dimensional partial differential equation (PDE) in the relative coordinate system. When expressed in hyperspherical coordinates, a single scalar coordinate, the hyperradius R defined later, is singled out for special treatment within an adiabatic formulation. It is possible in general to formally transform the d -dimensional PDE, specifically the time-independent Schrödinger equation $\hat{H}\Psi = E\Psi$ for any potential energy function dependent on the relative position coordinates only, into an infinite set of ordinary coupled differential equations in a single adiabatic coordinate R . Moreover, a conceptual advantage of hyperspherical coordinates is that every possible fragmentation mode for any system of particles occurs in the limit $R \rightarrow \infty$.

The basic equations of the adiabatic representation are simple to derive. First, write the full time-independent Hamiltonian in the form

$$\hat{H} = \hat{T}_R + H_{R=\text{const}}, \quad (1)$$

where the term $H_{R=\text{const}}$ depends on R only as a parameter and is a Hermitian partial differential operator in all other (hyperangular) coordinates of the system plus spins, denoted collectively here as $\{\varpi\}$. Next, solve the eigenvalue equation at each value of R :

$$H_{R=\text{const}}\Phi_\nu(R; \varpi) = u_\nu(R)\Phi_\nu(R; \varpi). \quad (2)$$

The exact eigenfunctions of the full \hat{H} can now be expanded into the complete, orthonormal set of eigenfunctions $\Phi_\nu(R; \varpi)$ with R -dependent coefficients $F_{E\nu}(R)$ as

$$\Psi_E(R; \varpi) = R^{-(d-1)/2} \sum_\nu \Phi_\nu(R; \varpi) F_{E\nu}(R), \quad (3)$$

giving an infinite set of coupled differential equations for the hyperradial functions:

$$\left(-\frac{\hbar^2}{2\mu} \frac{d^2}{dR^2} + U_\nu(R) - E\right) F_{E\nu}(R) = -\sum_{\nu'} \hat{W}_{\nu\nu'} F_{E\nu'}(R), \quad (4)$$

where μ is the N -body reduced mass and its explicit form is given in Eq. (9). Observe that for a coordinate space with d dimensions, the hyperradial kinetic energy operator has the form

$$\hat{T}_R = -\frac{\hbar^2}{2\mu} \frac{1}{R^{d-1}} \frac{\partial}{\partial R} R^{d-1} \frac{\partial}{\partial R},$$

and the rescaling of the radial function eliminates the first-order derivative of $F_{E\nu}(R)$ on the left-hand side of Eq. (4). The rescaling also adds what Fano called a ‘‘mock-centrifugal term’’ to $u_\nu(R)$, giving the full effective hyperradial Born-Oppenheimer potential as

$$U_\nu(R) = u_\nu(R) + \frac{(d-1)(d-3)\hbar^2}{8\mu R^2}. \quad (5)$$

The coupling terms on the right-hand side of Eq. (4), which are responsible for nonadiabatic couplings, are given by

$$\hat{W}_{\nu\nu'} F_{E\nu'} = -\frac{\hbar^2}{2\mu} Q_{\nu\nu'}(R) F_{E\nu'}(R) - \frac{\hbar^2}{\mu} P_{\nu\nu'}(R) \frac{dF_{E\nu'}(R)}{dR}. \quad (6)$$

Here the two nonadiabatic coupling matrices are given by

$$Q_{\nu\nu'}(R) \equiv \left\langle\left\langle \Phi_\nu(R; \varpi) \left| \frac{\partial^2}{\partial R^2} \right| \Phi_{\nu'}(R; \varpi) \right\rangle\right\rangle^{(R)}$$

and

$$P_{\nu\nu'}(R) \equiv \left\langle\left\langle \Phi_\nu(R; \varpi) \left| \frac{\partial}{\partial R} \right| \Phi_{\nu'}(R; \varpi) \right\rangle\right\rangle^{(R)},$$

where the double bracket notation signifies an integral (and spin trace) only over the ϖ degrees of freedom. This set of coupled equations is sometimes treated in the hyperradial Born-Oppenheimer approximation which neglects the right-hand side of Eq. (4). In that approximation, the system moves along a single potential energy curve with no possibility of changing from one potential to another, and this approximation of course has no possibility of describing an inelastic collision. But in some cases it can give a reasonable description of energy levels and scattering phase shifts, although in most cases a more accurate result is obtained by retaining (except near close avoided crossings) the diagonal terms of Eq. (4) which is usually referred to as the hyperspherical *adiabatic approximation*.

While the hyperradial Born-Oppenheimer approximation, which considers only a single term in the expansion for Ψ_E in Eq. (4), is often reasonable, a far richer set of phenomena emerges when nonadiabatic coupling effects are incorporated, either by direct solution of the coupled radial equations or else using semiclassical methods such as Landau-Zener-Stückelberg or their improvements along the lines of Nikitin (1970) and Zhu, Teranishi, and Nakamura (2001). This in fact yields a quantitative description of phenomena such as three-body or four-body recombination and inelastic atom-dimer or dimer-dimer scattering.

The following development sketches one explicit version of this recasting of the Schrödinger equation into hyperspherical coordinates for an N -particle system in three dimensions. Note that a similar development for N 2D particles is presented by Daily, Wooten, and Greene (2015) in the context of the quantum Hall effect. One first transforms the N laboratory frame position vectors $\{\vec{r}_i\}$ in terms of a suitable set of $N-1$ mass-weighted relative Jacobi coordinate vectors $\{\vec{\rho}_i\}$, plus the center-of-mass vector which is trivial and is therefore ignored throughout. Extensive arbitrariness and flexibility exists for the choice of the Jacobi coordinate vectors, but for definiteness one simple choice is based on choosing the j th Jacobi vector as the (reduced-mass-weighted) relative vector between particle $j+1$ and the center of mass of the preceding group of particles 1 through j , i.e.,

$$\begin{aligned} \vec{\rho}_1 &= \sqrt{\frac{\mu_{12}}{\mu}} (\vec{r}_2 - \vec{r}_1), \\ \vec{\rho}_2 &= \sqrt{\frac{\mu_{12,3}}{\mu}} \left(\vec{r}_3 - \frac{m_1 \vec{r}_1 + m_2 \vec{r}_2}{m_1 + m_2} \right), \text{ etc.}, \end{aligned} \quad (7)$$

where the $N-1$ Jacobi reduced masses are

$$\mu_{12} = \frac{m_1 m_2}{m_1 + m_2}, \quad \mu_{12,3} = \frac{(m_1 + m_2) m_3}{m_1 + m_2 + m_3}, \text{ etc.}, \quad (8)$$

and where the N -body reduced mass is

$$\mu = (\mu_{12} \mu_{12,3} \cdots)^{1/(N-1)}. \quad (9)$$

Alternative choices for the overall reduced mass μ are possible and are sometimes utilized, but this choice in Eq. (9) is particularly desirable in many contexts because it preserves the overall volume element. With these definitions, the

nonrelativistic kinetic operator acquires a simple form, namely,

$$\hat{T} = -\frac{\hbar^2}{2\mu} \sum_{j=1}^{N-1} \vec{\nabla}_{\rho_j}^2 \equiv -\frac{\hbar^2}{2\mu} \sum_{i=1}^d \frac{\partial^2}{\partial x_i^2}. \quad (10)$$

The Cartesian coordinates of all these Jacobi vectors can thus be collected into a single d -dimensional relative vector $\underline{x} \equiv \{x_1, x_2, x_3, \dots, x_d\}$, and these can in turn be transformed into hyperspherical coordinates by defining the hyperradius R as the radius of the d -dimensional hypersphere:

$$R = \sqrt{x_1^2 + x_2^2 + x_3^2 + \dots + x_d^2}. \quad (11)$$

There are again many possible choices for the $d-1$ hyperangles α_k , but one simple generalization of our usual spherical coordinates is implied by the chain (Avery, 1989):

$$\begin{aligned} x_d &= R \cos \alpha_{d-1}, \\ x_{d-1} &= R \sin \alpha_{d-1} \cos \alpha_{d-2}, \\ x_{d-2} &= R \sin \alpha_{d-1} \sin \alpha_{d-2} \cos \alpha_{d-3}, \\ \dots x_2 &= R \prod_{j=1}^{d-1} \sin \alpha_j, \quad \text{and} \\ x_1 &= R \prod_{j=2}^{d-1} \sin \alpha_j \cos \alpha_1. \end{aligned} \quad (12)$$

This easily generalizable choice of the hyperangles is sometimes referred to as the canonical choice. The ranges spanned by these hyperangles are then

$$0 \leq \alpha_1 \leq 2\pi, \quad 0 \leq \alpha_i \leq \pi, \quad i = 2, \dots, d-1. \quad (13)$$

Now the nonrelativistic kinetic energy operator in hyperspherical coordinates can be conveniently written as

$$\hat{T} = T_R + \frac{\hbar^2 \Lambda^2}{2\mu R^2}, \quad (14)$$

where

$$T_R = -\frac{\hbar^2}{2\mu} \frac{1}{R^{d-1}} \frac{\partial}{\partial R} R^{d-1} \frac{\partial}{\partial R},$$

and Λ^2 is the isotropic Casimir operator for the group $O(d)$ (Knirk, 1974; Smirnov and Shitikova, 1977; Cavagnero, 1984, 1986) explicitly given by

$$\Lambda^2 = -\sum_{i>j} \Lambda_{ij}^2, \quad \Lambda_{ij} = x_i \frac{\partial}{\partial x_j} - x_j \frac{\partial}{\partial x_i}.$$

The operator Λ^2 is often referred to as the square of the ‘‘grand angular momentum’’ operator of the system. These equations now show how the physics of this d -dimensional problem can be mapped exactly onto an adiabatic representation in the single coordinate R , with potential energy curves $U_\nu(R)$

and nonadiabatic coupling terms as in standard Born-Oppenheimer theory. As particularly stressed by Macek (1968) and Fano (1981b, 1983), and as we document, this approach yields tremendous insight into many physical systems.

Some examples of applying the adiabatic hyperspherical representation to systems with many particles are summarized in Sec. IV. But before turning to examples, we show how far greater symmetry and simplicity emerge from a clever choice of the hyperangles for three-particle systems $N=3$ by adopting a ‘‘body-fixed’’ coordinate system of the type suggested by Whitten and Smith (1968). The particular variant described here adopts the conventions specified by Suno *et al.* (2002).

Usually we are interested in three-body systems that have exact separability in the relative and center-of-mass coordinates, whereby the relative degrees of freedom can be described by six coordinates, i.e., $d=6$ is the full dimensionality of this space. Three of these coordinates are conveniently chosen to be Euler angles $\{\alpha, \beta, \gamma\}$ that connect the body-fixed frame to the space-fixed frame. Three remaining coordinates in this system are the hyperradius R and two hyperangles θ and φ . Following Whitten and Smith (1968), Johnson (1983), Lepetit, Peng, and Kuppermann (1990), and Kendrick *et al.* (1999) with only minor modifications described by Suno *et al.* (2002), this begins from the mass-scaled Jacobi coordinates (Delves, 1960)

$$\vec{\rho}_1 = (\vec{r}_2 - \vec{r}_1)/\Delta, \quad (15)$$

$$\vec{\rho}_2 = \Delta \left[\vec{r}_3 - \frac{m_1 \vec{r}_1 + m_2 \vec{r}_2}{m_1 + m_2} \right], \quad (16)$$

with

$$\Delta^2 = \frac{1}{\mu} \frac{m_3(m_1 + m_2)}{m_1 + m_2 + m_3} \quad (17)$$

and μ is the three-body reduced mass as previously defined, namely,

$$\mu^2 = \frac{m_1 m_2 m_3}{m_1 + m_2 + m_3}. \quad (18)$$

In this expression, particle i with mass m_i has position \vec{r}_i . When the three particles have identical mass m , the parameters simplify to $\Delta = (4/3)^{1/4}$ and $\mu = m/\sqrt{3}$. And specializing the definition of the hyperradius R , it is given here by

$$R^2 = \rho_1^2 + \rho_2^2, \quad 0 \leq R < \infty. \quad (19)$$

The hyperangles θ and φ are determined by the four nonzero components of the two Jacobi vectors in the body frame $x-y$ plane by

$$\begin{aligned}
(\vec{\rho}_1)_x &= R \cos(\theta/2 - \pi/4) \sin(\varphi/2 + \pi/6), \\
(\vec{\rho}_1)_y &= R \sin(\theta/2 - \pi/4) \cos(\varphi/2 + \pi/6), \\
(\vec{\rho}_2)_x &= R \cos(\theta/2 - \pi/4) \cos(\varphi/2 + \pi/6), \\
(\vec{\rho}_2)_y &= -R \sin(\theta/2 - \pi/4) \sin(\varphi/2 + \pi/6),
\end{aligned} \tag{20}$$

where by definition $\rho_{1z} = 0 = \rho_{2z}$. For definiteness, note that the x , y , and z right-handed coordinate system of the body-fixed frame is chosen such that the z axis is parallel to $\vec{\rho}_1 \times \vec{\rho}_2$, and the x axis is that with the smallest moment of inertia. The ranges of the hyperangles are $0 \leq \theta \leq \pi/2$ and $0 \leq \varphi < 2\pi$ (Kendrick *et al.*, 1999). If the three equal mass particles are in fact truly identical, then the hyperangle φ can be further restricted to the range $[0, 2\pi/3]$. Note that in this case the interaction potential is symmetric under the operation $\varphi \rightarrow \pi/3 - \varphi$. Then the bosonic or fermionic symmetry of the Schrödinger solutions under exchange of any two particles is particularly simple to impose as a boundary condition in these coordinates. The volume element for integrals over $|\Psi|^2$ is equal to

$$dV \equiv d\varpi R^5 dR = 2 \sin 2\theta d\theta d\varphi d\alpha \sin \beta d\beta d\gamma R^5 dR,$$

and the Euler angle ranges are $0 \leq \alpha < 2\pi$, $0 \leq \beta < \pi$, and $0 \leq \gamma < \pi$. The full Schrödinger equation for the rescaled wave function $\psi_E = R^{5/2}\Psi$ describing three identical particles now takes the form

$$\left(-\frac{1}{2\mu} \frac{\partial^2}{\partial R^2} + \frac{15}{8\mu R^2} + \frac{\Lambda^2}{2\mu R^2} + V(R, \theta, \varphi) \right) \psi_E = E \psi_E. \tag{21}$$

In this expression, Λ^2 is the squared grand angular momentum operator and is given by (Lepetit, Peng, and Kuppermann, 1990; Kendrick *et al.*, 1999)

$$\frac{\Lambda^2}{2\mu R^2} = T_1 + T_2 + T_3, \tag{22}$$

where

$$T_1 = -\frac{2}{\mu R^2} \frac{\partial}{\sin 2\theta} \sin 2\theta \frac{\partial}{\partial \theta}, \tag{23}$$

$$T_2 = \frac{1}{\mu R^2 \sin^2 \theta} \left(i \frac{\partial}{\partial \varphi} - \cos \theta \frac{L_z}{2} \right)^2, \tag{24}$$

$$T_3 = \frac{L_x^2}{\mu R^2 (1 - \sin \theta)} + \frac{L_y^2}{\mu R^2 (1 + \sin \theta)} + \frac{L_z^2}{2\mu R^2}. \tag{25}$$

The total orbital angular momentum operator in the body frame is denoted here as $\vec{L} = \{L_x, L_y, L_z\}$. For an interacting three-body system, one frequently adopts a sum of two-body potential energy functions for $V(R, \theta, \varphi)$, but some explorations are carried out with explicit nonpairwise additive terms as well. That is, most explorations of universal physics have used an approximate three-particle V of the form

$$V(R, \theta, \varphi) = v(r_{12}) + v(r_{23}) + v(r_{31}), \tag{26}$$

where r_{ij} are the interparticle distances. For three equal mass particles, these distances are expressed in terms of the hyperspherical coordinates as

$$\begin{aligned}
r_{12} &= 3^{-1/4} R [1 + \sin \theta \sin(\varphi - \pi/6)]^{1/2}, \\
r_{23} &= 3^{-1/4} R [1 + \sin \theta \sin(\varphi - 5\pi/6)]^{1/2}, \\
r_{31} &= 3^{-1/4} R [1 + \sin \theta \sin(\varphi + \pi/2)]^{1/2}.
\end{aligned} \tag{27}$$

As indicated, the first step in implementing the adiabatic representation is to solve the fixed- R adiabatic eigenvalue equation for a given symmetry L^Π to obtain the fixed- R adiabatic eigenfunctions (Φ_ν , sometimes referred to as channel functions) and eigenvalues [potential energy curves $U_\nu(R)$]. Here we adopt an abbreviated notation with $\Omega \equiv (\theta, \varphi, \alpha, \beta, \gamma)$ and for some systems Ω includes spin degrees of freedom as well. For the body-frame choice of hyperangles, it is simplest to expand the Euler angle dependence of the Φ_ν in terms of normalized Wigner D functions $\tilde{D}_{MK}^L(\alpha\beta\gamma)$, i.e., as

$$\Phi_\nu^{L^\Pi}(R; \Omega) = \sum_K \phi_{K\nu}(R; \theta, \varphi) \tilde{D}_{MK}^L(\alpha\beta\gamma). \tag{28}$$

This representation guarantees that $\Phi_\nu^{L^\Pi}$ is automatically an eigenfunction of L^2 , and it is also an even (odd) eigenfunction of the parity operator $\hat{\Pi}$ provided K is restricted to even (odd) values, respectively. A few more details of this body-frame representation are useful when using this representation to convert the five-dimensional PDE (21) into a set of coupled 2D PDEs in θ, φ only. In this body-frame representation of angular momentum, the raising and lowering operators are defined (owing to the anomalous commutation relations of body-frame operators) as

$$L_\pm = L_x \mp iL_y, \tag{29}$$

where

$$\begin{aligned}
L_\pm \tilde{D}_{M,K}^L(\alpha\beta\gamma) &= \sqrt{(L \mp K)(L \pm K + 1)} \tilde{D}_{M, K \pm 1}^L(\alpha\beta\gamma), \\
L_z \tilde{D}_{M,K}^L(\alpha\beta\gamma) &= K \tilde{D}_{M,K}^L(\alpha\beta\gamma).
\end{aligned}$$

After inserting these expressions, one obtains for each value of $\{L, M, \Pi\}$ a finite number of coupled 2D PDEs in θ, φ . The terms involving L_x^2 and L_y^2 cause couplings between components K and $K \pm 2$. While these PDEs are for complex solutions, as written here, it is possible to take linear combinations, e.g., $\phi_K(R; \theta, \varphi) \pm \phi_{-K}(R; \theta, \varphi)$ and reformulate the PDEs in terms of real functions everywhere.

A. Recombination cross sections and rate coefficients

It was proven by Delves that the hyperspherical representation preserves the usual desired properties of continuum scattering solutions, such as flux conservation when the Hamiltonian is Hermitian which ensures unitarity of the scattering matrix S and symmetry of the S matrix when the Hamiltonian is time reversal invariant. One simple conceptual aspect of Macek's adiabatic hyperspherical representation involving potential energy curves and nonadiabatic

couplings is that the computation of the unitary S matrix can utilize any of the powerful techniques already developed for treating two-body inelastic scattering processes. In other words, just as in standard multichannel scattering theory (Rodberg and Thaler, 1970) or multichannel quantum defect theory (Fano, 1970; Seaton, 1983; Mies, 1984; Greene and Jungen, 1985; Aymar, Greene, and Luc-Koenig, 1996; Burke, Greene, and Bohn, 1998; Mies and Raoult, 2000; Gao, 2001; Ruzic, Greene, and Bohn, 2013), one simply propagates solutions of the coupled equations in Eq. (4) out to large distances, fits to linear combinations of energy normalized regular and irregular radial functions $\{f_{E\nu}(R), g_{E\nu}(R)\}$ and in this manner obtain a real, symmetric reaction matrix $K_{\nu\nu'}(E)$ characterizing solutions from some large matching radius R_0 out to infinity:

$$\Psi_{E\nu}(R; \varpi) = \sum_{\nu'} \frac{\Phi_{\nu'}(R; \varpi)}{R^{(d-1)/2}} [f_{E\nu}(R)\delta_{\nu\nu'} - g_{E\nu}(R)K_{\nu\nu'}]. \quad (30)$$

Then linear combinations of those solutions can be taken to enforce any appropriate boundary conditions at $R \rightarrow \infty$ for the observable quantities of interest (Fano and Rau, 1986; Aymar, Greene, and Luc-Koenig, 1996). The usual relations are obtained for quantities such as $S = (1 + iK)(1 - iK)^{-1}$ with extra long-range phase factors sometimes needed to satisfy outgoing-wave or incoming-wave boundary conditions [see, e.g., Sec. II of Aymar, Greene, and Luc-Koenig (1996)]. Of particular interest in the context of ultracold quantum gases is the three-body recombination rate coefficient which was derived by Esry, Greene, and Burke (1999). The relevant formula for three identical bosonic particles which are in a thermal gas rather than a BEC, after correcting for a factor of 6 error in the formulas reported in that paper, is

$$K_3(E) = \frac{\hbar k}{\mu} \frac{192\pi^2}{k^5} \sum_{\nu\nu'} |S_{\nu\nu'}|^2. \quad (31)$$

Here $k = \sqrt{2\mu E/\hbar^2}$ and the sum includes all entrance three-body continuum channels ($A + A + A, \nu$) for the symmetry of interest, and over all final state two-body bound channels ($A_2 + A, \nu'$). A few words are relevant to explain how this recombination rate coefficient is to be used in rate equations used to model this reaction in a cold gas. This quantity $K_3(E)$ is the fundamental coefficient relevant to a single triad of particles in the gas. The coefficient in the rate equations for the disappearance of atoms or the appearance of dimers is another rate coefficient L_3 , which is determined by the following points. If one imagines that there are N atoms in a thermal gas volume V , then there are $g_N = N(N-1)(N-2)/3! \approx N^3/6$ distinct triads of the type $A + A + A$ in the system. If we define a density as $n \equiv N/V$, then the rate equation for the disappearance of atoms from a cold trapped gas is

$$\frac{dn}{dt} = -L_3 n^3, \quad (32)$$

where for a thermal trapped gas,

$$L_3 = 3K_3 \frac{g_N}{N^3} \approx \frac{K_3}{2}.$$

In this last equation, the leading factor of 3 in the middle is the number of atoms lost in each recombination event, and the value of 3 reflects the fact that for a typical trapped gas of atoms, a recombination event releases so much kinetic energy that both the final dimer and the final atom following recombination will be ejected, i.e., all three of the initially free atoms. If an unusually deep trap is implemented, or if the binding energy of the dimer produced is far less than the trap depth, then that factor of 3 would of course be changed to 2 since only the dimer would escape the atom trap, although one should then also keep track of the energy deposited into the cloud by the remaining hot atom. As is also well known (Kagan, Svistunov, and Shlyapnikov, 1985; Burt *et al.*, 1997; Söding *et al.*, 1999), if the initial atom cloud is in a pure BEC rather than a thermal gas, then the preceding K_3 needs to be reduced by a factor of 3!

Some of the simplest and most important early predictions of the low-energy recombination rate behavior include an expected a^4 scaling (Fedichev, Reynolds, and Shlyapnikov, 1996), which was later seen to be modified in a nontrivial way that differs depending on whether the atom-atom scattering length a is positive (Esry, Greene, and Burke, 1999; Nielsen and Macek, 1999) or negative (Esry, Greene, and Burke, 1999). If a is large and positive, then there exists a weakly bound dimer state whose energy is approximately $-\hbar^2/ma^2$, and the recombination rate into that universal dimer channel should have Stückelberg interference minima at scattering lengths $a_+^{(i)}$ whose spacings should scale geometrically with the Efimov scaling parameter $a_+^{(i+1)}/a_+^{(i)} = e^{\pi/s_0} \sim 22.7$. If instead a is negative, then this implies that there is no weakly bound universal dimer, and recombination can occur only into deeper nonuniversal dimer channels. On this side, even though the attraction is not strong enough to bind two atoms together into a universal dimer, the Efimov effect can bind trimers at certain values of $a^{(i)} < 0$. Moreover, the successive values of a where a trimer can form at zero energy also obey the Efimov scaling $a^{(i+1)}/a^{(i)} \sim 22.7$. While the first experiments (Ferlandino *et al.*, 2008, 2009, 2011; Gross *et al.*, 2009, 2010, 2011; Knoop *et al.*, 2009, 2010; Pollack, Dries, and Hulet, 2009; Zaccanti *et al.*, 2009; Berninger *et al.*, 2011, 2013; Machtey, Kessler, and Khaykovich, 2012; Machtey *et al.*, 2012; Dyke, Pollack, and Hulet, 2013; Zenesini *et al.*, 2013) were able only to observe a single Efimov resonance ($i = 1$) for homonuclear systems, a recent experiment by Huang, Sidorenkov *et al.* (2014) observed the $i = 1, 2$ resonances and confirmed their approximate ratio to be close to Efimov's predicted value.

Much subsequent theory has treated the physics of recombination and developed compact analytical formulas within the framework of zero-range models and/or effective field theory, which are particularly convenient for analyzing experimental data (Braaten and Hammer, 2006; Macek, Yu Ovchinnikov, and Gasaneo, 2006; Gogolin, Mora, and Egger, 2008; Mora, Gogolin, and Egger, 2011). A different direction of extending and generalizing recombination theory has been the treatment of recombination processes for $N > 3$

particles. A generalization of Eq. (31) presented for recombination of N identical bosons into any number of bound fragments was derived by Mehta *et al.* (2009):

$$K_N(E) = N! \frac{\hbar k}{\mu} \left(\frac{2\pi}{k} \right)^{d-1} \frac{\Gamma(d/2)}{2\pi^{d/2}} \sum_{\nu\nu} |S_{\nu\nu}|^2. \quad (33)$$

Here d is the number of dimensions in the relative coordinate space after eliminating the trivial center-of-mass motion, i.e., for N particles in three dimensions, $d = 3N - 3$. This last formula of course reduces to the above expression for K_3 when $N = 3$.

III. THE BIRTH OF FEW-BODY PHYSICS: THE EFFECTS OF THOMAS AND EFIMOV

A. The Thomas collapse

In the early days of nuclear physics, in 1935, a mere three years following the Chadwick discovery of the neutron, L. H. Thomas published a seminal work about the structure of the triton ${}^3\text{H}$ (Thomas, 1935). In particular, Thomas studied the existence of the triton ground state obtained with different assumptions for the neutron-proton interaction, but neglecting neutron-neutron interactions as depicted in Fig. 2. As a result, Thomas (1935) found that the neutron-neutron potential energy should have a repulsive character at short range, and that the neutron-proton interaction cannot be confined to a distance very small compared with 1 fm. These findings constitute the very first exploration of few-body physics with finite-range forces, and they sparked the interest of many physicists in different fields of physics, especially atomic physics and molecular physics in addition to nuclear physics.

The key point of Thomas (1935) is that it is possible to account for nucleon-nucleon (or atom-atom) interactions having an arbitrary scattering length a with many different two-body interaction models. For a two-body model with arbitrarily short range r_0 there must be a corresponding potential depth of order $\hbar^2/2mr_0^2$ in order to yield a value of a that is independent of the potential range and fixed at an experimentally measured value. For instance, in a spherical square well model having depth V_0 and range r_0 , the zero-energy two-body scattering length for two equal mass particles of mass m and reduced mass $m/2$ is equal to $a = r_0 - \tan qr_0/q$, where $q = \sqrt{mV_0/\hbar^2}$. As r_0 is decreased to smaller and smaller values, q must increase approximately in proportion to $1/r_0$ in order to maintain any given fixed scattering length. Thomas then examined the nature of the three-body ground state energy in this limit of decreasing potential range r_0 but fixed two-body scattering length. The qualitative argument is rather simple, namely, that when a third particle is brought into the system having equal scattering lengths a , this adds two new potential energy terms to the Hamiltonian of the same depth and range, while adding only one new kinetic energy term. As a result, the three-body system is shown by Thomas to have a ground state energy that must be of the order of $-\hbar^2/mr_0^2$, which becomes arbitrarily large and negative as $r_0 \rightarrow 0$.

B. Efimov physics and universality in ultracold gases

Efimov considered an analogous three-body problem which also involved two-body scattering lengths a much larger in magnitude than the potential range, i.e., $|a|/r_0 \gg 1$, except that Efimov visualized the two-body interaction range r_0 to be fixed, and $|a| \rightarrow \infty$.

Three identical particles with resonant two-body interaction showed an infinite series of three-body bound states as predicted by Efimov (1970, 1971, 1973) more than 40 years ago. This infinity of trimer states follows a discrete symmetry scaling, i.e., the energy of the n th and $(n+1)$ th states are related through $E_{n+1} = \lambda^2 E_n$, where for the particular case of three identical bosons $\lambda = e^{\pi/s_0}$ with $s_0 = 1.0062$ (Efimov, 1970; Braaten and Hammer, 2006; Greene, 2010; Ferlaino *et al.*, 2011; Wang, D’Incao, and Esry, 2013), and hence $\lambda \approx 22.7$. Efimov introduced the universal theory of three-body collisions thinking in nuclear systems as the preferable scenario for the quest of his predictions. However, the first experimental evidence of the prediction of Efimov came from ultracold gases (Kraemer *et al.*, 2006), and this early evidence triggered an explosive growth in research into few-body ultracold physics.

In ultracold systems the exciting capability exists to tune a two-body atomic scattering length, using magnetic, optical, or radio-frequency-induced Fano-Feshbach resonances (Inouye *et al.*, 1998; Köhler, Góral, and Julienne, 2006; Chin *et al.*, 2010; Hanna, Tiesinga, and Julienne, 2010; Tscherbul *et al.*, 2010; Owens, Xie, and Hutson, 2016). This tunability of ultracold system Hamiltonians makes them perfect candidates to study few-body universality. However, the formation of universal trimers must be detected and characterized in such systems. The most usual route to such detection is to measure the three-body loss coefficient L_3 as a function of the two-body scattering length a , as schematically shown in Fig. 1. Specifically, the universal Efimov trimers cause an enhancement of L_3 at a given two-body negative scattering length $a_-^{(n)}$, and the Efimov physics exhibits interference minima at values of the positive two-body scattering length $a_+^{(n)}$, as shown in Fig. 1. Efimov states can also be studied by radiative or oscillatory field association as was achieved in ${}^6\text{Li}$ by Lompe, Ottenstein, Serwane, Wenz *et al.* (2010) and Nakajima *et al.* (2011) and in ${}^7\text{Li}$ by Machtey *et al.* (2012).

C. Faddeev equations for three identical bosons: Bound states

1. Hamiltonian and Faddeev operator equations

In the following, three spinless and equal mass particles of bosonic character are considered which interact via short-range fields. Note that the notation introduced for deriving the Faddeev equations follows Gloeckle (1983). Then the total Hamiltonian for three s -wave interacting bosons obeys the following form:

$$H = H_0 + \hat{V}_{23} + \hat{V}_{31} + \hat{V}_{12}, \quad (34)$$

where H_0 is the three-body kinetic operator, and \hat{V}_{ij} indicates the short-range potential between the i th and j th particles. For simplicity the following notation is introduced $\hat{V}_i \equiv \hat{V}_{jk}$ with

cyclic permutation of (i, j, k) . The three-body Schrödinger equation reads

$$\left(H_0 + \sum_i \hat{V}_i\right)\Psi = E\Psi, \quad (35)$$

where Ψ indicates the three-body wave function. Employing now the three-body noninteraction Green's function, i.e., $\hat{G}_0 \equiv [E - H_0]^{-1}$, Eq. (35) can be recast to the following form:

$$\Psi = \hat{G}_0 \sum_i \hat{V}_i \Psi = \underbrace{\hat{G}_0 \hat{V}_1 \Psi}_{\psi^{(1)}} + \underbrace{\hat{G}_0 \hat{V}_2 \Psi}_{\psi^{(2)}} + \underbrace{\hat{G}_0 \hat{V}_3 \Psi}_{\psi^{(3)}}, \quad (36)$$

where this holds as long as the Green's function is free of poles. In our case this is valid since we focus on the description of three-body bound states, i.e., the energy of any bound state is negative while the zeroth-order Hamiltonian has only kinetic energy and is positive definite. As Eq. (36) illustrates the total three-body wave function Ψ can be decomposed in three components, namely, $\Psi = \sum_i \psi^{(i)}$ with $i = 1, \dots, 3$ where each $\psi^{(i)}$ indicates the i th Faddeev component of the total three-body wave function Ψ . Physically, the i th Faddeev component, i.e., $\psi^{(i)}$ implies that the i th particle is a spectator particle with respect to the interacting pair (j, k) . Employing this decomposition ansatz in Eq. (36) yields a system of three coupled Faddeev equations which describe the bound state properties of the three-body system

$$\begin{pmatrix} \psi^{(1)} \\ \psi^{(2)} \\ \psi^{(3)} \end{pmatrix} = \hat{G}_0 \begin{pmatrix} 0 & \hat{t}_1 & \hat{t}_1 \\ \hat{t}_2 & 0 & \hat{t}_2 \\ \hat{t}_3 & \hat{t}_3 & 0 \end{pmatrix} \begin{pmatrix} \psi^{(1)} \\ \psi^{(2)} \\ \psi^{(3)} \end{pmatrix}, \quad (37)$$

where the term \hat{t}_i represents the two-body transition operator. More specifically, \hat{t}_i obeys the following Lippmann-Schwinger equation:

$$\hat{t}_i = \hat{V}_i + \hat{V}_i \hat{G}_0 \hat{t}_i, \quad \text{for } i = (1, 2, 3), \quad (38)$$

where the term \hat{G}_0 denotes the Green's function of three noninteracting bosons. This implies that the transition operator \hat{t}_i is considered as a two-body operator embedded in a three-body Hilbert space.

The Faddeev equations in Eq. (37) can be decoupled by taking into account the exchange symmetry between the three particles. Formally the exchange symmetry can be addressed by a permutation operator P_{ij} which permutes the i th with the j th particle. In addition, the considered system consists of three identical bosons, and therefore the total wave function Ψ is symmetric. Because of this the exchange operator permutes only the particles in the Faddeev components. By using the permutation operator, a pair of Faddeev components $(\psi^{(j)}, \psi^{(k)})$ can be expressed in terms of $\psi^{(i)}$ and vice versa. The $\psi^{(i)}$ component of the Faddeev equations in Eq. (37) then takes the following form:

$$\psi^{(i)} = \hat{G}_0 \hat{t}_i (P_{ij} P_{jk} + P_{ik} P_{jk}) \psi^{(i)}, \quad \text{for } (i, j, k = 1, 2, 3), \quad (39)$$

where the indices (i, j, k) form a cyclic permutation.

Equation (39) represents the operator form of the Faddeev equations and in the following Eq. (39) is expressed in momentum space. For completeness reasons in the following the Jacobi coordinates and the corresponding momenta are briefly reviewed.

2. Faddeev equations in momentum representation

Consider that the motion of three bosonic particles with masses m_i with $i = 1, \dots, 3$ are described by the lab coordinates \mathbf{x}_i whereas their corresponding momentum is \mathbf{k}_i with $i = 1, \dots, 3$. Then in order to describe the relative motion of three particles the following three sets of Jacobi coordinates are introduced:

$$\boldsymbol{\rho}_i = \mathbf{x}_i - \frac{m_j \mathbf{x}_j + m_k \mathbf{x}_k}{m_j + m_k} \quad \text{and} \quad \mathbf{r}_i = \mathbf{x}_j - \mathbf{x}_k, \quad (40)$$

where $(i, j, k = 1, 2, 3)$ form a cyclic permutation and the Jacobi vector \mathbf{r}_i denotes the relative distance between the j th and k th particles whereas the vectors $\boldsymbol{\rho}_i$ indicate the distance of the i th particle, i.e., the spectator particle, from the center of mass of the (j, k) pair of atoms. Note that the coordinate of the center of mass of three particles obeys the simple relation $\mathbf{R} = \sum_{i=1}^3 m_i \mathbf{x}_i / M$, where $M = \sum_{i=1}^3 m_i$ denotes the total mass of the system.

Similarly, for the Jacobi momenta we obtain the following relations:

$$\begin{aligned} \mathbf{q}_i &= \frac{m_k \mathbf{k}_j - m_j \mathbf{k}_k}{m_j + m_k} \quad \text{and} \\ \mathbf{p}_i &= \frac{(m_j + m_k) \mathbf{k}_i - m_i (\mathbf{k}_j + \mathbf{k}_k)}{M}, \end{aligned} \quad (41)$$

where $(i, j, k = 1, 2, 3)$ form a cyclic permutation, \mathbf{q}_i denotes the relative momentum of the (j, k) pair, and \mathbf{p}_i indicates the momentum of the the spectator particle relative to the center of mass of the (j, k) pair. The total momentum is given by $\mathbf{P} = \sum_{i=1}^3 \mathbf{k}_i$.

According to these definitions the kinetic operator \hat{H}_0 in the momentum space takes the following form:

$$H_0 = \frac{\mathbf{P}^2}{2M} + \frac{\mathbf{p}_i^2}{2\bar{\mu}_i} + \frac{\mathbf{q}_i^2}{2\mu_i}, \quad (42)$$

where $\mu_i = m_j m_k / (m_j + m_k)$ is the reduced mass of the (j, k) pair particles and $\bar{\mu}_i = m_i (m_j + m_k) / M$ denotes the reduced mass of the spectator particle and the center of mass of the (j, k) pair.

In the following we assumed that the collisions occur in the frame of the total center of mass; this means $\mathbf{P} = 0$. Therefore, the term $\mathbf{P}^2 / (2M)$ can be removed from the total Hamiltonian which then takes the form

$$H' = \frac{\mathbf{p}_i^2}{2\bar{\mu}_i} + \frac{\mathbf{q}_i^2}{2\mu_i} + V_i(\boldsymbol{\rho}_i) + V_j\left(\mathbf{r}_i + \frac{m_j}{m_j + m_k}\boldsymbol{\rho}_i\right) + V_k\left(\mathbf{r}_i - \frac{m_k}{m_j + m_k}\boldsymbol{\rho}_i\right). \quad (43)$$

Since the Jacobi coordinates and momenta are introduced, the reduced Faddeev equation [see Eq. (39)] can be transformed into the momentum space. For this purpose a certain set of Jacobi momenta is chosen, i.e., $(\mathbf{p}_1, \mathbf{q}_1)$. This means that in this particular set of Jacobi coordinates the particle 1 is the spectator of the pair (2,3). Upon introducing a complete set of states $|\mathbf{q}_1\mathbf{p}_1\rangle$, Eq. (39) becomes

$$\langle \mathbf{q}_1\mathbf{p}_1 | \psi^{(1)} \rangle = G_0(\mathbf{q}_1, \mathbf{p}_1) \int \frac{d\mathbf{q}'_1}{(2\pi)^3} \frac{d\mathbf{p}'_1}{(2\pi)^3} \langle \mathbf{q}_1\mathbf{p}_1 | \hat{t}_1 | \mathbf{q}'_1\mathbf{p}'_1 \rangle \times \langle \mathbf{q}'_1\mathbf{p}'_1 | P_{12}P_{23} + P_{13}P_{23} | \psi^{(1)} \rangle, \quad (44)$$

where the three-body Green's function in momentum space is given by

$$G_0(\mathbf{q}_1, \mathbf{p}_1) = \left[E - \frac{q_1^2}{2\mu_1} - \frac{p_1^2}{2\bar{\mu}_1} \right]^{-1}.$$

Note that for the bound trimer spectrum the total energy E is negative; thus in this case the G_0 Green's function is free of poles.

The matrix elements of the transition operator \hat{t}_1 in Eq. (44) can be evaluated with the help of the corresponding Lippmann-Schwinger equation (38):

$$\langle \mathbf{q}_1\mathbf{p}_1 | \hat{t}_1 | \mathbf{q}'_1\mathbf{p}'_1 \rangle = \delta(\mathbf{p}_1 - \mathbf{p}'_1) \langle \mathbf{q}_1 | t \left(E - \frac{p_1^2}{2\bar{\mu}_1} \right) | \mathbf{q}'_1 \rangle, \quad (45)$$

where the term $t(E - p_1^2/2\bar{\mu}_1)$ is the two-body transition amplitude embedded in the two-body Hilbert space. This means that the transition amplitude obeys a two-body Lippmann-Schwinger equation of the following form:

$$\langle \mathbf{q}_1 | t(\varepsilon) | \mathbf{q}'_1 \rangle = \langle \mathbf{q}_1 | \hat{V}_1 | \mathbf{q}'_1 \rangle + \int \frac{d\mathbf{q}''_1}{(2\pi)^3} \langle \mathbf{q}_1 | \hat{V}_1 | \mathbf{q}''_1 \rangle \times \left[\varepsilon - \frac{q_1''^2}{2\mu_1} \right]^{-1} \langle \mathbf{q}''_1 | t(\varepsilon) | \mathbf{q}'_1 \rangle. \quad (46)$$

In addition the exchange operators in Eq. (44) for equal masses, namely, $m_1 = m_2 = m_3 = m$ obey the following relation:

$$\begin{aligned} & \langle \mathbf{q}'_1\mathbf{p}'_1 | P_{12}P_{23} + P_{13}P_{23} | \mathbf{q}''_1\mathbf{p}''_1 \rangle \\ &= \delta\left(\mathbf{q}'_1 + \frac{3}{4}\mathbf{p}''_1 + \frac{\mathbf{q}''_1}{2}\right) \delta\left(\mathbf{p}'_1 - \mathbf{q}''_1 + \frac{\mathbf{p}''_1}{2}\right) \\ &+ \delta\left(\mathbf{q}'_1 - \frac{3}{4}\mathbf{p}''_1 + \frac{\mathbf{q}''_1}{2}\right) \delta\left(\mathbf{p}'_1 + \mathbf{q}''_1 + \frac{\mathbf{p}''_1}{2}\right). \end{aligned} \quad (47)$$

By substituting the Eqs. (45), (46), and (47) into the reduced Faddeev equation, namely, Eq. (44), we get the following expression:

$$\begin{aligned} \langle \mathbf{q}_1\mathbf{p}_1 | \psi^{(1)} \rangle &= \left(E - \frac{q_1^2}{m} - \frac{3p_1^2}{4m} \right)^{-1} \\ &\times \int \frac{d\mathbf{p}'_1}{(2\pi)^3} \left[\left\langle \mathbf{q}_1 \left| t \left(E - \frac{3p_1^2}{4m} \right) \right| -\mathbf{p}'_1 - \frac{\mathbf{p}_1}{2} \right\rangle \right. \\ &\times \left\langle \mathbf{p}_1 + \frac{\mathbf{p}'_1}{2}; \mathbf{p}'_1 \left| \psi^{(1)} \right\rangle \right. \\ &+ \left\langle \mathbf{q}_1 \left| t \left(E - \frac{3p_1^2}{4m} \right) \right| \mathbf{p}'_1 + \frac{\mathbf{p}_1}{2} \right\rangle \\ &\left. \times \left\langle -\mathbf{p}_1 - \frac{\mathbf{p}'_1}{2}; \mathbf{p}'_1 \left| \psi^{(1)} \right\rangle \right]. \end{aligned} \quad (48)$$

3. Separable potential approximation: Two-body transition elements and the reduced Faddeev equation

In the following we consider that the two-body interactions can be modeled by a separable potential, such as the Yamaguchi potential (Yamaguchi, 1954). This particular type of potentials simplifies the Faddeev equations [see Eq. (48)] into a one-dimensional integral equation. Assume that the two particles interact via s -wave interactions only through the following nonlocal potential:

$$\langle \mathbf{q}_1 | \hat{V}_1 | \mathbf{q}'_1 \rangle = -\frac{\lambda}{m} \chi(\mathbf{q}_1) \chi(\mathbf{q}'_1), \quad (49)$$

where λ denotes the strength of the two-body interactions, m indicates the mass of the particles, and the $\chi(\cdot)$ functions are the so-called form factors. Typically, the χ form factors are chosen such that the potential V yields the same scattering length and effective-range correction as the real two-body interactions. Note that since we are interested in three-body bosonic collisions of neutral atoms in Sec. III.D we provide the form factors χ which are derived from a van der Waals potential. This particular choice of form factor incorporates in a transparent way the pairwise two-body interactions of the three neutral atoms.

After insertion of Eq. (46), the two-body transition matrix elements for the separable potential in Eq. (49) obey

$$\begin{aligned} \langle \mathbf{q}_1 | t(\varepsilon) | \mathbf{q}'_1 \rangle &= -\frac{\lambda}{m} \chi(\mathbf{q}_1) \tau(\varepsilon) \chi(\mathbf{q}'_1), \text{ with} \\ \tau^{-1}(\varepsilon) &= 1 + \frac{\lambda}{m} \int \frac{d\mathbf{q}_1}{(2\pi)^3} \frac{|\chi(\mathbf{q}_1)|^2}{\varepsilon - q_1^2/m}. \end{aligned} \quad (50)$$

After specializing to states where the three particles have total angular momentum $L = 0$ and using the separable potential from Eq. (49), as well as the two-body transition matrix elements from Eq. (50), the reduced Faddeev equation in Eq. (48) reads

$$\begin{aligned} \langle \mathbf{q}_1\mathbf{p}_1 | \psi^{(1)} \rangle &= -2\frac{\lambda}{m} \left(E - \frac{q_1^2}{m} - \frac{3p_1^2}{4m} \right)^{-1} \tau \left(E - \frac{3p_1^2}{4m} \right) \\ &\times \chi(\mathbf{q}_1) \int \frac{d\mathbf{p}'_1}{(2\pi)^3} \chi \left(\mathbf{p}'_1 + \frac{\mathbf{p}_1}{2} \right) \left\langle \mathbf{p}_1 + \frac{\mathbf{p}'_1}{2}; \mathbf{p}'_1 \left| \psi^{(1)} \right\rangle \right. \\ &\left. \right). \end{aligned} \quad (51)$$

This integral equation can be further simplified by employing the following ansatz for the Faddeev component $|\psi^{(1)}\rangle$:

$$\langle \mathbf{q}_1 \mathbf{p}_1 | \psi^{(1)} \rangle = \left(E - \frac{q_1^2}{m} - \frac{3p_1^2}{4m} \right)^{-1} \chi(\mathbf{q}_1) \mathcal{F}(\mathbf{p}_1). \quad (52)$$

Substituting the ansatz of Eq. (52) into the reduced Faddeev equation, namely, Eq. (50), an integral equation for the amplitudes \mathcal{F} is obtained where its arguments depend only on the magnitude of the \mathbf{p}_1 vector states due to the s -wave character of the two-body interactions. Under these considerations the integral equation of the amplitudes \mathcal{F} reads

$$\begin{aligned} \mathcal{F}(p_1) = & -2 \frac{\lambda}{m} \tau \left(E - \frac{3p_1^2}{4m} \right) \\ & \times \int \frac{d\mathbf{p}'_1}{(2\pi)^3} \frac{\chi(|\mathbf{p}'_1 + \mathbf{p}_1/2|) \chi(|\mathbf{p}_1 + \mathbf{p}'_1/2|)}{E - p_1'^2/m - p_1'^2/m - \mathbf{p}_1 \cdot \mathbf{p}'_1/m} \mathcal{F}(p'_1), \end{aligned} \quad (53)$$

where for a particular choice of χ form factors the preceding equation is transformed into a matrix equation. For a given s -wave scattering length and effective range parameters, numerically the energy is varied in searching for roots of the corresponding determinantal equation of Eq. (53).

Finally, note that replacement of the χ form factor by $\chi(\mathbf{q}_1) \rightarrow 1$ in the reduced Faddeev equation in Eq. (51) one obtains the Skorniakov–Ter-Martirosian (STM) equation (Skorniakov and Ter-Martirosian, 1957) for three bosons colliding with zero-range s -wave interactions. The following section focuses on deriving a separable potential which is suitable for the two-body interactions of neutral atoms, i.e., van der Waals forces.

D. Separable potentials for van der Waals pairwise interactions

In order to study the universal aspects of the three-body spectrum of bosonic gases it is necessary to focus on the two-body interactions which govern the collisional behavior of ultracold gaseous matter. More specifically, it is well known that neutral bosonic atoms at large separation distances experience an attractive van der Waals type of force which asymptotically vanishes as $\sim -1/r^6$. Note that we ignore the Casimir-Polder modification due to retardation (Casimir and Polder, 1948), which modifies this at very long range but is largely irrelevant to the energy scale of interest here. This particular type of interaction potential imprints universal features onto the corresponding wave function (Gao, 1998; Flambaum, Gribakin, and Harabati, 1999) which becomes manifested in the spectra of three interacting bosons.

However, as shown in the preceding Sec. III.C.3, the Faddeev equations are best simplified by using the separable potential approach. Thus it is of major interest to construct a separable potential which encapsulates the main features of the van der Waals forces. Naidon, Endo, and Ueda (2014a, 2014b) showed that such a potential can be derived simply by using the analytically known *zero-energy* wave function of two particles in the presence of the van der Waals potential (Flambaum, Gribakin, and Harabati, 1999). Namely, the zero-energy two-body wave function for van der Waals interaction is given by the following relation:

$$\begin{aligned} \phi(r) = & \Gamma\left(\frac{5}{4}\right) \sqrt{\frac{r}{\ell_{\text{vdW}}}} J_{1/4}\left(2\frac{\ell_{\text{vdW}}^2}{r^2}\right) \\ & - \frac{\ell_{\text{vdW}}}{a_s} \Gamma\left(\frac{3}{4}\right) \sqrt{\frac{r}{\ell_{\text{vdW}}}} J_{-1/4}\left(2\frac{\ell_{\text{vdW}}^2}{r^2}\right), \end{aligned} \quad (54)$$

where a_s is the s -wave scattering length, and $\ell_{\text{vdW}} = \frac{1}{2}(mC_6/\hbar^2)^{1/4}$ is the van der Waals length scale with C_6 the dispersion coefficient. The quantities $\Gamma(\cdot)$ and $J_{\pm 1/4}(\cdot)$ represent the gamma and Bessel functions, respectively.

Figure 6 depicts the wave function in Eq. (54) for an s -wave scattering length $a_s = 50\ell_{\text{vdW}}$. At short distances the two-body wave function oscillates fast enough which in essence reflects the fact that the van der Waals potential contains many two-body bound states. At large distances the wave function of Eq. (54) obtains the form $\phi(r) \rightarrow 1 - r/a_s$. It is evident that a separable potential based on the two-body wave function as well as effective range effects due to the short-range oscillatory part of $\phi(r)$. The latter is of particular importance since Naidon, Endo, and Ueda (2014a, 2014b) demonstrated that the universality of the three-body parameter of the Efimov states relies exactly on the short-range oscillatory part of the two-body wave function. The Yamaguchi potential from Eq. (49) is adopted, where the χ function in the momentum space is defined by

$$\chi(q_1) = 1 - q_1 \int_0^\infty dr \left[1 - \frac{r}{a_s} - \phi(r) \right] \sin(q_1 r), \quad (55)$$

where $\phi(r)$ is the zero-energy two-body rescaled radial wave function [see Eq. (54)]. Note that the argument of the χ form factor depends only on the magnitude of the vector \mathbf{q}_1 due to the s -wave character of the wave function. The strength λ of the Yamaguchi potential is determined by

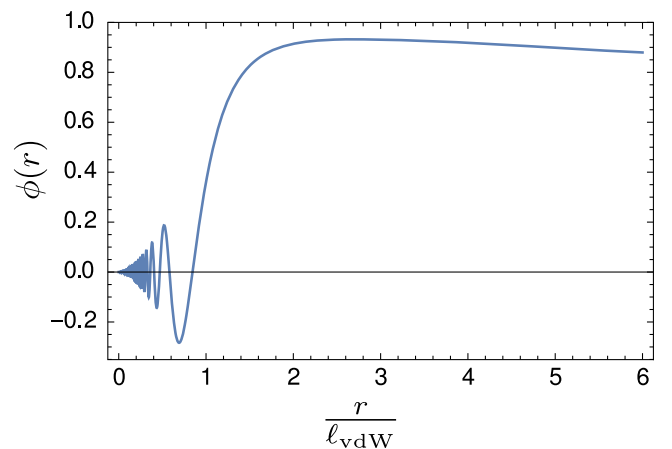


FIG. 6. The two-body zero-energy wave function $\phi(r)$ for the van der Waals potential as a function of the scaled interparticle distance r/ℓ_{vdW} , for an s -wave scattering length $a_s = 50\ell_{\text{vdW}}$. Note that ℓ_{vdW} denotes the van der Waals length scale defined in the text.

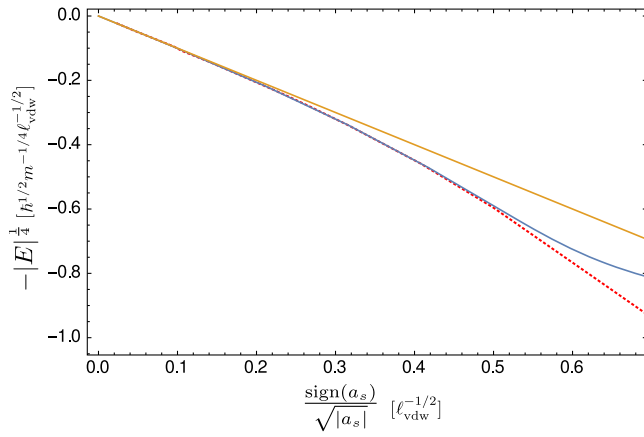


FIG. 7. The two-body binding energy as a function of the s -wave scattering length. The orange curve (top) refers to the universal dimer energy, the solid blue line (bottom) indicates the effective range theory for van der Waals interactions, and the dotted red curve denotes the binding energy within the separable potential approximation.

$$\lambda = \left[-\frac{1}{4\pi a_s} + \frac{1}{2\pi^2} \int_0^\infty dq_1 |\chi(q_1)|^2 \right]^{-1}. \quad (56)$$

Substitution of Eqs. (55) and (56) for the nonlocal interaction into Eq. (49) specifies a separable potential which mimics a van der Waals interaction between two neutral atoms. Namely, the van der Waals separable potential in the momentum space reads

$$\langle \mathbf{q}_1 | V_1 | \mathbf{q}_1' \rangle = \frac{\chi(q_1)\chi(q_1')}{m/4\pi a_s - (m/2\pi^2) \int_0^\infty dq_1 |\chi(q_1)|^2}. \quad (57)$$

As an example, Fig. 7 illustrates the binding energies versus the s -wave scattering length a_s . The two-body dimer energies within the separable potential approximation [see Eq. (57)] (dotted red line) are compared with the effective range theory of van der Waals interactions given by Flambaum, Gribakin, and Harabati (1999) (solid blue line, bottom). The solid orange line (top) indicates the universal dimer energies. Evidently, Fig. 7 depicts that the separable potential introduced in Eq. (57) captures the essential two-body physics beyond the effective range approximation.

E. The Efimov spectrum and its universal aspects

This section focuses on the impact of van der Waals forces on the Efimov spectrum of three identical s -wave-interacting bosons, the typical situation for three ultracold atoms but irrelevant for the few-nucleon problem. In particular, the reduced Faddeev equation (44) is numerically solved within the separable potential approximation. The separable potential is constructed according to the prescription given in Sec. III.D. Specifically, use of the potential in Eq. (57) ensures that it contains all the relevant zero-energy information about the van der Waals potential. Under these considerations, Fig. 8 depicts the Efimov spectrum of three neutral atoms as a function of the s -wave scattering length. In particular, the blue curve (bottom)

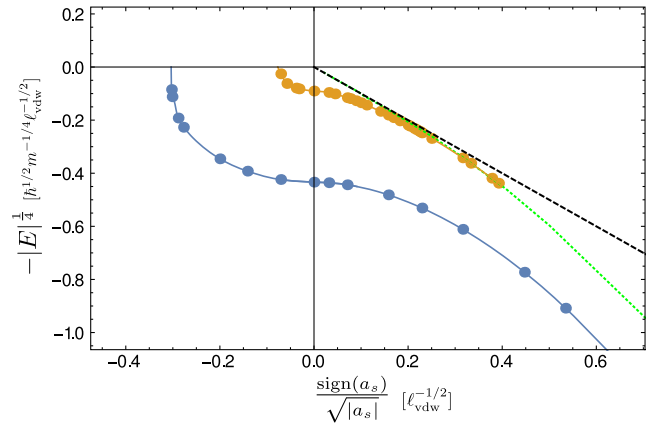


FIG. 8. The Efimov spectrum for the ground state (blue line and dots, bottom) and the first excited (orange line and dots, top) three-body state. The dashed black line is the universal dimer energies. The dotted green curve refers to the dimer binding energies calculated within the separable van der Waals potential approach.

and dots indicate the ground Efimov trimer state. The orange dots and curve (top) denote the first excited state. The dashed black curve refers to the universal dimer threshold, i.e., $E = -\hbar^2/m a_s^2$, whereas the dotted green curve corresponds to the two-body binding energies given for the potential in Eq. (57). Deeply in the regime of unitarity, namely, $|a_s| \rightarrow \infty$, the trimer energies for the ground and first excited states are $E_1 = 0.035338\ell_{vdW}^{-2}$ and $E_2 = 6.6806 \times 10^{-5}\ell_{vdW}^{-2}$, respectively, or in wave vectors we have that $\kappa_1 = 0.1879\ell_{vdW}^{-1}$ and $\kappa_2 = 0.00817\ell_{vdW}^{-1}$. For the first two κ wave vectors a scaling factor is obtained which is equal to $\kappa_1/\kappa_2 = 22.9988$. The latter deviates from the universal scaling law obtained within the zero-range approximation which is given by $\kappa_1^{ZR}/\kappa_2^{ZR} = 22.6944$. This discrepancy between the van der Waals approach and the zero-range approximation can be attributed to the fact that the latter method completely neglects effective range corrections. Specifically, the ground Efimov state is strongly influenced by finite-range effects in the two-body interaction potentials (Ji *et al.*, 2015). Note that the value obtained for κ_0 is in reasonable agreement within 16% with the corresponding calculation in Wang, D’Incao, Esry, and Greene (2012), which was based on a local position space van der Waals interaction. More specifically, for a hard-core van der Waals potential tail Wang, D’Incao, Esry, and Greene (2012) obtained the value $\kappa_0 = 0.226(2)\ell_{vdW}^{-1}$ at unitarity for the ground Efimov state.

Away from unitarity and for negative values of the scattering length, Fig. 8 shows that the trimer states cross the three-body threshold and become resonances in the three particle scattering continuum. In particular, the ground state crosses the threshold at $a_-^{(1)} = -10.849\ell_{vdW}$, whereas the first excited Efimov trimer merges with the three-body continuum at $a_-^{(2)} = -169.199\ell_{vdW}$. Note that the $a_-^{(1)}$ for the ground Efimov state is in good agreement with the hyperspherical approach employed by Wang, D’Incao, Esry, and Greene (2012). More specifically, Wang, D’Incao, Esry, and Greene (2012) for a hard-core van der Waals potential tail obtained the

value $a_{-}^{(1)} = -9.73(3)\ell_{\text{vdW}}$ for the ground Efimov state. In addition, the Naidon *et al.* model result agrees well with the corresponding experimental values, i.e., $a_{-}^{(1)} = -9.1\ell_{\text{vdW}}$ (Ferlandi *et al.*, 2011). Remarkably, the separable potential model presented by Naidon, Endo, and Ueda (2014a, 2014b) reproduced the universal features of the Efimov spectrum without utilizing any auxiliary parameter of the type that is needed within the zero-range approximation. Recall that the three-body spectrum for the Efimov effect is not bounded from below in the zero-range approximation; thus an additional parameter (three-body parameter) is employed in order to properly define the “ground Efimov state.” In the van der Waals separable potential model the auxiliary parameter becomes unnecessary due to the fact that the potential itself describes not only the asymptotic behavior of the two-body wave function but also its behavior at short distances which oscillates rapidly. Indeed, the fast oscillations of the two-body wave function in regions of the three-body configuration space where two particles approach each other translates into an effective repulsive hyperradial barrier, which in return suppresses the probability to find three bosons at distances less than $R \sim 2\ell_{\text{vdW}}$. This suppression effect was initially understood by Wang, D’Incao, Esry, and Greene (2012) using the hyperspherical approach where the steep attraction of the van der Waals forces leads to an effective three-body potential barrier at this somewhat surprisingly large hyperradius.

In order to illustrate this point from the reduced Faddeev equation in Eq. (49) the three-body wave function is first obtained in the momentum representation at $a_{-}^{(1)}$. Then following a Fourier transformation the corresponding configuration space three-body wave function is expressed in hyperspherical coordinates. After integrating the density over all the hyperangles α , taking the square root and applying the hyperradius kinetic operator to the resulting hyperradial wave function, an effective potential is obtained as a function of the hyperradius R . This effective potential is compared with the corresponding adiabatic potential curve which contains the diagonal correction from the diagonal nonadiabatic coupling term Q_{00} . Figure 9 compares the resulting implied hyperradial potential curve from Naidon, Endo, and Ueda (2014b) with the direct adiabatic hyperspherical solution from Wang, D’Incao, Esry, and Greene (2012), showing good general agreement. The dotted gray curve illustrates the asymptotic $-R^{-2}$ Efimov potential curve at unitarity for comparison. While the effective potential curve possesses some additional structure, Naidon, Endo, and Ueda (2014b) stated that this structure is an artifact which mainly arises from the oscillatory behavior of the Faddeev three-body wave function.

F. Efimov states in homonuclear systems

1. ${}^6\text{Li}$

Ultracold gases of fermionic ${}^6\text{Li}$ have been the object of different studies about Efimov physics and universality in three-body physics (Ottensstein *et al.*, 2008; Huckans *et al.*, 2009; Wenz *et al.*, 2009; Williams *et al.*, 2009; Lompe, Ottensstein, Serwane, Viering *et al.*, 2010; Nakajima *et al.*, 2010, 2011). It should be pointed out that it is a bit of a stretch to include the ${}^6\text{Li}$ system in our discussion of the Efimov

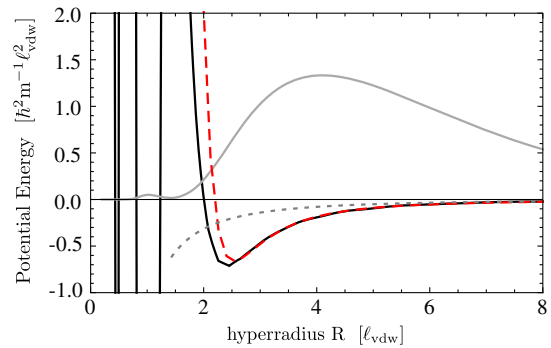


FIG. 9. The solid gray curve depicts the three-body Faddeev wave function in arbitrary units within the separable potential approach as a function of the hyperradius. The dashed red line corresponds to the hyperspherical potential curve including the diagonal adiabatic correction term Q_{00} , while the dotted gray curve indicates the asymptotic Efimov potential curve at unitarity. The solid black curve indicates the effective potential implied by the Faddeev equation solution determined within the separable potential approximation. Adapted from Naidon, Endo, and Ueda, 2014b.

effect for three identical bosonic atoms. Owing to the fermionic nature of ${}^6\text{Li}$ there is no s -wave scattering between atoms in identical spin substates, but atoms in different substates do have an s -wave scattering length. The studies just quoted have in fact considered atoms in three distinguishable substates, but unlike the case of three identical bosons, the three interparticle scattering lengths are in general different in the ${}^6\text{Li}$ system. However, they are all large and negative and therefore the system can be approximately mapped onto and compared with an Efimov system with three identical bosons in identical spin substates. In the following discussion, it should be kept in mind that this mapping is an approximation. Wenz *et al.* (2009) argued that one conjectured mapping, a definition of an effective “homonuclear” scattering length a_{ave} that applies when all three interspecies scattering lengths are large and negative, is

$$a_{\text{ave}}^4 \equiv \frac{1}{3}(a_{12}^2 a_{23}^2 + a_{13}^2 a_{23}^2 + a_{12}^2 a_{13}^2). \quad (58)$$

Nevertheless, quantities in Efimov physics such as the loss to deeply bound dimers and the three-body parameter should more rigorously be understood to depend in general on all three separate scattering lengths for a fermionic atom such as ${}^6\text{Li}$, i.e., on a_{12} , a_{23} , and a_{13} . In general, many of the experimental investigations have relied upon rf techniques for the identification of Efimov trimers. These methods employ rf pulses to form different Efimov states, which are detected as atom loss, thus leading to the characterization of their binding energies (Wenz *et al.*, 2009; Lompe, Ottensstein, Serwane, Viering *et al.*, 2010; Nakajima *et al.*, 2010, 2011). The measured trimer energies show a clear dependence on the applied magnetic field close to the two-body Feshbach resonances, which has been viewed as evidence for deviations from Efimov’s universal three-body physics scenario. In particular, the geometric scaling factor $\lambda = 22.7$ is not observed between successive resonances, and this has been

TABLE I. Fitting parameters to a universal theory obtained by measuring the three-body loss coefficient in ${}^7\text{Li}$. From [Gross *et al.*, 2010](#).

m_F	$a_+^{(1)} (a_0)$	$-a_-^{(1)} (a_0)$	$ a_-^{(1)} /\ell_{\text{vdW}}$
0	243 ± 35	264 ± 11	8.52 ± 0.35
+1	247 ± 12	268 ± 12	8.65 ± 0.39

interpreted as a magnetic field dependence of the three-body parameter.

The apparent nonuniversality of ${}^6\text{Li}$ has been an open question in the last decade, leading two different nonuniversal models beyond nonuniversal two-body interactions ([Nakajima *et al.*, 2010](#)). However, ([Huang, O'Hara *et al.* \(2014\)](#)) showed that accounting for a realistic two-body energy-dependent scattering length and taking into account finite temperature effects the three-body parameter for ${}^6\text{Li}$ turns out to be $a_-^{(1)}/\ell_{\text{vdW}} = -7.11 \pm 0.6$ which is very similar to the results obtained for identical bosons in [Tables I and II](#). Moreover, the geometric scaling factor shows a 10% deviation with respect to $\lambda = 22.7$, the universal expected value.

2. ${}^7\text{Li}$

The Efimov physics in bosonic ${}^7\text{Li}$ has been extensively studied through characterizations of maxima and minima of the three-body loss coefficient ([Gross *et al.*, 2009, 2010, 2011](#); [Pollack, Dries, and Hulet, 2009](#); [Machtey, Kessler, and Khaykovich, 2012](#); [Dyke, Pollack, and Hulet, 2013](#)), as well as using radio-frequency fields to measure the binding energies of weakly bound trimers ([Machtey *et al.*, 2012](#)). In particular, the Rice group identified the ground Efimov state for ${}^7\text{Li}$ in the $|m_F = 1\rangle$ hyperfine state as a resonance in the three-body loss coefficient for $a < 0$. An initial suggestion by [Pollack, Dries, and Hulet \(2009\)](#) that they had also observed the first excited Efimov resonance $a_-^{(2)}$ was later attributed to a calibration error. The recalibration, published in [Dyke, Pollack, and Hulet \(2013\)](#), also corrected the position of the first Efimov resonance to $a_-^{(1)} = -252 \pm 10$. Efimov physics was also observed on the $a > 0$ branch of the spectrum as the expected minima in the three-body loss

TABLE II. Experimentally determined three-body parameter a_- for different Feshbach resonances and spin states m_F in ${}^{39}\text{K}$. R^* represents the intrinsic length scale and associated with it, the resonance strength s_{res} . The value for the three-body parameter as a function of the van der Waals length $\ell_{\text{vdW}} = 64.49 a_0$ is also reported, as well as the initial temperature T , which implies a saturation limit of the three-body recombination rate because the S matrix is unitary. From [Roy *et al.*, 2013](#).

m_F	$R^* (a_0)$	s_{res}	$-a_-^{(1)} (a_0)$	$ a_-^{(1)} /\ell_{\text{vdW}}$	T (nK)
0	22	2.8	640 ± 100	10.0 ± 1.6	50 ± 5
0	456	0.14	950 ± 250	14.7 ± 3.9	330 ± 30
0	556	0.11	950 ± 150	14.7 ± 2.3	400 ± 80
+1	22	2.8	690 ± 40	10.7 ± 0.6	90 ± 6
-1	23	2.6	830 ± 140	12.9 ± 2.2	120 ± 10
-1	24	2.5	640 ± 90	10.0 ± 1.4	20 ± 7
-1	59	1.1	730 ± 120	11.3 ± 1.9	40 ± 5

coefficient ([Pollack, Dries, and Hulet, 2009](#)), yielding $a_+^{(1)} = 89 \pm 4$ and $a_+^{(2)} = 1420 \pm 100$ when the recalibration of [Dyke, Pollack, and Hulet \(2013\)](#) was applied. The ratio $a_+^{(2)}/a_+^{(1)} = 16 \pm 2$ deviates appreciably from the expected universal ratio of 22.7 ([Esry, Greene, and Burke, 1999](#); [Nielsen and Macek, 1999](#)), but this level of deviation for the first two Efimov features is not unexpected, based on theoretical calculations.

Similar results for the maxima of the three-body loss rate were obtained by [Gross *et al.* \(2009, 2010, 2011\)](#) for two different hyperfine states $|m_F = 1\rangle$ and $|m_F = 0\rangle$ as shown in [Table I](#). However, different results for $a_+^{(1)}$ in comparison with [Pollack, Dries, and Hulet \(2009\)](#) were obtained as displayed in [Table I](#). This discrepancy for $a_+^{(1)}$ has been explained as a distinct magnetic field-scattering length conversion through a different characterization of the same Feshbach resonance ([Gross *et al.*, 2010](#)). In [Table I](#) the universal character is also observed for the three-body parameter $a_-^{(1)}$ in terms of the van der Waals length ℓ_{vdW} for ${}^7\text{Li}$ - ${}^7\text{Li}$. In particular, the values obtained for $a_-^{(1)}/\ell_{\text{vdW}}$ are very similar to the values observed in cesium ([Berninger *et al.*, 2011](#)), rubidium ([Wild *et al.*, 2012](#)), and potassium ([Roy *et al.*, 2013](#)).

3. ${}^{39}\text{K}$

The study of Efimov states in bosonic ${}^{39}\text{K}$ at ultracold temperatures was developed mainly by the LENS group ([Zaccanti *et al.*, 2009](#); [Roy *et al.*, 2013](#)). In particular, the study of [Roy *et al.* \(2013\)](#) is a remarkable exploration of the $a_-^{(1)}$ three-body parameter universality, even including narrow Feshbach resonances. This study was carried out by employing different spin states m_F , as well as different Feshbach resonances in an ultracold gas of ${}^{39}\text{K}$, some showing open-channel dominance while others are narrower closed-channel-dominated resonances.

Resonances with a small resonance strength s_{res} ([Chin *et al.*, 2010](#)), i.e., narrow resonances, have an intrinsic length scale $R^* = \hbar^2/m a_{\text{bg}} \delta\mu$ ([Chin *et al.*, 2010](#)), where a_{bg} represents the background scattering length, m is the reduced mass, and $\delta\mu$ is the change in the magnetic moment between the initial and final states. Such a scenario predicted that the Efimov physics would be dominated by the intrinsic length associated with the resonance R^* , in particular, $a_-^{(1)} = -12.90R^*$ ([Petrov, 2004](#); [Gogolin, Mora, and Egger, 2008](#); [Mora, Gogolin, and Egger, 2011](#)). However, the experimental work of [Roy *et al.* \(2013\)](#) revealed a completely different behavior, as shown in [Table II](#), where the three-body parameter $|a_-^{(1)}|/\ell_{\text{vdW}} \sim 10$, which turns out to be very similar to the experimental and theoretical values for the case of broad two-body resonances ([Berninger *et al.*, 2011](#); [Wang, D'Incao, Wang, and Greene, 2012](#); [Naidon, Endo, and Ueda, 2014a](#)), i.e., $|a_-^{(1)}|/\ell_{\text{vdW}} = 9.5$. This striking result implies that the intrinsic length scale associated with a narrow resonance apparently plays no role in the determination of the three-body parameter. Thus, for systems with long-range dominant van der Waals interactions, the three-body parameter seems to be universal.

4. ^{85}Rb

The study of Tan's contact in an ultracold gas of ^{85}Rb was realized by Wild *et al.* (2012). In particular, the two-body and three-body contacts were determined, as well as the three-body recombination rate constant, by varying the two-body scattering length in a sweep of the magnetic field through a Feshbach resonance. The two-body contact is an extensive thermodynamic magnitude proportional to the derivative of the internal energy of the ultracold gas with respect to the scattering length (Tan, 2008a, 2008b, 2008c; Combescot, Alzetto, and Leyronas, 2009; Werner, Tarruell, and Castin, 2009; Schakel, 2010), i.e., $C_2 \propto dE/da$. The three-body contact C_3 is defined in terms of the derivative of the internal energy with respect to the three-body parameter $C_3 \propto dE/da_-$ (Braaten, Kang, and Platter, 2011; Castin and Werner, 2011).¹

The measurements of the three-body recombination rate were performed in dilute, ultracold, noncondensed clouds containing 1.5×10^5 atoms of ^{85}Rb at a temperature $T = 80$ nK. Then the magnetic field was varied through a Feshbach resonance in order to explore the region of negative scattering lengths. The obtained three-body recombination rate was fitted to the expected form for the Efimov three-body rate (Braaten and Hammer, 2006), obtaining $a_-^{(1)} = -(759 \pm 6)a_0$. The utilized fitting function is valid only at $T = 0$, and hence the fitting was realized for $a < 1/k_{\text{thermal}}$, where $k_{\text{thermal}} = \sqrt{2mk_B T}/\hbar$. The ratio between the measured three-body parameter and the van der Waals length is $a_-^{(1)}/\ell_{\text{vdW}} = -9.24 \pm 0.7$ (Wild *et al.*, 2012). This value is very similar to the reported values for ^{133}Cs (Kraemer *et al.*, 2006; Berninger *et al.*, 2011) and ^7Li (Gross *et al.*, 2009, 2010, 2011).

5. ^{133}Cs

The first experimental evidence of the Efimov effect was observed in an ultracold gas of ^{133}Cs (Kraemer *et al.*, 2006) by tuning the Cs-Cs scattering length through a Feshbach resonance and measuring the enhancement and decreases of the three-body loss coefficient for negative and positive scattering lengths, respectively. At the same time, this pioneering work readily showed the possibility of using ultracold physics in order to explore universal physics in few-body physics (Esry and Greene, 2006).

A few years after the observation of Efimov states in ultracold systems, Berninger *et al.* (2011) employed four different Feshbach resonances to study variations of the three-body parameter in an ultracold sample of ^{133}Cs . For these four observed Efimov resonances shown in Table III, the ratio of the three-body parameter $a_-^{(1)}$ to the van der Waals length ℓ_{vdW} is approximately equal for all the Feshbach resonances analyzed in the experiment to within only about 15% variations. More recently, Huang, O'Hara *et al.* (2014) realized an exhaustive experimental work on the negative scattering length branch of the two-body interaction in Cs,

¹Usually C_3 is defined in terms of the so-called three-body interaction parameter k_* (Braaten, Kang, and Platter, 2011; Castin and Werner, 2011), which is related to the three-body parameter by $a_-^{(1)} = (-1.56 \pm 5)/k_*$ (Braaten and Hammer, 2006).

TABLE III. Experimentally determined three-body parameter a_- for different Feshbach taken from Berninger *et al.* (2011). The positions of the Feshbach resonances employed are denoted by B_{res} , the three-body parameter as a function of the van der Waals length ($\ell_{\text{vdW}} = 101 a_0$) is reported, and finally η_- is a nonuniversal quantity that reflects the decay into deeply bound diatomic states (Wenz *et al.*, 2009).

B_{res} (G)	$ a_-^{(1)} /\ell_{\text{vdW}}$	η_-
7.56 ± 0.17	8.63 ± 0.22	0.10 ± 0.03
553.30 ± 0.4	10.19 ± 0.57	0.12 ± 0.01
554.71 ± 0.80	9.48 ± 0.79	0.19 ± 0.02
853.07 ± 0.56	9.45 ± 0.28	0.08 ± 0.01

confirming the universality of the Efimov scaling by seeing for the first time two successive Efimov resonances in a homonuclear system. Note, however, that more than one previous experiment has observed the expected Efimov scaling between two successive destructive interference Stückelberg minima $a_+^{(n)}$; it should be remembered that this behavior of three-body recombination at positive scattering lengths is a nonresonant manifestation of universal Efimov physics.

G. Four-body and five-body bound states and recombination resonances

Normally one views three-body recombination as a comparatively rare process in a dilute, ultracold gas. Typical Bose-Einstein condensates, for instance, can have lifetimes of the order of many seconds. Thus it may come as a surprise that higher order processes involving even more than three atoms simultaneously colliding in 3D can have even higher inelastic collision rates in some regimes of scattering length and density. There are theoretical predictions of this resonant N -body recombination (Mehta *et al.*, 2009; Wang and Esry, 2009; von Stecher, D'Incao, and Greene, 2009; Rittenhouse *et al.*, 2011; Blume, 2012b; Wang, Laing *et al.*, 2012; Blume and Yan, 2014; Yan and Blume, 2015), and a few experimental observations (Ferralino *et al.*, 2009b; Pollack, Dries, and Hulet, 2009; Dyke, Pollack, and Hulet, 2013; Zenesini *et al.*, 2013; Ulmanis, Häfner, Pires, Kuhnle *et al.*, 2016). While these usually cause difficulty for applications of interest with quantum degenerate gases or optical lattices, they can be especially interesting and informative to study in their own right, especially from a few-body point of view.

The four-body problem has challenged theorists for many years (Lazauskas and Carbonell, 2006) and is still of fundamental importance and interest. Extensive attention has been devoted to the question of whether there is an Efimov effect for four or more particles. For four or more identical particles, an early theoretical study by Amado and Greenwood (1973) concluded: "Hence the remarkable Efimov effect seems even more remarkably to be a property of the three-body system only." Later, however, a treatment by Kröger and Perne (1980) based on a separable potential model concluded that in certain parameter ranges there is an Efimov effect for four bosons. To add to this apparent discrepancy between the preceding two references mentioned, the possible existence of an Efimov effect in a 3D four-body system with three heavy particles and

one light particle was treated theoretically by Adhikari and Fonseca (1981) and later by Naus and Tjon (1987), reaching opposite conclusions (no and yes, respectively). A subsequent study by Adhikari, Frederico, and Goldman (1995) suggests that an additional short-range length (or high-momentum) scale is required for each successively larger number N of particles, in order to pin down the energy even of low-lying states. Another treatment by Yamashita *et al.* (2006) concluded that four-body bound states can exist in the universal regime of large atom-atom scattering lengths, but they will normally not be fixed in energy by two-body and three-body physics alone and will require an independent four-body parameter. This conclusion was supported by a later study as well, namely, Hadizadeh *et al.* (2011).

Based on four-identical boson bound state calculations using low-energy effective field theory, it was conjectured by Platter, Hammer, and Meißner (2004) and Hammer and Platter (2007) that there should be two four-boson bound states at unitarity lying at energies between each successive pair of Efimov trimer energies. These studies suggested, in apparent disagreement with Yamashita *et al.* (2006), that the energies are largely fixed by the three-body parameter, and at least to a good approximation, this would mean that no additional four-body parameter is needed. A four-body hyperspherical calculation was carried out (von Stecher, D’Incao, and Greene, 2009) that was based on the use of correlated Gaussian basis functions (Suzuki and Varga, 1998) adapted to the adiabatic hyperspherical representation (von Stecher and Greene, 2009; Rakshit and Blume, 2012; Mitroy *et al.*, 2013; Daily and Greene, 2014). Using that method, D’Incao, von Stecher, and Greene (2009), Mehta *et al.* (2009), Wang and Esry (2009), and von Stecher, D’Incao, and Greene (2009) gave supporting evidence to that conjecture and advanced the theory to the point where detailed predictions could be made of four-body recombination rate coefficients and resonance positions. In the universal limit, for instance, theory predicted (von Stecher, D’Incao, and Greene, 2009) that the two-body scattering lengths, where four-boson resonances would be observable as zero-energy recombination resonances, should be at the following values of the boson-boson scattering length: $a_{4B,1}^- \approx 0.43a_{4B,1}^{(1)}$ and $a_{4B,2}^- \approx 0.9a_{4B,1}^{(1)}$. These have since been confirmed in experimental studies (Ferlandino *et al.*, 2009) of homonuclear recombination processes involving four or more free bosonic atoms, although von Stecher, D’Incao, and Greene (2009) pointed out that there was already some evidence for a four-body process in Kraemer *et al.* (2006). Exciting theoretical progress in developing a highly quantitative theoretical treatment was subsequently reported for four-body resonances and recombination by Deltuva (2010, 2011, 2012), in a momentum space treatment based on a separable two-body interaction, a treatment that does not utilize hyperspherical coordinates. One interesting aspect of those theoretical and experimental efforts is the suggested implication that no additional four-body parameter is needed to fix the universal behavior of four interacting identical bosons, as it appears to be fixed once the three-body parameter is known. The extent to which this remains true for interactions of much shorter range than van der Waals potentials remains an active topic of investigation.

These developments in turn spawn a fundamental question: Are the universal properties also fixed for five, six, seven, and even more bosonic particles once the three-body parameter is known? If the answer is yes, this is a crucial point that can greatly simplify the development of realistic many-body theories for interacting bosons. A number of studies (Blume and Greene, 2000; Yamashita, Fedorov, and Jensen, 2010; von Stecher, 2010, 2011; Gattobigio, Kievsky, and Viviani, 2012) bear directly on this question. In particular, von Stecher (2011) predicted that a universal resonance of five identical bosons should occur at zero energy when the two-body scattering length is equal to $a_{5B,1}^- \approx (0.65 \pm 0.01)a_{4B,1}^-$. That prediction was tested and confirmed experimentally by the Innsbruck group (Zenesini *et al.*, 2013); this study also compared a detailed theoretical and experimental estimate of the direct five-body recombination rate, apparently the first time a direct (i.e., nonstepwise) recombination process could be observed experimentally and computed theoretically. While this is suggestive of a general universality for all N -boson systems, recent work by Yan and Blume (2015) suggested that this may apply only to systems whose long-range two-body interaction is dominated by van der Waals interactions, as shorter range interacting systems apparently exhibit extensive variability in their N -boson binding energies at unitarity (Yamashita, Fedorov, and Jensen, 2010).

Following the prediction by von Stecher (2010, 2011), the possible existence of a universal five-body recombination resonance was tested and confirmed by Zenesini *et al.* (2013). Figure 10 shows the comparison between theory and experiment, in a region that includes both a universal four-body resonance and a universal five-body resonance. These predictions of universal resonances observable in N -body recombination have been extended in some impressive recent calculations to even larger numbers of identical bosons by Gattobigio, Kievsky, and Viviani (2011, 2012).

H. Efimov states in heteronuclear mass-imbalanced systems

The existence of an infinite series of three-body bound states for resonant two-body interaction, as predicted by Efimov (1970), is not only present for homonuclear systems, as such universal three-body bound states should appear as well for heteronuclear systems (Efimov, 1973, 1979; D’Incao and Esry, 2006a, 2006b; Helfrich, Hammer, and Petrov, 2010; Wang, Wang *et al.*, 2012; Mikkelsen *et al.*, 2015; Petrov and Werner, 2015). In particular, in heteronuclear systems the mass-imbalanced nature of the three-body system preserves but modifies in an interesting way the discrete symmetry scaling characteristic of Efimov states, i.e., $a_{\underline{n}}^{(n)} = \lambda a_{\underline{n}}^{(n-1)}$, and hence preserving the universality of the three-body bound states. Most importantly, it influences the scaling factor λ , which depends on the masses of the three particles involved. In particular, λ gets smaller as the mass imbalance of the HHL system increases, which has sparked the study of highly mass-imbalanced systems as the best possible scenario for studying multiple excited Efimov states and hence exploring as deeply and unambiguously as possible the universal characteristics of such states. To date, heteronuclear Efimov states have been searched for in ^{41}K - ^{87}Rb - ^{87}Rb (Barontini *et al.*, 2009; Wacker *et al.*, 2016), ^{39}K - ^{87}Rb - ^{87}Rb (Wacker *et al.*, 2016),

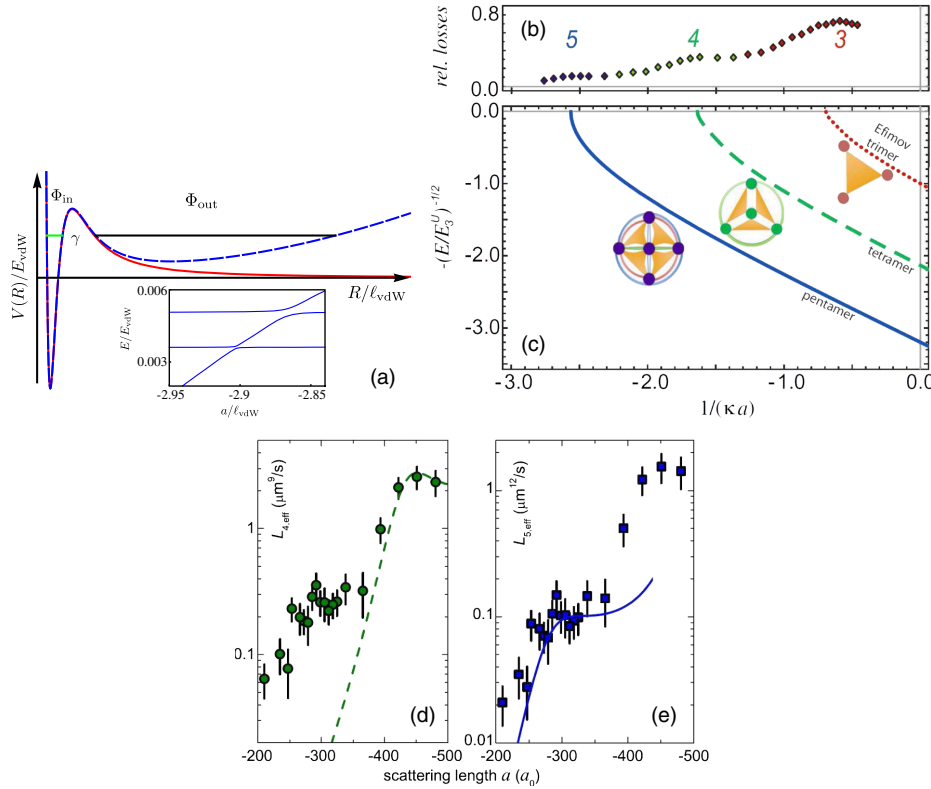


FIG. 10. (a) Schematic hyperspherical potential curve relevant to five-boson recombination when the two-body scattering length is negative, $a < 0$. The curve has also labeled the JWKB phases ϕ in the two classically allowed regions or R as well as the tunneling exponent that characterizes the region of negative incident kinetic energy. The inset shows energy levels for this five-boson system in a spherically symmetric harmonic trap, which has avoided crossings between inner and outer region states, whose strengths enable an estimate of the tunneling exponent γ that is important in obtaining the five-body recombination rate. (b) The experimental atom loss in a Cs gas vs the inverse two-body scattering length, rescaled by a characteristic wave number κ of the order of $2/\ell_{\text{vdW}}$. (c) The energies of trimer, tetramer, and pentamer states and the points where they merge into the zero-energy continuum. The measured loss rate coefficients vs a in units of Bohr radii, compared with theory that includes either (d) four-body recombination only $L_{4,\text{eff}}$ or else (e) five-body recombination only $L_{5,\text{eff}}$. From Zenesini *et al.*, 2013.

^{40}K - ^{87}Rb - ^{87}Rb (Bloom *et al.*, 2013), ^7Li - ^{87}Rb - ^{87}Rb (Maier *et al.*, 2015), and ^6Li - ^{133}Cs - ^{133}Cs (Tung *et al.*, 2014; Ulmanis *et al.*, 2015; Johansen *et al.*, 2016; Ulmanis, Häfner, Pires, Kuhnle *et al.*, 2016; Ulmanis, Häfner, Pires, Werner *et al.*, 2016).

The study of three-body losses in an ultracold mixture ^{41}K - ^{87}Rb performed by the LENS group led to the first claimed observation of heteronuclear Efimov states, specifically for ^{41}K - ^{87}Rb - ^{87}Rb and ^{41}K - ^{41}K - ^{87}Rb (Barontini *et al.*, 2009). In particular, a three-body parameter $a_{\text{tr}}^{(1)} = (-246 \pm 14)a_0$ was claimed to be observed for K-Rb-Rb. However, this claimed observation of an Efimov resonance has been questioned in the literature, in part because it is so far from the expected theoretical range for this system. Owing to the positive value of the Rb-Rb scattering length $a \sim 100a_0$, the first Efimov resonance is expected to occur in K-Rb-Rb at around $a_{\text{tr}}^{(1)}(\text{K-Rb}) \leq -30\,000$ a.u.. In a very recent follow-up by the Aarhus experimental group, they found that there is a two-body p -wave feature in the vicinity of the LENS group's claimed Efimov resonance ^{41}K - ^{87}Rb - ^{87}Rb , which adds doubts about the classification of that loss feature which does not fit universal expectations for the three-body system (Wang,

Wang *et al.*, 2012; Ulmanis, Häfner, Pires, Kuhnle *et al.*, 2016) Similarly, the K-K-Rb system is Efimov-unfavored (LLH) since it has two lighter and one heavier atom, and its first Efimov resonance was predicted to occur only for $a_{\text{tr}}^{(1)}(\text{K-Rb}) \leq -10^6$ a.u. Other experiments on potassium mixtures with ^{87}Rb with either the fermionic isotope ^{40}K (Bloom *et al.*, 2013) or the bosonic isotope ^{39}K (Wacker *et al.*, 2016) have failed to observe Efimov resonances at a reasonable value of the K-Rb scattering length, results which are more consistent with theoretical expectations. In particular, the JILA group (Bloom *et al.*, 2013) studied an ultracold Bose-Fermi mixture ^{40}K - ^{87}Rb , in which only ^{40}K - ^{87}Rb - ^{87}Rb supports Efimov resonances because ^{40}K - ^{40}K - ^{87}Rb is suppressed by spin statistics. The JILA group measured the three-body recombination rate with the aim of testing whether they could observe approximately the same Efimov resonant position as had been seen for ^{41}K - ^{87}Rb - ^{87}Rb (Barontini *et al.*, 2009). This expectation was of course fueled by the assumption of universality of the three-body parameter (Wang, Wang *et al.*, 2012). However, no trace of any Efimov resonances was observed at the expected two-body scattering length (Bloom *et al.*, 2013), consistent with our

current theoretical understanding (Wang, Wang *et al.*, 2012; Ulmanis, Häfner, Pires, Kuhnle *et al.*, 2016).

Recently an Efimov resonance for ${}^7\text{Li}-{}^{87}\text{Rb}-{}^{87}\text{Rb}$ was reported (Maier *et al.*, 2015) as a consequence of a first exploration of the negative Li-Rb scattering length in an ultracold mixture of bosonic ${}^7\text{Li}$ and ${}^{87}\text{Rb}$. The observed resonance is found at $a_{\perp}^{(1)} = (-1870 \pm 121)a_0$ in at least approximate agreement with the universal Efimov expectation (Wang, Wang *et al.*, 2012), and it should be stressed that it is vital to include in the analysis the correct heavy-heavy scattering length (Maier *et al.*, 2015). Note that with current experimental capabilities it is extremely difficult to reliably create and control atom-atom scattering lengths beyond about $10\,000a_0$ in absolute magnitude. Only one experiment to date, a heroic effort by the Innsbruck group in a homonuclear Cs gas (Huang, O'Hara *et al.*, 2014), has been able to measure Efimov physics at a scattering length as large and negative as $-22\,000a_0$.

The most convincing tests of universal Efimov scaling are for the highly mass-imbalanced case of ${}^6\text{Li}-{}^{133}\text{Cs}-{}^{133}\text{Cs}$, studied independently by the Heidelberg (Pires, Ulmanis *et al.*, 2014; Ulmanis *et al.*, 2015; Ulmanis, Häfner, Pires, Kuhnle *et al.*, 2016; Ulmanis, Häfner, Pires, Werner *et al.*, 2016; Häfner *et al.*, 2017) and Chicago groups (Tung *et al.*, 2014; Johansen *et al.*, 2016). Theoretically, the universal Efimov scaling factor for this system should be $\lambda = 4.88$ (D'Incao and Esry, 2006a; Wang, Wang *et al.*, 2012), which enables experiments to observe and characterize multiple resonances in a single Efimov series for the first time. As in many other approaches to Efimov physics with ultracold atoms, the Chicago and Heidelberg groups use a magnetic Fano-Feshbach resonance for Li-Cs to vary the two-body scattering length. The results for the observed Efimov resonances, characterized by the analysis of the maxima in the three-body loss coefficient, are shown in Table IV, where the three-body parameter reported by the Chicago and Heidelberg groups can be seen to agree approximately to within the error bars. Another interesting difference probed in the experiments by Ulmanis, Häfner, Pires, Kuhnle *et al.* (2016) is the

TABLE IV. Experimental Efimov resonances for ${}^6\text{Li}-{}^{133}\text{Cs}-{}^{133}\text{Cs}$, with the Li-Cs scattering lengths denoted here as $a_{\perp}^{(n)}$. For the spin states utilized in these experiments, the background Cs-Cs scattering length in this region of magnetic field near 843G is approximately in the range $-1600a_0 < a_{\text{CsCs}} < -1000a_0$. The maxima of the three-body loss rate occur at the indicated value $a_{\perp}^{(n)}$, where n stands for the ordering of the different associated Efimov states. The three-body parameter is denoted here as $a_{\perp}^{(1)}$. The discrete symmetry scaling factor for two successive Efimov states is denoted by λ . The Heidelberg group results of Ulmanis *et al.* (2015) are shown in the second and third columns, and the results of the Chicago group (Tung *et al.*, 2014) in the fourth and fifth columns. Note that the Heidelberg group also suggests a recalibration of the Chicago group's data in Table 2 of Ulmanis *et al.* (2015), but those results are not shown here.

n	$a_{\perp}^{(n)} (a_0)$	λ	$a_{\perp}^{(n)} (a_0)$	λ
1	-311 ± 3		-323 ± 8	
2	-1710 ± 70	5.48 ± 0.28	-1635 ± 60	5.1 ± 0.2
3	-8540 ± 2700	5.00 ± 1.8	-7850 ± 1100	4.8 ± 0.7

contrasting value of the first Efimov resonance depending on the sign of the Cs-Cs scattering length. For instance, when the Cs-Cs scattering length is large and negative as in the cases reported in Table IV, the first resonance occurs at a Li-Cs scattering length value equal to $a_{\perp}^{(1)} \approx -320$ a.u. But for a different range of magnetic fields where the Cs-Cs scattering length is positive [$a(\text{Cs} - \text{Cs}) \approx 200a_0$], the first resonance occurs at $a_{\perp}^{(1)} \approx -2000$ a.u. As argued by Ulmanis, Häfner, Pires, Kuhnle *et al.* (2016), this major difference can be understood qualitatively already in the zero-range theory, without invoking van der Waals interactions, although a full model including van der Waals finite-range interactions is needed to make the description quantitatively accurate. These experiments are of course extremely difficult, and we stress the importance of developing highly accurate two-body scattering models before undertaking the analysis of departures from expected universal behavior.

The prediction of Efimov and the universality of the three-body physics (Efimov, 1970, 1971) is strictly true in the case of two-body resonant interactions and assuming $T = 0$, since no consideration was given to the kinetic energy of the three-body system. A few studies have carried out the appropriate Boltzmann average needed to derive finite temperature predictions of the three-body recombination rate, as in Rem *et al.* (2013) and Petrov and Werner (2015). Thus, in realistic systems one would expect some deviations from Efimov's prediction. However, the experimental observations seem to indicate that most of the Efimov states are accurately universal.

I. Efimov and universal bound states for fermionic systems

It is well known that there is no Efimov effect for homonuclear trimers composed of identical fermions in a single intrinsic spin substate. This is easy to understand because the requirement of antisymmetry adds nodes to the spatial wave function and this raises the kinetic energy of the trimer internal degrees of freedom substantially. For a system of two heavy fermions of mass M in the same spin state and a lighter distinguishable particle of mass m , the nodal constraint of antisymmetry is weaker and some interesting predictions for this case have been presented by Kartavtsev and Malykh (2007, 2014). The Efimov effect emerges for this FFX system with divergent $F + X$ scattering length, provided the mass ratio is sufficiently large, namely, $M/m > 13.607$. For smaller mass ratios than this critical ratio just mentioned, one observes one or two universal states, usually denoted as “Kartavtsev-Malykh universal trimers,” but there is no true Efimov effect and the number of energy levels remains finite. Some level perturbations that can affect these universal trimer states have been identified by Safavi-Naini *et al.* (2013). For a detailed recent treatment that revises some of the conclusions for the range of mass ratios $M/m < 13.607$, see Kartavtsev and Malykh (2016).

The possibility of a four-particle Efimov effect is another intriguing prediction by Castin, Mora, and Pricoupenko (2010), with three heavier identical fermions of mass M and one lighter distinguishable particle of mass m . Specifically, they predict that only in the small mass ratio range $13.384 < M/m < 13.607$ should one be able to observe

the infinite number of energy levels converging geometrically to zero binding that characterizes Efimov physics. Recently [Bazak and Petrov \(2017\)](#) predicted a pure five-body Efimov effect, for a system of four heavy identical fermions and one distinguishable particle, again in a small range between $13.279 \pm 0.002 < M/m < 13.384$, based on a stochastic solution of the generalized STM equation ([Pricoupenko, 2011](#)), with techniques analogous to diffusion Monte Carlo (MC) methods. The study by [Bazak and Petrov \(2017\)](#) also predicted mass ratios where one expects universal five-body states in regimes where no true Efimov effect exists, and a conjecture that the $5 + 1$ hexamer and higher particle numbers will be qualitatively different rather than simply continuing the trend, a conjecture certainly deserving to be explored. This study agrees and improves on the accuracy of a prediction by [Blume \(2012b\)](#) that a universal $3 + 1$ tetramer should exist at a mass ratio around $M/m \geq 9.5$, with the new and improved computed ratio equal to $M/m \geq 8.862 \pm 1$.

J. Naturally occurring Efimov physics in the helium trimer

The study of helium clusters—their aggregation, formation, and collision dynamics—has been an active research topic in chemical physics, in particular, in the field of molecular beams ([Campargue, 2001](#)). Molecular beam experiments rely on the supersonic expansion of a chosen gas in vacuum, which induces the cooling of the different molecular degrees of freedom as the gas expands in the chamber. This cooling mechanism is due to inelastic collisions involving electronic, rotational, and vibrational degrees of freedom, and hence it strongly depends on the inelastic cross sections as well as the number of collisions through the density of the gas ([Zucrow and Hoffman, 1976](#); [Zhdanov, 2002](#); [Montero and Pérez-Ríos, 2014](#)). The diluteness of the gas as it moves away from the nozzle can be controlled by the initial conditions of the expansion: temperature, pressure, and mass flow, through the conservation of enthalpy and mass flow of the fluid. Therefore, any property or process related with the dynamics of the gas, such as cluster formation, could be controlled to some degree in those experiments. Using such methods,

[Schöllkopf and Toennies \(1994, 1996\)](#) experimentally observed the helium dimer and the ground state of the helium trimer.

Although the ground state ${}^4\text{He}_3$ was observed two decades ago, the first excited state of ${}^4\text{He}_3$, which has Efimov character, was not observed until recently ([Kunitski *et al.*, 2015](#)). Figure 11 summarizes both the key theoretical and experimental results for the system. This remarkably challenging experiment was performed by joining the technology of molecular beam experiments, atom interferometry, and modern ionization and detection techniques. In particular, very well-controlled nozzle conditions leading to a supersonic expansion of He, where He trimers were selected by means of matter-wave diffraction through a grating. Then all three atoms of the trimer are ionized by means of a strong ultrashort pulse, leading to the subsequent Coulomb explosion of the trimer compounds. The momenta of the ions after the Coulomb explosion were detected by cold target recoil ion momentum spectroscopy (COLTRIMS) ([Jagutzki *et al.*, 2002](#); [Ullrich *et al.*, 2003](#)), which allowed analysis of the reconstruction of the initial probability distribution of the trimer atom positions and thereby allowed a deduction of the trimer binding energy. In this way, [Kunitski *et al.* \(2015\)](#) studied the formation of two different He trimer states as functions of the pressure in the nozzle, leading to the first observation of the excited state of ${}^4\text{He}_3$.

The findings of [Kunitski *et al.* \(2015\)](#) revealed the geometry of the ground state and first excited state of the helium trimer. In particular, for the ground trimer state a unimodal radial distribution was observed for the atom-atom distance in the trimer, in relation to the expected equilateral geometry. However, for the first excited trimer state the radial distribution function shows a bimodal character, thus resembling an isosceles triangular geometry. These results demonstrate the Efimov character of the first excited state of the helium trimer. In particular, the obtained binding energy is 2.60 ± 0.2 mK in good agreement with recent theoretical predictions ([Hiyama and Kamimura, 2012](#); [Kunitski *et al.*, 2015](#)); however, the bimodal radial distribution deviates from what is expected from the universal Efimov predictions for resonant two-body

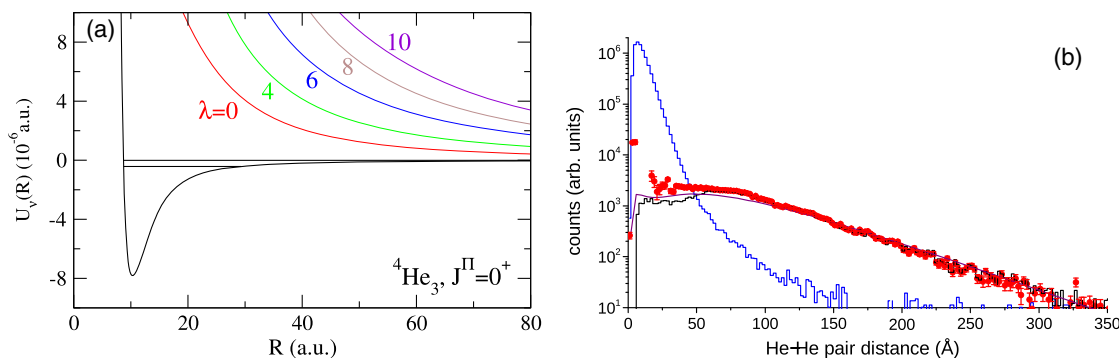


FIG. 11. (a) Adiabatic $J^\pi = 0^+$ hyperspherical potential curves, with the two bound state energies predicted for this symmetry drawn into the potentials. The higher energy of the two, which has an energy so small that it appears to coincide with $E = 0$, was predicted to be an observable Efimov state. From [Suno and Esry, 2008](#). (b) Experimentally measured pair distribution functions of the two helium trimer bound states, with a theory comparison for the more diffuse state that is concluded to be an Efimov state. This measurement used laser ionization followed by Coulomb explosion of the three resulting ions, with detection in a COLTRIMS apparatus. From [Kunitski *et al.*, 2015](#).

interaction at unitarity, which is not surprising in view of the finite value of the He-He scattering length (Blume, Greene, and Esry, 2000, 2014).

The most recent hyperspherical coordinate calculations of the helium trimer properties in the electronic ground state appear to be those of Suno and Esry (2008). Their $J^\pi = 0^+$ adiabatic potential energy curves obtained with an up to date potential surface, which includes three-body as well as realistic retarded two-body potential terms, are shown in Fig. 11. The energies drawn into the lowest potential curve are the two computed bound state energies, namely, -130.86 and -2.5882 mK. The more weakly bound of these is the one expected to have significant Efimov state character, and it is in fact so weakly bound that its energy is indistinguishable from $E = 0$ on the scale of Fig. 11.

IV. FEW-BODY PERSPECTIVES ON MANY-BODY SYSTEMS

There are multiple ways in which few-body physics is useful for understanding, interpreting, and predicting new many-body phenomena. The most obvious is through the development of detailed theoretical understanding of the microscopic processes involving two, three, four, or some cases even a handful more particles within a gas or lattice array of particles. The detailed studies previously described and other review articles (Köhler, Góral, and Julienne, 2006; Chin *et al.*, 2010; Wang, D’Incao, and Esry, 2013; Wang, Julienne, and Greene, 2015a) have focused largely on two-body phenomena such as Fano-Feshbach resonances, and on the three-body phenomena that arise such as Efimov

resonances in three-body recombination and related behavior such as Stückelberg interference minima. The initially surprising experimental result (Cubizolles *et al.*, 2003; Strecker, Partridge, and Hulet, 2003; Regal, Greiner, and Jin, 2004a) that large universal fermionic dimers have remarkably small losses despite their large size was understood theoretically by Petrov, Salomon, and Shlyapnikov (2005a, 2005b). This played a key role in stimulating experiments in the Bardeen-Cooper-Schrieffer (BCS)-BEC crossover problem and in triggering explorations of other phenomena in unitary Fermi gases. Figure 12 shows a later theoretical treatment of the two-component four-fermion system in hyperspherical coordinates, including the computed dimer-dimer scattering information. For instance, it has now become possible to map out an extremely accurate equation of state for unitary Fermi gases (Chevy *et al.*, 2011; Ku *et al.*, 2012).

Another way few-body theories have provided some useful perspectives on Bose-Einstein condensates and degenerate Fermi gases has simply been through applying the few-body toolkit and ideas, such as adiabatic hyperspherical potential curves, to the many-particle system directly. In some cases this is done by treating only a modest number of particles accurately, while in other cases the many-particle limit is examined but at a relatively crude level of approximation to estimate the many-particle potential energy curves.

Few-body physics also produces insight into systems of trapped atoms through the use of the idea of an artificially strong trap. The premise here is that frequently in a trapped quantum gas with thousands or even millions of atoms, the physical trap frequency might be only of the order of 10 Hz and determines only a largely irrelevant energy scale for the

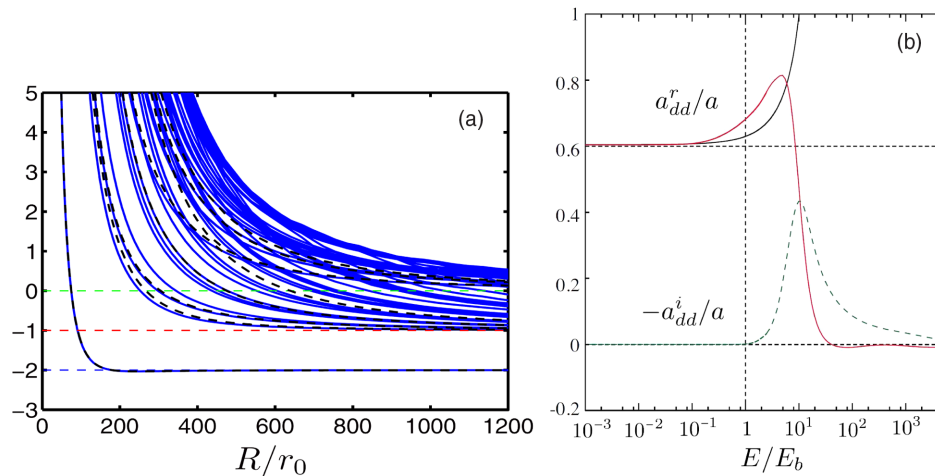


FIG. 12. (a) Adiabatic $J^\pi = 0^+$ four-fermion hyperspherical potential curves for two spin-up and two spin-down identical fermions with a large positive interspecies scattering length, i.e., on the BEC side of the BCS-BEC crossover problem. The dashed horizontal lines mark the fragmentation thresholds, the lowest of which represents the dissociation of two bound universal dimers ($FF' + FF'$), the next highest representing one bound dimer plus two free atoms ($FF' + F + F'$), and the highest which denotes the threshold energy $E = 0$ for complete four-body dissociation. Using these adiabatic potential energy curves and the nonadiabatic couplings, the elastic and inelastic collision properties could be computed for this system. From von Stecher and Greene, 2009. (b) The computed elastic a_{dd}^r and inelastic a_{dd}^i scattering lengths for collisions between two universal dimers, i.e., in an $FF' + FF'$ collision, shown in units of the two-body scattering length $a(F + F')$ as a function of energy measured in units of the dimer binding energy. Note the smallness of the inelastic (imaginary) scattering length, first understood theoretically by Petrov, Salomon, and Shlyapnikov (2005a, 2005b), which was crucial for understanding why the two-component Fermi gas has minimal losses close to unitarity (Cubizolles *et al.*, 2003; Strecker, Partridge, and Hulet, 2003; Regal, Greiner, and Jin, 2004a). These low losses were crucial in enabling the BCS-BEC crossover experiments to be successful and create long-lived quantum gases. From D’Incao, Rittenhouse *et al.*, 2009.

system. More relevant by far are the typical scale of interparticle interactions and the average kinetic energy or temperature, reflected in the separation of atoms Δr . The physical content of this separation length scale is sometimes referred to as the “Fermi wave number” $k_F = 2\pi/\Delta r$ even when the gas consists of some or even all bosonic particles. Then one can gain insight by treating only two, three, or four particles in an unphysical artificially tight “theoretical trap” designed to have a high frequency with particle separation Δr comparable to the Δr in the actual many-particle system. An example where this strategy enables a simple interpretation (Borca, Blume, and Greene, 2003) of a complicated many-body problem is the famous “atom-molecule” coherent oscillations or quantum beats observed in an ^{85}Rb experiment (Donley *et al.*, 2002), depicted in Fig. 13.

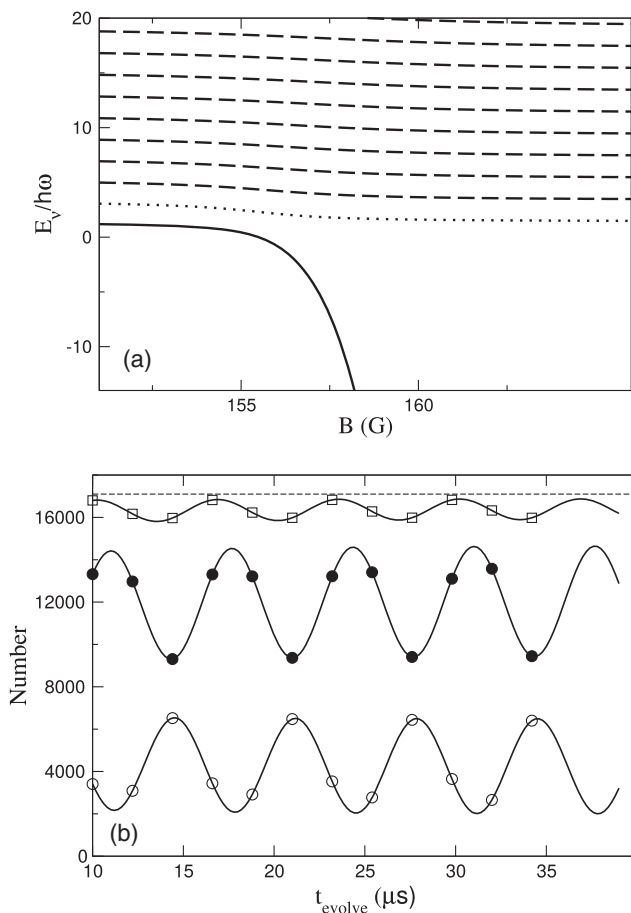


FIG. 13. (a) Two-body s -wave energy levels in ^{85}Rb are shown as a function of magnetic field near the 155 G Fano-Feshbach resonance that was used by Donley *et al.* (2002) to study quantum beats between atomic states of a quantum degenerate Rb gas and molecular states. (b) Calculated quantum beats reflecting interference between one pathway where a given pair of atoms remained atomic and another pathway where that pair of atoms was bound into a long-range universal dimer for a delay time T . These two-body calculations use an artificially tight trap ($\omega' = 2\pi$ kHz) whose peak density approximately equals the density of 17 100 atoms trapped in the actual experiment whose geometric mean trapping frequency was $\omega = 2\pi \times 12$ Hz. From Borca, Blume, and Greene, 2003.

A. Polaron physics attacked from a few-body viewpoint

When a slow electron moves inside a bulk material such as a polar crystal or helium liquid, it attracts other particles from the bulk and the entity behaves as a quasiparticle, as described in early studies by Fröhlich (1954) and Feynman (1955). Such a quasiparticle was denoted a polaron, and this term has been generalized to describe a more general situation in which an interaction-dressed minority particle moves in the field of other particles in a medium. An active field of research to this day, polarons have attracted extensive attention from experimental (Michaud and Sanche, 1987) as well as theoretical studies (Basak and Cohen, 1979; Fano and Stephens, 1986; Stephens and Fano, 1988) in condensed-matter physics. In recent years polaron physics has become a topic of great interest in the ultracold atomic physics community, owing to the promise of great control and observability. The few-body side of polaron physics has two major areas of interest. One aspect is to discern the details of a single quasiparticle in the many-body environment and the more advanced topic of interactions among two, three, or four quasiparticles, i.e., the effect of a many-body bosonic or fermionic bath of particles on the interactions, energy levels, and recombination of the quasiparticles (Bellotti *et al.*, 2016). The second area that has received extensive attention is the behavior of few-body analogs of a polaronic system, with small numbers of minority and majority particles, such as the HHL and HHHL and related problems discussed elsewhere in this review.

Polarons have received attention in ultracold atom experiments and theory over the past decade or so by Astrakharchik and Pitaevskii (2004), Cucchietti and Timmermans (2006), Kalas and Blume (2006), Bruderer, Bao, and Jaksch (2008), Bei-Bing and Shao-Long (2009), Schirotzek *et al.* (2009), Tempere *et al.* (2009), Catani *et al.* (2012), Kohstall *et al.* (2012), Koschorreck *et al.* (2012), Spethmann *et al.* (2012), Rath and Schmidt (2013), Scelle *et al.* (2013), Li and Das Sarma (2014), Grusdt *et al.* (2015), and Levinsen, Parish, and Bruun (2015) and recently, as in Hu *et al.* (2016) and Jørgensen *et al.* (2016). Some work has considered an impurity with internal degrees of freedom called an “angulon” which is a quasiparticle consisting of a rotating impurity dressed by the quantal many-body environment (Schmidt and Lemeshko, 2016; Lemeshko, 2017). To date the explorations have concentrated on the behavior of a single impurity in a BEC or degenerate Fermi gas (DFG), but a future few-body topic that is still in its infancy is the study of interactions among two or more impurities dressed by the many-body environment. An initial foray along those lines by Naidon (2016) treats two-body polaron-polaron interactions. We refer the reader to the review by Naidon and Endo (2017) and references therein.

B. Bose-Einstein condensates viewed in hyperspherical coordinates

In the Russian nuclear physics literature, a technique evolved during the 1960s and 1970s to treat the many-nucleon problem, which was referred to as the “ K -harmonic” theory. This treatment was based on a particularly simple approximation formulated in hyperspherical coordinates. The basic idea was to find the lowest grand angular momentum state, the

K -harmonic $|KQ\rangle$. This eigenfunction of hyperangular kinetic energy and various symmetry operators is usually an appropriately antisymmetrized linear combination of hyperspherical harmonics; they are constrained to obey the symmetries of the system such as the Pauli exclusion principle, definite parity, and so on. This approximation then uses this single harmonic to describe the hyperangular wave function of the system. When this technique is applied to the description of a single-component BEC, it is particularly simple because the K harmonic for this system is simply the state of vanishing grand angular momentum $K = 0$, which is a constant in the hyperangular space of any N -particle system. While the resulting wave function is not sufficiently realistic to describe the true short-range interactions that occur whenever any two particles approach each other, the use of the Fermi pseudopotential in the many-body Hamiltonian implies that the average energy of interaction can be approximately represented perturbatively (Bohn, Esry, and Greene, 1998). In our terminology today, we can view this as approximating the lowest adiabatic hyperangular eigenfunction as this K harmonic, after which perturbation theory can be applied to the interparticle interaction term in the Hamiltonian to determine the approximate ground state potential energy curve for the many-particle system, namely, $U_0(R)$; see Fig. 14. This treatment does a reasonable job of predicting the approximate maximum number of atoms that can exist in a harmonic trap when the scattering length is negative, beyond which the system undergoes a macroscopic collapse often referred to as the “Bosenova” (Bradley, Sacket, and Hulet, 1997; Donley *et al.*, 2001). More recently, the hyperspherical BEC theory has been extended via a renormalization technique to treat properties of the quantum degenerate Bose gas in the unitary limit $a \rightarrow \infty$ (Ding and Greene, 2017).

Since that simple study of Bohn, Esry, and Greene (1998), other studies have considered improvements of the hyperspherical BEC treatment, including generalizations to asymmetrical traps and attempts to better include the two-body correlation physics beyond the simplest mean-field approximations (Watson and McKinney, 1999; Kim and Zubarev, 2002; Kushibe *et al.*, 2004; Sorensen, Fedorov, and Jensen, 2004).

C. The unitary Bose gas

Based on what has been learned from studies of dilute Bose gas recombination theory and experiments, one expects it to be impossible to create a long-lived Bose-Einstein condensate in the unitary limit where $a \rightarrow \infty$. This conclusion is based on the fact that three-body losses are seen to scale with the scattering length overall as a^4 , aside from quantum resonance and interference factors. Nevertheless this is a fascinating limit, in part because it can test whether the recombination loss rates continue to scale as a^4 all the way to $a \rightarrow \infty$ and in part because the many-body behavior implied by the Gross-Pitaevskii equation looks so qualitatively different for large negative (infinitely attractive and immediate collapse) versus large positive scattering lengths (infinitely strong repulsion).

These questions have long been of theoretical interest (Cowell *et al.*, 2002; Radzihovsky, Weichman, and Park, 2008; Lee and Lee, 2010), and recently they have begun to receive experimental attention. One way to deal with the transient nature of any short-lived quantum gas is to perform the experiment as a “quench,” i.e., begin with a BEC at small positive scattering length and then suddenly ramp to the range of unitarity $a \rightarrow \infty$. A recent experiment at JILA by Makotyn *et al.* (2014) quickly stimulated extensive theoretical work (Hudson *et al.*, 2014; Jiang *et al.*, 2014; Laurent, Leyronas, and Chevy, 2014; Piatecki and Krauth, 2014; Rancon and Levin, 2014; Sykes *et al.*, 2014; Ancilotto *et al.*, 2015; Kira, 2015; Corson and Bohn, 2016; Jiang, Maki, and Zhou, 2016; Yin and Radzihovsky, 2016; Ding and Greene, 2017) to understand their main observations, which were the following.

(i) The a^4 scaling of three-body loss is no longer applicable at very large scattering lengths, i.e., when $na^3 \gg 1$ where n is the density. To understand this, Makotyn *et al.* (2014) defined a characteristic wave number of the system (analogous to the Fermi wave number) as $K \equiv (6\pi^2 n)^{1/3}$, which is comparable to the inverse of the average interparticle spacing. They proposed that in any formula involving the scattering length a , it should be viewed as saturating at a constant value of the order of $1/K$ as soon as you reach the regime $Ka \approx 1$. In other words, as soon as $a \rightarrow \infty$, it is no longer a relevant length

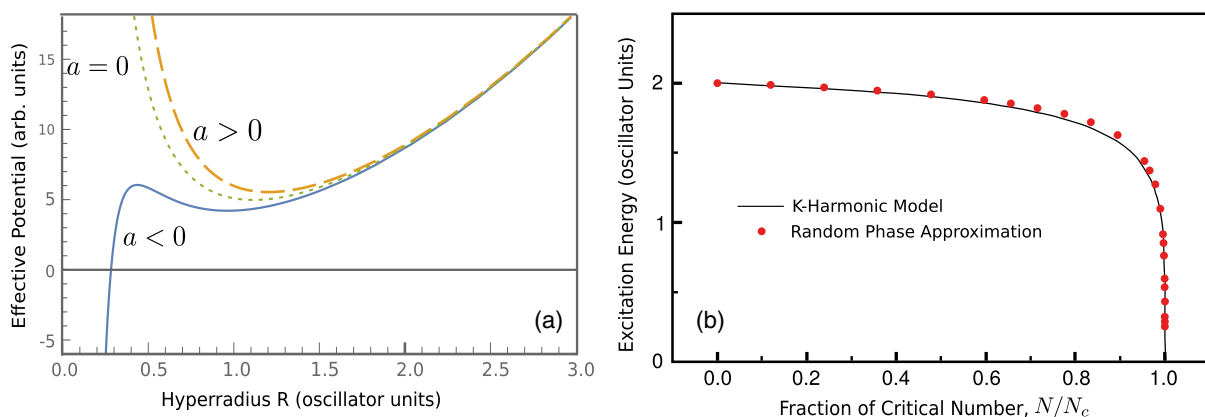


FIG. 14. (a) Adiabatic hyperspherical potential curves for an attractive BEC, a noninteracting BEC, and a repulsively interacting BEC. (b) Excitation energy calculated for an attractive ($a < 0$) BEC in the hyperspherical adiabatic theory, compared with the random phase approximation which is essentially identical to Bogoliubov theory. Adapted from Bohn, Esry, and Greene, 1998.

scale in the system, and the premise is that the interparticle spacing becomes the largest relevant scale instead. (ii) The momentum distribution of the atom cloud was measured as a function of time after the jump to unitarity, and it settled down to a quasistable distribution, which was the target of various many-body and few-body theory efforts to try to understand.

One of the main items of interest in this system, from a few-body physics perspective, is the saturation of losses at a value far smaller than would be expected from the zero-temperature a^4 scaling. An estimate (Sykes *et al.*, 2014) was made of the three-body rate coefficient. $L_3 \approx 3 \times 10^{-23} \text{ cm}^6/\text{s}$ is reasonably close (around half as large as) the measured value in the JILA experiment of Makotyn *et al.* (2014). This theoretical estimate is made using the few-body “artificial trap model” which considers only three atoms but places them in an artificially tight trap such that the atom density approximately matches the experimental average density, which was $\langle n \rangle = 5.5(3) \times 10^{12} \text{ cm}^{-3}$. As discussed by Sykes *et al.* (2014), one obtains somewhat poorer quantitative agreement but still the correct order of magnitude for the loss rate at unitarity by replacing the value of a in the universal three-body loss rate formulas by $1/K$ as defined above in terms of the average density in the gas. Other experimental studies of the unitary Bose gas that have focused on the three-body loss rate include Fletcher *et al.* (2013), Rem *et al.* (2013), and Eismann *et al.* (2016). And another intriguing “universality limit” where the scattering length is no longer a relevant length scale is the opposite limit $a \approx 0$, recently explored experimentally with some phenomenological conjectures by Shotan *et al.* (2014).

D. Two-component Fermi gases and the BCS-BEC crossover problem

One fascinating type of dilute quantum gas experiment consists of distinguishable fermions, either in two or more spin substates or else composed of two or more types of distinguishable particles. This system received extensive attention from many theoretical (Hui *et al.*, 2004; Hu, Liu, and Drummond, 2006; Hu, Drummond, and Liu, 2007; Yin and Blume, 2015; Yan and Blume, 2016) and experimental groups (Houbiers *et al.*, 1997; DeMarco and Jin, 1999; Zwierlein *et al.*, 2004, 2006; Schunck *et al.*, 2005; Ketterle and Zwierlein, 2008; Ku *et al.*, 2012) with particularly keen interest in the community around a decade ago. Conceptually, one typically starts the experiment by forming a two-component degenerate Fermi gas without interactions, i.e., with vanishing scattering length between the two component atoms. Interactions between like fermions can usually be ignored, unless one is close to a p -wave Fano-Feshbach resonance. Now one increases the attraction by making the scattering length a between unlike atoms small and negative, i.e., $-1 \ll k_f a < 0$. This is the regime usually referred to as the Bardeen-Cooper-Schrieffer region, because the weak attraction tends to cause pairing. These BCS-type pairs are sometimes referred to as “preformed pairs” because the pairing occurs before the attraction is strong enough to form true isolated dimer bound states. Of course true molecular bound states can be formed only after the attraction has increased beyond $k_f a < -1$, to infinite a and then a is large and positive which allows true universal dimers to form with

binding energy $1/2\mu a^2$. At that point, when the gas has large and positive a , the quantum gas has experienced a “crossover” from a degenerate Fermi gas to a BEC of weakly bound molecules (Sá de Melo, Randeria, and Engelbrecht, 1993). Remarkably, such a system allows an exploration of either Fermi or Bose quantum statistics depending on the range of scattering lengths chosen experimentally. An impressive series of experiments has observed precisely these phenomena (Loftus *et al.*, 2002; Greiner, Regal, and Jin, 2003; Regal, Greiner, and Jin, 2004b; Regal *et al.*, 2005), and this crossover physics has been reviewed by Regal and Jin (2007).

Of course the single-component Fermi gas is also of interest, with all fermionic atoms in the same intrinsic spin state. Owing to the absence of s -wave collisions in such systems, the cross sections for two-body elastic collisions that are needed for thermalization of the gas are generally quite small at ultracold temperatures. Use of a p -wave Fano-Feshbach resonance can enhance the cross sections, although two-body losses also usually grow in the vicinity of such resonances (Regal *et al.*, 2003). A two-component Fermi gas has its three-body recombination losses suppressed since the low-temperature behavior of the rate coefficient is linear in the temperature T , in contrast to a gas of bosons or of three distinguishable particles which have a constant low-temperature three-body recombination rate. A spin-polarized gas of fermions, on the other hand, has an even stronger suppression of the low-temperature recombination rate, which varies as T^2 . This might be expected to give very long-lived Fermi gases when fully polarized, but near a p -wave Fano-Feshbach resonance in spin-polarized ^{40}K (the point where the p -wave scattering volume $V_p \rightarrow \infty$), the recombination coefficient has been measured (Regal *et al.*, 2003) and calculated (Suno, Esry, and Greene, 2003a, 2003b), and found to approach within an appreciable fraction of the unitarity limit for the atom loss rate at total relative energy E :

$$K_3^{\max} = \frac{\hbar^5 144\sqrt{3}\pi^2}{m^3 E^2}. \quad (59)$$

In addition to an explosion of effort to understand the many-body physics of the BCS-BEC crossover problem, there has also been extensive fruitful effort directed toward understanding this system from a few-body point of view; see, in particular, Bulgac, Drut, and Magierski (2006), Werner and Castin (2006), Akkineni, Ceperley, and Trivedi (2007), Chang and Bertsch (2007), Kestner and Duan (2007), Alhassid, Bertsch, and Fang (2008), and Zinner *et al.* (2009). And in fact one limit of the many-body problem, the “high energy limit,” can be accurately treated using the virial or cluster expansion. Exciting progress in computing virial coefficients for three particles (Liu, Hu, and Drummond, 2009; Castin and Werner, 2013) and for four particles (Yan and Blume, 2016) has been contributed in landmark theoretical papers during the past decade, as well as tested in a few impressive experiments (Nascimbene *et al.*, 2010).

E. A step beyond independent particles: The Tan contact

The standard methods used in most many-body calculations usually start with a mean-field wave function ansatz, in some

cases going one step farther to the level of Bogoliubov theory or, what is essentially equivalent, the random phase approximation (Esry, 1997; Fetter and Walecka, 2003). These approximations have a demonstrated track record of describing gross global properties of many-body systems, for properties such as chemical potentials, total energies, and excitation frequencies (Dalfovo *et al.*, 1999; Giorgini, Pitaevskii, and Stringari, 2008). One thing that should be kept in mind about such treatments is that they are based on ridiculously inaccurate cartoon-level wave functions of the many-body system at interparticle distances less than the van der Waals length. However, the behavior over larger distances of the order of the long de Broglie wavelengths in the system turns out to be reasonable. To understand the flaws in the full many-body wave function ansatz used to derive the Gross-Pitaevskii equation, the workhorse equation of Bose-Einstein condensation theory, recall that it is a product of independent orbitals ψ , i.e., $\Psi(\vec{r}_1, \vec{r}_2, \dots, \vec{r}_N) = \psi(\vec{r}_1)\psi(\vec{r}_2) \cdots \psi(\vec{r}_N)$. Why is this an absurd hypothesis? Because it says that each particle's probability amplitude is independent of the instantaneous positions of all other particles; but in reality, there simply must be, in the “true” wave function of the system, a two-body character when the distance between any two particles of the gas becomes comparable to the interaction length scale in the potential energy function between those particles (the van der Waals length in the case of isotropic atoms). For two ^{87}Rb atoms in spin-stretched magnetic substates, for instance, the zero-energy wave function of any two approaching atoms in the Rb BEC must have the 39 nodes as the interparticle distance is varied which is guaranteed to be there by Levinson's theorem (Rodberg and Thaler, 1970; Taylor, 1972) since the Rb dimer has 39 triplet bound states in the $L = 0$ orbital partial wave. (For an ultracold atomic gas, higher partial wave physics is normally suppressed by the centrifugal barrier, so we focus only on the s -wave physics in this discussion.) This behavior is often incorporated into MC calculations by using a “Jastrow-type” variational trial function (or a guiding function in the case of diffusion MC), which includes a product of all zero-energy two-body pair wave functions (Dalfovo *et al.*, 1999; Giorgini, Pitaevskii, and Stringari, 2008; Carlson *et al.*, 2015).

To see why the cartoon-level approximation gives such a good description of many properties, consider the zero-range Fermi pseudopotential representation of the interaction between two low-energy particles, i.e.,

$$V(r_{ij}) = \frac{2\pi a_{ij} \hbar^2}{\mu_{ij}} \delta(\vec{r}_{ij}),$$

where a_{ij} is the scattering length between particles i and j and μ_{ij} is their reduced mass. In the important paper by Fermi (1934), he proved that this potential gives an accurate interaction energy of two particles with finite-range potentials in the zero-energy limit, even when highly inaccurate zeroth-order wave functions are utilized; this rescues many-body predictions of energies and other gross properties of the many-body system. The success of this “rescue” was documented by Holzmann and Castin (1999) who demonstrated that the behaviors over large distance scales of mean field and

Bogoliubov wave functions are quite reasonable, even though their Hamiltonian does not contain the large number of two-body bound states whose presence would cause rapid, short-range oscillations in any “exact” wave function of all alkali metal atoms in a many-body gas.

Nevertheless, some properties of the many-body system go beyond those global properties that are well described by a separable wave function ansatz and its crude improvements at the next level of approximation. One such property identified by Shina Tan in a ground-breaking series of papers (Tan, 2008a, 2008b, 2008c) is the high energy limit of the pair correlation function. This Tan contact parameter has now been measured for a Fermi gas (Sagi *et al.*, 2012, 2013) as well as for a BEC (Wild *et al.*, 2012), and those experiments have confirmed the basis two-body physics on which Tan's ideas are based. In brief, one way of looking at the Tan contact is to acknowledge that there will be a range of distances, as two zero-energy particles begin to approach each other at smaller and smaller distances r_{ij} , where the wave function must be proportional to

$$\Psi \propto \frac{1}{a_{ij}} - \frac{1}{r_{ij}}. \quad (60)$$

In a sense the physics of the Tan contact is just the tip of the iceberg, because at higher momenta one begins to probe the full momentum space wave function of two-body subsystems, which have a complicated structure that in general depends on the detailed nature of their short-range interactions. For instance, in a gas of Rb or K atoms, one can expect that the momentum space wave function above $k_{\text{vdW}} \sim 1/\ell_{\text{vdW}}$ or at energies above a few MHz should exhibit deviations from the contact prediction based on the scattering length alone. Experimental measurements to date appear to be mostly in the 10–100 kHz regime. Nevertheless, there is a wide energy range, high compared to many-body excitation frequencies but low compared to van der Waals energy scales, where Tan's contact and scattering length two-body physics control the major departure of the atomic quantum gas from a description in terms of noninteracting independent particle wave functions (Blume and Daily, 2009; Braaten and Platter, 2009; Braaten, Kang, and Platter, 2010; Yan and Blume, 2013; Hudson *et al.*, 2014; Sykes *et al.*, 2014; Yin and Blume, 2015; Corson and Bohn, 2016; Yin and Radzihovsky, 2016).

F. Toward many-body theory with realistic interactions

If a mean-field separable wave function ansatz is attempted in a variational calculation that uses realistic atom-atom interactions, the results are disastrous and the total energy is overestimated by many orders of magnitude (Esry and Greene, 1999). Basically, the mean-field wave function is unable to make the wave function negligibly small at small distances where the atom-atom potential is largely repulsive. An exact solution of the Schrödinger equation would of course make the wave functions exponentially small in such classically forbidden regions, something that no independent particle wave function is “smart enough” to accomplish. Quantum Monte Carlo calculations, however, are able to solve for ground states of many-particle systems and they are

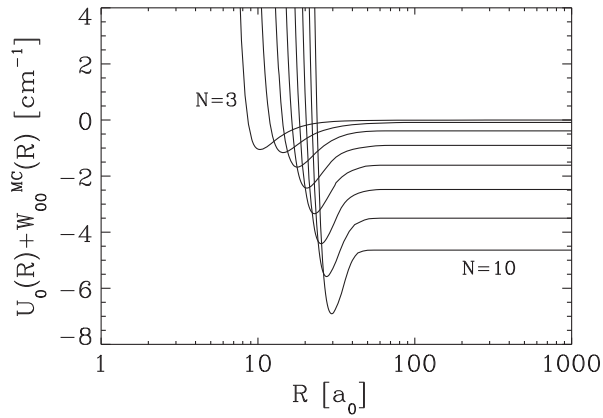


FIG. 15. Lowest energy adiabatic hyperspherical potential curves for N ^4He atoms with $N = 3$ – 10 . These potential curves are for total angular momentum $L = 0$. They were computed in a hybrid hyperspherical-diffusion Monte Carlo method. Based on these potentials, approximate scattering lengths were computed, for instance, $a(\text{He}_9 + \text{He}) = 67a_0$. Note that the potential curve for He_N converges asymptotically to the ground state energy of the He_{N-1} cluster. From Blume and Greene, 2000.

smart enough to make the wave functions exponentially small in regions of strong repulsion. For instance, some of the best calculations of helium cluster energies have been obtained using diffusion Monte Carlo calculations (Lewerenz, 1997; Blume and Greene, 2002). Obtaining excited state information from Monte Carlo calculations is notoriously difficult and limited, however, which makes the technique difficult to use for determining scattering properties.

One hybrid theory that has shown promise combines Monte Carlo and adiabatic hyperspherical ideas (Blume and Greene, 2000). The basic idea is to carry out a diffuse Monte Carlo calculation to find the energy of the system at a fixed hyperradius. By repeating the calculation for many different hyperradii, one maps out the ground state potential energy curve of the system. Then, within the adiabatic approximation that neglects coupling to higher potential curves, at least elastic scattering and a class of excited bound state properties can be computed. That approach has been used to compute hyperspherical potential curves (including diagonal adiabatic correction terms) for clusters of up to $N = 10$ ^4He atoms, as shown in Fig. 15, and observable properties such as binding energies and atom-cluster scattering lengths. There appear to be no competing calculations to date of the atom-cluster scattering lengths, for instance, beyond about $N = 6$ helium atoms, although excellent progress has been achieved up to $N = 6$, and in some cases beyond, by using Gaussian wave functions in combination with a Hamiltonian based on soft-core model potentials.

V. ULTRACOLD ATOMS IN LOW-DIMENSIONAL TRAPS

The experimental realization of Bose-Einstein condensation in a dilute gas of alkali atoms in 1995 (Anderson *et al.*, 1995; Bradley *et al.*, 1995; Davis *et al.*, 1995) enabled the investigation of pure quantum systems that lie at the interface among atomic, molecular, quantum optical physics, and

many-body physics. A key breakthrough emerging from the control of ultracold gaseous matter is the capability to tune interatomic interactions in strength and sign by means of magnetic or optical Fano-Feshbach resonances (Inouye *et al.*, 1998; Köhler, Góral, and Julienne, 2006; Chin *et al.*, 2010). Nowadays, this has triggered the next generation of quantum technologies that allow experimental creation and manipulation of low-dimensional ultracold gases (Kolomeisky and Straley, 1996; Bongs and Sengstock, 2004; Giamarchi, 2004; Lieb, Seiringer, and Yngvason, 2004; Lewenstein *et al.*, 2007; Bloch, Dalibard, and Zwerger, 2008; Cazalilla *et al.*, 2011; McKay and DeMarco, 2011; Imambekov, Schmidt, and Glazman, 2012; Lewenstein, Sanpera, and Ahufinger, 2012) of bosonic or fermionic or mixed symmetry (Giorgini, Pitaevskii, and Stringari, 2008).

Degenerate ultracold atomic gases of reduced dimensionality then serve as a vehicle for experimental realizations and theoretical investigations of exotic quantum phases such as the Tonks-Girardeau (TG) gas (Tonks, 1936; Girardeau, 1960). The TG many-body phase consists of a one-dimensional gas of impenetrable bosons with infinite pairwise repulsion. A fundamental property of the TG gas is that it can be viewed as displaying a *fermionization* of the bosons. In this context, fermionization indicates that the infinite repulsion of the bosons creates a node when any two particles touch, so that the squared wave function of the infinitely repelling bosons coincides with that of a noninteracting fermionic gas. When the repulsive 1D interaction coefficient is cranked up beyond the pole and onto the side representing infinite attraction, the bosonic ensemble experiences a metastable many-body state, namely, the “super Tonks-Girardeau” gas phase (Astrakharchik *et al.*, 2005). Clearly the strength and the sign of interactions play an essential role in creating and probing these exotic many-body phases. It is therefore crucial to study in detail the collisional processes as modified by external confining potentials. Indeed, in these particular low-dimensional two-body systems, the confinement generates significant modifications to the colliding pair scattering properties. Existing theoretical studies on bosonic collisions show that resonant scattering can be induced by the confinement, yielding the so-called confinement-induced resonance (CIR) effect (Yurovsky, Olshanii, and Weiss, 2008; Dunjko *et al.*, 2011a). A CIR occurs when the length scale of the confinement becomes comparable to the s -wave scattering length of the colliding bosons and it produces a divergence in the 1D coupling coefficient that is interpreted as a Fano-Feshbach-like resonance. The additional control of low-dimensional gaseous matter by varying the confinement frequency led to the experimental creation of the TG gas (Kinoshita, Wenger, and Weiss, 2004; Paredes *et al.*, 2004) and the super-TG gas (Haller *et al.*, 2009) in cigar-shaped traps.

Evidently, the deepening understanding of collision physics in the low-dimensional ultracold gases translates into an ability to manipulate and even to design new many-body phases by means of the external confinement.

A. Confinement-induced resonances: An interlude

Early seminal work by Demkov and Drukarev (1966) treated the motion of an electron in the presence of a uniform magnetic field as well as a zero-range potential. That study

showed that the motion of the charged particle is bounded in the presence of the magnetic and zero-range potentials, whereas in the magnetic free case the zero-range potential cannot bind the electron. Another physical system that exhibits similar effects is the negative-ion photodetachment in a uniform magnetic field (Blumberg, Itano, and Larson, 1979; Clark, 1983; Larson and Stoneman, 1985; Greene, 1987; Crawford, 1988; Grozdanov, 1995; Robicheaux, Giannakeas, and Greene, 2015), where in this particular case the electron-atom interaction is treated as a short-range potential. Note that all these cases are half-collisions, in the sense that they arise in photofragmentation processes, and involve only an escape to infinity, whereas a full collision involves both an incoming wave and an outgoing wave.

In the realm of ultracold atomic physics, Olshanii (1998) showed in his seminal work that boson-boson collisions in an axially symmetric waveguide rely on virtually identical mathematics as the system treated by Demkov and Drukarev, except with the trapping potential playing the role of the transverse diamagnetic confinement caused by the magnetic field. More specifically, Olshanii showed that the confinement not only can create a new bound state, but it can also nontrivially enhance the resonant two-body collision amplitude. In many cases the reduced-dimensional bound state is not strictly new, but can be viewed as having been shifted from its position in the 3D or 2D system. For this reason, the term “confinement-induced resonance” is often used synonymously with the term “confinement-shifted resonance.” The following briefly summarizes the two-body scattering and its modification under the influence of the trapping potential and highlights the physical implications.

1. Two-body collisions in a cigar-shaped trap

Two bosonic particles in the presence of a quasi-1D waveguide have s -wave collisions that can be modeled using a Fermi-Huang regularized pseudopotential. The waveguide constrains the motion of the particles transversely, and they propagate freely in the longitudinal direction. The quadratic nature of the trapping potential allows separation of the Schrödinger equation into center-of-mass and relative degrees of freedom. The relative coordinate Hamiltonian describes the relevant collisional physics, which in cylindrical coordinates reads

$$H = -\frac{\hbar^2}{2\mu}\nabla_r^2 + V_{sh}(r) + \frac{1}{2}\mu\omega_\perp^2\rho^2, \quad (61)$$

where μ is the reduced mass of the two bosons, and ω_\perp is the frequency of the confining potential. As usual, ρ denotes the radial polar coordinate and V_{sh} is the 3D Fermi-Huang pseudopotential operator defined by

$$V_{sh}(\mathbf{r})\Psi = \frac{2\pi\hbar^2 a_s(E)}{\mu}\delta(\mathbf{r})\frac{d}{dr}(r\Psi), \quad (62)$$

where a_s indicates the s -wave scattering length, $\delta(\mathbf{r})$ denotes the three-dimensional delta function, and the quantity $d/dr(r\cdot)$ is the regularization operator. Note that the s -wave scattering length in Eq. (62) depends on the relative collision

energy E in the pseudopotential, although in the ultracold limit this energy dependence is often negligible.

The waveguide symmetry implies that the transverse degrees of freedom in the scattering solutions can be expanded in terms of two-dimensional harmonic oscillator eigenstates in the potential $\frac{1}{2}\mu\omega_\perp^2\rho^2$ and the transverse part of the Laplacian in the Hamiltonian H [see Eq. (61)]. The corresponding transverse eigenenergies are given by $E_{nm} = \hbar\omega_\perp(n + |m| + 1)$, with $n = 2n_\rho = 0, 2, 4, \dots$ the quantum number associated with the nodes of the wave function in the ρ direction and m the azimuthal angular momentum. This relative Hamiltonian H possesses azimuthal symmetry, so m is a good quantum number throughout all the configuration space. Here we concentrate on the case $m = 0$.

Remarkably, the prescription given by Demkov and Drukarev (1966) to regularize a divergent sum that arises in the derivation involves a very similar mathematical analysis as was used in the CIR treatment of Olshanii (1998) that results in a Hurwitz zeta function that is well defined.

This means that the system strongly interacts at a finite value of the 3D scattering length, whereas in the absence of the confinement the two bosons exhibit a comparatively weak interaction. This particular phenomenon is the so-called confinement-induced resonance. The main feature of this effect is that the corresponding resonance condition $a_s(E)/a_\perp = -1/c_1$ can be met either by tuning the trapping frequency or by adjusting the scattering length via a Fano-Feshbach resonance, where $a_\perp = \sqrt{\mu\omega_\perp/\hbar}$.

The treatment by Olshanii (1998) showed that the full Hamiltonian in Eq. (61) can be mapped onto an effective one-dimensional Hamiltonian with a delta function interaction between the two bosons of strength g_{1D} :

$$H_{\text{eff}} = -\frac{\hbar^2}{2\mu}\frac{d^2}{dz^2} + g_{1D}\delta(z), \quad g_{1D} = \frac{\hbar^2}{\mu a_\perp a_\perp + c_1 a_s(E)}, \quad (63)$$

where the constant c_1 is given by

$$c_1(k) = \zeta\left(\frac{1}{2}, 1 - \frac{1}{4}(ka_\perp)^2\right), \quad (64)$$

with $\zeta(\cdot, \cdot)$ the Hurwitz zeta function and for $ka_\perp \ll 1$ we have the value $c_1 \approx -1.46035$. Here k is the wave number associated with the total colliding energy E .

This effective two-body interaction derived from first principles can be directly utilized in a many-body Hamiltonian, which permits an exploration of the underlying physics associated with the Tonks-Girardeau gas. The effective Hamiltonian based on the coupling strength g_{1D} encapsulates all the relevant scattering information in the full Hamiltonian as well as the nontrivial modifications due to the trap. More specifically, as the ratio $a_s(E)/a_\perp$ tends to $-1/c_1$ the quantity $g_{1D} \rightarrow \infty$. This particular feature is depicted in Fig. 16 by the vertical dotted line where the position of the CIR is indicated by the red star. In Fig. 16 the coupling constant g_{1D} is shown as a function of the ratio $a_s(E)/a_\perp$. The black dots correspond to the full numerical solution of the Hamiltonian given in Eq. (61) where the two-body interactions are modeled by a 6-10 potential, i.e.,

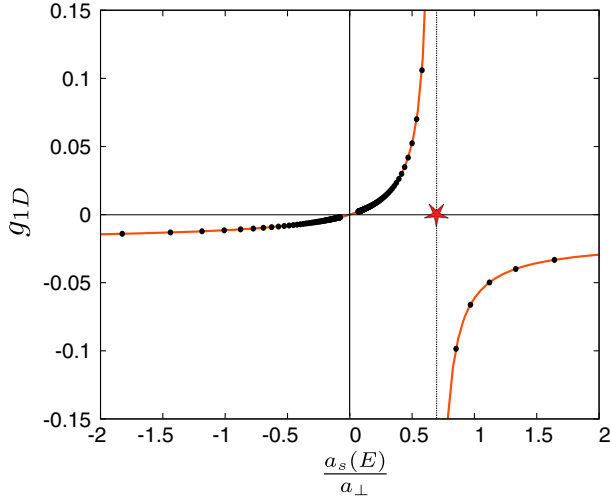


FIG. 16. The one-dimensional coupling strength g_{1D} (in units of $\hbar^2/\mu a_{\perp}$) as a function of the ratio $a_s(E)/a_{\perp}$. The solid orange line corresponds to the analytical expression given in Eq. (63). The black dots correspond to full numerical calculations where the two-body interactions are modeled via a 6-10 potential. The red star denotes the position of the confinement-induced resonance.

$V(r) = C_{10}/r^{10} - C_6/r^6$. The solid orange line denotes the analytical result of the coupling constant g_{1D} given in Eq. (63) which agrees accurately with the numerical solution. Furthermore, Fig. 16 shows that as the ratio $a_s(E)/a_{\perp}$ tends to infinity the coupling constant tends asymptotically to a weakly attractive limit in the effective 1D potential energy. The resonant 3D free-space two-body interactions, on either the repulsive or attractive side, are modified into weakly attractive 1D forces due to the trapping geometry. This attractive force in the waveguide is determined solely by the $c_1(k)$ constant and the oscillator length a_{\perp} . Indeed, for $a_s(E)/a_{\perp} \rightarrow \infty$ the coupling strength is $g_{1D} \rightarrow \hbar^2/2\mu a_{\perp} c_1$.

Qualitatively, the CIR can be viewed as a bound state supported by all the closed channels whose energy coincides with the lowest channel threshold, as in a usual Fano-Feshbach resonance (Bergeman, Moore, and Olshanii, 2003). This multichannel bound state produces only a single pole in the reactance operator, i.e., the tangent of the 1D even z -parity phase shift. To follow up on this idea, one can obtain the binding energies of the closed-channel supported bound state from the following transcendental equation, and its solution is the CIR resonance condition:

$$\frac{a_{\perp}}{a_s} = -\zeta\left(\frac{1}{2}, \frac{3}{2} - \frac{E_r}{2\hbar\omega_{\perp}}\right), \quad (65)$$

where $\zeta(\cdot, \cdot)$ is the Hurwitz zeta function. Note that the appropriate value of E_r in the ultracold limit is in the range of a few tens of kHz. On the other hand, the theoretical treatment suggests that at energies below the threshold of the open channel confinement-induced molecular states might be supported. Equation (66) is derived by requiring all the scattering channels to be closed yielding a wave function that vanishes asymptotically. In this case the molecular

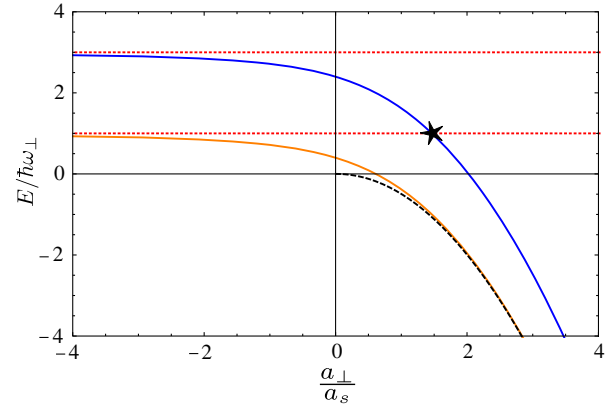


FIG. 17. Illustration of the physical origin of confinement-induced resonances. Bound state energies in units of $\hbar\omega_{\perp}$, i.e., $E/\hbar\omega_{\perp}$ are depicted vs the ratio a_{\perp}/a_s . The dotted red lines indicate the energy levels of the unperturbed two-dimensional harmonic oscillator, which act here as channel threshold energies. The black star denotes the position of the confinement-induced resonance relevant in the ultracold limit. The dashed curve illustrates the s -wave bound state in the absence of the trapping potential. The solid orange curve corresponds to the molecular confinement-induced resonance. The blue curve (top) is the CIR bound state energy supported by all the closed channels.

confinement-induced energies obey the following transcendental equation:

$$\frac{a_{\perp}}{a_s} = -\sqrt{\frac{2\hbar\omega_{\perp}}{\hbar\omega_{\perp} - E_r}} - \zeta\left(\frac{1}{2}, \frac{3}{2} - \frac{E_r}{2\hbar\omega_{\perp}}\right). \quad (66)$$

Figure 17 illustrates the relations in Eqs. (65) and (66), where the corresponding closed-channel bound state (solid blue curve, top) and molecular CIR state (solid orange curve, bottom) energies are given as a function of the ratio a_{\perp}/a_s . The dashed red lines indicate the two-dimensional harmonic oscillator eigenenergies in the absence of short-range interactions, i.e., the values $E^{(1)} = \hbar\omega_{\perp}$ and $E^{(2)} = 3\hbar\omega_{\perp}$. The dashed black curve corresponds to the energy of an s -wave molecular pair in the absence of a confining trap, i.e.,

$$E_{\text{free}}/\hbar\omega_{\perp} = -\frac{a_{\perp}^2}{2a_s^2}.$$

We observe that the closed-channel bound state (solid blue curve, top) tends to $3\hbar\omega_{\perp}$ as the ratio $a_{\perp}/a_s \rightarrow -\infty$, i.e., in the absence of a short-range interaction. As the ratio a_{\perp}/a_s approaches the value $-c_1 = 1.46035$ the bound state from the closed channels becomes degenerate with the threshold of the open channel $E^{(1)} = \hbar\omega_{\perp}$ (see the black star in Fig. 17), and not coincidentally the CIR resonance occurs at $a_{\perp}/a_s = -c_1 = 1.46035$. Note that at $a_{\perp}/a_s > 1.46035$ and for energies less than $E^{(1)}$ the depicted blue line (top) does not have any physical significance and it is just an analytic continuation of Eq. (65). In this energy regime all the channels should be closed and Eq. (65) refers to the case where the system possess a single open channel.

This analysis illustrates that the CIR has the character of a Fano-Feshbach resonance, where the collective bound state attached to all the closed channels lies in the low-energy continuum of the open channel. In addition, the confinement-induced molecular state (see the solid orange line, bottom) exists regardless of the strength of the short-range interactions. This is a manifestation of the impact of the confinement since in free-space collisions the bosonic pair forms a weakly bound state only for positive values of the s -wave scattering length. On the positive side of the abscissa in Fig. 17 as the ratio a_{\perp}/a_s increases we observe that the energy of the free-space weakly bound molecule (dashed black line) coincides with the energy of the confinement-induced molecular state (solid orange line, bottom). This occurs at these values of scattering length since the two-body potential is deep enough forcing the wave function to vanish before the trapping potential becomes important. Therefore, in this limit the confinement-induced molecular state behaves as a free-space bound state. Note that similar behavior was observed by Demkov and Drukarev (1966).

An experiment by Moritz *et al.* (2005) considered a Fermi gas of ^{40}K atoms in the presence of harmonic confinement. The ^{40}K atoms are prepared in two hyperfine states $|F = 9/2, m_F = -9/2\rangle$ and $|F = 9/2, m_F = -7/2\rangle$. Note that the third hyperfine $|F = 9/2, m_F = -5/2\rangle$ is not populated initially. The mutual interactions are tuned via a Feshbach resonance whose position is located at $B = 202.1$ G and its zero crossing is at $B = 210$ G. Thereafter, by employing radio-frequency spectroscopy confinement-induced molecules are generated and their binding energy is measured as a function of the scattering length and the confinement frequency. In Fig. 18 the binding energies of the confinement-induced (solid black line and squares) and Feshbach (solid blue line and circles) molecules are depicted as a function of the magnetic field. The solid lines denote the theoretical predictions of Dickerscheid and Stoof (2005) whereas the scattered data are the experimental measurements. The dashed blue line indicates the position of the Feshbach resonance where a Feshbach molecule (blue line and circles) is

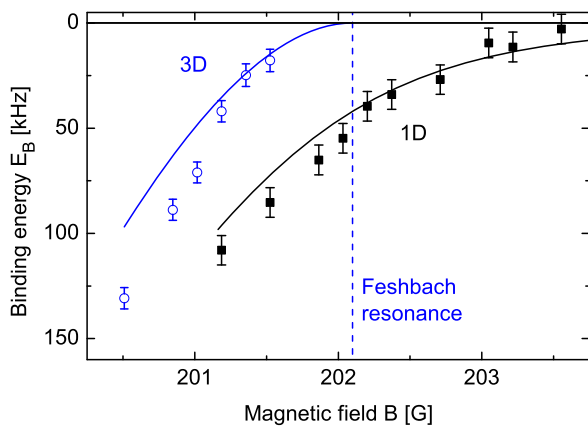


FIG. 18. Confinement-induced (black squares and line) and Feshbach (blue line and circles) molecules. The solid lines correspond to the theoretical predictions whereas the circles and squares indicate the experimental measurements. The vertical dashed line indicates the position of the Feshbach resonance. From Moritz *et al.*, 2005.

formed only on the positive side of the resonance whereas no measurement occurs on the negative side. On the other hand, in the case of confinement-induced molecule (black line and squares) we observe that there is always a bound state regardless the sign of the s -wave interactions. This is in accordance with the theoretical predictions. In addition, note that the intersection point of the black line with the dashed blue line, i.e., at the position of infinite scattering length, the binding energy acquires its universal value, i.e., $E_B \approx 0.6\hbar\omega_{\perp}$. At this universal value the binding energy of the confinement-induced molecules depends solely on the strength of the confinement. Note that the strength of the confinement in Moritz *et al.* (2005) is tuned by changing the lattice depth V_0 . Figure 19 depicts the binding energy of the confinement-induced molecule as a function of the confinement strength in units of recoil energy E_r . The solid black line refers to theoretical calculations and the scatter data indicate the radio-frequency measurements. Both theory (Dickerscheid and Stoof, 2005) and experiment show sufficient agreement. The minor disagreements between theory and experiment in Figs. 18 and 19 associated with the effective-range corrections are not included as pointed out by Peng *et al.* (2012).

In the analysis of s -wave confinement-induced resonances it is evident that zero-range approximations are employed. This means that the short-range part of the Hamiltonian is treated in essence as a single channel. In experiments, however (see Fig. 18), the main toolkit to tune the interactions or the s -wave scattering length is the Feshbach resonances. This particular aspect implies that the short-range part must be treated as a two-channel model in order to obtain a direct comparison with the corresponding experimental advances. Toward this pathway a tremendous amount of theoretical effort is focused in order to adequately incorporate the two-channel nature of Feshbach resonances in the confinement-induced physics (Yurovsky, 2005, 2006; Peng *et al.*, 2012; Saeidian, Melezhik, and Schmelcher, 2012; Kristensen and Pricoupenko, 2015). All these works pointed out the importance of the effective range corrections particularly on the calculation of the binding energy of confinement-induced molecules. In addition, it was shown that the effective range

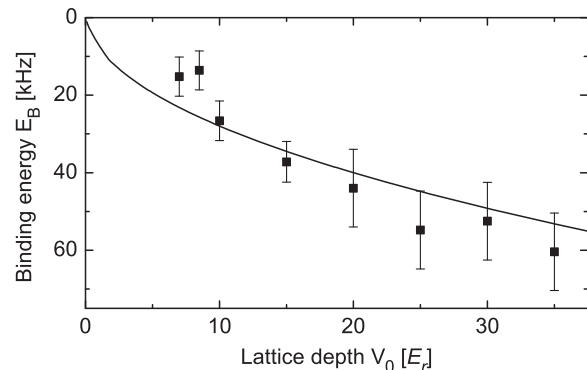


FIG. 19. The binding energy of the confinement-induced molecules as a function of the lattice depth V_0 in recoil units (E_r). The spectra are measured very close to the Feshbach resonance at magnetic field $B = 202$ G. The solid black line indicates the corresponding theoretical calculations. From Moritz *et al.*, 2005.

corrections become more important for narrow Feshbach resonances. Note that similar conclusions were also drawn for fermionic species in harmonic waveguides (Saeidian, Melezhik, and Schmelcher, 2015).

Another aspect which was excluded from the work of Demkov and Drukarev (1966), Olshanii (1998), and Bergeman, Moore, and Olshanii (2003) was that the total colliding energy is sufficient for the pair atoms such that no excitation will occur before and after the collision. Lifting this constraint, i.e., going beyond the single mode regime (Moore, Bergeman, and Olshanii, 2004; Saeidian, Melezhik, and Schmelcher, 2008; Heß, Giannakeas, and Schmelcher, 2015) predicted numerically (Saeidian, Melezhik, and Schmelcher, 2008) and analytically (Moore, Bergeman, and Olshanii, 2004; Heß, Giannakeas, and Schmelcher, 2015) the emergent inelastic confinement-induced resonances for bosonic and fermionic exchange symmetries. In particular, Heß, Giannakeas, and Schmelcher (2015) also considered the higher partial wave interactions going beyond s - and p -wave interactions and obtained universal expressions for the position of all the inelastic confinement-induced resonances.

Kim, Melezhik, and Schmelcher (2006) studied distinguishable particle collisions in the presence of a harmonic waveguide which yield the effect of dual confinement-induced resonances. These types of resonances correspond to total transmission due to the destructive interference of s and p -partial waves. The importance of high partial waves on bosonic or fermionic systems in a cigar-shaped trap were considered by Giannakeas, Diakonov, and Schmelcher (2012). Because of the anisotropy of the trap all the partial waves associated with either bosonic or fermionic exchange symmetry are interacting, which yields in this manner coupled ℓ -wave confinement-induced resonances. The analysis of this particular system is based on the idea of the local frame transformation. This framework was employed for highlighting the underlining physics of fermionic collisions in matter waveguides by Granger and Blume (2004) avoiding the complications of zero-range and two-channel models. The following focuses on a system of spin-polarized fermions in the presence of cigar-shaped traps and the underlying details of the local frame transformation theory.

2. Fermions in a cigar-shaped trap

It is also of extensive experimental and theoretical interest to explore near-degenerate fermionic gases in low-dimensional traps, which requires a detailed understanding of confinement-induced resonances between identical fermions. Granger and Blume (2004) developed a scattering theory to describe collisions between identical spin-polarized fermions in the presence of an axially symmetric harmonic trap. Owing to the Pauli exclusion principle, ultracold fermions interact in 3D with p -wave interactions instead of s -wave interactions that were considered in the previous section. The p -wave theory requires somewhat different considerations, which we therefore consider in this section from the general viewpoint of the K -matrix theory; this highlights the behavior imposed on spin-polarized fermionic ensembles by the transverse trapping potential.

Again, the relative Hamiltonian for two spin-polarized fermions expressed in cylindrical coordinates has the same form as given in Eq. (61). In contrast with the previous s -wave treatment, the spherically symmetric two-body interaction is not modeled by a pseudopotential. Instead the formulation works directly with the short-range phase shift caused by the spherical symmetric two-body atomic interaction. In the following, azimuthal symmetry is assumed and our analysis is restricted to only $m = 0$.

In practice the length scales associated with the two potential terms in Hamiltonian H are well separated, with r_0 the short-range potential typically orders of magnitude smaller than the waveguide potential oscillator length in a typical ultracold experiment $a_\perp = \sqrt{\hbar/\mu\omega_\perp}$. At small inter-particle distance $r \ll a_\perp$, the orbital angular momentum is approximately conserved and therefore the two fermions experience a free-space collision with total colliding energy $E = \hbar^2 k^2 / (2\mu)$. As usual, μ denotes the two-body reduced mass. In this case the ℓ' th linearly independent energy eigenstate expressed in spherical coordinates has the following form at $r_0 \ll r \ll a_\perp$:

$$\Psi_{\ell'}(\mathbf{r}) = \sum_{\ell} F_{\ell}(r, \theta) \delta_{\ell\ell'} - G_{\ell}(r, \theta) K_{\ell\ell'}^{3D}, \quad (67)$$

where $F_{\ell}(r, \theta)$ [$G_{\ell}(r, \theta)$] is the energy normalized regular [irregular] solution expressed in terms of spherical Bessel $j_{\ell}(r)$ [spherical Neumann $n_{\ell}(r)$] functions multiplied by the corresponding spherical harmonic $Y_{\ell, m=0}(\theta, \phi)$. The summation is performed over all odd ℓ angular momentum due to the Pauli exclusion principle. The quantity $K_{\ell\ell'}^{3D}$ represents the elements of the reaction matrix \underline{K}^{3D} in three dimensions. This K matrix incorporates all the scattering information due to the short-range potential $V_{sh}(\mathbf{r})$, and for a spherically symmetric potential it is diagonal, but for anisotropic interactions such as the dipole-dipole type it could acquire off-diagonal elements in other contexts (Giannakeas, Melezhik, and Schmelcher, 2013).

At large distances the waveguide geometry prevails and imposes cylindrical symmetry on the wave function, and the total collision energy gets apportioned between the transversal and longitudinal degrees of freedom. The energy can be expressed at $|z| > r_0$ as $E = \hbar\omega_\perp(2n + |m| + 1) + \hbar^2 q_n^2 / (2\mu)$, where the term $\hbar\omega_\perp(2n + |m| + 1)$ refers to the energy of the transversal part of the Hamiltonian and q_n is the channel momentum, i.e., the momentum of the particles in the z direction. In this region the n' th linearly independent scattering wave function at energy E can be expressed in cylindrical coordinates as

$$\Psi_{n'}(\mathbf{r}) = \sum_n f_n(z, \rho) \delta_{nn'} - g_n(z, \rho) K_{nn'}^{1D}, \quad (68)$$

where the quantity $K_{nn'}^{1D}$ represents the elements of the quasi-1D reaction matrix \underline{K}^{1D} and $(f_n(z, \rho), g_n(z, \rho))$ are the energy normalized (regular, irregular) standing-wave solutions solely in the presence of the trap. The specific form of the regular and irregular solutions which obey the Pauli exclusion principle have odd z parity for $m = 0$ and are given by

$$\begin{pmatrix} f_n(z, \rho) \\ g_n(z, \rho) \end{pmatrix} = (2\pi^2 q_n)^{-1/2} \Phi_n(\rho) \left\{ \begin{pmatrix} \sin q_n z \\ -\frac{z}{|z|} \cos q_n z \end{pmatrix}, \quad (69)$$

where $\Phi_n(\rho)$ are the $m=0$ eigenfunctions of the two-dimensional harmonic oscillator and the z dependence describes motion in the unbounded coordinate. For collisions of spin-polarized fermions the factor $z/|z|$ corresponds to the antisymmetrization operator.

From the Hamiltonian H in Eq. (61) it is evident that the corresponding Schrödinger equation is nonseparable over all the configuration space. However, as mentioned there are two distinct subspaces where the resulting Schrödinger equation is separable and all the relevant scattering information can be expressed in terms of reaction matrices, namely, K^{3D} [see Eq. (67)] and K^{1D} [see Eq. (68)]. The main idea is to define a frame transformation which will permit one to express the K^{1D} reaction matrix in terms of the short range K^{3D} . Intuitively, the frame transformation U permits us to propagate outward to the asymptotic region the information of the collisional events occurring close to the origin.

An unusual property of this frame transformation is that it is not unitary. This arises due to the fact that the solutions given in Eqs. (67) and (68) obey different Schrödinger equations. However, the Hamiltonian H in Eq. (61) possesses length scale separation implying the existence of an intermediate region where both potentials are negligible. This means that in this subspace Eqs. (67) and (68) approximately satisfy the same Schrödinger equation, i.e., the Helmholtz equation. Therefore, in this Helmholtz region one locally employs the frame transformation. The concept of the local frame transformation was introduced by Fano (1981a) and Harmin (1982a, 1982b) and extended by Greene (1987), Wong, Rau, and Greene (1988), Granger and Blume (2004), Zhang and Greene (2013), Robicheaux, Giannakeas, and Greene (2015), and Giannakeas, Greene, and Robicheaux (2016).

The local frame transformation is derived by matching the energy normalized regular solutions $f_n(\mathbf{r})$ and $F_\ell(\mathbf{r})$ on a surface σ at a finite distance $r_0 < r < a_\perp$ inside the Helmholtz region. Formally, for $r < a_\perp$ U obeys

$$f_n(\mathbf{r}) = \sum_\ell F_\ell(\mathbf{r}) U_{\ell n}^T, \quad \text{with } U_{\ell n}^T = \langle\langle F_\ell | f_n \rangle\rangle, \quad \text{for } r < a_\perp, \quad (70)$$

where U^T denotes the transpose of the frame transformation matrix U , and $\langle\langle \cdot | \cdot \rangle\rangle$ indicates that the solutions F_ℓ and f_n are integrated only over the solid angle $\Omega = (\theta, \phi)$. Note that the matrix elements U are independent of the distance r . This occurs since the matching of the regular solutions takes place in the Helmholtz region where both solutions possess the same r dependence. In addition, since the set of solutions in Eqs. (67) and (68) are real standing-wave solutions, the matrix U is real.

Fano (1981a) pointed out that the irregular parts of Eqs. (67) and (68) can be interconnected by matching in the Helmholtz region the corresponding principal value Green's functions, written in the different coordinate systems. Formally, the irregular solutions obey

$$g_n(\mathbf{r}) = \sum_\ell G_\ell(\mathbf{r}) [U^{-1}]_{\ell n}, \quad \text{for } r < a_\perp. \quad (71)$$

After inserting Eqs. (70) and (71) into the scattering wave function $\Psi(\mathbf{r})$ in Eq. (67), the K^{1D} matrix can be expressed in terms of the short range K^{3D} compactly as

$$K^{1D} = U K^{3D} U^T, \quad (72)$$

where the short range K^{3D} includes all the odd partial waves for the spin-polarized fermions. Also, the K^{1D} matrix depends on the total collision energy E .

The K^{1D} matrix contains information about the asymptotically open- and closed-channel components of the wave functions. To describe the closed-channel components, solutions given in Eq. (68) can be analytically continued by setting the channel momentum q_n to be $q_n \rightarrow i|q_n|$ in the usual spirit of quantum defect theory. Then one can derive the local frame transformation U which possesses the same functional form as for the open channels. Note that the local frame transformation U in the open channels only for p -wave interactions obeys the relation

$$U_{\ell=1n} = \frac{\sqrt{2}}{a_\perp} \sqrt{\frac{3}{kq_n}} P_{\ell=1} \left(\frac{q_n}{k} \right),$$

where $P_\ell(\cdot)$ indicates the ℓ th Legendre polynomial. This yields the same expression for K^{1D} shown in Eq. (72). The only drawback from these manipulations is that the resulting K^{1D} matrix corresponds to a scattering solution which does not (yet) obey the proper boundary conditions asymptotically. This is because the closed-channel parts of the wave function given in Eq. (68) contains exponentially growing pieces at $|z| \rightarrow \infty$. One sees readily after substituting $q_n \rightarrow i|q_n|$ that the regular and irregular solutions in Eq. (69) for the closed-channel components have exponentially both decaying and growing pieces. Therefore, in order to enforce the physically accepted asymptotic boundary conditions in Eq. (68) concepts from multichannel quantum defect theory are employed Aymar, Greene, and Luc-Koenig (1996).

Initially, the scattering wave function in Eq. (68) is separated into open (o) and closed (c) channels. Then, linear combinations are chosen by demanding that the exponentially growing pieces in the closed channels are canceled. Formally, we have the following relation for the wave function:

$$\begin{pmatrix} \Psi_{oo} & \Psi_{oc} \\ \Psi_{co} & \Psi_{cc} \end{pmatrix} \begin{pmatrix} B_{oo} \\ B_{co} \end{pmatrix} = \left[\begin{pmatrix} f_o & 0 \\ 0 & f_c \end{pmatrix} - \begin{pmatrix} g_o & 0 \\ 0 & g_c \end{pmatrix} \right. \\ \left. \begin{pmatrix} K_{oo}^{1D} & K_{oc}^{1D} \\ K_{co}^{1D} & K_{cc}^{1D} \end{pmatrix} \right] \begin{pmatrix} B_{oo} \\ B_{co} \end{pmatrix},$$

where the matrices B_{oo} and B_{co} denote the linear combination coefficients. By eliminating the closed channels the linear combination coefficients acquire the values

$$B_{oo} = \mathbb{1} \quad \text{and} \quad B_{co} = \left(\frac{f_c}{g_c} - K_{cc}^{1D} \right)^{-1} K_{co}^{1D}, \quad (73)$$

where the term $f_c/g_c \xrightarrow{|z| \rightarrow \infty} -i\mathbb{1}$.

The physical wave function, which involves only open channels asymptotically since the closed-channel components decay exponentially, acquires the following form at $|z| \rightarrow \infty$:

$$\Psi^{\text{phys}} = f_o - g_o [K_{oo}^{1D} + iK_{oc}^{1D}(\mathbb{1} - iK_{cc}^{1D})^{-1}K_{co}^{1D}]. \quad (74)$$

Here the effects of the closed channels on the open channel scattering are included in the corresponding physical K matrix, given by

$$K_{oo}^{1D,\text{phys}} \equiv K_{oo}^{1D} + iK_{oc}^{1D}(\mathbb{1} - iK_{cc}^{1D})^{-1}K_{co}^{1D}. \quad (75)$$

The resonances of the collision complex appear as poles of the $K_{oo}^{1D,\text{phys}}$ matrix. More specifically, the $K_{oo}^{1D,\text{phys}}$ exhibits resonant features at zero eigenvalues of the matrix $(\mathbb{1} - iK_{cc}^{1D})$. Therefore, this argument can be recast into the form of a determinantal equation:

$$\det(\mathbb{1} - iK_{cc}^{1D}) = 0. \quad (76)$$

Note that despite the appearance of the imaginary unit i in the preceding equations, all of these physical wave functions and reaction matrices are real. When all channels are closed, the roots of Eq. (76) yield the bound state energies. When one or more channels are energetically open, the roots of the above closed-channel determinant approximately identify the real parts of resonance energies. Equation (76) shows why a confinement-induced resonance can be viewed as a Fano-Feshbach type of resonance.

Consider next the situation where the two fermions collide in the single mode regime, meaning that the relative collision energy lies between the lowest two transverse thresholds. In addition, these ultracold spin-polarized fermions interact at short distances via p -wave interactions only. Phase shifts associated with higher 3D partial waves are entirely neglected. Accordingly, the determinantal equation has one nonzero root, and the $K_{oo}^{1D,\text{phys}}$ matrix takes the following form:

$$K_{oo}^{1D,\text{phys}} = K_{oo}^{1D} + iK_{oc}^{1D} \left(\mathbb{1} + \frac{i}{1 - i\gamma} K_{cc}^{1D} \right)^{-1} K_{co}^{1D}, \quad (77)$$

where $\gamma = \text{Tr}(K_{cc,\ell}^{1D})$. Note that the $\text{Tr}(K_{cc,\ell}^{1D})$ is an infinite sum which formally diverges and in order to obtain a meaningful answer an auxiliary regularization scheme is employed. In the particular case a Riemann zeta function regularization scheme is used. Note that such techniques are totally avoided in the generalized form of the local frame transformation theory (Robicheaux, Giannakeas, and Greene, 2015; Giannakeas, Greene, and Robicheaux, 2016). In addition, Eq. (77) is further simplified by substituting $(K^{3D})_{\ell'\ell''} = \tan \delta_{\ell=1}(E) \delta_{\ell',1} \delta_{\ell'',1}$, i.e., using the fact that only p -wave phase shifts $\delta_{\ell=1}(E)$ are nonzero. Next, in Eq. (77) we substitute the corresponding local frame transformation for the closed channels only

$$U_{\ell=1n} = \frac{\sqrt{2}}{a_{\perp}} \sqrt{\frac{3}{ik|q_n|}} P_{\ell=1} \left(\frac{i|q_n|}{k} \right),$$

where $P_{\ell}(\cdot)$ indicates the ℓ th Legendre polynomial. Equation (77) now reads

$$K_{oo}^{1D,\text{phys}} = -\frac{6V_p}{a_{\perp}^3} q_0 a_{\perp} \left[1 - 12 \frac{V_p}{a_{\perp}^3} \zeta \left(-\frac{1}{2}, \frac{3}{2} - \frac{E}{2\hbar\omega_{\perp}} \right) \right]^{-1}, \quad (78)$$

where the terms inside the square brackets provide the resonance condition for the position of the p -wave confinement-induced resonances. The term V_p denotes the energy-dependent 3D scattering volume which is defined by $V_p(E) = -\tan \delta_{\ell=1}(E)/k^3$ ($k = \sqrt{2\mu E/\hbar^2}$).

The quantity of greatest experimental relevance is the effective interaction strength between two 1D spin-polarized fermions which contains the corresponding p -wave confinement-induced physics. As shown by Girardeau and Olshanii (2004), Kanjilal and Blume (2004), and Pricoupenko (2008) this effective 1D interaction is related to the corresponding K matrix [see Eq. (78)] according to

$$g_{1D}^{-} = -\frac{\hbar^2 a_{\perp}}{\mu q_0} K_{oo}^{1D,\text{phys}}. \quad (79)$$

This coefficient controls the strength of the effective zero-range pseudopotential that is relevant for describing the interaction of identical fermions in 1D in both few-body and many-body contexts, namely,

$$V^{\text{pseudo}}(z) = g_{1D}^{-} \frac{\overleftarrow{d}}{dz} \delta(z) \frac{\overrightarrow{d}}{dz}. \quad (80)$$

The left (or right) arrow indicates that the derivative operator acts on the bra (or ket), respectively. In the idealized limit of a zero-range potential, this pseudopotential produces a discontinuous wave function that obeys the required antisymmetry of the identical fermion wave function. This might seem problematical since one normally requires wave functions in Schrödinger wave mechanics to be continuous, but it can be accommodated theoretically as discussed, for instance, by Cheon and Shigehara (1999).

Figure 20 illustrates the dependence of the effective coupling constant g_{1D}^{-} as a function of the V_p/a_{\perp}^3 in the

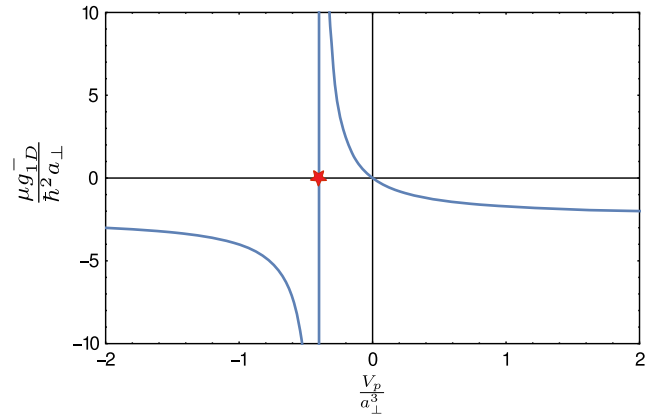


FIG. 20. The low-energy effective interaction g_{1D}^{-} for two spin-polarized fermions in the presence of a harmonic confinement as a function of V_p/a_{\perp}^3 . The red star denotes the position of the p -wave confinement-induced resonance.

low-energy regime. The two fermions strongly interact at the position of p -wave confinement-induced resonance (see the red star in Fig. 20) whereas in the limit of $V_p/a_\perp^3 \rightarrow 0$ the corresponding effective interaction vanishes. Interestingly, for strong p -wave interactions, i.e., $V_p/a_\perp^3 \rightarrow \pm\infty$ the spin-polarized fermions experience a weak attraction due to the transversal harmonic confinement. The location of this divergent interaction strength is called the p -wave confinement-induced resonance, and it occurs where the scattering volume of the p -wave phase shift is finite and satisfies the resonance condition, namely, $V_p/a_\perp^3 = [12\zeta(-1/2, 3/2 - E/2\hbar\omega_\perp)]^{-1}$.

Apparently, the theoretical scope of confinement-induced resonances is addressed mainly to the elastic collisional aspects of particles with either bosonic or fermionic exchange symmetry. However, in the experimental advances of Günter *et al.* (2005), Haller *et al.* (2010), Lamporesi *et al.* (2010), and Sala *et al.* (2013) the confinement-induced physics is probed via atom loss measurements which inherently are inelastic scattering processes. These processes mainly emerge due to mechanisms, such as three-body recombination, coupling of the two-body center-of-mass and relative degrees of freedom, spin flips, etc. Theoretically, the few-body collisions in the presence of external confinement were investigated by Mora *et al.* (2004, 2005), Mora, Egger, and Gogolin (2005), Gharashi, Daily, and Blume (2012), and Blume (2014) addressing the three- and four-body aspects of the confinement-induced physics where a detailed discussion can be found in the excellent review by Blume (2012a).

Günter *et al.* (2005) experimentally investigated p -wave collisions of spin-polarized fermions in the presence of cigar-shaped and pancake traps. The degenerate gas constitutes of fermionic ^{40}K atoms where their mutual interactions are tuned by means of a p -wave Feshbach resonance at 198 G which possesses a double-peaked feature. As shown by Ticknor *et al.* (2004) the doublet structure of a p -wave magnetic Feshbach

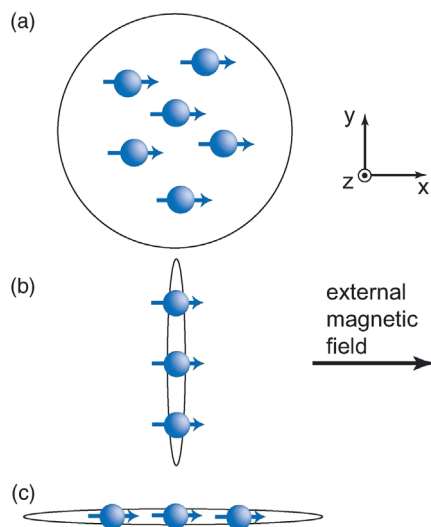


FIG. 21. Schematic illustration of the alignment of the spins with respect to pancake and cigar-shaped traps. (a) In a pancake configuration all the spin alignments are permitted. (b), (c) Cigar-shaped traps where only the $|m| = 1$ ($m = 0$) spin configuration of the p -wave interactions is allowed. From Günter *et al.*, 2005.

resonance is associated with the different projections of the orbital angular momentum, i.e., $|m| = 1$ and $m = 0$ for $\ell = 1$ and it occurs due to the magnetic dipole-dipole interactions. Günter *et al.* (2005) showed that this feature also yields particular signatures in low-dimensional arrangements. Qualitatively the impact of the double-peaked Feshbach resonance is depicted in Fig. 21 where three configurations are considered for pancake and cigar-shaped traps. In particular, Fig. 21(a) corresponds in a pancake trap where all the projection alignments, i.e., $|m| = 1$ and $m = 0$, are considered. In Fig. 21(b) a cigar-shaped trap is considered whose longitudinal direction is perpendicular to the magnetic field. This implies that the $|m| = 1$ configuration of the p -wave Feshbach resonance mainly contributes in the scattering process whereas collisional events associated with $m = 0$ component of the Feshbach resonance are suppressed. Finally, in Fig. 21(c) the quasi-one-dimensional trap is aligned with the magnetic field, whereby the $m = 0$ component dominates the p -wave collisions.

By measuring the atom loss signal the impact of the multiplet Feshbach resonance is illustrated in Fig. 22 for five different trap configurations. In particular, Fig. 22(a) a three-dimensional optical trap where the double-peaked feature of the p -wave resonance stands out. In Fig. 22(b) the potassium atoms are confined in a pancake-shaped trap and the two

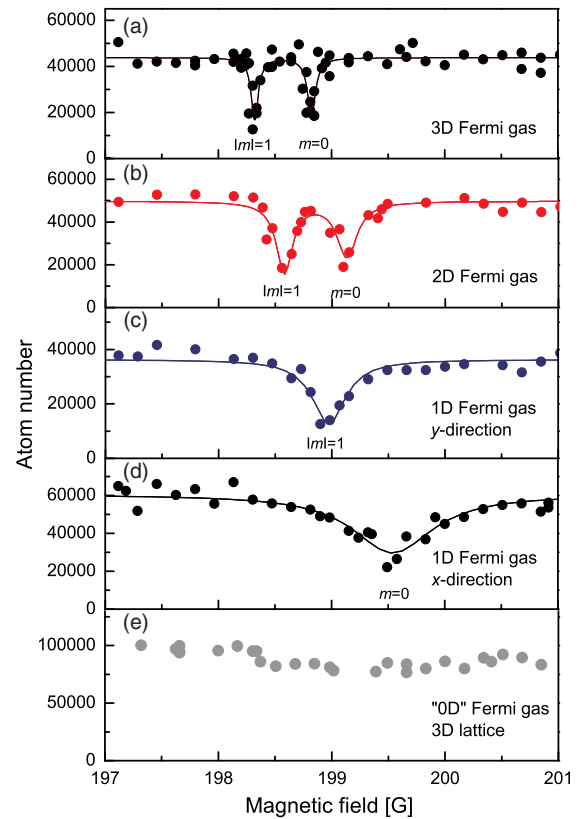


FIG. 22. Atom loss measurements for ^{40}K atoms around a multiplet p -wave Feshbach resonance for (a) a three-dimensional dipole trap, (b) a two-dimensional pancake trap, (c), (d) a quasi-one-dimensional cigar-shaped trap whose longitudinal direction is perpendicular (parallel) to the magnetic field, and (e) a three-dimensional optical lattice. From Günter *et al.*, 2005.

components of the Feshbach resonance prevail where a confinement-induced shift is observed with respect to the measurements of Fig. 22(a). In Fig. 22(c) the Fermi gas is confined in a quasi-one-dimensional trap with its longitudinal direction positioned perpendicular to the magnetic field. In contrast to Figs. 22(a) and 22(b), only the $|m| = 1$ component of p -wave resonance is pronounced whereas the trapping potential induces a shift with respect to the corresponding resonance in Fig. 22(a). Similarly, in Fig. 22(d) the Fermi gas is confined in a cigar-shaped trap with the longitudinal direction being aligned with the magnetic field. In this case, solely the $|m| = 0$ component of the Feshbach resonance contributes appreciably, and it is shifted toward larger values of field strength with respect to the corresponding measurements of Fig. 22(a) verifying in this manner the theoretical predictions of Granger and Blume (2004). Finally, a tight three-dimensional optical lattice is considered in Fig. 22(e) where no pronounced losses are observed since the atoms are effectively confined in “zero” dimensions and asymptotic scattering states are restricted.

From a theoretical viewpoint, Peng, Tan, and Jiang (2014) considered fermionic collisions around a p -wave Feshbach resonance in the presence of quasi-two- and quasi-one-dimensional traps. In particular, Peng, Tan, and Jiang (2014) took into account the multiplet structure of the p -wave Feshbach resonance and studied within a zero-range model the impact of the relative orientation of the magnetic field with the trapping potentials on the collisional processes. In this manner, the experimentally (Günter *et al.*, 2005) observed spin alignment-dependent confinement-induced resonances for spin-polarized fermions were also verified theoretically by Peng, Tan, and Jiang (2014).

B. Confinement-induced resonances: Delving deeper

The previous discussion considered only a quasi-one-dimensional harmonic type of confinement for producing confinement-induced resonances. The rapid technological advances in laser trapping techniques have opened a new avenue that enables ultracold atoms to be confined in arbitrary geometries. From a theoretical viewpoint, this requires extensions of the boundaries of our understanding of confinement-induced physics to include more general types of trapping potentials. Many of the generalizations discussed in this section were reviewed by Blume (2012a) and Zinner (2012).

In this direction, Petrov, Holzmann, and Shlyapnikov (2000), Petrov and Shlyapnikov (2001), Idziaszek and Calarco (2006), and Pricoupenko (2008) considered ultracold collisions in the presence of quasi-two-dimensional traps. In particular, Petrov and Shlyapnikov (2001) studied bosonic collisions in pancake-shaped traps within the zero-range approximation. The pancake trap modifies the properties of 3D binary collisions yielding two-dimensional confinement-induced resonances. This particular type of resonance also fulfills a Fano-Feshbach scenario as do the quasi-one-dimensional resonances. However, due to the pancake geometry a confinement-induced resonance occurs when the two-body potential is not sufficiently deep to produce a true 3D universal bound state, i.e., where the corresponding free-space scattering length is negative. Again, this differs from the

quasi-one-dimensional confinement-induced resonances in the low-energy limit, which occur at positive values of the s -wave scattering length. The theoretical predictions of Petrov and Shlyapnikov (2001) were experimentally confirmed by Fröhlich *et al.* (2011). Fröhlich *et al.* (2011) explored the collisional aspects of a two-component Fermi gas in a pancake trap around a free-space Fano-Feshbach resonance. By employing radio-frequency techniques the molecule formation is measured on the negative side of Fano-Feshbach resonance.

Idziaszek and Calarco (2005) and Peng *et al.* (2010) studied confinement-induced resonances in the presence of an anisotropic waveguide, using a pseudopotential model of the two-body collisions. The anisotropy is induced by considering a transverse harmonic potential in the x - y plane, with different frequencies in the x and y directions. Theory suggests that the system in this type of geometry possesses only one confinement-induced resonance, whose position can be tuned by adjusting the confining frequency aspect ratio (Peng *et al.*, 2010). Moreover, similar conclusions emerged from Zhang and Zhang (2011) that considered a two-channel model for the short-range 3D interaction. The simple fact that an anisotropic harmonic waveguide exhibits only one confinement-induced resonance was not confirmed by the experiment of Haller *et al.* (2010). More specifically, Haller *et al.* (2010) conducted experiments on Cs atoms confined in quasi-one-to-quasi-two-dimensional traps. In the regime of anisotropic traps through atom loss measurements the corresponding observations showed signatures of *two* confinement-induced resonances.

The double peak feature was theoretically resolved by proposing two possible loss mechanisms. One was associated with multichannel inelastic processes (Melezhik and Schmelcher, 2011) and the second one was related to the mere fact that the trapping potential in Haller *et al.* (2010) exhibits an anharmonicity (Peng *et al.*, 2011; Sala, Schneider, and Saenz, 2012). The anharmonicity of the trap induces a coupling between the center-of-mass and relative degrees of freedom of the colliding pair. This coupling enables the two particles to form a molecule without requiring a third particle since the binding energy can be distributed to the center-of-mass degrees of freedom. After implementing these considerations in the theory, two confinement-induced resonances do indeed emerge which confirm the experimental observations of Haller *et al.* (2010). More recently, in order to pinpoint the physical origin of the double confinement-induced resonances, Sala *et al.* (2013) considered experiments with ${}^6\text{Li}$ atoms in an anharmonic waveguide. More specifically, in that experiment, the trapping potential was loaded with only two ${}^6\text{Li}$ atoms in the ground state of the external potential. Therefore, three-body effects as well as multichannel inelastic multichannel effects were excluded (Melezhik and Schmelcher, 2011). In this manner, a double peak structure was observed in atom loss measurements which are attributed to two confinement-induced resonances.

Dealing with ultracold collisions in arbitrarily shaped transversal potentials Zhang and Greene (2013) and Robicheaux, Giannakeas, and Greene (2015) developed theories based on local frame transformation theory, which can predict a broader class of confinement-induced resonances. These theoretical treatments also include two-body

collisions beyond s - or p -wave character. In addition, Robicheaux, Giannakeas, and Greene (2015) using ideas related to the Schwinger variational principle provided infinity-free calculations of scattering observables based on physical grounds and avoided the need for additional regularization schemes which were previously utilized in the pseudopotential approaches of Olshanii (1998), Petrov and Shlyapnikov (2001), and Granger and Blume (2004). However, in the treatments of Zhang and Greene (2013) and Robicheaux, Giannakeas, and Greene (2015) the center of mass is coupled with the relative degrees of freedom for particles of finite mass, so they have thus far only been applied in the limit of an infinitely massive particle which is struck by a much lighter one. Peano *et al.* (2005) considered the coupling of the center of mass in an arbitrary transversal potential, using the Green's function formalism to solve the corresponding Schrödinger equation directly in the laboratory frame. Apart from arbitrary quasi-one-dimensional potentials, Peano *et al.* (2005) considered also the case of two-component ultracold gases in harmonic traps where atoms have different polarizabilities; they therefore experience different harmonic oscillator confining frequencies which results in coupled center-of-mass and relative degrees of freedom. In both cases, Peano *et al.* (2005) theoretically predicted that the corresponding scattering observables should exhibit more than one resonant feature associated with the confinement-induced resonances. Similarly, Kim, Schmiedmayer, and Schmelcher (2005) developed a theory yielding only qualitative predictions since the Hilbert space associated with the closed-channel physics was not taken into account. This aspect, however, was taken into account by Melezhik and Schmelcher (2009) which predicted confinement-induced resonant molecular formation.

Massignan and Castin (2006) and Nishida and Tan (2008, 2010, 2011) focused on mixed-dimension collisions in ultracold gases under the assumption that different atomic species experience move in different numbers of spatial dimensions, such as when a 3D gas of atoms interacts with either different atoms or the same atoms in different internal states that are trapped in an optical lattice. Again, for this mixed-dimension system the center-of-mass and relative degrees of freedom are inherently coupled. The concept of mixed dimensionality arises from the fact that in a mixture of ultracold gas different particles, i.e., A and B species, experience different confinement frequencies. The confinement frequencies depend on each atom's polarizability and the laser frequency. Therefore, by adjusting the laser frequency at a zero of polarizability of one atomic species, i.e., A atoms, only the B atoms will experience the trapping potential. The proposed technique of Massignan and Castin (2006) and LeBlanc and Thywissen (2007) for species-selective dipole potentials was first realized by Catani *et al.* (2009). Nishida and Tan (2010) studied this idea by considering one atomic species, e.g., A atoms, to be totally unconfined, i.e., they move in three dimensions, while the B atoms are trapped in a tight spherical trap (a "zero dimension" configuration), a cigar-shaped (quasi-one-dimensional configuration) trapping potential, or a pancake-shaped trap (quasi-two-dimensional configuration). In addition, particles A and B are assumed to collide at small distances with s -wave interactions only. This gives rise to an infinite series of

a particular type of confinement-induced resonances which possess high orbital angular momentum character despite the fact that the two-body collisions are dominated by s -wave interactions (Massignan and Castin, 2006). This effect emerges from the combination of pure s -wave interactions and the fact that the two-body collisions take place in mixed dimensions which couples the angular momenta of the A and B atomic species. The theoretical predictions (Nishida and Tan, 2008, 2010) have apparently been observed by Lamporesi *et al.* (2010), who created a mixed-dimensional confinement of two ultracold atomic species, namely, ^{41}K and ^{87}Rb . The ^{41}K atoms are trapped in two dimensions whereas the ^{87}Rb atoms move in three dimensions, which is achieved by implementing species-selective dipole trapping techniques (Massignan and Castin, 2006; LeBlanc and Thywissen, 2007; Catani *et al.*, 2009). In this mixed-dimensional configuration Lamporesi *et al.* (2010) observed up to five resonances by measuring three-body losses, in good agreement with theoretical resonance positions.

Pair collisions within a three-dimensional optical lattice were theoretically investigated by Fedichev, Bijlsma, and Zoller (2004) and Cui, Wang, and Zhou (2010). Fedichev, Bijlsma, and Zoller (2004) utilized the tight-binding framework and assumed that the range of the two-body interactions is far smaller than the lattice spacing d and the size of the ground state in a lattice side ℓ_0 . Also the curvature within the lattice sites is approximated as a harmonic oscillator, which permits a decoupling of the center-of-mass and relative degrees of freedom. Furthermore, using the tight-binding model Fedichev, Bijlsma, and Zoller (2004) assumed that the effective mass of the particles is large enough such that the size of the ground state within the lattice site is small compared to the lattice spacing, whereas effects arising from higher Bloch bands were excluded. Based on these considerations Fedichev, Bijlsma, and Zoller (2004) predicted a confinement-induced resonance that occurs at negative values of the s -wave scattering length. The resonance condition simply reads $a_s \sim \ell^*$, where $\ell^* = \ell_0 \sqrt{D_0} / (4 \ln 2)$, with D_0 the tunneling amplitude to neighboring lattice sides in the lowest Bloch band. Köhl *et al.* (2005) conducted experiments on a degenerate Fermi gas in the presence of a three-dimensional optical lattice. They observed that the Feshbach resonance within the optical lattice exhibits an additional shift from the corresponding Feshbach resonance in the absence of the external potential, which verified the theoretical predictions of Fedichev, Bijlsma, and Zoller (2004). Cui, Wang, and Zhou (2010) extended the theoretical studies of Fedichev, Bijlsma, and Zoller (2004) and quantitatively described Bloch wave scattering at different lattice depths. Also, higher Bloch bands are taken into account as well as intraband effects which occur in the lowest Bloch band. Cui, Wang, and Zhou (2010) showed that in the case of true molecular states and at moderate lattice depths the higher Bloch band effects play crucial role since their neglect overestimates binding energies.

C. Synthetic spin-orbit coupled systems

Experimental and theoretical efforts on the confinement-induced physics in low-dimensional systems consider a regime where the two-body interactions are short ranged

and isotropic. Lifting the latter constraint permits us to generalize the concept of the confinement-induced resonances in physical systems which are mainly governed by anisotropic binary interactions.

The experimental realization of spin-orbit coupled Bose-Einstein condensates opens new avenues to explore the collisional aspects of such exotic systems. Developments in this rapidly evolving field have been reviewed by Williams *et al.* (2012) and Zhai (2015). For example, in free-space collisions, spin-orbit coupling yields a mixed-partial wave scattering process that alters the corresponding Wigner threshold law (Cui, 2012; Duan, You, and Gao, 2013; Wang and Greene, 2015). Zhang, Zhang, and Zhang (2012), Zhang and Zhang (2013), and Zhang, Song, and Liu (2014) studied the impact of reduced dimensionality on these physical systems in the presence of quasi-one- and quasi-two-dimensional traps.

In particular, Zhang, Song, and Liu (2014) considered resonant collisions of spin-orbit coupled cold atoms with Raman coupling in the presence of an axially symmetric harmonic waveguide. As a first-order approximation, effects due to the coupling of the center-of-mass and relative degrees of freedom are neglected by considering the case of zero center-of-mass momentum. Then the relative Hamiltonian, apart from the kinetic energy, two-body, and confinement potential terms, possesses two additional terms: (i) the spin-orbit coupling term $H_{\text{SOC}} = (\gamma k/m)(\sigma_2^x - \sigma_1^x)$ and (ii) the Raman coupling term $H_{\text{Raman}} = (\Omega/2)(\sigma_2^z + \sigma_1^z)$. $\sigma_{1,2}^i$ with $i = x$ and z represents the spin Pauli matrices for each particle, k indicates the relative kinetic energy, and m is the atom's mass. Ω represents the strength of the two-photon Raman coupling and $\gamma = 2\pi\hbar \sin(\theta/2)/\lambda$ indicates the spin-orbit coupling constant, where λ is the Raman laser wavelength and θ denotes the angle between the lasers.

Both spin-orbit and Raman coupling inherently influence the position of the resulting confinement-induced resonance. A confinement-induced resonance always exists regardless of the sign of the s -wave scattering length only in the case where the Raman coupling strength is less than the spin-orbit coupling strength, i.e., $\Omega < 2\gamma$. For strong Raman coupling, i.e., $\Omega \gg 2\gamma$ the position of the confinement-induced resonance occurs only at smaller values of the ratio a_s/a_\perp , namely, $a_s/a_\perp \sim 1/\sqrt{2\Omega}$. This provides in essence an extra means to manipulate the position of a CIR without the need of a Fano-Feshbach resonance to tune the magnitude of the 3D scattering length. Note that similar findings were also reported by Zhang and Zhang (2013).

D. Confined dipoles and dynamical CIR

Collisions of magnetic dipolar atoms or polar molecules pose another physical system whose two-body interactions are inherently anisotropic. The concept of confinement-induced resonances for anisotropic two-body interactions has been considered for both quasi-two- and quasi-one-dimensional waveguide geometries. Such dipolar systems hold particular interest in the many-body realm for their potential to create novel new topological phases of matter in addition to quantum information applications (Baranov, 2008; Baranov *et al.*,

2012). In a numerical study, Hanna *et al.* (2012) explored the impact of a pancake geometry on nonreactive polar molecules where despite the fact that the confining potential yielded broader resonances than the absence of a trap, the locations of the resonances are extremely sensitive to the dipole moment strength.

Apart from pancake geometries, the concept of dipolar confinement-induced resonances is also investigated in harmonic waveguides, i.e., in quasi-one-dimensional traps (Sinha and Santos, 2007; Bartolo *et al.*, 2013; Giannakeas, Melezhik, and Schmelcher, 2013) where the dipoles are aligned by an external field in a head-to-tail configuration. In particular, Giannakeas, Melezhik, and Schmelcher (2013) and Shi and Yi (2014) applied the local frame transformation theory and the pseudopotential techniques, respectively, showing the existence of a broad class of dipolar confinement-induced resonances which are characterized by mixed orbital angular momentum character due to the dipole-dipole interactions and the confinement.

Moreover, for s -wave dominated dipolar confinement-induced resonances their position depends linearly on the ratio of the length scale of dipolar forces over the trapping length scale, i.e., $\sim l_d/a_\perp$. Note that $(l_d, a_\perp) = (\mu d^2/\hbar^2, \sqrt{\hbar/\mu\omega_\perp})$, where μ indicates the reduced mass of the dipoles, d is the corresponding dipole moment, and ω_\perp indicates the confinement frequency. This linear dependence of position of the dipolar confinement-induced resonances on the ratio l_d/a_\perp means that the collisional properties of dipoles in the presence of a confinement can be controlled by adjusting the strength of an external field and confining potential frequency in a regime accessible by the experimental advances.

Furthermore, Shi and Yi (2014) showed that by tilting the relative orientation of the external electric field with respect to the longitudinal axis of the harmonic waveguide provides additional means to refine the tuning of dipolar confinement-induced resonance positions. Simoni *et al.* (2015) studied the case of reactive polar molecules in cigar-shaped traps. In more detail, Simoni *et al.* (2015) numerically studied the impact of the reduced dimensionality on elastic, inelastic, and reaction rates of collision of the reactive molecules in terms of the collisional energy and the strength of the dipole moments. The full four-body calculations are simplified by employing an asymptotic effective two-body model at large distances where the reactions are suppressed (Micheli *et al.*, 2010). The reaction physics is introduced through a JWKB-type boundary condition at short distances that accounts for atom exchange phenomena. By varying the angle of an external electric field with respect to the longitudinal direction of the trap, i.e., trap axis, it is observed that the reaction rate is greatly suppressed for angles normal to the trap's axis. For the case of a bosonic KRb molecule the reaction rate can only be efficiently suppressed under strong confinement without yielding any significant advantages over the reaction rate suppression in quasi-two-dimensional trapping geometries.

Photon-assisted confinement-induced resonances arise when there is a dynamical mechanism to enhance resonant collisions in the presence of a waveguide. Leyton *et al.* (2014) considered s -wave binary collisions in the presence of an rf driven harmonic waveguide whose confining frequency

modulation permits the separation of the center-of-mass degrees freedom. The resulting time-dependent Schrödinger equation is solved within a zero-range approximation, i.e., using a Bethe-Peierls boundary condition at the origin of the relative degrees of freedom. The rf modulation of the transversal frequency allows the two counterpropagating atoms to perform a transition from the continuum state to the confinement-induced molecular state by emitting one or multiple photons. This dynamical mechanism of photon-assisted confinement-induced resonances can result in a series of resonant features for a given number of photons.

E. Inelastic few-body collisions in 1D

An intriguing implication of the exact integrability of the 1D Schrödinger equation for N equal mass particles that experience zero-range two-body potentials and the existence of an analytically known solution due to McGuire (1964) is that there are no inelastic collisions. One way to understand this is that every time two particles collide, the final state of the two particles in momentum space is kinematically identical to the initial state, since transmission and reflection are indistinguishable. While the absence of all inelasticity including three-body recombination for this system is straightforwardly clear, given the exact solution of McGuire (1964), it is far from obvious how the inelasticity turns out to vanish when studied in the adiabatic hyperspherical representation. One way all inelasticity would vanish for a system would be if the hyperradial degree of freedom in the Schrödinger equation turns out to be exactly separable, because in that case all nonadiabatic coupling matrices would vanish. It is not that simple, however, in the case of identical 1D bosons with zero-range interactions, because the nonadiabatic coupling matrices are nonzero. Hence, the different adiabatic hyperspherical channels are coupled, at least locally. This issue was explored by Mehta and Shepard (2005), who numerically solved the coupled hyperradial equations that described atom-dimer scattering.

Later, three-body recombination was calculated in this 1D identical boson system both for the zero-range potential case and for a finite-range potential by Mehta, Esry, and Greene (2007), again using the adiabatic hyperspherical representation. That study confirmed as well that there is no inelasticity, i.e., vanishing three-body recombination rate coefficient. In the hyperspherical representation, the recombination rate and the rates of all other inelastic processes vanish because there is complete destructive interference in the zero-range limit. For a 1D potential of finite range L , however, the study showed how the recombination rate increases for nonzero $L > 0$. The near-threshold behavior of the recombination rate is of interest for 1D and quasi-1D experiments, and it was demonstrated by Mehta, Esry, and Greene (2007) that three identical particles have the same threshold behavior $K_3^{1D} \propto k^7$ regardless of whether the particles are spin-polarized fermions or bosons. For three identical bosons, in particular, this study showed more concretely that in strict 1D, $K_3^{1D} = C(L)(\hbar k/\mu)(ka)^6$, where k is the 1D wave number and a is the 1D two-body scattering length. Experimental evidence is quite limited on this topic, but the results measured to date by Tolra *et al.* (2004) appear not to have reached a regime very close to the strict 1D results and are

probably better viewed as probes of the crossover regime between 1D and 3D or between 1D and 2D.

F. 2D, quasi-2D systems, and the super-Efimov effect

Two-dimensional systems in both few-body and many-body physics exhibit rich and fascinating behavior, involving logarithmic dependences of nearly all quantities that depend on distance and energy. In many-particle condensed-matter systems, prototypical phenomena that have generated extensive interest include the Berezinskii-Kosterlitz-Thouless (BKT) transition (Berezinskii, 1971; Kosterlitz and Thouless, 1973; Thouless *et al.*, 1982) relating to the formation and binding of 2D vortices, and of course the fractional quantum Hall effect (Stormer, Tsui, and Gossard, 1999). Underlying the theoretical description of striking many-body phenomena in 2D are the effective two-body and three-body interactions that are modified when a three-dimensional gas is squeezed into a pancake-shaped trap geometry.

The modification of the 3D atom-atom scattering information into an effective 2D interaction was addressed by Wódkiewicz (1991) and Kanjilal and Blume (2006), with a more comprehensive list of references in Dunjko *et al.* (2011b). Implications of 2D confinement for three-body recombination and for the formation of many-body phases were treated by Petrov, Holzmann, and Shlyapnikov (2000) for a gas consisting of particles with finite-range interactions. The three-body problem in 2D for short-range interactions has recently been examined in a hyperspherical coordinate framework by D’Incao and Esry (2014) and D’Incao, Anis, and Esry (2015), including a nonperturbative study of three-body recombination in that geometry. Two-body dipole-interacting particles in a 2D or quasi-2D gas are treated in many publications, two of which are Kanjilal, Bohn, and Blume (2007) and D’Incao and Greene (2011). The intriguing many-body phenomena that arise in dipolar systems have received extensive theoretical and experimental attention, as was reviewed by Baranov (2008) and Baranov *et al.* (2012).

One class of few-body treatments in two dimensions relates to fractional quantum Hall droplets having modest numbers of particles, typically from 3 to 10 electrons, or in the ultracold physics context, atoms or polar molecules. A few such explorations in recent years can be found by Daily, Wooten, and Greene (2015), Rittenhouse, Wray, and Johnson (2016), and Wooten, Yan, and Greene (2017), which are just a sampling of the work that followed Laughlin (1983) on three 2D electrons in a perpendicular magnetic field. A degenerate perturbation theory treatment of semiconductor quantum dots in a strong magnetic field, which has numerous cases that can serve as useful benchmark calculations for comparison with few-body theory, can be found in Jeon, Chang, and Jain (2007).

A provocative few-body prediction in recent years has been the super-Efimov effect, which deals with bound states of three p -wave interacting fermions in 2D (Nishida, Moroz, and Son, 2013; Gridnev, 2014; Moroz and Nishida, 2014; Volosniev *et al.*, 2014; Gao, Wang, and Yu, 2015). The interactions are assumed in the derivation of this effect to have a finite range, and each interacting pair in the trimer is assumed to have a zero-energy bound state in the symmetry with $|L_z| = 1$, also referred

to as a resonant p -wave interaction. The resulting trimer energy level formula predicted in this case takes the double-exponential form $E_n \propto \exp[-2e^{3\pi n/4+\theta}]$, where θ is a nonuniversal constant defined modulo $3\pi/4$. Because the size of these super-Efimov states grows so rapidly with n , and also the successive binding energies shrink dramatically as n increases, these will be challenging to observe experimentally. Whereas the successive energy levels in the ordinary homonuclear Efimov effect are less bound by a factor of 515, the corresponding ratio in the super-Efimov effect exceeds 10^9 . More promising than the homonuclear systems are heavy-heavy-light heteronuclear trimers, whose super-Efimov states can display a more favorable scaling (Moroz and Nishida, 2014) as is also the case in the ordinary Efimov effect for heteronuclear trimers. Another exploration of heavy-heavy-light trimers in 2D with resonant p -wave interactions is based on the conventional Born-Oppenheimer approximation (Efremov *et al.*, 2013).

Recently, a theoretical treatment by Nishida (2017) introduced the “semi-super-Efimov effect.” This is in a system of four bosons in 2D, which exhibit a different scaling possible for an infinite pattern of energy levels and state sizes, in a scenario where the three-boson interactions are resonant but the two-body interactions are negligible. In the semi-super-Efimov case, the state sizes are predicted to scale with the integer quantum number $n > 0$ in proportion to $\exp[(\pi n)^2/27]$.

The theory of the quasi-2D homonuclear three-boson problem was treated in detail by Levinsen, Massignan, and Parish (2014) and Yamashita *et al.* (2015). This topic is also sometimes referred to as the crossover from 3D to 2D. This study demonstrated how the finite number of universal three-body states in 2D, where there is no true Efimov effect (Bruch and Tjon, 1979; Nielsen *et al.*, 2001; Nishida and Tan, 2011), connects with true Efimov states in 3D as one varies the degree of confinement in the transverse dimension. Three fermions in 2D are also treated theoretically by Ngampruetikorn, Parish, and Levinsen (2013), by solving the STM integral equation (Skorniakov and Ter-Martirosian, 1957).

VI. FEW-BODY PHYSICS IN NUCLEAR AND CHEMICAL SYSTEMS

In previous sections, the current state of the art of few-body ultracold atomic physics was presented, with an extended discussion of universality in three-body and four-body physics. However, the domain of few-body physics extends beyond atomic systems, reaching many different branches of physics such as chemistry or nuclear or particle physics, among others. Indeed, few-body physics was born in nuclear physics motivated by the seminal paper of Thomas (1935), as previously pointed out.

The premise of long de Broglie wavelength effective field theory is that for the low-energy physics of a few- or many-body system below a certain characteristic energy scale, the behavior of the system should not be sensitive to the details of the Hamiltonian at distances much less than λ . Indeed, the physics behind such behavior is closely related to the concept of renormalization group theory (Wilson, 1971, 1983; Wilson and Kogut, 1974). One of the best pedagogical introductions to the strategy of systematically building in the correct long

wavelength physics was presented by Lepage (1989, 1997) in the context of nonrelativistic Schrödinger quantum mechanics. In fact, the concept of effective field theory was spawned by the seminal work of Weinberg that attempted to understand the role of pion exchange in nuclear forces (Weinberg, 1979, 1990, 1991). Example applications to Efimov physics and related few-body systems have been developed in detail by Braaten and Hammer (2006). Other studies that utilize model two-body and three-body Hamiltonians that produce key information such as the low-energy two-body scattering length and effective range are making use of the spirit of low-energy effective field theories even when they proceed via a more direct solution of the few-body Schrödinger equation. Note that trions, excitons, and biexcitons occur as few-body problems in semiconductor physics, as discussed by Patton, Langbein, and Woggon (2003).

This section is devoted to the study of major developments in few-body physics relevant for nuclear physics and chemistry. The few-body physics in chemical sciences will be presented through classical trajectory calculations in hyperspherical coordinates involving neutrals and charged particles.

A. Hyperspherical methods in nuclear physics

The adiabatic hyperspherical technique was introduced in previous sections of this review, with examples of its methodology and applications in the field of atomic and molecular collisions. Reiterating, the basic idea behind this method is to reduce a complex multidimensional problem into a set of coupled second-order ordinary differential equations in a single variable. The same idea can of course be applied in a field with tremendously different energy and length scales: nuclear physics, where the nature of the nucleon-nucleon and related interactions exhibit all the complexities of the strong nuclear force. For instance, both exotic nuclear systems and the three-nucleon problem, to name two classes of problems, have been studied using the adiabatic hyperspherical representation.

In nuclear physics the adiabatic hyperspherical technique follows the same scheme as previously presented: the first step involves a solution of the hyperangular equation where the hyperradius R is treated as a parameter, thereby giving hyperspherical potential energy curves and couplings. Then, these are employed to solve a set of coupled ordinary differential equations in the radial coordinate. With this strategy one can tackle the few- or many-nucleon interaction problem at different levels of sophistication. For instance, the cosmologically important reaction of three alpha particles to form ^{12}C via the intermediate Hoyle state was treated within the coupled-channel adiabatic representation by Alvarez-Rodriguez *et al.* (2007, 2008) and Suno, Suzuki, and Descouvemont (2015). The calculation of hyperspherical potential curves and couplings by Suno, Suzuki, and Descouvemont (2015) was based on a binary $\alpha - \alpha$ model Hamiltonian that accurately describes the ^8Be resonance state, and a three-body term was chosen to represent some experimentally known properties of ^{12}C such as some particular energy levels. The final calculation gives a good energy and width in agreement with experimental values for the $J_\pi^\pi = 0_2^+$

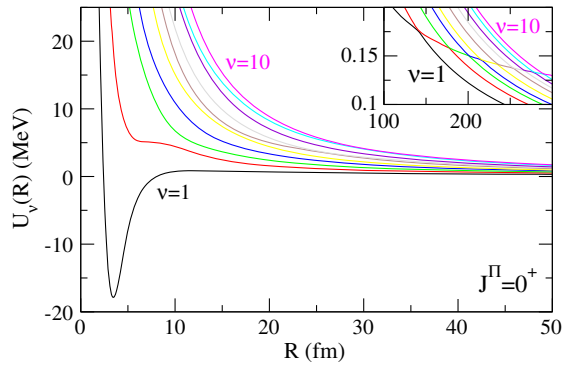


FIG. 23. Adiabatic hyperspherical potential curves computed for the triple- α system for the $J^\pi = 0^+$ symmetry which contains the famous Hoyle resonance thought to be important in nucleosynthesis. Inset: the adiabatic potential curves at large hyper-radius. From Suno, Suzuki, and Descouvemont, 2015.

Hoyle resonance state. The relevant adiabatic hyperspherical potential curves are shown in Fig. 23.

Note that when this technique is applied to few-nucleon systems, one must keep in mind the distinctively different nature of the nucleon-nucleon forces compared to the atom-atom interactions. This difference comes from the fact that nuclear collisions can be understood to first order as resulting from the exchange of virtual pions between nucleons. In this sense, pions (π) can be viewed as the *quanta* of the nuclear force, and since they represent a massive scalar field their influence is associated with a Yukawa potential $e^{-m_\pi r}/4\pi r$ (Weinberg, 1991). Indeed, the nucleon-nucleon potential can be modeled using an effective field theory based on the exchange of pions. This exchange leads to new and complicated interaction terms in the nucleon-nucleon potential, among them, the tensor interaction reads

$$V(\mathbf{r}_{ij}) = V_i(r_{ij})(\boldsymbol{\tau}_i \cdot \boldsymbol{\tau}_j) \left[3 \frac{(\boldsymbol{\sigma}_i \cdot \mathbf{r}_{ij})(\boldsymbol{\sigma}_j \cdot \mathbf{r}_{ij})}{r_{ij}^2} - \boldsymbol{\sigma}_i \cdot \boldsymbol{\sigma}_j \right], \quad (81)$$

where $\boldsymbol{\sigma}_i$ and $\boldsymbol{\tau}_i$ represent the nuclear spin and isospin of nucleon i , respectively. For a more detailed modern view of the nucleon-nucleon forces, including pionless theories and chiral effective field theory, see Epelbaum, Hammer, and Meissner (2009).

The very complicated nature of the nucleon-nucleon interaction does not prevent the success of the adiabatic hyperspherical technique in nuclear physics, indeed hyperspherical coordinates were applied in the context of nuclear physics by Delves (1960) and Smith (1960) to study three-body nuclear systems (Levinger, 1974; Valliers, Das, and Coelho, 1976; Fang and Tomusiak, 1977; Verma and Sural, 1979). Those studies, however, did not implement the adiabatic formulation and thus could not benefit from its insights and accelerated convergence. Hyperspherical methods were also applied to exotic nuclei, such as the hypertriton, and complex nuclei by including realistic nucleon-nucleon potentials (Verma and Sural, 1979, 1982; Clare and Levinger, 1985). The potential employed included the tensor interaction and many other components of the nucleon-nucleon force. In general, many

theorists preferred to work with a set of coupled integral equations instead of coupled differential equations, which can be regarded as a procedure different from the adiabatic hyperspherical machinery most frequently adopted in atomic physics. More recently, however, the adiabatic hyperspherical approach has been employed to compute the triton bound state energy (Daily, Kievsky, and Greene, 2015) in a convergence exploration, using realistic nucleon-nucleon potentials with a three-body force as well. Other systems that have been considered include exotic species such as kaonic clusters involving three and four particles (Kezerashvili, Tsiklauri, and Takibayev, 2015).

B. Universality in nuclear systems

As previously discussed, the nuclear forces are fundamentally different from the interactions in the context of ultracold atomic physics, since they derive from the electromagnetic interaction. Therefore, due to the very strong and short-ranged nature of the nuclear interactions, some aspects of universality can be expected to differ in nuclear systems compared with atomic and molecular species. In particular, some nuclear systems form halo nuclei (Zhukov, 1993; Tanihata, 1996; Cobis, Fedorov, and Jensen, 1998; Jensen *et al.*, 2004), which is a nuclear bound state formed by a tightly bound core and one or two valence nucleons. These valence nucleons are characterized to have a very small binding energy in comparison with the binding energy of the core nucleons, which is reflected in a highly extended bound state wave function. For this reason, halo nuclei exhibit very large radii compared to the core radius. The most familiar example of a halo nucleus is the deuteron, with an average neutron-proton separation of 3.1 fm that is 3 times larger than both the size of its component nucleons and the range of their interaction potential (both ≈ 1 fm). While halos also exist in atomic and molecular physics, they are far more prevalent in nuclear systems, with many studies even in large or medium-sized nuclei; see, for instance, Hove *et al.* (2014, 2016) and references therein. In fact, Efimov physics can be relevant to describing aspects of the wave function of a medium-sized nucleus such as ^{62}Ca with two outlying nucleons (Hagen *et al.*, 2013). Nevertheless this type of system exemplifies the *Efimov-unfavored scenario* with two light particles and one heavier particle discussed by Wang, Wang *et al.* (2012); based on the arguments presented there, it is unlikely that a “true Efimov state” exists in such systems.

Halo nuclei with two valence nucleons represent a good playground for three-body physics, since these nuclear systems are potential candidates to exhibit some properties associated with Efimov physics despite being Efimov unfavored. These nuclides are found in the bottom of the neutron drip line, the line that describes the boundary beyond which the neutron-rich nuclides are unstable. Among the different kinds of two-nucleon halo nuclei, the Borromean² halo nuclei

²The term Borromean is associated with the coat of arms of the house of the Borromeo family in northern Italy, which consists of three interlayer rings. In particular, the symbol appears in the left escutcheon of the coat of arms. However, a similar symbol involving three triangles was already used in Norse mythology around the 7th century.

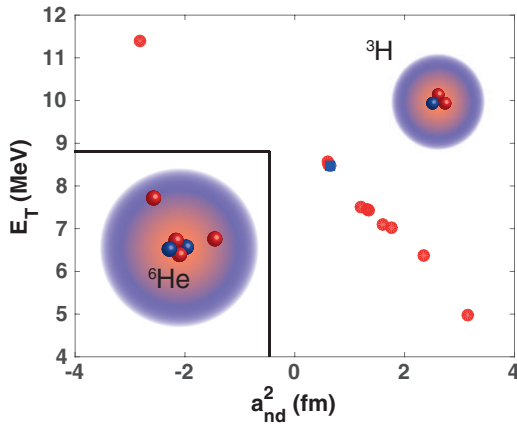


FIG. 24. Phillips plot for the triton energy E_T as a function of the doublet nd scattering length a_{nd}^2 . The red dots stand for different theoretical calculations based on different kinds of two-body and three-body interactions (Benayoun, Cignoux, and Chauvin, 1981; Friar *et al.*, 1984; Fedorov and Jensen, 2002), whereas the blue square represents the experimental result. For a more detailed presentation of the Phillips plot for the triton, see Efimov and Tkachenko (1988). Inset: schematic representation of a halo nuclei with two valence nucleons, namely, ${}^6\text{He}$.

have received special attention since these have a three-body bound state, despite the fact that none of the two-body subsystems are bound. The most studied Borromean halo nuclei to date have been ${}^6\text{He}$ and ${}^{11}\text{Li}$ (Zhukov, 1993; Tanihata, 1996). A schematic representation of one such nucleus is shown in the inset of Fig. 24, concretely for ${}^6\text{He}$. In this case, the core is an α particle and the two valence nucleons are neutrons.

On the other hand, three-body bound states in some nuclear systems show a universal behavior: a correlation between the dimer-nucleon scattering length and the nucleon trimer binding energy, which is known as the Phillips line (Phillips, 1968). This correlation is independent of the model employed for the calculations: such as a two-body contact interaction, three-body interaction terms, and it should also be present regardless of the method employed, i.e., an effective field theory approach, adiabatic hyperspherical treatment, or low-energy Faddeev equations. Figure 24 presents a Phillips plot for the triton including different theoretical results as well as the experimental data. This figure exhibits a linear correlation between the triton binding energy and the doublet neutron-deuteron scattering length a_{nd}^2 . However, other kinds of correlation may occur in different three-body nuclear bound states (Fedorov and Jensen, 2002).

At least two halo nuclei have been seen as potential candidates to exhibit Efimov universality. However, the universality can be claimed convincingly only if the different excited state of the three-body system follows the predicted scaling law by Efimov, and those are not experimentally accessible by any currently existing capabilities. For instance in the case of ${}^6\text{He}$, which is also Borromean, it has been proven that a p -wave resonance exists in the $J = 3/2$ channel of $n - \alpha$ scattering which explains the nature of the three-body bound state. However, in the 1990s Fedorov, Jensen, and Riisager (1994) and Amorim, Frederico, and Tomio (1997)

explored the Efimov character of several halo nuclei, assuming that the ground state is also an Efimov state. Their study suggested that ${}^{20}\text{C}$ is the only halo nucleus candidate that has appreciable Efimov state character, other than the triton.

Apart from normal nuclei, namely, those that appear in the table of nuclides, there other hypernuclei that contain strange quarks and are the so-called strange nuclei. Some of these are classified as halo nuclei, and among them the simplest case is the hypertriton ${}^3_{\Lambda}\text{H}$: a three-body bound state formed by a neutron, a proton, and the Λ^0 . The Λ^0 is the lightest Λ hyperon, a neutrally charged baryon similar to a neutron but slightly heavier, and its quark structure is uds ; it has a strangeness of -1 . The total binding energy of ${}^3_{\Lambda}\text{H}$ is ≈ 2.4 MeV (Fujiwara *et al.*, 2008), whereas its breakup energy is ~ 0.14 MeV (Fujiwara *et al.*, 2008), which is very small in comparison with the binding energy of the deuteron 2.22 MeV, and hence it can be considered as a two-nucleon halo nucleus. Indeed, it was extensively studied (Gongleton, 1992; Cobis, Jensen, and Fedorov, 1997; Fedorov and Jensen, 2002). All of these studies suffer, however, from needing better experimental information concerning the n - Λ scattering length, so these works might be considered as qualitative or semiquantitative approaches to the Efimov nature of the hypertriton. Nevertheless, new data coming from ALICE and STAR may help to better understand the nature of the n - Λ interaction, as well as to yield more accurate measurements of the lifetime of ${}^3_{\Lambda}\text{H}$ (Abelev *et al.*, 2010; Zhu, 2013; ALICE Collaboration, 2016). On the other hand, a good understanding of the hyperon-nucleon interaction is needed for a proper understanding of high-density matter systems, such as neutron stars (Lattimer and Prakash, 2004; Weber *et al.*, 2007; Vidaña, 2013; Lonardonì, Pederiva, and Gandolfi, 2014).

In nuclear systems, universal properties in the four-body sector can be identified. The clearest example is the case of the Tjon line (Tjon, 1975): a correlation between the binding energy of the α particle and the triton binding energy that persists across nearly all nucleon interaction models; in particular, this correlation is approximately linear. The origin of the Tjon correlation can be explained as an approximate independence of the four-body energy level spectrum on any four-body parameter. In other words, the Tjon analysis suggests that there is no need for a four-body parameter for the renormalization at leading order in the four-body sector (Platter, Hammer, and Meißner, 2004, 2005), for energy levels in the universal regime. However, higher order corrections break the expected correlation leading to a band with some scatter depending on the short-range physics, instead of a simple, well-defined line (Nogga, Kamada, and Glöckle, 2000).

C. Few-body physics and universality in chemistry

Traditionally the term *few-body physics* has been employed in nuclear physics, and subsequently it became adopted in the context of atomic physics, especially in ultracold atomic systems (Hess *et al.*, 1983, 1984; de Goey *et al.*, 1986; Fedichev *et al.*, 1996; Burt *et al.*, 1997; Esry, Greene, and Burke, 1999; Suno, Esry, and Greene, 2003a; Weber *et al.*,

2003). However, in chemical physics it has not been the case, even though chemical physics studies hinge on our understanding of few-body physics. And of course a deep understanding of fundamental processes in chemical physics is frequently needed in other fields of physics and chemistry, notably in astrophysics, such as the three-body recombination of hydrogen in stellar formation (Flower and Harris, 2007; Forrey, 2013); in theoretical chemistry: transport coefficients in gases (Hirschfelder, Curtiss, and Bird, 1954; Snider, 1960; Mason and Monchick, 1962; Wang-Chang, Uhlenbeck, and deBoer, 1964; Köhl and Schaefer, 1983; McCourt *et al.*, 1991; Montero and Pérez-Ríos, 2014), reactive and nonreactive scattering (Shui, 1972; Child, 1974; Truhlar and Muckerman, 1975; Levine and Bernstein, 1987) and three-body recombination (Mansbach and Keck, 1969; Robicheaux, 2006; Ermolova, Rusin, and Sevryuk, 2014), dissociative recombination of H_3^+ (Kokoouline, Greene, and Esry, 2001; Kokoouline and Greene, 2003; Petrigiani *et al.*, 2011); plasma physics (Zhdanov, 2002); and in cold chemistry (Willitsch *et al.*, 2008; Hall and Willitsch, 2012; Härter *et al.*, 2012, 2013; Willitsch, 2012; Härter and Denschlag, 2014; Krüchow *et al.*, 2016). Some of these characteristic and fundamental processes in chemical physics are reviewed from a few-body perspective in the present section, in particular, those involving three-body processes, such as three-body recombination. Special emphasis will be given to universality in three-body recombination processes which are relevant to hybrid trap experiments.

Three-body processes can be viewed as a chemical reaction that converts three free atoms (or molecules or other particles) into diatomic molecules in the absence of external fields, i.e., the reaction $A + A + A \rightarrow A_2 + A$. One of the first theoretical treatments of this reaction was developed by Keck (1960, 1967) using a variational principle following a very early approach proposed by Wigner (1937). In particular, an upper bound for the three-body recombination rate was computed by dividing regions of phase space by a trial surface that acts as the boundary between reactants and products; this is now denoted the phase-space theory of reaction rates. Almost in parallel, Smith (1962) developed a more microscopic treatment for three-body recombination, and later Shui, Appleton, and Keck (1970) extended the previous theory of Keck, applying this theory to the recombination of nitrogen. An application to the recombination of hydrogen (Shui, 1972, 1973) found fair agreement with the fairly crude early experiments.

The phase-space theory of reaction rates was introduced by Keck (1960) and an alternative was presented by Smith (1962). Next, the mathematical foundations of a recent approach to calculation of classical three-body recombination rates are presented, after which applications to different systems involving neutrals as well as charged particles will be reviewed. Classical trajectory calculations in hyperspherical approach have been employed to derive different classical Newtonian threshold laws, which are reviewed here, with special emphasis on their universality.

1. General classical treatment of few-body collisions

Classically, a two-body collision is envisioned as one particle with a definite momentum moving toward a scattering

center. The cross section is defined as an effective area on the plane perpendicular to the initial momentum of the incoming particle which contains the scattering center (Levine and Bernstein, 1987). In classical mechanics, the scattering cross section is determined in terms of the scattering probability for a given value of the impact parameter \mathbf{b} . Recall that \mathbf{b} is defined as the component of the position vector which is perpendicular to the momentum vector of the incoming particle at infinite distance.

The concept of a two-body collision cross section is readily generalized to an arbitrary number (n) of dimensions. In particular, the cross section is defined as the effective scattering volume of the $n - 1$ hyperplane perpendicular to the initial momentum of the incoming particle, for a given impact parameter \mathbf{b} and initial momentum \mathbf{P}_0 :

$$\sigma_{\text{process}}(\mathbf{P}_0) = \int \wp_{\text{process}}(\mathbf{b}, \mathbf{P}_0) d^{n-1}\mathbf{b}. \quad (82)$$

Here the opacity function $\wp_{\text{process}}(\mathbf{b}, \mathbf{P}_0)$ is the probability that a trajectory with particular initial conditions leads to the collisional process under investigation, e.g., an inelastic collision, or formation of a particular product, etc.

The classical dynamics of a few-body system can be obtained by recasting the degrees of freedom of the system at hand d as a two-body collision in a d -dimensional space, as shown in Fig. 25. This figure represents the usual case where the center-of-mass motion is decoupled from the relative motion of the interacting particles. In this picture the three-body recombination cross section is written

$$\sigma_{\text{rec}}(P_0) = \frac{\int \wp_{\text{rec}}(\mathbf{b}, \mathbf{P}_0) d\Omega_{P_0}^6 d\Omega_b^5 b^4 db}{\int d\Omega_{P_0}^6}, \quad (83)$$

where the quantity $d\Omega_{P_0}^6$ represents the differential element associated with the hyperangles of the initial momentum \mathbf{P}_0 . In Eq. (83) the averaging over the degrees of freedom associated with the initial momentum is shown explicitly,

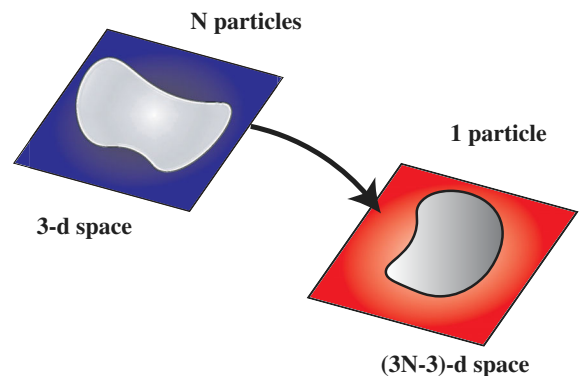


FIG. 25. Schematic representation of a general classical treatment of few-body collisions. The method is based on the mapping of the degrees of freedom of the system at hand into a problem involving a single effective particle moving in higher dimensional space, in particular, the dimension (n) is equal to the number of independent relative coordinates of the system.

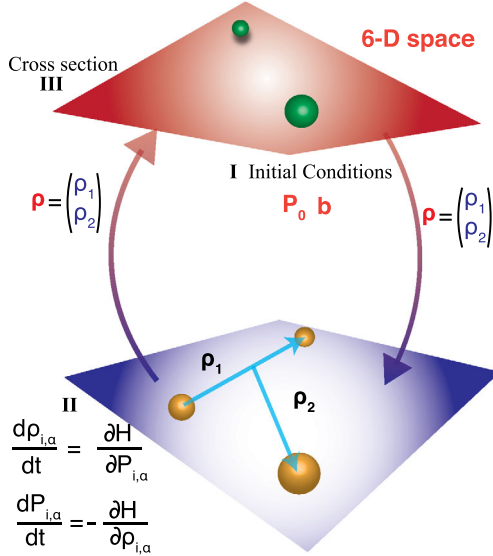


FIG. 26. Schematic representation of the method developed for treating three-body collisions. We start with the description of the initial conditions in the 6D space associated with the three-body problem at hand. Then, as indicated in step I, the initial conditions are transformed into the coordinates associated with the three-body problem in the usual 3D space. Step II represents the solution of the Hamilton's equations of motion in the 3D space. Finally, by means of step III, the results are transformed back into the 6D space, where the cross section is calculated.

whereby the final average cross section depends only on the energy.

2. Classical trajectory calculations in hyperspherical coordinates

The classical Hamiltonian for three particles with masses m_1 , m_2 , and m_3 moving in a given potential energy landscape $V(\mathbf{r}_1, \mathbf{r}_2, \mathbf{r}_3)$ is

$$H = \frac{\mathbf{p}_1^2}{2m_1} + \frac{\mathbf{p}_2^2}{2m_2} + \frac{\mathbf{p}_3^2}{2m_3} + V(\mathbf{r}_1, \mathbf{r}_2, \mathbf{r}_3), \quad (84)$$

where \mathbf{p}_i and \mathbf{r}_i represent the momentum and the vector position of the i th particle, respectively. This Hamiltonian can be recast in terms of the Jacobi coordinates $(\boldsymbol{\rho}_1, \boldsymbol{\rho}_2)$ depicted in Fig. 26 as in (Karplus, Porter, and Sharma, 1965)

$$H = \frac{\mathbf{P}_1^2}{2m_{12}} + \frac{\mathbf{P}_2^2}{2m_{3,12}} + \frac{\mathbf{P}_{\text{CM}}^2}{2M} + V(\boldsymbol{\rho}_1, \boldsymbol{\rho}_2). \quad (85)$$

Here

$$\frac{1}{m_{12}} = \frac{1}{m_1} + \frac{1}{m_2},$$

$$\frac{1}{m_{3,12}} = \frac{1}{m_3} + \frac{1}{m_1 + m_2},$$

$V(\boldsymbol{\rho}_1, \boldsymbol{\rho}_2)$ is the potential energy in terms of the relative Jacobi coordinates with the c.m. momentum a separated constant of

motion. \mathbf{P}_1 , \mathbf{P}_2 , and \mathbf{P}_{CM} represent the canonical momenta conjugate to $\boldsymbol{\rho}_1$, $\boldsymbol{\rho}_2$, and $\boldsymbol{\rho}_{\text{CM}}$, respectively. Finally, the relative Hamiltonian is

$$H = \frac{\mathbf{P}_1^2}{2m_{12}} + \frac{\mathbf{P}_2^2}{2m_{3,12}} + V(\boldsymbol{\rho}_1, \boldsymbol{\rho}_2). \quad (86)$$

For three particles, the Hamilton equations of motion can be expressed in terms of Jacobi coordinates and momenta as follows:

$$\frac{d\rho_{i,\alpha}}{dt} = \frac{\partial H}{\partial P_{i,\alpha}}, \quad (87a)$$

$$\frac{dP_{i,\alpha}}{dt} = -\frac{\partial H}{\partial \rho_{i,\alpha}}, \quad (87b)$$

where $i = 1, 2$ and $\alpha = x, y,$ and z label the Cartesian coordinates of each Jacobi vector. Upon adopting the representation of Smith (1962), a 6D position vector is constructed from the two mass-weighted Jacobi vectors as

$$\boldsymbol{\rho} = \begin{pmatrix} \sqrt{\frac{m_{12}}{\mu}} \boldsymbol{\rho}_1 \\ \sqrt{\frac{m_{3,12}}{\mu}} \boldsymbol{\rho}_2 \end{pmatrix}, \quad (88)$$

where

$$\mu = \sqrt{\frac{m_1 m_2 m_3}{M}}.$$

On the other hand, an equivalent 6D vector position can be expressed in terms of the bare Jacobi vectors as (Pérez-Ríos *et al.*, 2014)

$$\boldsymbol{\rho}_{\text{bare}} = \begin{pmatrix} \boldsymbol{\rho}_1 \\ \boldsymbol{\rho}_2 \end{pmatrix}. \quad (89)$$

Similarly the canonical momenta are given by

$$\mathbf{P} = \begin{pmatrix} \mathbf{P}_1 \\ \mathbf{P}_2 \end{pmatrix} \quad (90)$$

and

$$\mathbf{P}_{\text{bare}} = \begin{pmatrix} \sqrt{\frac{\mu}{m_{12}}} \mathbf{P}_1 \\ \sqrt{\frac{\mu}{m_{3,12}}} \mathbf{P}_2 \end{pmatrix}, \quad (91)$$

respectively. It can be shown that the relation between the coordinates $(\boldsymbol{\rho}, \mathbf{P})$ and $(\boldsymbol{\rho}_{\text{bare}}, \mathbf{P}_{\text{bare}})$ defines a canonical transformation (Whittaker, 1937; Landau and Lifshitz, 1976; Maslov and Fedoriuk, 1981), and hence both sets of coordinates will describe the same phase-space volume. In other words, the scattering observables will be the same for either of these sets of coordinates, as one would expect. The 6D position vector $\boldsymbol{\rho}$ or $\boldsymbol{\rho}_{\text{bare}}$ links the three-body problem in

3D and the single particle problem in 6D, as schematically presented in Fig. 26.

In the present approach the mass-weighted 6D vector position ρ will be employed, with a minor difference from the conventions utilized by Pérez-Ríos *et al.* (2014). Then the Hamiltonian is

$$H = \frac{\mathbf{P}^2}{2\mu} + V(\rho). \quad (92)$$

Now that the position and the momentum vectors have been defined in this 6D space, the concept of an impact parameter as the projection of the position vector onto a hyperplane perpendicular to the initial momentum is clear. We implement hyperspherical coordinates for the representation of the 6D vectors. In particular, it is convenient to implement Avery's definition of the hyperangles (Avery, 1989), where all the vectors can be represented by means of their magnitude r and five different hyperangles (α_i , $i = 1, 2, 3, 4$, and 5) as

$$\mathbf{r} = \begin{pmatrix} r_{x_1} \\ r_{x_2} \\ r_{x_3} \\ r_{x_4} \\ r_{x_5} \\ r_{x_6} \end{pmatrix} = \begin{pmatrix} r \sin \alpha_1 \sin \alpha_2 \sin \alpha_3 \sin \alpha_4 \sin \alpha_5 \\ r \cos \alpha_1 \sin \alpha_2 \sin \alpha_3 \sin \alpha_4 \sin \alpha_5 \\ r \cos \alpha_2 \sin \alpha_3 \sin \alpha_4 \sin \alpha_5 \\ r \cos \alpha_3 \sin \alpha_4 \sin \alpha_5 \\ r \cos \alpha_4 \sin \alpha_5 \\ r \cos \alpha_5 \end{pmatrix}. \quad (93)$$

Here the ranges of each angle are $0 \leq \alpha_1 \leq 2\pi$, $0 \leq \alpha_i \leq \pi$, $i = 2, 3, 4$, and 5. In particular, choosing the 3D z axis parallel to \mathbf{P}_2 expresses the initial momentum \mathbf{P}_0 as

$$\mathbf{P}_0 = \begin{pmatrix} P_0 \sin \alpha_1^P \sin \alpha_2^P \sin \alpha_5^P \\ P_0 \cos \alpha_1^P \sin \alpha_2^P \sin \alpha_5^P \\ P_0 \cos \alpha_2^P \sin \alpha_5^P \\ 0 \\ 0 \\ P_0 \cos \alpha_5^P \end{pmatrix}, \quad (94)$$

where $0 \leq \alpha_1^P \leq 2\pi$, $0 \leq \alpha_2^P \leq \pi$, and $0 \leq \alpha_5^P \leq \pi$.

The impact parameter represents the components of the initial vector position of the system in the hyperplane perpendicular to the initial momentum of the incoming particle, as was introduced previously. Let us define $\tilde{\mathbf{b}}$ as the impact parameter when the 6D vector position is ρ :

$$\tilde{\mathbf{b}} = \begin{pmatrix} \tilde{b} \sin \alpha_1^{\tilde{b}} \sin \alpha_2^{\tilde{b}} \sin \alpha_3^{\tilde{b}} \sin \alpha_4^{\tilde{b}} \\ \tilde{b} \cos \alpha_1^{\tilde{b}} \sin \alpha_2^{\tilde{b}} \sin \alpha_3^{\tilde{b}} \sin \alpha_4^{\tilde{b}} \\ \tilde{b} \cos \alpha_2^{\tilde{b}} \sin \alpha_3^{\tilde{b}} \sin \alpha_4^{\tilde{b}} \\ \tilde{b} \cos \alpha_3^{\tilde{b}} \sin \alpha_4^{\tilde{b}} \\ \tilde{b} \cos \alpha_4^{\tilde{b}} \\ 0 \end{pmatrix}, \quad (95)$$

where $0 \leq \alpha_1^{\tilde{b}} \leq 2\pi$, $0 \leq \alpha_i^{\tilde{b}} \leq \pi$, $i = 2, 3$, and 4. Thus, $\tilde{\mathbf{b}}$ is a mass-weighted version of the bare impact parameter \mathbf{b} . These two impact parameters are related by $d^5 \tilde{\mathbf{b}} = (m_{12}^3 m_{3,12}^3 / \mu^6)^{1/2} d^5 \mathbf{b}$, and hence the classical cross section is given by

$$\sigma_{\text{process}}(\mathbf{P}) = \frac{\int \mathcal{S}_{\text{process}}(\tilde{\mathbf{b}}, \mathbf{P}) d\Omega_p^6 d\Omega_b^5 \tilde{b}^4 d\tilde{b}}{(m_{12}^3 m_{3,12}^3 / \mu^6)^{1/2} \int d\Omega_p^6}, \quad (96)$$

where a normalization mass factor emerges as a consequence of the mass-weighted character of the 6D vector position.

The initial vector position $|\rho_0| = R$ is chosen in the asymptotic region where the interaction potential is negligible, thus the initial momentum satisfies $E = P_0^2 / 2\mu$, where E is the incident collision kinetic energy. The hyperangles α_i^P with $i = 1, 2$, and 5, and the impact parameter hyperangles $\alpha_j^{\tilde{b}}$ with $j = 1, 2, 3$, and 4 are randomly generated subject to the constrained magnitude of the impact parameter $|\tilde{\mathbf{b}}|$. The random distribution of those angles must of course be chosen consistent with their appropriate probability density function (Pérez-Ríos *et al.*, 2014). Exploiting the orthogonality of the initial momentum \mathbf{P}_0 and the impact parameter $\tilde{\mathbf{b}}$, the initial vector position is written as

$$\rho_0 = \tilde{\mathbf{b}} - \frac{\sqrt{R^2 - \tilde{b}^2}}{P_0} \mathbf{P}_0. \quad (97)$$

Equation (97) generates ρ_0 from R , $\tilde{\mathbf{b}}$, and \mathbf{P}_0 . For a given set of initial conditions ρ_0 , R , \mathbf{P}_0 , and $\tilde{\mathbf{b}}$, the information is transformed into the usual 3D space by means of Eqs. (88) and (90), where Hamilton's classical equations of motion are numerically integrated up to a certain final time (Press *et al.*, 1986; Pérez-Ríos *et al.*, 2014). Then the coordinates are mapped back into the 6D space, and the classical three-body

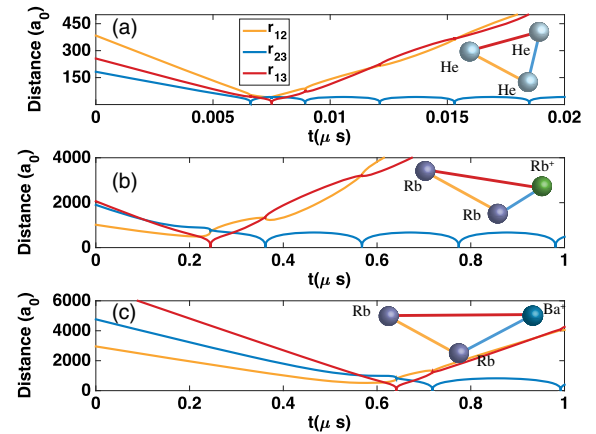


FIG. 27. Classical trajectories for three-body collisions at a relative collision energy $E = k_B T_{\text{in}}$ with $T_{\text{in}} = 1$ mK. (The Boltzmann constant k_B is usually omitted in quoting energies in the following.) Classical trajectories associated with a three-body recombination event (a) $\text{He} + \text{He} + \text{He} \rightarrow \text{He}_2 + \text{He}$ with $b = 97a_0$, (b) $b = 1000a_0$ for $\text{Rb} + \text{Rb} + \text{Rb}^+ \rightarrow \text{Rb}_2^+ + \text{Rb}$, and (c) $\text{Rb} + \text{Rb} + \text{Ba}^+ \rightarrow \text{Rb} - \text{Ba}^+ + \text{Rb}$ with $b = 1000a_0$.

cross section is calculated by means of Eq. (96). This protocol is schematically presented in Fig. 26.

The present approach has been applied to neutral three-body recombination (Pérez-Ríos *et al.*, 2014) and also to neutral-neutral-ion three-body recombination (Pérez-Ríos and Greene, 2015). Figure 27 exhibits different trajectories associated with recombination events in several atomic systems: He + He + He in Fig. 27(a), Rb + Rb + Rb⁺ in Fig. 27(b), and Rb + Rb + Ba⁺ in Fig. 27(c). These trajectories have been obtained by assuming a pairwise potential $V(\mathbf{r}_1, \mathbf{r}_2, \mathbf{r}_3) = v(r_{12}) + v(r_{23}) + v(r_{31})$, where r_{ij} are the interparticle distances. In particular, for the helium atom-atom interaction the potential of Aziz, Janzen, and Moldover (1995), designated HFD-B3-FC11, was employed. The $^3\Sigma$ potential of Strauss *et al.* (2010) for Rb-Rb was employed, and no spin-flip transitions are allowed in the theoretical model. The ion-atom interactions are described by the model potential $-\alpha_d[1 - (r_m/r)^2]/2r^4$, where α_d denotes the static dipole polarizability of Rb, which is taken as $\alpha_d = 320$ a.u., and r_m represents the position of the minimum of the potential. For Rb⁺-Rb, r_m is taken from the quantum chemistry calculations of Jraj *et al.* (2003), and the information needed for Ba⁺-Rb is adapted from Krych *et al.* (2011). For details about the numerical solution method, Monte Carlo sampling, and convergence, see Pérez-Ríos *et al.* (2014) and Pérez-Ríos and Greene (2015).

3. Classical three-body recombination for neutrals and ion-neutral-neutral systems

The hyperspherical classical trajectory method (Pérez-Ríos *et al.*, 2014; Pérez-Ríos and Greene, 2015) has been applied to the recombination of three neutral atoms and to the ion-neutral-neutral recombination process. For a given collision energy $E_k = P_0^2/2\mu$, the average classical three-body cross section is given by

$$\sigma_{\text{rec}}(P_0) = \frac{\int \wp_{\text{rec}}(\mathbf{b}, P_0) d\Omega_{P_0}^6 d\Omega_b^5 \tilde{b}^4 db}{\int d\Omega_b^5 \Omega_{P_0}^6}, \quad (98)$$

where $d\Omega_b^5$ and $d\Omega_{P_0}^6$ stand for the differential elements in the hyperangles associated with the impact parameter b and the initial momentum P_0 , respectively. $\wp_{\text{rec}}(\mathbf{b}, \mathbf{P})$ represents the opacity function or reaction probability for three-body recombination, that is, the probability that the reactants transform into the products of interest for a given set of initial conditions and impact parameter. Generally, such a probability shows a stereochemical dependence, but the hyperangular degrees of freedom can be averaged out, leading to

$$\wp_{\text{rec}}(b, P_0) = \frac{\int \wp_{\text{rec}}(\mathbf{b}, P_0) d\Omega_{P_0}^6 d\Omega_b^5}{\int d\Omega_{P_0}^6}. \quad (99)$$

This integral is evaluated by Monte Carlo sampling over the different initial conditions and impact parameters. The sampling is performed by means of the probability distribution function in each degree of freedom, which can be laborious but is trivially parallelizable. The solution for $\wp_{\text{rec}}(b, P_0)$ in Eq. (99) implies the maximum impact parameter that can

produce a recombination process for a fixed P_0 , denoted as $b_{\text{max}}(P_0)$. In other words, $\wp_{\text{rec}}(b, P_0) = 0$ for $b > b_{\text{max}}(P_0)$. Finally, the three-body recombination cross section can be expressed as

$$\sigma_{\text{rec}}(P_0) = \Omega_b^5 \int_0^{b_{\text{max}}(P_0)} \wp_{\text{rec}}(b, P_0) b^4 db, \quad (100)$$

where $\Omega_b^5 = 8\pi^2/3$ is the total integrated hyperangular solid angle associated with \mathbf{b} for a collision of three particles in 3D. This integral is evaluated by means of Monte Carlo importance sampling (Shui, 1972). Next, the energy-dependent three-body rate constant is defined as

$$k_3(P_0) = \frac{P_0}{\mu} \sigma_{\text{rec}}(P_0). \quad (101)$$

The results for the He-He-He classical three-body recombination rate are shown in Fig. 28. The quantum mechanical results shown in Fig. 28 were obtained using the *R*-matrix method to solve the coupled hyperradial equations in the adiabatic hyperspherical representation (Lin, 1995; Esry, Lin, and Greene, 1996; Wang, D'Incao, and Greene, 2011) to obtain the scattering matrix (Aymar, Greene, and Luc-Koenig, 1996). Figure 28 shows that classical trajectory results for $J = 0$ are in reasonably good agreement with the quantum results at collision energies ~ 1 K, which is the same order of magnitude as the van der Waals energy: this serves approximately as the transition energy between ultracold physics and thermal physics, as was pointed out by Pérez-Ríos *et al.* (2014).

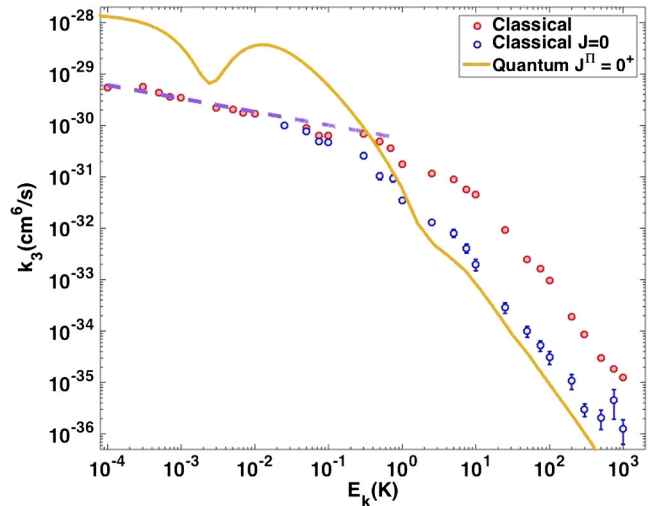


FIG. 28. Energy dependence of the three-body recombination rate of helium atoms in cm^6/s , i.e., $\text{He} + \text{He} + \text{He} \rightarrow \text{He}_2 + \text{He}$. Classical trajectory results following the classical treatment in 6D by means of hyperspherical coordinates are shown as red points. The same results but restricted to total angular momentum $J = |\boldsymbol{\rho}_1 \times \mathbf{P}_1 + \boldsymbol{\rho}_2 \times \mathbf{P}_2| = 0$ are shown as blue circles. The quantum calculation for a fixed angular momentum and parity $J^\pi = 0^+$ is plotted as the solid line. The quantum results show a convergence within better than about 15% for $E = 1000$ K regarding the number of channels included and the parameters employed in the calculations.

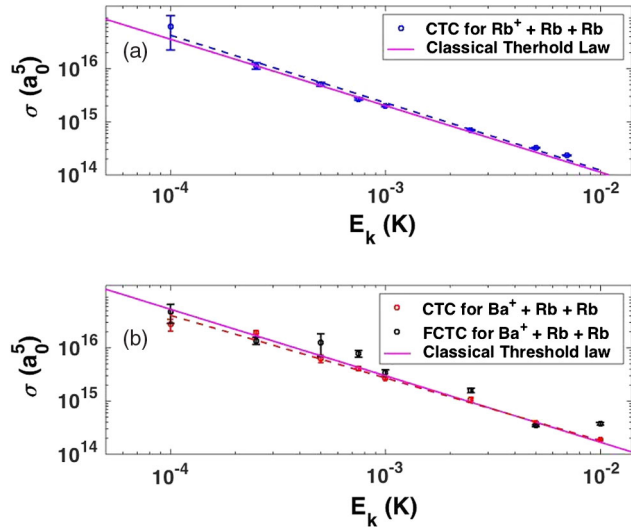


FIG. 29. Three-body recombination cross section (in a_0^5) as a function of the collision energy (in K). (a) $^{87}\text{Rb}^+ - ^{87}\text{Rb} - ^{87}\text{Rb}$; the circles represent the numerical results by means of CTC whereas the dashed line stands for the power-law fit of the points. (b) $^{138}\text{Ba}^+ - ^{87}\text{Rb} - ^{87}\text{Rb}$; red circles represent the numerical results by means of CTC, the black circles denote the results using FCTC (see text for details), and the dashed line stands for the fit of the obtained CTC results. In both panels, the solid magenta line represents the prediction based on the derived classical threshold law. The fitting function assumed for both systems is $\sigma(E_k) = \gamma E_k^\beta$. Adapted from Pérez-Ríos and Greene, 2015.

The same classical approach has been applied to the study of ion-neutral-neutral three-body recombination at cold temperatures (Pérez-Ríos and Greene, 2015; Krüchow *et al.*, 2016), which is important in ion-neutral hybrid trap experiments. Indeed three-body recombination reaction is the main loss mechanism for certain ionic species immersed in an ultracold high-density neutral cloud (Härter *et al.*, 2012, 2013; Härter and Denschlag, 2014; Krüchow *et al.*, 2016). In particular, $^{87}\text{Rb}^+ - ^{87}\text{Rb} - ^{87}\text{Rb}$ and $^{138}\text{Ba}^+ - ^{87}\text{Rb} - ^{87}\text{Rb}$ were studied following the hyperspherical classical approach for collision energies ranging from 100 μK up to 10 mK, and the results are shown in Fig. 29.

The classical trajectory results in Figs. 29(a) and 29(b) have been obtained by restricting one of the hyperangles associated with the momentum, guaranteeing that 95% of the collision energy goes along the vector joining the ion and the center of mass of the neutrals. This dynamical constraint is a consequence of the typical experimental conditions: the energy of the ion is typically orders of magnitude higher than the energy of the neutrals (Willitsch *et al.*, 2008; Willitsch, 2012; Härter and Denschlag, 2014) because of the trapped ion micromotion. As for the trajectories shown in Fig. 27, the same assumptions about the potential energy landscape and the same potentials were employed. In Figs. 29(a) and 29(b), the three-body recombination rate versus collision energy shows a power-law dependence. The physics behind this numerical observation, including its derivation, was explained by Pérez-Ríos and Greene (2015) and is summarized next.

4. Classical threshold law for three-body recombination: Universality in cold chemistry

In quantum mechanics the existence of threshold laws for elastic and inelastic collisions is familiar: the well-known Wigner threshold laws. These threshold laws represent the general trend of the cross section for different processes (here elastic and inelastic collisions) as functions of the collision energy. Analogously, there are also classical threshold laws, such as the famous Langevin cross section (Langevin, 1905) which establishes the behavior of the cross section at low collision energies for two-body ion-neutral collisions. Several years after that, Wannier (1953) found the classical threshold law for three-body collisions involving charged particles, implementing a different approach than Langevin developed. Interestingly, in the case of three mixed-charge particles, e.g., two negative electrons escaping from a positive ion, the exponent in the energy-dependent rate constant is an irrational number which has been experimentally confirmed by measuring the double photoionization of He (Van der Wiel, 1972; Kossmann, Schmidt, and Andersen, 1988). The unusual threshold law exponent 1.127... was also verified experimentally for the escape of two electrons from a singly charged positive ion, as was discussed previously in Sec. I (Cvejanovic and Read, 1974; Donahue *et al.*, 1982). More recently, the classical threshold law for three-body recombination involving neutral atoms with dominant long-range van der Waals attraction, as well as for two neutral atoms and a single ion, was obtained (Pérez-Ríos *et al.*, 2014; Pérez-Ríos and Greene, 2015) following a classical capture model (Levine and Bernstein, 1987).

At low collision energies the scattering properties are mainly dominated by the long-range tail of the two-body interaction, which here are represented as $V(R) \rightarrow -C_s/R^s$, with $s > 2$. We define the maximum impact parameter \tilde{b}_{\max} as the distance where the interaction potential is equal to the collision energy, i.e.,

$$E = \frac{C_s}{\tilde{b}_{\max}^s}. \quad (102)$$

This denotes the distance where the motion of the colliding particles starts to deviate from the rectilinear uniform trajectory. This distance is the equivalent to the classical capture radius employed for the derivation of the Langevin cross section (Langevin, 1905; Levine and Bernstein, 1987), but assuming $V(R) = -\alpha_d/2R^4$ in that case. In analogy with the classical capture model, it is assumed that all the trajectories with $\tilde{b} \leq \tilde{b}_{\max}$ will lead to a three-body recombination event, which of course is likely to be an overestimate. The three-body recombination cross section can then be expressed as [by virtue of Eq. (98)]

$$\begin{aligned} \sigma_{\text{rec}}(E_k) &= \left(\frac{m_{12}^3 m_{3,12}^2}{\mu^5} \right)^{-1/2} \frac{8\pi^2}{3} \int_0^{\tilde{b}_{\max}(E_k)} \tilde{b}^4 d\tilde{b} \\ &\propto \tilde{b}_{\max}^5(E_k). \end{aligned} \quad (103)$$

Equations (102) and (103), after incorporating the relationship between momentum and energy ($P \propto E_k^{1/2}$), yield

$$k_3(E_k) \propto E_k^{1/2} \frac{1}{E_k^{5/s}} = E_k^{(s-10)/2s}. \quad (104)$$

Thus, the neutral three-body recombination rate constant at low collision energies should vary with energy in proportion to $k_3(E_k) \propto E_k^{1/3}$ (Pérez-Ríos *et al.*, 2014). Figure 28 displays a numerical calculation of the three-body recombination rate coefficient for helium, showing that at low collision energies $k_3(E_k)$ follows a power-law dependence as a function of E_k . A fit of the classical trajectory results to the functional form $[k_3(E_k) = aE_k^b]$ gives the dashed purple line. The fitting parameters obtained are $a = 5.89 \pm 3.145 \times 10^{-31} \text{ cm}^6/\text{s}$ and $b = -0.26 \pm 0.07$, which is consistent with the predicted $k_3(E_k) \propto E_k^{-1/3}$ behavior (Pérez-Ríos *et al.*, 2014).

The preceding derivation has assumed that all of the two-body interactions share identical long-range behavior, but an important case to consider is when different particle pairs have different interactions. This case has been explored in the context of determining the threshold law for ion-neutral-neutral three-body recombination (Pérez-Ríos and Greene, 2015). For that system, the two neutral atoms interact through a long-range van der Waals potential $V(R) = -C_6/R^6$, whereas the two ion-neutral interaction is dominated by the charge induced dipole interaction $V(R) = -\alpha_d/2R^4$. A classical capture model can be employed in analogy to the neutral three-body recombination derivation, but in this case the capture radius is given by

$$E = \frac{\alpha_d}{\bar{b}_{2\text{max}}^4}. \quad (105)$$

Here it has been assumed that the longer-range attractive ion-neutral interaction dominates over the neutral-neutral interaction. Plugging Eq. (105) into Eq. (103) the threshold behavior of the ion-neutral-neutral three-body recombination cross section is obtained as (Pérez-Ríos and Greene, 2015)

$$\sigma(E_k) \propto E_k^{-5/4}, \quad (106)$$

and the associated rate constant reads as

TABLE V. Classical threshold law for the three-body recombination (TBR) cross section. A power-law dependence of the TBR cross section as a function of the collision energy is assumed and used as a fitting function for the classical trajectory calculations (CTC) numerical results presented in Fig. 29. The errors quoted for the fitting parameters are associated with a confidence interval of 95%. Adapted from Pérez-Ríos and Greene, 2015.

System	γ (a_0^5)	β (dimensionless)
$^{87}\text{Rb}^+ - ^{87}\text{Rb} - ^{87}\text{Rb}$	$(7.94 \pm 2.72) \times 10^{11}$	-1.178 ± 0.068
$^{138}\text{Ba}^+ - ^{87}\text{Rb} - ^{87}\text{Rb}$	$(3.57 \pm 0.07) \times 10^{11}$	-1.269 ± 0.132
Classical threshold law		-1.25

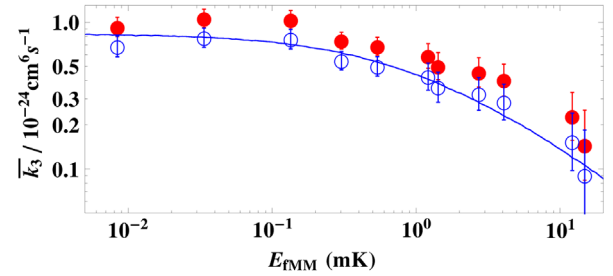


FIG. 30. The three-body recombination rate for $^{138}\text{Ba}^+ - ^{87}\text{Rb} - ^{87}\text{Rb}$ is presented as a function of the controlled micromotion energy. The experimental values are represented by solid circles, whereas the theoretical predictions based on classical trajectory calculations are shown as the open circles. Adapted from Krüchow *et al.*, 2016.

$$k_3(E_k) \propto E_k^{-3/4}. \quad (107)$$

Figure 29 presents the numerical results for ion-neutral-neutral three-body recombination computed classically at low collision energies, as the points in both panes of the figure. Also shown is the threshold law given by Eq. (106) as the solid magenta line. Power-law fits of the numerical results are represented by the dashed lines, and the fitting parameters are shown in Table V. Figure 29 is a numerical confirmation of the predicted threshold law. And the fitted exponents in Table V confirm the validity of the derived classical threshold law.

Ion-neutral-neutral collisions play an important role in hybrid trap experiments where a high density of neutral atoms is in the presence of a single ion or several of them (Härter *et al.*, 2012, 2013; Härter and Denschlag, 2014; Krüchow *et al.*, 2016), and hence hybrid trap experiments may elucidate the nature of ion-neutral-neutral three-body recombination. Indeed, recently the three-body recombination rate for $^{138}\text{Ba}^+ - ^{87}\text{Rb} - ^{87}\text{Rb}$ has been experimentally studied (Krüchow *et al.*, 2016), and the results of the experimental three-body recombination rate as a function of the micromotion energy E_{fMM} are shown as solid symbols in Fig. 30. In the same figure the open symbols stand for the classical trajectory results computed using hyperspherical coordinates (Pérez-Ríos *et al.*, 2014). The theoretical three-body recombination rate constant presented in Fig. 30 is calculated by using the realistic energy distribution of the ion by means of a Monte Carlo simulation (Krüchow *et al.*, 2016). Figure 30 shows good agreement between the classical trajectory calculations and the experimental results, confirming, on the one hand, the validity of the classical Newtonian treatment in cold chemistry, and, on the other hand, supporting the classical threshold law, Eq. (107). Apart from the confirmation of the threshold law, this also has important implications in the chemistry that occurs after a three-body recombination event in a hybrid trap experiment, since the classical results suggest that the dominant product channel will be the formation of shallow molecular ions (Pérez-Ríos and Greene, 2015; Krüchow *et al.*, 2016). In fact our estimates suggest that classical mechanics should give a reasonable description of the three-body recombination process for $\text{Ba}^+ - \text{Rb} - \text{Rb}$ down to energies of the order of 100–200 nK.

VII. CONCLUSIONS

This article reviews developments in only a modest subset of the many extremely vigorous and dynamic topics in the field of few-body physics. Anyone interested in exploring the multifaceted aspects of this field and its interconnections with nuclear physics, chemical physics, and ultracold atomic and molecular physics is encouraged to explore the broader literature, and a good start would be the following set of review articles: Lin (1995), Sadeghpour *et al.* (2000), Nielsen *et al.* (2001), Jensen *et al.* (2004b), Braaten and Hammer (2006), Rittenhouse *et al.* (2011), Baranov *et al.* (2012), Blume (2012a), Frederico *et al.* (2012), Petrov (2012), Wang, D’Incao, and Esry (2013), Zinner and Jensen (2013), Wang, Julienne, and Greene (2015a), and Naidon and Endo (2017). The ability to control interparticle interactions through Fano-Feshbach resonances or confinement-induced resonances continues to trigger novel experimental efforts, and theoretical progress on many fronts continues to be rapid as well. This field promises to continue stimulating new surprises in few-body and many-body physics in the years ahead. Here is one wish list for desirable development of improved understanding in several areas:

- (1) Further insight into the extent of universality for heavy-heavy-light systems with short-range interactions, including the role of van der Waals forces and the dependence on all parameters including the mass ratio.
- (2) Detailed theory and experiment to map out the universality of three-particle systems with all masses different, including of course the possible role of van der Waals universality.
- (3) Determination of N -body cluster states and recombination rates for both homonuclear and heteronuclear systems, with $N > 3$. There is a large parameter space to explore here, just for $N = 4$, for instance.
- (4) Controlled applications of external electromagnetic field dressing of the few-body systems to suppress or enhance inelastic processes. Progress in this area could potentially lead to the formation of a long-lived degenerate Bose gas at infinite two-body scattering length, currently limited by three-body recombination processes.
- (5) Further development of experiments and theory for mixed-dimension few-body systems.
- (6) Experimental observation of log-periodic *energy dependence* of three-body recombination, which has been predicted to be visible for very large scattering lengths.
- (7) In the BCS-BEC crossover problem with a Fermi gas having more than two spin components, it will be interesting to see whether macroscopic collapse of the gas is possible when the interaction scattering lengths are negative, as predicted by Blume *et al.* (2008) and Rittenhouse and Greene (2008).
- (8) The three-body and four-body systems with strong electric and/or magnetic dipolar interactions has received some theoretical attention (Wang, D’Incao, and Greene, 2011a, 2011b) but little in the way of experimental tests to date, and in view of extensive current interest in polar

molecule quantum gases, or strong magnetic dipolar atomic condensates and Fermi gases, far more work is needed from both perspectives (Baranov *et al.*, 2012; Zinner and Jensen, 2013; Kotochigova, 2014; Wang, Julienne, and Greene, 2015a).

- (9) It should be kept in mind that an accurate description of the two-body scattering length dependence of few-body phenomena hinges critically on having an accurate description of the atom-atom scattering lengths as functions of static and/or oscillating electromagnetic fields. Theory has improved to the point where a number of alternative techniques can provide these data, when developed in conjunction with experiments, including full close-coupling calculations (Berninger *et al.*, 2013), the asymptotic bound state model (Tiecke *et al.*, 2010), and variants of multichannel quantum defect theory with or without the additional frame transformation approximation (Burke, Greene, and Bohn, 1998; Gao, 2008; Ruzic, Greene, and Bohn, 2013). Pires, Repp *et al.* (2014) provide comparisons of these different treatments, with application to the recently important heteronuclear system ^6Li - ^{133}Cs . While these theoretical descriptions have been generally successful, extensions and improvements are still desirable in order to gain the fullest possible control of the two-body physics underlying all of the few-body physics addressed in this review.
- (10) Further insight is also desired for systems such as the few-body version of the fractional quantum Hall problem, both in condensed-matter systems and in ultracold atomic systems. Initial studies by Daily, Wooten, and Greene (2015), Rittenhouse, Wray, and Johnson (2016), and Wooten, Daily, and Greene (2016) into that subject from the adiabatic hyperspherical perspective suggest that the corresponding 2D N -particle Schrödinger equation nearly separates in the hyperradial degree of freedom, for both bosons and fermions, as can be deduced from potential energy curves in those references. Moreover, some of the intriguing degeneracy patterns observed in that problem are deserving of further exploration.

ACKNOWLEDGMENTS

Different aspects of this work have been supported over the years by the National Science Foundation, the Department of Energy Office of Science, the AFOSR-MURI program on cold polar molecules, and the Bi-National Science Foundation. C. H. G. specifically thanks many present and former colleagues, especially Doerte Blume, Brett Esry, and Jose D’Incao for extended collaborations and access to their unpublished results and innumerable discussions. C. H. G. also acknowledges the Alexander von Humboldt Foundation for supporting an extended stay at the Max-Planck Institute for Nuclear Physics and the University of Heidelberg, where part of this review was completed. Many of the extensive revisions following submission were carried out with partial support from the Max-Planck Institute for the Physics of Complex Systems in Dresden.

REFERENCES

- Abelev, B. I., *et al.* (STAR Collaboration), 2010, “Observation of an antimatter hypernucleus,” *Science* **328**, 58–62.
- Adhikari, Sadhan K., and António C. Fonseca, 1981, “Four-body efimov effect in a born-oppenheimer model,” *Phys. Rev. D* **24**, 416–425.
- Adhikari, Sadhan K., T. Frederico, and I. D. Goldman, 1995, “Perturbative renormalization in quantum few-body problems,” *Phys. Rev. Lett.* **74**, 487–491.
- Akkineni, Vamsi K., D. M. Ceperley, and Nandini Trivedi, 2007, “Pairing and superfluid properties of dilute fermion gases at unitarity,” *Phys. Rev. B* **76**, 165116.
- Alhassid, Y., G. F. Bertsch, and L. Fang, 2008, “New effective interaction for the trapped Fermi gas,” *Phys. Rev. Lett.* **100**, 230401.
- ALICE Collaboration, 2016, “ ${}^3\Lambda\text{H}$ and ${}^3\Lambda\bar{H}$ production in Pb-Pb collisions at $\sqrt{s_{NN}} = 2.76$ TeV,” *Phys. Lett. B* **754**, 360.
- Alt, E. O., P. Grassberger, and W. Sandhas, 1967, “Reduction of the three-particle collision problem to multi-channel two-particle Lippmann-Schwinger equations,” *Nucl. Phys. B* **2**, 167–180.
- Alvarez-Rodriguez, R., E. Garrido, A. S. Jensen, D. V. Fedorov, and H. O. U. Fynbo, 2007, “Structure of low-lying c-12 resonances,” *Eur. Phys. J. A* **31**, 303–317.
- Alvarez-Rodriguez, R., A. S. Jensen, E. Garrido, D. V. Fedorov, and H. O. U. Fynbo, 2008, “Momentum distributions of alpha particles from decaying low-lying c-12 resonances,” *Phys. Rev. C* **77**, 064305.
- Amado, R. D., and F. C. Greenwood, 1973, “There is no Efimov effect for four or more particles,” *Phys. Rev. D* **7**, 2517–2519.
- Amorim, A. E. A., T. Frederico, and L. Tomio, 1997, “Universal aspects of Efimov states and light halo nuclei,” *Phys. Rev. C* **56**, R2378.
- Ancilotto, F., M. Rossi, L. Salasnich, and F. Toigo, 2015, “Quenched dynamics of the momentum distribution of the unitary Bose gas,” *Few-Body Syst.* **56**, 801.
- Anderson, M. H., J. R. Ensher, M. R. Matthews, C. E. Wieman, and E. A. Cornell, 1995, “Observation of Bose-Einstein condensation in a dilute atomic vapor,” *Science* **269**, 198–201.
- Andresen, G. B., *et al.*, 2010, “Trapped antihydrogen,” *Nature (London)* **468**, 673.
- Andresen, G. B., *et al.*, 2011, “Confinement of antihydrogen for 1,000 seconds,” *Nat. Phys.* **7**, 558.
- Astrakharchik, G. E., J. Boronat, J. Casulleras, and S. Giorgini, 2005, “Beyond the Tonks-Girardeau gas: Strongly correlated regime in quasi-one-dimensional Bose gases,” *Phys. Rev. Lett.* **95**, 190407.
- Astrakharchik, G. E., and L. P. Pitaevskii, 2004, “Motion of a heavy impurity through a Bose-Einstein condensate,” *Phys. Rev. A* **70**, 013608.
- Avery, J., 1989, *Hyperspherical Harmonics: Applications in Quantum Theory* (Kluwer Academic Publishers, Norwell, MA).
- Aymar, M., C. H. Greene, and E. Luc-Koenig, 1996, “Multichannel Rydberg spectroscopy of complex atoms,” *Rev. Mod. Phys.* **68**, 1015–1123.
- Aziz, R. A., A. R. Janzen, and M. R. Moldover, 1995, “*Ab Initio* calculations for helium: A standard for transport property measurements,” *Phys. Rev. Lett.* **74**, 1586.
- Baranov, M. A., 2008, “Theoretical progress in many-body physics with ultracold dipolar gases,” *Phys. Rep.* **464**, 71–111.
- Baranov, M. A., M. Dalmonte, G. Pupillo, and P. Zoller, 2012, “Condensed Matter Theory of Dipolar Quantum Gases,” *Chem. Rev.* **112**, 5012–5061.
- Barletta, P., and A. Kievsky, 2008, “Continuum three-body states using the hyperspherical adiabatic basis set,” *Few-Body Syst.* **44**, 371–373.
- Barletta, P., and A. Kievsky, 2009, “Scattering states of three-body systems with the hyperspherical adiabatic method,” *Few-Body Syst.* **45**, 123–125.
- Barletta, P., C. Romero-Redondo, A. Kievsky, M. Viviani, and E. Garrido, 2009, “Integral relations for three-body continuum states with the adiabatic expansion,” *Phys. Rev. Lett.* **103**, 090402.
- Barnea, N., 1999, “A recursive method for the construction of irreducible representations of the orthogonal group $O(N)$,” *J. Math. Phys. (N.Y.)* **40**, 1011.
- Barnea, N., and A. Novoselsky, 1997, “Construction of hyperspherical functions symmetrized with respect to the orthogonal and the symmetric groups,” *Ann. Phys. (N.Y.)* **256**, 192.
- Barontini, G., C. Weber, F. Rabatti, J. Catani, G. Thalhammer, M. Inguscio, and F. Minardi, 2009, “Observation of heteronuclear atomic Efimov resonances,” *Phys. Rev. Lett.* **103**, 043201.
- Bartlett, P. L., I. Bray, S. Jones, A. T. Stelbovics, A. S. Kadyrov, K. Bartschat, G. L. V. Steeg, M. P. Scott, and P. G. Burke, 2003, “Unambiguous ionization amplitudes for electron-hydrogen scattering,” *Phys. Rev. A* **68**, 020702.
- Bartolo, N., D. J. Papoular, L. Barbiero, C. Menotti, and A. Recati, 2013, “Dipolar-induced resonance for ultracold bosons in a quasi-one-dimensional optical lattice,” *Phys. Rev. A* **88**, 023603.
- Basak, Soumen, and Morrel H. Cohen, 1979, “Deformation-potential theory for the mobility of excess electrons in liquid argon,” *Phys. Rev. B* **20**, 3404–3414.
- Bazak, B., and D. S. Petrov, 2017, “Five-body Efimov effect and universal pentamer in fermionic mixtures,” *Phys. Rev. Lett.* **118**, 083002.
- Bedaque, P. F., E. Braaten, and H.-W. Hammer, 2000, “Three-body recombination in Bose gases with large scattering length,” *Phys. Rev. Lett.* **85**, 908–911.
- Bei-Bing, Huang, and Wan Shao-Long, 2009, “Polaron in Bose-Einstein-Condensation System,” *Chin. Phys. Lett.* **26**, 080302.
- Bellotti, F. F., T. Frederico, M. T. Yamashita, D. V. Fedorov, A. S. Jensen, and N. T. Zinner, 2016, “Three-body bound states of two bosonic impurities immersed in a fermi sea in 2d,” *New J. Phys.* **18**, 043023.
- Benayoun, J. J., C. Cignoux, and J. Chauvin, 1981, “Neutron-deuteron scattering at zero energy with realistic nucleon-nucleon interactions,” *Phys. Rev. C* **23**, 1854.
- Berezinskii, V. L., 1971, “Destruction of long-range order in one-dimensional and 2-dimensional systems having a continuous symmetry group 1—classical systems,” *Sov. Phys. JETP* **32**, 493 [*Zh. Eksp. Teor. Fiz.* **59**, 907 (1971)].
- Bergeman, T., M. G. Moore, and M. Olshanii, 2003, “Atom-atom scattering under cylindrical harmonic confinement: Numerical and analytic studies of the confinement induced resonance,” *Phys. Rev. Lett.* **91**, 163201.
- Berninger, M., A. Zenesini, B. Huang, W. Harm, H.-C. Nägerl, F. Ferlaino, R. Grimm, P. S. Julienne, and J. M. Hutson, 2011, “Universality of the three-body parameter for Efimov states in ultracold cesium,” *Phys. Rev. Lett.* **107**, 120401.
- Berninger, M., A. Zenesini, B. Huang, W. Harm, H.-C. Nägerl, F. Ferlaino, R. Grimm, P. S. Julienne, and J. M. Hutson, 2013, “Feshbach resonances, weakly bound molecular states, and coupled-channel potentials for cesium at high magnetic fields,” *Phys. Rev. A* **87**, 032517.
- Bloch, I., J. Dalibard, and W. Zwerger, 2008, “Many-body physics with ultracold gases,” *Rev. Mod. Phys.* **80**, 885–964.
- Bloom, R. S., M. G. Hu, T. D. Cumby, and D. S. Jin, 2013, “Tests of universal three-body physics in an ultracold Bose-Fermi mixture,” *Phys. Rev. Lett.* **111**, 105301.

- Blumberg, W. A. M., Wayne M. Itano, and D. J. Larson, 1979, "Theory of the photodetachment of negative ions in a magnetic field," *Phys. Rev. A* **19**, 139–148.
- Blume, D., 2012a, "Few-body physics with ultracold atomic and molecular systems in traps," *Rep. Prog. Phys.* **75**, 046401.
- Blume, D., 2012b, "Universal four-body states in heavy-light mixtures with a positive scattering length," *Phys. Rev. Lett.* **109**, 230404.
- Blume, D., 2014, "Three-body bound states in a harmonic waveguide with cylindrical symmetry," *Phys. Rev. A* **89**, 053603.
- Blume, D., and K. M. Daily, 2009, "Universal relations for a trapped four-Fermion system with arbitrary s-wave scattering length," *Phys. Rev. A* **80**, 053626.
- Blume, D., and C. H. Greene, 2000, "Monte Carlo hyperspherical description of helium cluster excited states," *J. Chem. Phys.* **112**, 8053–8067.
- Blume, D., and C. H. Greene, 2002, "Lowest breathing mode of bosonic helium clusters," *Eur. Phys. J. D* **18**, 83–86.
- Blume, D., C. H. Greene, and B. D. Esry, 2000, "Comparative study of He_3 , Ne_3 , and Ar_3 using hyperspherical coordinates," *J. Chem. Phys.* **113**, 2145–2158.
- Blume, D., C. H. Greene, and B. D. Esry, 2014, Comparative study of He_3 , Ne_3 , and Ar_3 using hyperspherical coordinates," *J. Chem. Phys.* **141**, 069901; **113**, 2145(E) (2000).
- Blume, D., S. T. Rittenhouse, J. von Stecher, and C. H. Greene, 2008, "Stability of inhomogeneous multicomponent Fermi gases," *Phys. Rev. A* **77**, 033627.
- Blume, D., and Y. Yan, 2014, "Generalized Efimov Scenario for Heavy-Light Mixtures," *Phys. Rev. Lett.* **113**, 213201.
- Bohn, J. L., B. D. Esry, and C. H. Greene, 1998, "Effective potentials for dilute Bose-Einstein condensates," *Phys. Rev. A* **58**, 584–597.
- Bohr, A., S. Paolini, R. C. Forrey, N. Balakrishnan, and P. C. Stancil, 2014, "A full-dimensional quantum dynamical study of $\text{H}_2 + \text{H}_2$ collisions: Coupled-states versus close-coupling formulation," *J. Chem. Phys.* **140**, 064308.
- Bongs, K., and K. Sengstock, 2004, "Physics with coherent matter waves," *Rep. Prog. Phys.* **67**, 907.
- Borca, B., D. Blume, and C. H. Greene, 2003, "A two-atom picture of coherent atom-molecule quantum beats," *New J. Phys.* **5**, 111.
- Botero, J., and C. H. Greene, 1985, "Positronium negative-ion—an adiabatic study using hyperspherical coordinates," *Phys. Rev. A* **32**, 1249–1251.
- Botero, J., and C. H. Greene, 1986, "Resonant photodetachment of the positronium negative-ion," *Phys. Rev. Lett.* **56**, 1366–1369.
- Braaten, E., and H.-W. Hammer, 2001, "Three-body recombination into deep bound states in a Bose gas with large scattering length," *Phys. Rev. Lett.* **87**, 160407.
- Braaten, E., and H.-W. Hammer, 2003, "Universality in the three-body problem for ^4He atoms," *Phys. Rev. A* **67**, 042706.
- Braaten, E., and H.-W. Hammer, 2006, "Universality in few-body systems with large scattering length," *Phys. Rep.* **428**, 259–390.
- Braaten, E., D. Kang, and L. Platter, 2010, "Short-time operator product expansion for rf spectroscopy of a strongly interacting Fermi gas," *Phys. Rev. Lett.* **104**, 223004.
- Braaten, E., D. Kang, and L. Platter, 2011, "Short-time operator product expansion for rf spectroscopy of a strongly interacting Fermi gas," *Phys. Rev. Lett.* **106**, 153005.
- Braaten, E., and L. Platter, 2009, "Universal relations for the strongly-interacting Fermi gas," *Laser Phys.* **19**, 550–553.
- Bradley, C. C., C. A. Sackett, and R. G. Hulet, 1997, "Bose-Einstein condensation of lithium: Observation of limited condensate number," *Phys. Rev. Lett.* **78**, 985–989.
- Bradley, C. C., C. A. Sackett, J. J. Tollett, and R. G. Hulet, 1995, "Evidence of Bose-Einstein condensation in an atomic gas with attractive interactions," *Phys. Rev. Lett.* **75**, 1687.
- Bray, I., and A. T. Stelbovics, 1993, "Calculation of the total ionization cross section and spin asymmetry in electron-hydrogen scattering from threshold to 500 eV," *Phys. Rev. Lett.* **70**, 746–749.
- Bruch, L. W., and J. A. Tjon, 1979, "Binding of three identical bosons in two dimensions," *Phys. Rev. A* **19**, 425–432.
- Bruderer, M., W. Bao, and D. Jaksch, 2008, "Self-trapping of impurities in Bose-Einstein condensates: Strong attractive and repulsive coupling," *Europhys. Lett.* **82**, 30004.
- Bulgac, A., J. E. Drut, and P. Magierski, 2006, "Spin 1/2 Fermions in the unitary regime: A superfluid of a new type," *Phys. Rev. Lett.* **96**, 090404.
- Burke, J. P., C. H. Greene, and J. L. Bohn, 1998, "Multichannel cold collisions: Simple dependences on energy and magnetic field," *Phys. Rev. Lett.* **81**, 3355–3358.
- Burt, E. A., R. W. Ghrist, C. J. Myatt, M. J. Holland, E. A. Cornell, and C. E. Wieman, 1997, "Coherence, correlations, and collisions: What one learns about Bose-Einstein condensates from their decay," *Phys. Rev. Lett.* **79**, 337–340.
- Campargue, R., 2001, *Atomic and Molecular Beams: The state of the Art 2000*, edited by R. Campargue (Springer, Heidelberg).
- Carlson, J., S. Gandolfi, F. Pederiva, Steven C. Pieper, R. Schiavilla, K. E. Schmidt, and R. B. Wiringa, 2015, "Quantum Monte Carlo methods for nuclear physics," *Rev. Mod. Phys.* **87**, 1067–1118.
- Casimir, H. B. G., and D. Polder, 1948, "The influence of retardation on the London-van der Waals forces," *Phys. Rev.* **73**, 360–372.
- Castin, Y., and F. Werner, 2011, "Single-particle momentum distribution of an Efimov trimer," *Phys. Rev. A* **83**, 063614.
- Castin, Yvan, Christophe Mora, and Ludovic Pricoupenko, 2010, "Four-Body Efimov Effect for Three Fermions and a Lighter Particle," *Phys. Rev. Lett.* **105**, 223201.
- Castin, Yvan, and Felix Werner, 2013, "The third coefficient of unitary Bose viral gas," *Can. J. Phys.* **91**, 382–389.
- Catani, J., G. Barontini, G. Lamporesi, F. Rabatti, G. Thalhammer, F. Minardi, S. Stringari, and M. Inguscio, 2009, "Entropy exchange in a mixture of ultracold atoms," *Phys. Rev. Lett.* **103**, 140401.
- Catani, J., G. Lamporesi, D. Naik, M. Gring, M. Inguscio, F. Minardi, A. Kantian, and T. Giamarchi, 2012, "Quantum dynamics of impurities in a one-dimensional Bose gas," *Phys. Rev. A* **85**, 023623.
- Cavagnero, M., 1984, "Electron correlations in atomic shells: Systematics of high-angular-momentum admixtures," *Phys. Rev. A* **30**, 1169–1174.
- Cavagnero, M., 1986, "Electron correlations in atomic shells. II. Antisymmetric basis functions," *Phys. Rev. A* **33**, 2877–2886.
- Cazalilla, M. A., R. Citro, T. Giamarchi, E. Orignac, and M. Rigol, 2011, "One dimensional bosons: From condensed matter systems to ultracold gases," *Rev. Mod. Phys.* **83**, 1405.
- Chang, S. Y., and G. F. Bertsch, 2007, "Local-density-functional theory for superfluid Fermionic systems: The unitary gas," *Phys. Rev. A* **76**, 021603(R).
- Cheon, Taksu, and T. Shigehara, 1999, "Fermion-boson duality of one-dimensional quantum particles with generalized contact interactions," *Phys. Rev. Lett.* **82**, 2536–2539.
- Chevy, F., S. Nascimbene, N. Navon, K. Jiang, C. Lobo, and C. Salomon, 2011, "Thermodynamics of the unitary Fermi gas," *J. Phys. Conf. Ser.* **264**, 012012.
- Child, M. S., 1974, *Molecular Collision Theory* (Academic Press, London, England).
- Chin, C., 2011, "Universal scaling of Efimov resonance positions in cold atom systems," arXiv:1111.1484.

- Chin, C., R. Grimm, P. S. Julienne, and E. Tiesinga, 2010, “Feshbach resonances in ultracold gases,” *Rev. Mod. Phys.* **82**, 1225–1286.
- Christensen-Dalsgaard, B. L., 1984, “Combined hyperspherical and close-coupling description of 2-electron wave-functions—application to e–H elastic-scattering phase-shifts,” *Phys. Rev. A* **29**, 2242–2244.
- Clapp, R. E., 1949, “The binding energy of the triton,” *Phys. Rev.* **76**, 873–874.
- Clare, R. B., and J. S. Levinger, 1985, “Hypertriton and hyperspherical harmonics,” *Phys. Rev. C* **31**, 2303.
- Clark, C. W., 1983, “Low-energy electron-atom scattering in a magnetic field,” *Phys. Rev. A* **28**, 83–90.
- Clark, C. W., and C. H. Greene, 1980, “Hyperspherical analysis of three-electron dynamics,” *Phys. Rev. A* **21**, 1786–1797.
- Clary, D. C., 1991, “Quantum reactive scattering of four-atom reactions with nonlinear geometry: $\text{OH} + \text{H}_2 \rightarrow \text{H}_2\text{O} + \text{H}$,” *J. Chem. Phys.* **95**, 7298–7310.
- Cobis, A., D. V. Fedorov, and A. S. Jensen, 1998, “Three-body halos. v. computations of continuum spectra for borromean nuclei,” *Phys. Rev. C* **58**, 1403–1421.
- Cobis, A., A. S. Jensen, and D. V. Fedorov, 1997, “The simplest strange three-body halo,” *J. Phys. G* **23**, 401.
- Combescot, R., F. Alzetto, and X. Leyronas, 2009, “Particle distribution tail and related energy formula,” *Phys. Rev. A* **79**, 053640.
- Corson, J. P., and J. L. Bohn, 2016, “Ballistic quench-induced correlation waves in ultracold gases,” *Phys. Rev. A* **94**, 023604.
- Côté, R., 2016, “Chapter two—ultracold hybrid atom ion systems,” *Adv. At. Mol. Opt. Phys.* **65**, 67.
- Cowell, S., H. Heiselberg, I. E. Mazets, J. Morales, V. R. Pandharipande, and C. J. Pethick, 2002, “Cold Bose gases with large scattering lengths,” *Phys. Rev. Lett.* **88**, 210403.
- Crawford, O. H., 1988, “Oscillations in photodetachment cross sections for negative ions in magnetic fields,” *Phys. Rev. A* **37**, 2432–2440.
- Cubizolles, J., T. Bourdel, S. J. J. M. F. Kokkelmans, G. V. Shlyapnikov, and C. Salomon, 2003, “Production of long-lived ultracold Li_2 molecules from a Fermi gas,” *Phys. Rev. Lett.* **91**, 240401.
- Cucchiatti, F. M., and E. Timmermans, 2006, “Strong-coupling polarons in dilute gas Bose-Einstein condensates,” *Phys. Rev. Lett.* **96**, 210401.
- Cui, X., 2012, “Mixed-partial-wave scattering with spin-orbit coupling and validity of pseudopotentials,” *Phys. Rev. A* **85**, 022705.
- Cui, X., Y. Wang, and F. Zhou, 2010, “Resonance scattering in optical lattices and molecules: Interband versus intraband effects,” *Phys. Rev. Lett.* **104**, 153201.
- Cvejanovic, S., and F. H. Read, 1974, “Studies of the threshold electron impact ionization of helium,” *J. Phys. B* **7**, 1841.
- Daily, K. M., and C. H. Greene, 2014, “Extension of the correlated Gaussian hyperspherical method to more particles and dimensions,” *Phys. Rev. A* **89**, 012503.
- Daily, K. M., A. Kievsky, and C. H. Greene, 2015, “Adiabatic hyperspherical analysis of realistic nuclear potentials,” *Few-Body Syst.* **56**, 753–759.
- Daily, K. M., R. E. Wooten, and C. H. Greene, 2015, “Hyperspherical theory of the quantum Hall effect: The role of exceptional degeneracy,” *Phys. Rev. B* **92**, 125427.
- Dalfovo, F., S. Giorgini, L. P. Pitaevskii, and S. Stringari, 1999, “Theory of Bose-Einstein condensation in trapped gases,” *Rev. Mod. Phys.* **71**, 463–512.
- Davis, K. B., M.-O. Mewes, M. R. van Andrews, N. J. Van Druten, D. S. Durfee, D. M. Kurn, and W. Ketterle, 1995, “Bose-Einstein condensation in a gas of sodium atoms,” *Phys. Rev. Lett.* **75**, 3969.
- de Goey, L. P. H., T. H. M. v. d. Berg, N. Mulders, H. T. C. Stoof, B. J. Verhaar, and W. Glöckle, 1986, “3-body recombination in spin-polarized atomic-hydrogen,” *Phys. Rev. B* **34**, 6183.
- Deltuva, A., 2010, “Efimov physics in bosonic atom-trimer scattering,” *Phys. Rev. A* **82**, 040701.
- Deltuva, A., 2011, “Universality in bosonic dimer-dimer scattering,” *Phys. Rev. A* **84**, 022703.
- Deltuva, A., 2012, “Momentum-space calculation of four-boson recombination,” *Phys. Rev. A* **85**, 012708.
- Delves, L. M., 1958, “Tertiary and general-order collisions,” *Nucl. Phys.* **9**, 391.
- Delves, L. M., 1960, “Tertiary and general-order collisions part II,” *Nucl. Phys.* **20**, 275.
- DeMarco, B., and D. S. Jin, 1999, “Onset of Fermi degeneracy in a trapped atomic gas,” *Science* **285**, 1703.
- Demkov, Yu. N., and G. F. Drukarev, 1965, “Particle of low binding energy in a magnetic field,” *Sov. Phys. JETP* **22**, 182 [*Zh. Eksp. Teor. Fiz.* **49**, 257 (1965)].
- Dickerscheid, D. B. M., and H. T. C. Stoof, 2005, “Feshbach molecules in a one-dimensional Fermi gas,” *Phys. Rev. A* **72**, 053625.
- D’Incao, J. P., 2003, “Hyperspherical angular adiabatic separation for three-electron atomic systems,” *Phys. Rev. A* **67**, 024501.
- D’Incao, J. P., Fatima Anis, and B. D. Esry, 2015, “Ultracold three-body recombination in two dimensions,” *Phys. Rev. A* **91**, 062710.
- D’Incao, J. P., and B. D. Esry, 2005, “Scattering length scaling laws for ultracold three-body collisions,” *Phys. Rev. Lett.* **94**, 213201.
- D’Incao, J. P., and B. D. Esry, 2006a, “Mass dependence of ultracold three-body collision rates,” *Phys. Rev. A* **73**, 030702.
- D’Incao, J. P., and B. D. Esry, 2006b, “Enhancing the observability of the Efimov effect in ultracold atomic gas mixtures,” *Phys. Rev. A* **73**, 030703.
- D’Incao, J. P., and B. D. Esry, 2014, “Adiabatic hyperspherical representation for the three-body problem in two dimensions,” *Phys. Rev. A* **90**, 042707.
- D’Incao, J. P., S. T. Rittenhouse, N. P. Mehta, and C. H. Greene, 2009, “Dimer-dimer collisions at finite energies in two-component Fermi gases,” *Phys. Rev. A* **79**, 030501.
- D’Incao, J. P., J. von Stecher, and C. H. Greene, 2009, “Universal four-boson states in ultracold molecular gases: Resonant effects in dimer-dimer collisions,” *Phys. Rev. Lett.* **103**, 033004.
- D’Incao, José P., and C. H. Greene, 2011, “Collisional aspects of bosonic and fermionic dipoles in quasi-two-dimensional confining geometries,” *Phys. Rev. A* **83**, 030702.
- Ding, Yijue, and C. H. Greene, 2017, “Renormalized contact interaction in degenerate unitary Bose gases,” *Phys. Rev. A* **95**, 053602.
- Domke, M., C. Xue, A. Puschmann, T. Mandel, E. Hudson, D. A. Shirley, G. Kaindl, C. H. Greene, H. R. Sadeghpour, and H. Petersen, 1991, “Extensive double-excitation states in atomic helium,” *Phys. Rev. Lett.* **66**, 1306–1309.
- Donahue, J. B., P. A. M. Gram, M. V. Hynes, R. W. Hamm, C. A. Frost, H. C. Bryant, K. B. Butterfield, David A. Clark, and W. W. Smith, 1982, “Observation of two-electron photoionization of the h^- ion near threshold,” *Phys. Rev. Lett.* **48**, 1538–1541.
- Donley, E. A., N. R. Clausen, S. L. Cornish, J. L. Roberts, E. A. Cornell, and C. E. Wieman, 2001, “Dynamics of collapsing and exploding Bose-Einstein condensates,” *Nature (London)* **412**, 295–299.
- Donley, E. A., N. R. Clausen, S. T. Thompson, and C. E. Wieman, 2002, “Atom-molecule coherence in a Bose-Einstein condensate,” *Nature (London)* **417**, 529–533.
- Duan, Hao, Li You, and Bo Gao, 2013, “Ultracold collisions in the presence of synthetic spin-orbit coupling,” *Phys. Rev. A* **87**, 052708.

- Dunjko, V., M. G. Moore, T. Bergeman, and M. Olshanii, 2011a, “Confinement-induced resonances,” *Adv. At. Mol. Opt. Phys.* **60**, 461–510.
- Dunjko, Vanja, Michael G. Moore, Thomas Bergeman, and Maxim Olshanii, 2011b, “Confinement-induced resonances,” in *Advances in Atomic, Molecular, and Optical Physics*, Vol. 60, edited by P. R. Berman, E. Arimondo, and C. C. Lin (Academic Press, New York), Chap. 10, pp. 461–510.
- Dyke, P., S. E. Pollack, and R. G. Hulet, 2013, “Finite range corrections near a Feshbach resonance and their role in the Efimov effect,” *Phys. Rev. A* **88**, 023625.
- Efimov, V., 1970, “Energy levels arising from resonant two-body forces in a three-body system,” *Phys. Lett. B* **33**, 563–564.
- Efimov, V., 1971, “Weakly-bound states of three resonantly-interacting particles,” *Sov. J. Nucl. Phys.* **12**, 589–595 [*Yad. Fiz.* **12**, 1080–1091 (1970)].
- Efimov, V., 1973, “Energy levels of three resonantly interacting particles,” *Nucl. Phys. A* **210**, 157–188.
- Efimov, V., 1979, “Low-energy properties of three resonantly interacting particles,” *Sov. J. Nucl. Phys.* **29**, 546 [*Yad. Fiz.* **29**, 1058–1069 (1979)].
- Efimov, V., and E. G. Tkachenko, 1988, “On the correlation between the triton binding energy and the neutron-deuteron doublet scattering length,” *Few-Body Syst.* **4**, 71–88.
- Efremov, Maxim A., Lev Plimak, Misha Yu. Ivanov, and Wolfgang P. Schleich, 2013, “Three-body bound states in atomic mixtures with resonant p -wave interaction,” *Phys. Rev. Lett.* **111**, 113201.
- Eismann, U., *et al.*, 2016, “Universal loss dynamics in a unitary Bose gas,” *Phys. Rev. X* **6**, 021025.
- Epelbaum, E., H. W. Hammer, and Ulf-G Meissner, 2009, “Modern theory of nuclear forces,” *Rev. Mod. Phys.* **81**, 1773–1825.
- Ermolova, E. V., L. Yu. Rusin, and M. B. Sevryuk, 2014, “A hard sphere model for direct three-body recombination of heavy ions,” *Russ. J. Phys. Chem. B* **8**, 769.
- Esry, B. D., 1997, “Hartree-Fock theory for Bose-Einstein condensates and the inclusion of correlation effects,” *Phys. Rev. A* **55**, 1147–1159.
- Esry, B. D., and C. H. Greene, 1999, “Validity of the shape-independent approximation for Bose-Einstein condensates,” *Phys. Rev. A* **60**, 1451–1462.
- Esry, B. D., and C. H. Greene, 2006, “Quantum physics: a ménage à trois laid bare,” *Nature (London)* **440**, 289–290.
- Esry, B. D., C. H. Greene, and J. P. Burke, 1999, “Recombination of three atoms in the ultracold limit,” *Phys. Rev. Lett.* **83**, 1751–1754.
- Esry, B. D., C. H. Greene, Y. Zhou, and C. D. Lin, 1996, “Role of the scattering length in three-boson dynamics and Bose-Einstein condensation,” *J. Phys. B* **29**, L51–L57.
- Esry, B. D., C. D. Lin, and C. H. Greene, 1996, “Adiabatic hyperspherical study of the helium trimer,” *Phys. Rev. A* **54**, 394–401.
- Esry, B. D., and H. R. Sadeghpour, 2003, “Ultraslow $\bar{p} - H$ collisions in hyperspherical coordinates: Hydrogen and protonium channels,” *Phys. Rev. A* **67**, 012704.
- Fabre de la Ripelle, M., 1993, “Green function and scattering amplitudes in many-dimensional space,” *Few-Body Syst.* **14**, 1.
- Fang, K. K., and E. L. Tomusiak, 1977, “Three-body model of ${}^6\text{Li}$ using hyperspherical harmonics,” *Phys. Rev. C* **16**, 2117.
- Fano, U., 1970, “Quantum defect theory of l uncoupling in H_2 as an example of channel-interaction treatment,” *Phys. Rev. A* **2**, 353–365.
- Fano, U., 1976, “Dynamics of electron excitation,” *Phys. Today* **29**, No. 9, 32.
- Fano, U., 1981a, “Stark effect of nonhydrogenic Rydberg spectra,” *Phys. Rev. A* **24**, 619–622.
- Fano, U., 1981b, “Unified treatment of collisions,” *Phys. Rev. A* **24**, 2402–2415.
- Fano, U., 1983, “Correlations of two excited electrons,” *Rep. Prog. Phys.* **46**, 97–165.
- Fano, U., and A. R. P. Rau, 1986, *Atomic Collisions and Spectra* (Academic Press, Orlando, FL).
- Fano, U., and J. A. Stephens, 1986, “Slow electrons in condensed matter,” *Phys. Rev. B* **34**, 438–441.
- Fedichev, P. O., M. J. Bijlsma, and P. Zoller, 2004, “Extended molecules and geometric scattering resonances in optical lattices,” *Phys. Rev. Lett.* **92**, 080401.
- Fedichev, P. O., Yu. Kagan, G. V. Shlyapnikov, and J. T. M. Walraven, 1996, “Influence of nearly resonant light on the scattering length in low-temperature atomic gases,” *Phys. Rev. Lett.* **77**, 2913–2916.
- Fedichev, P. O., M. W. Reynolds, and G. V. Shlyapnikov, 1996, “Three-body recombination of ultracold atoms to a weakly bound s level,” *Phys. Rev. Lett.* **77**, 2921–2924.
- Fedorov, D. V., and A. S. Jensen, 2002, “Regularized zero-range model and an application to the triton and the hypertriton,” *Nucl. Phys. A* **697**, 783–801.
- Fedorov, D. V., A. S. Jensen, and K. Riisager, 1994, “Efimov states in halo nuclei,” *Phys. Rev. Lett.* **73**, 2817.
- Ferlaino, F., S. Knoop, M. Berninger, W. Harm, J. P. D’Incao, H. C. Naegerl, and R. Grimm, 2009, “Evidence for universal four-body states tied to an Efimov trimer,” *Phys. Rev. Lett.* **102**, 140401.
- Ferlaino, F., S. Knoop, M. Mark, M. Berninger, H. Schoebel, H. C. Naegerl, and R. Grimm, 2008, “Collisions between tunable halo dimers: Exploring an elementary four-body process with identical bosons,” *Phys. Rev. Lett.* **101**, 023201.
- Ferlaino, F., A. Zenesini, M. Berninger, B. Huang, H.-C. Nägerl, and R. Grimm, 2011, “Efimov resonances in ultracold quantum gases,” *Few-Body Syst.* **51**, 113–133.
- Fermi, E., 1934, “Sopra lo spostamento per pressione delle righe elevate delle serie spettrali,” *Il Nuovo Cimento* **11**, 157–166.
- Fetter, A. L., and J. D. Walecka, 2003, *Quantum Theory of Many-particle Systems*, Dover Books on Physics (Dover Publications, New York).
- Feynman, R. P., 1955, “Slow electrons in a polar crystal,” *Phys. Rev.* **97**, 660–665.
- Fink, M. G. J., and P. Zoller, 1985, “One- and two-photon detachment of negative hydrogen ions: a hyperspherical adiabatic approach,” *J. Phys. B* **18**, L373.
- Flambaum, V. V., G. F. Gribakin, and C. Harabati, 1999, “Analytical calculation of cold-atom scattering,” *Phys. Rev. A* **59**, 1998.
- Fletcher, R. J., A. L. Gaunt, N. Navon, R. P. Smith, and Z. Hadzibabic, 2013, “Stability of a unitary Bose gas,” *Phys. Rev. Lett.* **111**, 125303.
- Flower, D. R., and G. J. Harris, 2007, “Three-body recombination of hydrogen during primordial star formation,” *Mon. Not. R. Astron. Soc.* **377**, 705–710.
- Fock, V., 1958, “Hyperspherical expansion,” *K. Nor. Vidensk. Selsk. Forh.* **31**, 138–52.
- Forrey, R. C., 2013, “Rate of formation of hydrogen molecules by three-body recombination during primordial star formation,” *Astrophys. J. Lett.* **773**, L25.
- Frederico, T., A. Delfino, Lauro Tomio, and M. T. Yamashita, 2012, “Universal aspects of light halo nuclei,” *Prog. Part. Nucl. Phys.* **67**, 939–994.
- Friar, J. L., B. F. Gibson, G. L. Payne, and C. R. Chen, 1984, “Configuration space Faddeev continuum calculations: N-d s -wave scattering lengths with tensor-force interactions,” *Phys. Rev. C* **30**, 1121.

- Fröhlich, B., M. Feld, E. Vogt, M. Koschorreck, W. Zwerger, and M. Köhl, 2011, “Radio-frequency spectroscopy of a strongly interacting two-dimensional Fermi gas,” *Phys. Rev. Lett.* **106**, 105301.
- Fröhlich, H., 1954, “Electrons in lattice fields,” *Adv. Phys.* **3**, 325–361.
- Fujiwara, Y., Y. Suzuki, M. Kohno, and K. Miyagawa, 2008, “Addendum to triton and hypertriton binding energies calculated from SU_6 quark-model baryon-baryon interactions,” *Phys. Rev. C* **77**, 027001.
- Fukuda, H., T. Ishihara, and S. Hara, 1990, “Hyperradial adiabatic treatment of $d\mu + t$ collisions at low energies,” *Phys. Rev. A* **41**, 145–149.
- Gao, B., 1998, “Quantum-defect theory of atomic collisions and molecular vibration spectra,” *Phys. Rev. A* **58**, 4222–4225.
- Gao, B., 2001, “Angular-momentum-insensitive quantum-defect theory for diatomic systems,” *Phys. Rev. A* **64**, 010701.
- Gao, B., 2008, “General form of the quantum-defect theory for $-1/r^\alpha$ type of potentials with $\alpha > 2$,” *Phys. Rev. A* **78**, 012702.
- Gao, Chao, Jia Wang, and Zhenhua Yu, 2015, “Revealing the origin of super efimov states in the hyperspherical formalism,” *Phys. Rev. A* **92**, 020504.
- Gattobigio, M., A. Kievsky, and M. Viviani, 2011, “Spectra of helium clusters with up to six atoms using soft-core potentials,” *Phys. Rev. A* **84**, 052503.
- Gattobigio, M., A. Kievsky, and M. Viviani, 2012, “Energy spectra of small bosonic clusters having a large two-body scattering length,” *Phys. Rev. A* **86**, 042513.
- Gharashi, S. E., K. M. Daily, and D. Blume, 2012, “Three s -wave-interacting fermions under anisotropic harmonic confinement: Dimensional crossover of energetics and virial coefficients,” *Phys. Rev. A* **86**, 042702.
- Giamarchi, T., 2004, *Quantum physics in one dimension* (Oxford University Press, London).
- Giannakeas, P., F. K. Diakonov, and P. Schmelcher, 2012, “Coupled ℓ -wave confinement-induced resonances in cylindrically symmetric waveguides,” *Phys. Rev. A* **86**, 042703.
- Giannakeas, P., C. H. Greene, and F. Robicheaux, 2016, “Generalized local-frame-transformation theory for excited species in external fields,” *Phys. Rev. A* **94**, 013419.
- Giannakeas, P., V. S. Melezhik, and P. Schmelcher, 2013, “Dipolar confinement-induced resonances of ultracold gases in waveguides,” *Phys. Rev. Lett.* **111**, 183201.
- Giorgini, S., L. P. Pitaevskii, and S. Stringari, 2008, “Theory of ultracold atomic Fermi gases,” *Rev. Mod. Phys.* **80**, 1215–1274.
- Girardeau, M., 1960, “Relationship between systems of impenetrable bosons and fermions in one dimension,” *J. Math. Phys.* **1**, 516–523.
- Girardeau, M. D., and M. Olshanii, 2004, “Theory of spinor Fermi and Bose gases in tight atom waveguides,” *Phys. Rev. A* **70**, 023608.
- Gloeckle, W., 1983, *The Quantum Mechanical Few-Body Problem* (Springer, Berlin).
- Gogolin, A. O., C. Mora, and R. Egger, 2008, “Analytical solution of the bosonic three-body problem,” *Phys. Rev. Lett.* **100**, 140404.
- Gongleton, J. G., 1992, “A simple model of the hypertriton,” *J. Phys. G* **18**, 339.
- Granger, Brian E., and D. Blume, 2004, “Tuning the interactions of spin-polarized Fermions using quasi-one-dimensional confinement,” *Phys. Rev. Lett.* **92**, 133202.
- Greene, C. H., 1981, “Doubly excited-states of the alkaline-earth atoms,” *Phys. Rev. A* **23**, 661–678.
- Greene, C. H., 1987, “Negative-ion photodetachment in a weak magnetic field,” *Phys. Rev. A* **36**, 4236–4244.
- Greene, C. H., 2010, “Universal insights from few-body land,” *Phys. Today* **63**, No. 3, 40–45.
- Greene, C. H., and C. W. Clark, 1984, “Adiabatic hyperspherical treatment of lithium $^2P^0$ states,” *Phys. Rev. A* **30**, 2161.
- Greene, C. H., and C. Jungen, 1985, “Molecular applications of quantum defect theory,” *Adv. At. Mol. Phys.* **21**, 51–121.
- Greene, C. H., and A. R. P. Rau, 1982, “Double escape of 2 electrons at threshold—dependence on L , S , and π ,” *Phys. Rev. Lett.* **48**, 533–537.
- Greene, C. H., and A. R. P. Rau, 1983, “Effect of symmetry on 2-electron escape at threshold,” *J. Phys. B* **16**, 99–106.
- Greiner, M., C. A. Regal, and D. S. Jin, 2003, “Emergence of a molecular Bose-Einstein condensate from a Fermi gas,” *Nature (London)* **426**, 537–540.
- Gridnev, Dmitry K., 2014, “Three resonating fermions in flatland: proof of the super efimov effect and the exact discrete spectrum asymptotics,” *J. Phys. A* **47**, 505204.
- Gross, N., Z. Shotan, S. Kokkelmans, and L. Khaykovich, 2009, “Observation of universality in ultracold ^7Li three-body recombination,” *Phys. Rev. Lett.* **103**, 163202.
- Gross, N., Z. Shotan, S. Kokkelmans, and L. Khaykovich, 2010, “Nuclear-spin-independent short-range three-body physics in ultracold atoms,” *Phys. Rev. Lett.* **105**, 103203.
- Gross, N., Z. Shotan, O. Machtey, S. Kokkelmans, and L. Khaykovich, 2011, “Study of Efimov physics in two nuclear-spin sublevels of ^7Li ,” *C.R. Phys.* **12**, 4–12.
- Grozdanov, T. P., 1995, “Photodetachment of an electron bound by a zero-range potential in magnetic fields of arbitrary strength,” *Phys. Rev. A* **51**, 607–610.
- Grusdt, F., Y. E. Shchadilova, A. N. Rubtsov, and E. Demler, 2015, “Renormalization group approach to the Frohlich polaron model: application to impurity-BEC problem,” *Sci. Rep.* **5**, 12124.
- Günter, K., T. Stöferle, H. Moritz, M. Köhl, and T. Esslinger, 2005, “ p -wave interactions in low-dimensional fermionic gases,” *Phys. Rev. Lett.* **95**, 230401.
- Hadizadeh, M. R., M. T. Yamashita, Lauro Tomio, A. Delfino, and T. Frederico, 2011, “Scaling properties of universal tetramers,” *Phys. Rev. Lett.* **107**, 135304.
- Häfner, S., J. Ulmanis, E. D. Kuhnle, Y. Wang, C. H. Greene, and M. Weidemüller, 2017, “Role of the intraspecies scattering length in the Efimov scenario with large mass difference,” *Phys. Rev. A* **95**, 062708.
- Hagen, G., P. Hagen, H.-W. Hammer, and L. Platter, 2013, “Efimov physics around the neutron-rich ^{60}Ca isotope,” *Phys. Rev. Lett.* **111**, 132501.
- Hall, F. H. J., and S. Willitsch, 2012, “Millikelvin reactive collisions between sympathetically cooled molecular ions and laser-cooled atoms in an ion-atom hybrid trap,” *Phys. Rev. Lett.* **109**, 233202.
- Haller, E., M. Gustavsson, M. J. Mark, J. G. Danzl, R. Hart, G. Pupillo, and H.-C. Nägerl, 2009, “Realization of an excited, strongly correlated quantum gas phase,” *Science* **325**, 1224–1227.
- Haller, E., M. J. Mark, R. Hart, J. G. Danzl, L. Reichsöllner, V. S. Melezhik, P. Schmelcher, and H.-C. Nägerl, 2010, “Confinement-induced resonances in low-dimensional quantum systems,” *Phys. Rev. Lett.* **104**, 153203.
- Hammer, H.-W., and L. Platter, 2007, “Universal properties of the four-body system with large scattering length,” *Eur. Phys. J. A* **32**, 113–120.
- Hanna, G. J., and D. Blume, 2006, “Energetics and structural properties of three-dimensional bosonic clusters near threshold,” *Phys. Rev. A* **74**, 063604.

- Hanna, T. M., E. Tiesinga, and P. S. Julienne, 2010, “Creation and manipulation of Feshbach resonances with radiofrequency radiation,” *New J. Phys.* **12**, 083031.
- Hanna, T. M., E. Tiesinga, W. F. Mitchell, and P. S. Julienne, 2012, “Resonant control of polar molecules in individual sites of an optical lattice,” *Phys. Rev. A* **85**, 022703.
- Hara, S., H. Fukuda, and T. Ishihara, 1989, “Application of hyperspherical coordinates to HD^+ ,” *Phys. Rev. A* **39**, 35–38.
- Hara, S., H. Fukuda, T. Ishihara, and A. V. Matveenko, 1988, “Hyper-radial adiabatic expansion for a muonic molecule $\text{dt} - \mu$,” *Phys. Lett. A* **130**, 22–25.
- Harmin, D. A., 1982a, “Theory of the nonhydrogenic Stark effect,” *Phys. Rev. Lett.* **49**, 128–131.
- Harmin, D. A., 1982b, “Theory of the Stark effect,” *Phys. Rev. A* **26**, 2656–2681.
- Härter, A., and J. H. Denschlag, 2014, “Cold atom-ion experiments in hybrid traps,” *Contemp. Phys.* **55**, 33–45.
- Härter, A., A. Krüchow, A. Brunner, W. Schnitzler, S. Schmid, and J. H. Denschlag, 2012, “Single ion as a three-body reaction center in an ultracold atomic gas,” *Phys. Rev. Lett.* **109**, 123201.
- Härter, A., A. Krüchow, M. Deiß, B. Drews, E. Tiemann, and J. H. Denschlag, 2013, “Population distribution of product states following three-body recombination in an ultracold atomic gas,” *Nat. Phys.* **9**, 512.
- Helfrich, K., H.-W. Hammer, and D. S. Petrov, 2010, “Three-body problem in heteronuclear mixtures with resonant interspecies interaction,” *Phys. Rev. A* **81**, 042715.
- Hess, H. F., D. A. Bell, G. P. Kochanski, R. W. Cline, D. Kleppner, and T. J. Greytak, 1983, “Observation of three-body recombination in spin-polarized hydrogen,” *Phys. Rev. Lett.* **51**, 483.
- Hess, H. F., D. A. Bell, G. P. Kochanski, D. Kleppner, and T. J. Greytak, 1984, “Temperature and magnetic field dependence of three-body recombination in spin-polarized hydrogen,” *Phys. Rev. Lett.* **52**, 1520.
- Heß, B., P. Giannakeas, and P. Schmelcher, 2015, “Analytical approach to atomic multichannel collisions in tight harmonic waveguides,” *Phys. Rev. A* **92**, 022706.
- Hino, K. I., and J. H. Macek, 1996, “Strong induced-dipole-field oscillations of the $\text{dt} \mu$ system above the $t\mu(n = 2)$ threshold,” *Phys. Rev. Lett.* **77**, 4310–4313.
- Hirschfelder, J. O., C. F. Curtiss, and R. B. Bird, 1954, *Molecular Theory of Transport and Processes in Gases* (Wiley, New York).
- Hiyama, E., and M. Kamimura, 2012, “Linear correlations between ^4He trimer and tetramer energies calculated with various realistic ^4He potentials,” *Phys. Rev. A* **85**, 062505.
- Holzmann, M., and Y. Castin, 1999, “Pair correlation function of an inhomogeneous interacting Bose-Einstein condensate,” *Eur. Phys. J. D* **7**, 425–432.
- Houbiers, M., R. Ferwerda, H. T. C. Stoof, W. I. McAlexander, C. A. Sackett, and R. G. Hulet, 1997, “Superfluid state of atomic ^6Li in a magnetic trap,” *Phys. Rev. A* **56**, 4864–4878.
- Hove, D., D. V. Fedorov, H. O. U. Fynbo, A. S. Jensen, K. Riisager, N. T. Zinner, and E. Garrido, 2014, “Borromean structures in medium-heavy nuclei,” *Phys. Rev. C* **90**, 064311.
- Hove, D., A. S. Jensen, H. O. U. Fynbo, N. T. Zinner, D. V. Fedorov, and E. Garrido, 2016, “Capture reactions into Borromean two-proton systems at r_p waiting points,” *Phys. Rev. C* **93**, 024601.
- Hu, H., P. D. Drummond, and X.-J. Liu, 2007, “Universal thermodynamics of strongly interacting Fermi gases,” *Nat. Phys.* **3**, 469–472.
- Hu, H., X.-J. Liu, and P. D. Drummond, 2006, “Equation of state of a superfluid Fermi gas in the BCS-BEC crossover,” *Europhys. Lett.* **74**, 574–580.
- Hu, Ming-Guang, Ruth S. Bloom, Deborah S. Jin, and Jonathan M. Goldwin, 2014, “Avalanche-mechanism loss at an atom-molecule Efimov resonance,” *Phys. Rev. A* **90**, 013619.
- Hu, Ming-Guang, Michael J. Van de Graaff, Dhruv Kedar, John P. Corson, Eric A. Cornell, and Deborah S. Jin, 2016, “Bose polarons in the strongly interacting regime,” *Phys. Rev. Lett.* **117**, 055301.
- Huang, B., K. M. O’Hara, R. Grimm, J. M. Hutson, and D. S. Petrov, 2014, “Three-body parameter for Efimov states in ^6Li ,” *Phys. Rev. A* **90**, 043636.
- Huang, B., L. A. Sidorenkov, and R. Grimm, 2015, “Finite-temperature effects on a triatomic Efimov resonance in ultracold cesium,” *Phys. Rev. A* **91**, 063622.
- Huang, B., L. A. Sidorenkov, R. Grimm, and J. M. Hutson, 2014, “Observation of the second triatomic resonance in Efimov’s scenario,” *Phys. Rev. Lett.* **112**, 190401.
- Huckans, J. H., J. R. Williams, E. L. Hazlett, R. W. Sities, and K. M. O’Hara, 2009, “Three-body recombination in a three-state Fermi gas with widely tunable interactions,” *Phys. Rev. Lett.* **102**, 165302.
- Hudson, S. D., E. Braaten, K. Daekyoung, and L. Platter, 2014, “Two-body and three-body contacts for identical bosons near unitarity,” *Phys. Rev. Lett.* **112**, 110402.
- Hui, H., A. Minguzzi, X.-J. Liu, and M. P. Tosi, 2004, “Collective modes and ballistic expansion of a Fermi gas in the BCS-BEC crossover,” *Phys. Rev. Lett.* **93**, 190403.
- Idziaszek, Z., and T. Calarco, 2005, “Two atoms in an anisotropic harmonic trap,” *Phys. Rev. A* **71**, 050701.
- Idziaszek, Z., and T. Calarco, 2006, “Analytical solutions for the dynamics of two trapped interacting ultracold atoms,” *Phys. Rev. A* **74**, 022712.
- Imambekov, A., T. L. Schmidt, and L. I. Glazman, 2012, “One-dimensional quantum liquids: Beyond the Luttinger liquid paradigm,” *Rev. Mod. Phys.* **84**, 1253.
- Inouye, S., M. R. Andrews, J. Stenger, H.-J. Miesner, D. M. Stamper-Kurn, and W. Ketterle, 1998, “Observation of Feshbach resonances in a Bose-Einstein condensate,” *Nature (London)* **392**, 151–154.
- Jagutzki, O., *et al.*, 2002, “Multiple readout of a microchannel plate detector with a three-layer delay-line anode,” *IEEE Trans. Nucl. Sci.* **49**, 2477–2483.
- Jensen, A. S., D. Riisager, D. V. Fedorov, and E. Garrido, 2004, “Structure and reactions of quantum halos,” *Rev. Mod. Phys.* **76**, 215.
- Jeon, Gun Sang, Chia-Chen Chang, and Jainendra K. Jain, 2007, “Semiconductor quantum dots in high magnetic fields,” *Eur. Phys. J. B* **55**, 271–282.
- Ji, C., E. Braaten, D. R. Phillips, and L. Platter, 2015, “Universal relations for range corrections to Efimov features,” *Phys. Rev. A* **92**, 030702.
- Jiang, S.-J., W.-M. Liu, G. W. Semenov, and F. Zhou, 2014, “Universal Bose gases near resonance: A rigorous solution,” *Phys. Rev. A* **89**, 033614.
- Jiang, S.-J., J. Maki, and F. Zhou, 2016, “Long-lived universal resonant Bose gases,” *Phys. Rev. A* **93**, 043605.
- Johansen, J., B. J. DeSalvo, K. Patel, and C. Chin, 2016, “Testing universality of Efimov physics across broad and narrow Feshbach resonances,” [arXiv:1612.05169](https://arxiv.org/abs/1612.05169).
- Johnson, B. R., 1973, “The Multichannel Log-Derivative Method for Scattering Calculations,” *J. Comput. Phys.* **13**, 445–449.
- Johnson, B. R., 1983, “The quantum dynamics of 3 particles in hyperspherical coordinates,” *J. Chem. Phys.* **79**, 1916–1925.
- Jørgensen, Nils B., Lars Wacker, Kristoffer T. Skalmstang, Meera M. Parish, Jesper Levinsen, Rasmus S. Christensen, Georg M. Bruun, and Jan J. Arlt, 2016, “Observation of attractive and repulsive

- polarons in a bose-einstein condensate,” *Phys. Rev. Lett.* **117**, 055302.
- Jraji, A., A. R. Allouche, M. Korek, and M. Aubert-Frécon, 2003, “Theoretical electronic structure of the alkali-dimer cation Rb_2^+ ,” *Chem. Phys.* **290**, 129.
- Kadomtsev, M. B., S. I. Vinitzky, and F. R. Yukajlovic, 1987, “Adiabatic representation for the 3-body problem in the limit of separated atoms in appropriate coordinates,” *Phys. Rev. A* **36**, 4652–4661.
- Kadyrov, A. S., I. Bray, A. M. Mukhamedzhanov, and A. T. Stelbovics, 2009, “Surface-integral formulation of scattering theory,” *Ann. Phys. (N.Y.)* **324**, 1516–1546.
- Kagan, Y., B. V. Svistunov, and G. V. Shlyapnikov, 1985, “Effect of Bose condensation on inelastic processes in gases,” *JETP Lett.* **42**, 209–212 [*Zh. Eksp. Teor. Fiz.* **42**, 169–172 (1985)].
- Kalas, R. M., and D. Blume, 2006, “Interaction-induced localization of an impurity in a trapped Bose-Einstein condensate,” *Phys. Rev. A* **73**, 043608.
- Kanjilal, K., and D. Blume, 2004, “Nondivergent pseudopotential treatment of spin-polarized fermions under one- and three-dimensional harmonic confinement,” *Phys. Rev. A* **70**, 042709.
- Kanjilal, K., and D. Blume, 2006, “Coupled-channel pseudopotential description of the Feshbach resonance in two dimensions,” *Phys. Rev. A* **73**, 060701.
- Kanjilal, K., John L. Bohn, and D. Blume, 2007, “Pseudopotential treatment of two aligned dipoles under external harmonic confinement,” *Phys. Rev. A* **75**, 052705.
- Karplus, M., R. N. Porter, and R. D. Sharma, 1965, “Exchange reactions with activation energy. I. Simple barrier potential for (H, H_2) ,” *J. Chem. Phys.* **43**, 3259.
- Kartavtsev, O. I., and J. H. Macek, 2002, “Low-energy three-body recombination near a Feshbach resonance,” *Few-Body Syst.* **31**, 249–254.
- Kartavtsev, O. I., and A. V. Malykh, 2007, “Low-energy three-body dynamics in binary quantum gases,” *J. Phys. B* **40**, 1429–1441.
- Kartavtsev, O. I., and A. V. Malykh, 2014, “Recent advances in description of few two-component fermions,” *Phys. At. Nucl.* **77**, 430–437.
- Kartavtsev, O. I., and A. V. Malykh, 2016, “Universal description of three two-component fermions,” *Europhys. Lett.* **115**, 36005.
- Kato, D., and S. Watanabe, 1995, “2-electron correlations in $e + \text{H}^- \rightarrow e + e + p$ near-threshold,” *Phys. Rev. Lett.* **74**, 2443–2446.
- Kato, D., and S. Watanabe, 1997, “Ab initio study of interelectronic correlations in electron-impact ionization of hydrogen,” *Phys. Rev. A* **56**, 3687–3700.
- Kazansky, A. K., P. Selles, and L. Malegat, 2003, “Hyperspherical time-dependent method with semiclassical outgoing waves for double photoionization of helium,” *Phys. Rev. A* **68**.
- Keck, J. C., 1960, “Variational theory of chemical reaction rates applied to three-body recombination,” *J. Chem. Phys.* **32**, 1035.
- Keck, J. C., 1967, “Variational theory of reaction rates,” *Adv. Chem. Phys.* **13**, 85.
- Kendrick, B. K., R. T. Pack, R. B. Walker, and E. F. Hayes, 1999, “Hyperspherical surface functions for nonzero total angular momentum. I. Eckart singularities,” *J. Chem. Phys.* **110**, 6673–6693.
- Kestner, J. P., and L.-M. Duan, 2007, “Level crossing in the three-body problem for strongly interacting Fermions in a harmonic trap,” *Phys. Rev. A* **76**, 033611.
- Ketterle, W., and M. W. Zwierlein, 2008, “Making, probing and understanding ultracold Fermi gases,” *Rivista del Nuovo Cimento* **31**, 247–422.
- Kezerashvili, R. Y., S. M. Tsiklauri, and N. Z. Takibayev, 2015, “Lighest kaonic nuclear clusters,” [arXiv:1510.00478v1](https://arxiv.org/abs/1510.00478v1).
- Kim, J. I., V. S. Melezhik, and P. Schmelcher, 2006, “Suppression of quantum scattering in strongly confined systems,” *Phys. Rev. Lett.* **97**, 193203.
- Kim, J. I., J. Schmiedmayer, and P. Schmelcher, 2005, “Quantum scattering in quasi-one-dimensional cylindrical confinement,” *Phys. Rev. A* **72**, 042711.
- Kim, Y. E., and A. L. Zubarev, 2000, “Equivalent linear two-body method for many-body problems,” *J. Phys. B* **33**, 55.
- Kim, Y. E., and A. L. Zubarev, 2002, “Equivalent linear two-body method for Bose-Einstein condensates in time-dependent harmonic traps,” *Phys. Rev. A* **66**, 053602.
- Kinoshita, T., T. Wenger, and D. S. Weiss, 2004, “Observation of a one-dimensional Tonks-Girardeau gas,” *Science* **305**, 1125–1128.
- Kira, M., 2015, “Coherent quantum depletion of an interacting atom condensate,” *Nat. Commun.* **6**, 6624.
- Klar, H., and W. Schlecht, 1976, “Threshold multiple ionization of atoms—energy-dependence for double and triple escape,” *J. Phys. B* **9**, 1699–1711.
- Knirk, Dwayne L., 1974, “Approach to the description of atoms using hyperspherical coordinates,” *J. Chem. Phys.* **60**, 66–80.
- Knoop, S., F. Ferlaino, M. Berninger, M. Mark, H.-C. Nägerl, R. Grimm, J. P. D’Incao, and B. D. Esry, 2010, “Magnetically controlled exchange process in an ultracold atom-dimer mixture,” *Phys. Rev. Lett.* **104**, 053201.
- Knoop, S., F. Ferlaino, M. Mark, M. Berninger, H. Schoebel, H.-C. Nägerl, and R. Grimm, 2009, “Observation of an Efimov-like trimer resonance in ultracold atom-dimer scattering,” *Nat. Phys.* **5**, 227–230.
- Köhl, M., H. Moritz, T. Stöferle, K. Günter, and T. Esslinger, 2005, “Fermionic atoms in a three dimensional optical lattice: Observing Fermi surfaces, dynamics, and interactions,” *Phys. Rev. Lett.* **94**, 080403.
- Köhl, W. E., and J. Schaefer, 1983, “Theoretical studies of $\text{H}_2 - \text{H}_2$ collisions. vs. Ab initio calculations of relaxation phenomena in parahydrogen gas,” *J. Chem. Phys.* **78**, 6602.
- Köhler, T., 2002, “Three-body problem in a dilute Bose-Einstein condensate,” *Phys. Rev. Lett.* **89**, 210404.
- Köhler, T., K. Góral, and P. S. Julienne, 2006, “Production of cold molecules via magnetically tunable Feshbach resonances,” *Rev. Mod. Phys.* **78**, 1311–1361.
- Kohstall, C., M. Zaccanti, M. Jag, A. Trenkwalder, P. Massignan, G. M. Bruun, F. Schreck, and R. Grimm, 2012, “Metastability and coherence of repulsive polarons in a strongly interacting Fermi mixture,” *Nature (London)* **485**, 615.
- Kokoouline, V., N. Douguet, and C. H. Greene, 2011, “Breaking bonds with electrons: Dissociative recombination of molecular ions,” *Chem. Phys. Lett.* **507**, 1–10.
- Kokoouline, V., and C. H. Greene, 2003, “Theory of dissociative recombination of D_{3h} triatomic ions applied to H_3^+ ,” *Phys. Rev. Lett.* **90**, 133201.
- Kokoouline, V., C. H. Greene, and B. D. Esry, 2001, “Mechanism for the destruction of H_3^+ ions by electron impact,” *Nature (London)* **412**, 891–894.
- Kolomeisky, E. B., and J. P. Straley, 1996, “Phase diagram and correlation exponents for interacting fermions in one dimension,” *Rev. Mod. Phys.* **68**, 175.
- Koschorreck, Marco, Daniel Pertot, Enrico Vogt, Bernd Froehlich, Michael Feld, and Michael Köhl, 2012, “Attractive and repulsive Fermi polarons in two dimensions,” *Nature (London)* **485**, 619.

- Kossmann, H., V. Schmidt, and T. Andersen, 1988, “Test of Wannier threshold laws: Double-photoionization cross section in helium,” *Phys. Rev. Lett.* **60**, 1266.
- Kosterlitz, J. M., and D. J. Thouless, 1973, “Ordering, Metastability and Phase-Transitions in 2 Dimensional Systems,” *J. Phys. C* **6**, 1181–1203.
- Kotochigova, Svetlana, 2014, “Controlling interactions between highly magnetic atoms with Feshbach resonances,” *Rep. Prog. Phys.* **77**, 093901.
- Kraemer, T., *et al.*, 2006, “Evidence for Efimov quantum states in an ultracold gas of caesium atoms,” *Nature (London)* **440**, 315–318.
- Kristensen, T., and L. Pricoupenko, 2015, “Ultracold-atom collisions in atomic waveguides: A two-channel analysis,” *Phys. Rev. A* **91**, 042703.
- Kröger, H., and R. Perne, 1980, “Efimov effect in the four-body case,” *Phys. Rev. C* **22**, 21–27.
- Krükow, A., A. Mohammadi, A. Härter, J. Hecker Denschlag, J. Pérez-Ríos, and C. H. Greene, 2016, “Energy scaling of cold atom-atom-ion three-body recombination,” *Phys. Rev. Lett.* **116**, 193201.
- Krych, M., W. Skomorowski, F. Pawłowski, R. Moszynski, and Z. Idziaszek, 2011, “Sympathetic cooling of the Ba⁺ ion by collisions with ultracold Rb atoms: Theoretical prospects,” *Phys. Rev. A* **83**, 032723.
- Ku, M. J. H., A. T. Sommer, L. W. Cheuk, and M. W. Zwierlein, 2012, “Revealing the Superfluid Lambda Transition in the Universal Thermodynamics of a Unitary Fermi Gas,” *Science* **335**, 563–567.
- Kunitski, M., *et al.*, 2015, “Observation of the Efimov state of the helium trimer,” *Science* **348**, 551–555.
- Kuppermann, A., and P. G. Hipes, 1986, “3-Dimensional quantum-mechanical reactive scattering using symmetrized hyperspherical coordinates,” *J. Chem. Phys.* **84**, 5962–5963.
- Kushibe, D., M. Mutou, T. Morishita, S. Watanabe, and M. Matsuzawa, 2004, “Aspects of hyperspherical adiabaticity in an atomic-gas Bose-Einstein condensate,” *Phys. Rev. A* **70**, 063617.
- Lamporesi, G., J. Catani, G. Barontini, Y. Nishida, M. Inguscio, and F. Minardi, 2010, “Scattering in mixed dimensions with ultracold gases,” *Phys. Rev. Lett.* **104**, 153202.
- Landau, L. D., and E. M. Lifshitz, 1976, *Mechanics* (Elsevier Butterworth-Heinemann, Burlington, MA).
- Landau, L. D., and E. M. Lifshitz, 1997, *Quantum Mechanics: Non-Relativistic Theory* (Butterworth-Heinemann, Stoneham, MA).
- Langevin, P., 1905, “Une formule fondamentale de théorie cinétique,” *C.R. Hebd. Seances Acad. Sci.* **140**, 35.
- Larson, D. J., and R. Stoneman, 1985, “Photodetachment of atomic negative ions near threshold in a magnetic field,” *Phys. Rev. A* **31**, 2210–2214.
- Lattimer, J. M., and M. Prakash, 2004, “The physics of neutron stars,” *Science* **304**, 536–542.
- Laughlin, R. B., 1983, “Quantized motion of three two-dimensional electrons in a strong magnetic field,” *Phys. Rev. B* **27**, 3383–3389.
- Launay, J. M., and M. Le Dourneuf, 1990, “Quantum-mechanical calculation of integral cross sections for the reaction $F + H_2(v = 0, j = 0) \rightarrow FH(v'j') + H$ by the hyperspherical method,” *Chem. Phys. Lett.* **169**, 473–481.
- Laurent, S., X. Leyronas, and F. Chevy, 2014, “Momentum distribution of a dilute unitary Bose gas with three-body losses,” *Phys. Rev. Lett.* **113**, 220601.
- Lazauskas, R., and J. Carbonell, 2006, “Description of ⁴He tetramer bound and scattering states,” *Phys. Rev. A* **73**, 062717.
- LeBlanc, L. J., and J. H. Thywissen, 2007, “Species-specific optical lattices,” *Phys. Rev. A* **75**, 053612.
- Lee, M. D., T. Köhler, and P. S. Julienne, 2007, “Excited Thomas-Efimov levels in ultracold gases,” *Phys. Rev. A* **76**, 012720.
- Lee, Yu-Li, and Yu-Wen Lee, 2010, “Universality and stability for a dilute Bose gas with a Feshbach resonance,” *Phys. Rev. A* **81**, 063613.
- Lemeshko, Mikhail, 2017, “Quasiparticle approach to molecules interacting with quantum solvents,” *Phys. Rev. Lett.* **118**, 095301.
- Lepage, G. P., 1989, *From Actions to Answers (TASI-89)*, edited by T. DeGrand and D. Toussaint (World Scientific, Singapore).
- Lepage, G. P., 1997, “How to renormalize the Schrödinger equation,” [arXiv:nucl-th/9706029](https://arxiv.org/abs/nucl-th/9706029).
- Lepetit, B., Z. Peng, and A. Kuppermann, 1990, “Calculation of bound rovibrational states on the first electronically excited state of the H₃ system,” *Chem. Phys. Lett.* **166**, 572.
- Levine, R. D., and R. B. Bernstein, 1987, *Molecular Reaction Dynamics and Chemical Reactivity* (Oxford University Press, New York).
- Levinger, J. S., 1974, *The two and three body problem* (Springer, Berlin), p. 88.
- Levinsen, Jesper, Pietro Massignan, and Meera M. Parish, 2014, “Efimov trimers under strong confinement,” *Phys. Rev. X* **4**, 031020.
- Levinsen, Jesper, Meera M. Parish, and Georg M. Bruun, 2015, “Impurity in a Bose-Einstein Condensate and the Efimov Effect,” *Phys. Rev. Lett.* **115**, 125302.
- Lewenstein, M., A. Sanpera, and V. Ahufinger, 2012, *Ultracold Atoms in Optical Lattices: Simulating quantum many-body systems* (Oxford University Press, London).
- Lewenstein, M., A. Sanpera, V. Ahufinger, B. Damski, A. Sen, and U. Sen, 2007, “Ultracold atomic gases in optical lattices: mimicking condensed matter physics and beyond,” *Adv. Phys.* **56**, 243–379.
- Lewerenz, M., 1997, “Structure and energetics of small helium clusters: Quantum simulations using a recent perturbational pair potential,” *J. Chem. Phys.* **106**, 4596–4603.
- Leyton, V., M. Roghani, V. Peano, and M. Thorwart, 2014, “Photon-assisted confinement-induced resonances for ultracold atoms,” *Phys. Rev. Lett.* **112**, 233201.
- Li, Weiran, and S. Das Sarma, 2014, “Variational study of polarons in Bose-Einstein condensates,” *Phys. Rev. A* **90**, 013618.
- Lieb, E. H., R. Seiringer, and J. Yngvason, 2004, “One-dimensional behavior of dilute, trapped Bose gases,” *Commun. Math. Phys.* **244**, 347–393.
- Lin, C. D., 1986, “Doubly excited-states, including new classification schemes,” *Adv. At. Mol. Phys.* **22**, 77–142.
- Lin, C. D., 1995, “Hyperspherical coordinate approach to atomic and other Coulombic three-body systems,” *Phys. Rep.* **257**, 1–83.
- Lin, C. D., and T. Morishita, 2000, “Few-body problems: The hyperspherical way,” *Phys. Essays* **13**, 367–376.
- Liu, Xia-Ji, Hui Hu, and Peter D. Drummond, 2009, “Virial Expansion for a Strongly Correlated Fermi Gas,” *Phys. Rev. Lett.* **102**, 160401.
- Loftus, T., C. A. Regal, C. Ticknor, J. L. Bohn, and D. S. Jin, 2002, “Resonant control of elastic collisions in an optically trapped Fermi gas of atoms,” *Phys. Rev. Lett.* **88**, 173201.
- Lompe, T., T. B. Ottenstein, F. Serwane, K. Viering, A. N. Wenz, G. Zürn, and S. Jochim, 2010, “Atom-dimer scattering in a three-component Fermi gas,” *Phys. Rev. Lett.* **105**, 103201.
- Lompe, T., T. B. Ottestein, F. Serwane, A. N. Wenz, G. Zürn, and S. Jochim, 2010, “Radio-frequency association of Efimov trimers,” *Science* **330**, 940–944.

- Lonardonì, D., F. Pederiva, and S. Gandolfi, 2014, “From hypernuclei to the inner core of neutron stars: A quantum Monte Carlo study,” *J. Phys. Conf. Ser.* **529**, 012012.
- Macek, J., 1968, “Properties of autoionizing states of He,” *J. Phys. B* **1**, 831.
- Macek, J., 1986, “Loosely bound states of three particles,” *Z. Phys. D* **3**, 31.
- Macek, J., and K. A. Jertjan, 1986, “Adiabatic hyperspherical treatment of HD^+ ,” *Phys. Rev. A* **33**, 233–241.
- Macek, J. H., 2002, “Multichannel zero-range potentials in the hyperspherical theory of three-body dynamics,” *Few-Body Syst.* **31**, 241–248.
- Macek, J. H., S. Ovchinnikov, and G. Gasaneo, 2005, “Solution for boson-diboson elastic scattering at zero energy in the shape-independent model,” *Phys. Rev. A* **72**, 032709.
- Macek, J. H., S. Yu Ovchinnikov, and G. Gasaneo, 2006, “Exact solution for three particles interacting via zero-range potentials,” *Phys. Rev. A* **73**, 032704.
- Machtey, O., D. A. Kessler, and L. Khaykovich, 2012, “Universal dimer in a collisionally opaque medium: Experimental observables and Efimov resonances,” *Phys. Rev. Lett.* **108**, 130403.
- Machtey, O., Z. Shotan, N. Gross, and L. Khaykovich, 2012, “Association of Efimov trimers from a three-atom continuum,” *Phys. Rev. Lett.* **108**, 210406.
- Maier, R. A. W., M. Eisele, E. Tiemann, and C. Zimmermann, 2015, “Efimov resonance and three-body parameter in a lithium-rubidium mixture,” *Phys. Rev. Lett.* **115**, 043201.
- Makotyn, P., C. E. E. Klauss, D. L. L. Goldberger, E. A. Cornell, and D. S. Jin, 2014, “Universal dynamics of a degenerate unitary Bose gas,” *Nat. Phys.* **10**, 116–119.
- Malegat, L., 2003, “On the theoretical treatment of the double electronic continuum,” *Phys. Scr.* **68**, C113–C117.
- Malegat, L., 2004, “(e, 2e) and (γ , 2e) processes: Open and closed questions,” *Phys. Scr.* **T110**, 83–89.
- Manolopoulos, David E., Michael J. Jamieson, and Atul D. Pradhan, 1993, “Johnson’s log derivative algorithm rederived,” *J. Comput. Phys.* **105**, 169–172.
- Mansbach, P., and J. Keck, 1969, “Monte Carlo trajectory calculations of atomic excitation and ionization by thermal electrons,” *Phys. Rev.* **181**, 275–289.
- Maslov, V. P., and M. V. Fedoriuk, 1981, *Semi-classical approximation in quantum mechanics* (D. Reidel Publishing Company, London, England).
- Mason, E. A., and L. Monchick, 1962, “Heat conductivity of polyatomic and polar gases,” *J. Chem. Phys.* **36**, 1622.
- Massignan, P., and Y. Castin, 2006, “Three-dimensional strong localization of matter waves by scattering from atoms in a lattice with a confinement-induced resonance,” *Phys. Rev. A* **74**, 013616.
- McCourt, F. R. W., J. J. M. Beenaker, W. E. Köhler, and I. Kuscer, 1991, *Nonequilibrium Phenomena in Polyatomic Gases* (Oxford University Press, Clarendon, Oxford).
- McCurdy, C. W., M. Baertschy, and T. N. Rescigno, 2004, “Solving the three-body Coulomb breakup problem using exterior complex scaling,” *J. Phys. B* **37**, R137.
- McCurdy, C. W., T. N. Rescigno, and D. Byrum, 1997, “Approach to electron-impact ionization that avoids the three-body Coulomb asymptotic form,” *Phys. Rev. A* **56**, 1958–1969.
- McGuire, J. B., 1964, “Study of exactly soluble one-dimensional n-body problems,” *J. Math. Phys. (N.Y.)* **5**, 622–636.
- McKay, D. C., and B. DeMarco, 2011, “Cooling in strongly correlated optical lattices: prospects and challenges,” *Rep. Prog. Phys.* **74**, 054401.
- Mehta, N. P., B. D. Esry, and C. H. Greene, 2007, “Three-body recombination in one dimension,” *Phys. Rev. A* **76**, 022711.
- Mehta, N. P., S. T. Rittenhouse, J. P. D’Incao, J. von Stecher, and C. H. Greene, 2009, “General theoretical description of N -body recombination,” *Phys. Rev. Lett.* **103**, 153201.
- Mehta, N. P., Seth T. Rittenhouse, J. P. D’Incao, and C. H. Greene, 2008, “Efimov states embedded in the three-body continuum,” *Phys. Rev. A* **78**, 020701.
- Mehta, N. P., and J. R. Shepard, 2005, “Three bosons in one dimension with short-range interactions: Zero-range potentials,” *Phys. Rev. A* **72**, 032728.
- Melezhik, V. S., and P. Schmelcher, 2009, “Quantum dynamics of resonant molecule formation in waveguides,” *New J. Phys.* **11**, 073031.
- Melezhik, V. S., and P. Schmelcher, 2011, “Multichannel effects near confinement-induced resonances in harmonic waveguides,” *Phys. Rev. A* **84**, 042712.
- Meyer, K. W., and C. H. Greene, 1994, “Double photoionization of helium using R-matrix methods,” *Phys. Rev. A* **50**, R3573–R3576.
- Meyer, K. W., C. H. Greene, and B. D. Esry, 1997, “Two-electron photoejection of He and H^- ,” *Phys. Rev. Lett.* **78**, 4902–4905.
- Michaud, M., and L. Sanche, 1987, “Absolute Vibrational-Excitation Cross-Sections for Slow-Electron (1–18 eV) Scattering in Solid H_2O ,” *Phys. Rev. A* **36**, 4684–4699.
- Micheli, A., Z. Idziaszek, G. Pupillo, M. A. Baranov, P. Zoller, and P. S. Julienne, 2010, “Universal rates for reactive ultracold polar molecules in reduced dimensions,” *Phys. Rev. Lett.* **105**, 073202.
- Mies, F. H., 1984, “A multichannel quantum defect analysis of diatomic predissociation and inelastic atomic scattering,” *J. Chem. Phys.* **80**, 2514.
- Mies, F. H., and M. Raoult, 2000, “Analysis of threshold effects in ultracold atomic collisions,” *Phys. Rev. A* **62**, 012708.
- Mikkelsen, M., A. S. Jensen, D. V. Fedorov, and N. T. Zinner, 2015, “Three-body recombination of two-component cold atomic gases into deep dimers in an optical model,” *J. Phys. B* **48**, 085301.
- Mitroy, Jim, Sergiy Bubin, Wataru Horiuchi, Yasuyuki Suzuki, Ludwik Adamowicz, Wojciech Cencek, Krzysztof Szalewicz, Jacek Komasa, D. Blume, and Kalman Varga, 2013, “Theory and application of explicitly correlated Gaussians,” *Rev. Mod. Phys.* **85**, 693–749.
- Moerdijk, A. J., H. M. J. M. Boesten, and B. J. Verhaar, 1996, “Decay of trapped ultracold alkali atoms by recombination,” *Phys. Rev. A* **53**, 916–920.
- Moerdijk, A. J., and B. J. Verhaar, 1996, “Collisional two- and three-body decay rates of dilute quantum gases at ultralow temperatures,” *Phys. Rev. A* **53**, R19–R22.
- Montero, S., and J. Pérez-Ríos, 2014, “Rotational relaxation in molecular hydrogen and deuterium: Theory versus acoustic experiments,” *J. Chem. Phys.* **141**, 114301.
- Moore, M. G., T. Bergeman, and M. Olshanii, 2004, “Scattering in tight atom waveguides,” *J. Phys. IV (France)* **116**, 69–86.
- Mora, C., R. Egger, and A. O. Gogolin, 2005, “Three-body problem for ultracold atoms in quasi-one-dimensional traps,” *Phys. Rev. A* **71**, 052705.
- Mora, C., R. Egger, A. O. Gogolin, and A. Komnik, 2004, “Atom-dimer scattering for confined ultracold Fermion gases,” *Phys. Rev. Lett.* **93**, 170403.
- Mora, C., A. Komnik, R. Egger, and A. O. Gogolin, 2005, “Four-body problem and BEC-BCS crossover in a quasi-one-dimensional cold Fermion gas,” *Phys. Rev. Lett.* **95**, 080403.
- Mora, Christophe, Alexander O. Gogolin, and Reinhold Egger, 2011, “Exact solution of the three-boson problem at vanishing energy,” *C.R. Phys.* **12**, 27–38.

- Morishita, T., and C. D. Lin, 1998, “Hyperspherical analysis of doubly and triply excited states of Li,” *Phys. Rev. A* **57**, 4268–4274.
- Morishita, T., and C. D. Lin, 1999, “Comprehensive analysis of electron correlations in three-electron atoms,” *Phys. Rev. A* **59**, 1835–1843.
- Morishita, T., and C. D. Lin, 2005, “Hyperspherical analysis of radial correlations in four-electron atoms,” *Phys. Rev. A* **71**, 012504.
- Morishita, T., O. I. Tolstikhin, S. Watanabe, and M. Matsuzawa, 1997, “Hyperspherical hierarchy of three-electron radial excitations,” *Phys. Rev. A* **56**, 3559–3568.
- Moritz, H., T. Stöferle, K. Günter, M. Köhl, and T. Esslinger, 2005, “Confinement induced molecules in a 1D Fermi gas,” *Phys. Rev. Lett.* **94**, 210401.
- Moroz, S., and Y. Nishida, 2014, “Super Efimov effect for mass-imbalanced systems,” *Phys. Rev. A* **90**, 063631.
- Morse, P. M., and H. A. Feshbach, 1953, *Methods of Theoretical Physics* (McGraw-Hill, New York), 1st ed.
- Naidon, P., 2016, “Two impurities in a Bose-Einstein condensate: from Yukawa to Efimov attracted polarons,” [arXiv:1607.04507](https://arxiv.org/abs/1607.04507).
- Naidon, P., and S. Endo, 2017, “Efimov Physics: a review,” *Rep. Prog. Phys.* **80**, 056001.
- Naidon, P., S. Endo, and M. Ueda, 2014a, “Microscopic origin and universality classes of the Efimov three-body parameter,” *Phys. Rev. Lett.* **112**, 105301.
- Naidon, P., S. Endo, and M. Ueda, 2014b, “Physical origin of the universal three-body parameter in atomic Efimov physics,” *Phys. Rev. A* **90**, 022106.
- Naidon, P., E. Hiyama, and M. Ueda, 2012, “Universality and the three-body parameter of ^4He trimers,” *Phys. Rev. A* **86**, 012502.
- Nakajima, S., M. Horikoshi, T. Mukaiyama, P. Naidon, and M. Ueda, 2010, “Nonuniversal Efimov atom-dimer resonances in a three-component mixture of ^6Li ,” *Phys. Rev. Lett.* **105**, 023201.
- Nakajima, S., M. Horikoshi, T. Mukaiyama, P. Naidon, and M. Ueda, 2011, “Measurement of an Efimov trimer binding energy in a three-component mixture of ^6Li ,” *Phys. Rev. Lett.* **106**, 143201.
- Nascimbene, S., N. Navon, K. J. Jiang, F. Chevy, and C. Salomon, 2010, “Exploring the thermodynamics of a universal Fermi gas,” *Nature (London)* **463**, 1057–U73.
- Naus, H. W. L., and J. A. Tjon, 1987, “The Efimov Effect in a 4-Body System,” *Few-Body Syst.* **2**, 121–126.
- Neuhauser, D., R. S. Judson, R. L. Jaffe, M. Baer, and D. J. Kouri, 1991, “Total integral reactive cross-sections for $\text{F} + \text{H}_2 \rightarrow \text{HF} + \text{H}$: comparison of converged quantum, quasi-classical trajectory and experimental results,” *Chem. Phys. Lett.* **176**, 546–550.
- Neumark, D. M., A. M. Wodtke, G. N. Robinson, C. C. Hayden, and Y. T. Lee, 1985, “Molecular-beam studies of the $\text{F} + \text{H}_2$ reaction,” *J. Chem. Phys.* **82**, 3045–3066.
- Ngampruetikorn, Vudtiwat, Meera M. Parish, and Jesper Levinsen, 2013, “Three-body problem in a two-dimensional Fermi gas,” *Europhys. Lett.* **102**, 13001.
- Nicholson, Amy N., 2012, “ n ,” *Phys. Rev. Lett.* **109**, 073003.
- Nielsen, E., D. V. Fedorov, A. S. Jensen, and E. Garrido, 2001, “The three-body problem with short-range interactions,” *Phys. Rep.* **347**, 373–459.
- Nielsen, Esben, and J. H. Macek, 1999, “Low-energy recombination of identical bosons by three-body collisions,” *Phys. Rev. Lett.* **83**, 1566–1569.
- Nikitin, E. E., 1970, *Teoriya Elementarnykh Atomnomolekulyarnykh Protssessov v Gazakh (Theory of Elementary Atom-molecule Processes in Gases)* (Izd. Khimiya, Moscow).
- Nishida, Y., 2017, “Semi-super Efimov effect of two-dimensional bosons at a three-body resonance,” *Phys. Rev. Lett.* **118**, 230601.
- Nishida, Y., S. Moroz, and D. T. Son, 2013, “Super Efimov effect of resonantly interacting fermions in two dimensions,” *Phys. Rev. Lett.* **110**, 235301.
- Nishida, Y., and S. Tan, 2008, “Universal Fermi gases in mixed dimensions,” *Phys. Rev. Lett.* **101**, 170401.
- Nishida, Y., and S. Tan, 2010, “Confinement-induced p -wave resonances from s -wave interactions,” *Phys. Rev. A* **82**, 062713.
- Nishida, Y., and S. Tan, 2011, “Liberating Efimov physics from three dimensions,” *Few-Body Syst.* **51**, 191–206.
- Nogga, A., H. Kamada, and W. Glöckle, 2000, “Modern nuclear forces predictions for the α particle,” *Phys. Rev. Lett.* **85**, 944.
- Ohsaki, A., and H. Nakamura, 1990, “Hyperspherical coordinate approach to atom-diatom chemical reactions in the sudden and adiabatic approximations,” *Phys. Rep.* **187**, 1–62.
- Olshani, M., 1998, “Atomic scattering in the presence of an external confinement and a gas of impenetrable bosons,” *Phys. Rev. Lett.* **81**, 938–941.
- Ottenstein, T. B., T. Lompe, M. Kohnen, A. N. Wenz, and S. Jochim, 2008, “Collisional stability of a three-component degenerate Fermi gas,” *Phys. Rev. Lett.* **101**, 203202.
- Owens, D. J., T. Xie, and J. M. Hutson, 2016, “Creating Feshbach resonances for ultracold molecule formation with radio-frequency fields,” *Phys. Rev. A* **94**, 023619.
- Pack, R. T., and G. A. Parker, 1987, “Quantum reactive scattering in three dimensions using hyperspherical (APH) coordinates,” *J. Chem. Phys.* **87**, 3888–3921.
- Pack, R. T., and G. A. Parker, 1989, “Quantum reactive scattering in three dimensions using hyperspherical (APH) coordinates. III. small theta behavior and corrigenda,” *J. Chem. Phys.* **90**, 3511–3519.
- Paredes, B., A. Widera, V. Murg, O. Mandel, S. Fölling, J. I. Cirac, G. V. Shlyapnikov, T. W. Hänsch, and I. Bloch, 2004, “Tonks-Girardeau gas of ultracold atoms in an optical lattice,” *Nature (London)* **429**, 277–281.
- Patton, B., W. Langbein, and U. Woggon, 2003, “Trion, biexciton, and exciton dynamics in single self-assembled cdse quantum dots,” *Phys. Rev. B* **68**, 125316.
- Peano, V., M. Thorwart, C. Mora, and R. Egger, 2005, “Confinement-induced resonances for a two-component ultracold atom gas in arbitrary quasi-one-dimensional traps,” *New J. Phys.* **7**, 192.
- Peng, S.-G., S. Bohloul, X.-J. J. Liu, H. Hu, and P. D. Drummond, 2010, “Confinement-induced resonance in quasi-one-dimensional systems under transversely anisotropic confinement,” *Phys. Rev. A* **82**, 063633.
- Peng, S.-G., H. Hu, X.-J. Liu, and P. D. Drummond, 2011, “Confinement-induced resonances in anharmonic waveguides,” *Phys. Rev. A* **84**, 043619.
- Peng, S.-G., H. Hu, X.-J. Liu, and K. Jiang, 2012, “Two-channel-model description of confinement-induced Feshbach molecules,” *Phys. Rev. A* **86**, 033601.
- Peng, S.-G., S. Tan, and K. Jiang, 2014, “Manipulation of p -wave scattering of cold atoms in low dimensions using the magnetic field vector,” *Phys. Rev. Lett.* **112**, 250401.
- Pérez-Ríos, J., and C. H. Greene, 2015, “Communication: Classical threshold law for ion-neutral-neutral three-body recombination,” *J. Chem. Phys.* **143**, 041105.
- Pérez-Ríos, J., S. Ragole, J. Wang, and C. H. Greene, 2014, “Comparison of classical and quantal calculations of helium three-body recombination,” *J. Chem. Phys.* **140**, 044307.
- Peterkop, R., 1971, “WKB approximation and threshold law for electron-atom ionization,” *J. Phys. B* **4**, 513.
- Peterkop, R., 1983, “On the derivation of the ionization threshold law,” *J. Phys. B* **16**, L587–L593.

- Petrignani, A., *et al.*, 2011, “Resonant structure of low-energy H_3^+ dissociative recombination,” *Phys. Rev. A* **83**, 032711.
- Petrov, D. S., 2004, “Three-boson problem near a narrow Feshbach resonance,” *Phys. Rev. Lett.* **93**, 143201.
- Petrov, D. S., 2012, “The few-atom problem,” [arXiv:1206.5752](https://arxiv.org/abs/1206.5752).
- Petrov, D. S., M. Holzmann, and G. V. Shlyapnikov, 2000, “Bose-Einstein condensation in quasi-2D trapped gases,” *Phys. Rev. Lett.* **84**, 2551–2555.
- Petrov, D. S., C. Salomon, and G. V. Shlyapnikov, 2005a, “Diatomic molecules in ultracold Fermi gases—novel composite bosons,” *J. Phys. B* **38**, S645–S660.
- Petrov, D. S., C. Salomon, and G. V. Shlyapnikov, 2005b, “Scattering properties of weakly bound dimers of Fermionic atoms,” *Phys. Rev. A* **71**, 012708.
- Petrov, D. S., and G. V. Shlyapnikov, 2001, “Interatomic collisions in a tightly confined Bose gas,” *Phys. Rev. A* **64**, 012706.
- Petrov, D. S., and F. Werner, 2015, “Three-body recombination in heteronuclear mixtures at finite temperature,” *Phys. Rev. A* **92**, 022704.
- Phillips, A. C., 1968, “Consistency of the low-energy three-nucleon observables and the separable interaction model,” *Nucl. Phys. A* **107**, 209.
- Piatecki, S., and W. Krauth, 2014, “Efimov-driven phase transitions of the unitary Bose gas,” *Nat. Commun.* **5**, 3503.
- Pindzola, M. S., and F. Robicheaux, 1998, “Correlated photoionization processes in H^- ,” *Phys. Rev. A* **58**, 4229–4231.
- Pindzola, M. S., *et al.*, 2007, “The time-dependent close-coupling method for atomic and molecular collision processes,” *J. Phys. B* **40**, R39.
- Pires, R., M. Repp, J. Ulmanis, E. D. Kuhnle, M. Weidemüller, T. G. Tiecke, C. H. Greene, B. P. Ruzic, J. L. Bohn, and E. Tiemann, 2014, “Analyzing Feshbach resonances: A $^6\text{Li} - ^{133}\text{Cs}$ case study,” *Phys. Rev. A* **90**, 012710.
- Pires, R., J. Ulmanis, S. Häfner, M. Repp, A. Arias, E. D. Kuhnle, and M. Weidemüller, 2014, “Observation of Efimov resonances in a mixture with extreme mass imbalance,” *Phys. Rev. Lett.* **112**, 250404.
- Platter, L., H.-W. Hammer, and U.-G. Meißner, 2004, “Four-boson system with short-range interactions,” *Phys. Rev. A* **70**, 052101.
- Platter, L., H.-W. Hammer, and U.-G. Meißner, 2005, “On the correlation between the binding energies of the triton and the α -particle,” *Phys. Lett. B* **607**, 254–258.
- Pohl, T., D. Vrinceanu, and H. R. Sadeghpour, 2008, “Rydberg atom formation in ultracold plasmas: Small energy transfer with large consequences,” *Phys. Rev. Lett.* **100**, 223201.
- Pollack, S. E., D. Dries, and R. G. Hulet, 2009, “Universality in three- and four-body bound states of ultracold atoms,” *Science* **326**, 1683–1685.
- Press, W. H., S. A. Teukolsky, W. T. Vetterling, and B. P. Flannery, 1986, *Numerical Recipes in Fortran 77* (Cambridge University Press, Cambridge, England).
- Pricoupenko, L., 2008, “Resonant scattering of ultracold atoms in low dimensions,” *Phys. Rev. Lett.* **100**, 170404.
- Pricoupenko, Ludovic, 2011, “Isotropic contact forces in arbitrary representation: Heterogeneous few-body problems and low dimensions,” *Phys. Rev. A* **83**, 062711.
- Radzihovsky, L., P. B. Weichman, and J. I. Park, 2008, “Superfluidity and phase transitions in a resonant Bose gas,” *Ann. Phys. (N.Y.)* **323**, 2376–2451.
- Rakshit, D., and D. Blume, 2012, “Hyperspherical explicitly correlated Gaussian approach for few-body systems with finite angular momentum,” *Phys. Rev. A* **86**, 062513.
- Rancon, A., and K. Levin, 2014, “Equilibrating dynamics in quenched Bose gases: Characterizing multiple time regimes,” *Phys. Rev. A* **90**, 021602.
- Rath, Steffen Patrick, and Richard Schmidt, 2013, “Field-theoretical study of the Bose polaron,” *Phys. Rev. A* **88**, 053632.
- Rau, A. R. P., 1971, “2 electrons in a Coulomb potential—double-continuum wave functions and threshold law for electron-atom ionization,” *Phys. Rev. A* **4**, 207.
- Rau, A. R. P., 1984, “The Wannier theory for 2 electrons escaping from a positive-ion,” *Phys. Rep.* **110**, 369–387.
- Rau, A. R. P., 1992, “Excitation and Decay of Correlated Atomic States,” *Science* **258**, 1444–1451.
- Read, F. H., 1984, “Extensions of the Wannier theory for near-threshold excitation and ionization of atoms by electron-impact,” *J. Phys. B* **17**, 3965–3986.
- Regal, C. A., M. Greiner, S. Giorgini, M. Holland, and D. S. Jin, 2005, “Momentum distribution of a Fermi gas of atoms in the BCS-BEC crossover,” *Phys. Rev. Lett.* **95**, 250404.
- Regal, C. A., M. Greiner, and D. S. Jin, 2004a, “Lifetime of molecule-atom mixtures near a Feshbach resonance in ^{40}K ,” *Phys. Rev. Lett.* **92**, 083201.
- Regal, C. A., M. Greiner, and D. S. Jin, 2004b, “Observation of resonance condensation of Fermionic atom pairs,” *Phys. Rev. Lett.* **92**, 040403.
- Regal, C. A., and D. S. Jin, 2007, “Experimental realization of the BCS-BEC crossover with a Fermi gas of atoms,” *Adv. At. Mol. Opt. Phys.* **54**, 1–79.
- Regal, C. A., C. Ticknor, J. L. Bohn, and D. S. Jin, 2003, “Tuning p -wave interactions in an ultracold Fermi gas of atoms,” *Phys. Rev. Lett.* **90**, 053201.
- Rem, B. S., *et al.*, 2013, “Lifetime of the Bose gas with resonant interactions,” *Phys. Rev. Lett.* **110**, 163202.
- Rittenhouse, S. T., M. J. Cavagnero, J. von Stecher, and C. H. Greene, 2006, “A hyperspherical variational approach to the N-Fermion problem,” *Few-Body Syst.* **38**, 85–90.
- Rittenhouse, S. T., and C. H. Greene, 2008, “The degenerate Fermi gas with density-dependent interactions in the large- n limit under the K-harmonic approximation,” *J. Phys. B* **41**, 205302.
- Rittenhouse, S. T., J. von Stecher, J. P. D’Incao, N. P. Mehta, and C. H. Greene, 2011, “The hyperspherical four-fermion problem,” *J. Phys. B* **44**, 172001.
- Rittenhouse, S. T., A. Wray, and B. L. Johnson, 2016, “Hyperspherical approach to a three-boson problem in two dimensions with a magnetic field,” *Phys. Rev. A* **93**, 012511.
- Robicheaux, F., 2006, “Three-body recombination for electrons in a strong magnetic field: Magnetic moment,” *Phys. Rev. A* **73**, 033401.
- Robicheaux, F., 2007, “Three-body recombination with mixed sign light particles,” *J. Phys. B* **40**, 271–280.
- Robicheaux, F., P. Giannakeas, and C. H. Greene, 2015, “Schwinger-variational-principle theory of collisions in the presence of multiple potentials,” *Phys. Rev. A* **92**, 022711.
- Robicheaux, F., S. D. Loch, M. S. Pindzola, and C. P. Ballance, 2010, “Contribution of near threshold states to recombination in plasmas,” *Phys. Rev. Lett.* **105**, 233201.
- Robicheaux, F., M. S. Pindzola, and D. R. Plante, 1997, “Time-dependent quantal calculations for $L = 0$ models of the electron-impact ionization of hydrogen near threshold,” *Phys. Rev. A* **55**, 3573–3579.
- Rodberg, L. S., and R. M. Thaler, 1970, *Introduction to the Quantum Theory of Scattering*, Pure and Applied Physics, A Series of Monographs and Textbooks, Vol. 26 (Academic Press, New York).

- Roy, S., M. Landini, A. Trenkwalder, G. Semeghini, G. Spagnolli, A. Simoni, M. Fattori, M. Inguscio, and G. Modugno, 2013, “Test of the universality of the three-body Efimov parameter at narrow Feshbach resonances,” *Phys. Rev. Lett.* **111**, 053202.
- Ruzic, B., C. H. Greene, and J. Bohn, 2013, “Quantum defect theory for high-partial-wave cold collisions,” *Phys. Rev. A* **87**, 032706.
- Sadeghpour, H. R., J. L. Bohn, M. J. Cavagnero, B. D. Esry, I. I. Fabrikant, J. H. Macek, and A. R. P. Rau, 2000, “Collisions near threshold in atomic and molecular physics,” *J. Phys. B* **33**, R93–R140.
- Sadeghpour, H. R., and C. H. Greene, 1990, “Dominant photodetachment channels in H^- ,” *Phys. Rev. Lett.* **65**, 313–316.
- Sá de Melo, C. A. R., M. Randeria, and J. R. Engelbrecht, 1993, “Crossover from BCS to Bose superconductivity: Transition temperature and time-dependent Ginzburg-Landau theory,” *Phys. Rev. Lett.* **71**, 3202.
- Saeidian, S., V. S. Melezhik, and P. Schmelcher, 2008, “Multichannel atomic scattering and confinement-induced resonances in waveguides,” *Phys. Rev. A* **77**, 042721.
- Saeidian, S., V. S. Melezhik, and P. Schmelcher, 2012, “Shifts and widths of Feshbach resonances in atomic waveguides,” *Phys. Rev. A* **86**, 062713.
- Saeidian, S., V. S. Melezhik, and P. Schmelcher, 2015, “Shifts and widths of p -wave confinement induced resonances in atomic waveguides,” *J. Phys. B* **48**, 155301.
- Safavi-Naini, A., Seth T. Rittenhouse, D. Blume, and H. R. Sadeghpour, 2013, “Nonuniversal bound states of two identical heavy fermions and one light particle,” *Phys. Rev. A* **87**, 032713.
- Sagi, Y., T. E. Drake, R. Paudel, R. Chapurin, and D. S. Jin, 2013, “Probing local quantities in a strongly interacting Fermi gas,” *J. Phys. Conf. Ser.* **467**, 012010.
- Sagi, Y., T. E. Drake, R. Paudel, and D. S. Jin, 2012, “Measurement of the homogeneous contact of a unitary Fermi gas,” *Phys. Rev. Lett.* **109**, 220402.
- Sala, S., P. I. Schneider, and A. Saenz, 2012, “Inelastic confinement-induced resonances in low-dimensional quantum systems,” *Phys. Rev. Lett.* **109**, 073201.
- Sala, S., G. Zürn, T. Lompe, A. N. N. Wenz, S. Murmann, F. Serwane, S. Jochim, and A. Saenz, 2013, “Coherent molecule formation in anharmonic potentials near confinement-induced resonances,” *Phys. Rev. Lett.* **110**, 203202.
- Scelle, R., T. Rentrop, A. Trautmann, T. Schuster, and M. K. Oberthaler, 2013, “Motional Coherence of Fermions Immersed in a Bose Gas,” *Phys. Rev. Lett.* **111**, 070401.
- Schakel, A. M. J., 2010, “Tan relations in dilute Bose gases,” [arXiv:1007.3452v1](https://arxiv.org/abs/1007.3452v1).
- Schirotzek, Andre, Cheng-Hsun Wu, Ariel Sommer, and Martin W. Zwierlein, 2009, “Observation of Fermi Polarons in a Tunable Fermi Liquid of Ultracold Atoms,” *Phys. Rev. Lett.* **102**, 230402.
- Schmidt, R., S. P. Rath, and W. Zwerger, 2012, “Efimov physics beyond universality,” *Eur. Phys. J. B* **85**, 386.
- Schmidt, Richard, and Mikhail Lemeshko, 2016, “Deformation of a quantum many-particle system by a rotating impurity,” *Phys. Rev. X* **6**, 011012.
- Schöllkopf, W., and J. P. Toennies, 1994, “Nondestructive mass selection of small van-der-Waals clusters,” *Science* **266**, 1345–1348.
- Schöllkopf, W., and J. P. Toennies, 1996, “The nondestructive detection of the helium dimer and trimer,” *J. Chem. Phys.* **104**, 1155.
- Schunck, C. H., M. W. Zwierlein, C. A. Stan, S. M. F. Raupach, and W. Ketterle, 2005, “Feshbach resonances in Fermionic ^6Li ,” *Phys. Rev. A* **71**, 045601.
- Seaton, M. J., 1983, “Quantum defect theory,” *Rep. Prog. Phys.* **46**, 167–257.
- Selles, P., L. Malegat, A. Huetz, A. K. Kazansky, S. A. Collins, D. P. Seccombe, and T. J. Reddish, 2004, “Convergence of the method of the hyperspherical R matrix with semiclassical outgoing waves,” *Phys. Rev. A* **69**.
- Selles, P., J. Mazeau, and A. Huetz, 1987, “Wannier theory for P^o and D^e states of 2 electrons,” *J. Phys. B* **20**, 5183–5193.
- Shepard, J. R., 2007, “Calculations of recombination rates for cold ^4He atoms from atom-dimer phase shifts and determination of universal scaling functions,” *Phys. Rev. A* **75**, 062713.
- Shi, T., and S. Yi, 2014, “Observing dipolar confinement-induced resonances in quasi-one-dimensional atomic gases,” *Phys. Rev. A* **90**, 042710.
- Shotan, Z., O. Machtey, S. Kokkelmans, and L. Khaykovich, 2014, “Three-body recombination at vanishing scattering lengths in an ultracold Bose gas,” *Phys. Rev. Lett.* **113**.
- Shui, V. H., 1973, “Thermal dissociation and recombination of hydrogen according to the reactions $H_2 + H \rightarrow H + H + H$,” *J. Chem. Phys.* **58**, 4868.
- Shui, V. H., J. P. Appleton, and J. C. Keck, 1970, “Three-body recombination and dissociation of nitrogen: A comparison between theory and experiment,” *J. Chem. Phys.* **53**, 2547.
- Shui, Ven H., 1972, “Monte Carlo Trajectory Calculations of the Three-Body Recombination and Dissociation of Diatomic Molecules,” *J. Chem. Phys.* **57**, 1704.
- Simoni, A., S. Srinivasan, J. M. Launay, K. Jachymski, Z. Idziaszek, and P. S. Julienne, 2015, “Polar molecule reactive collisions in quasi-1d systems,” *New J. Phys.* **17**, 013020.
- Sinha, S., and L. Santos, 2007, “Cold dipolar gases in quasi-one-dimensional geometries,” *Phys. Rev. Lett.* **99**, 140406.
- Skorniakov, G. V., and K. A. Ter-Martirosian, 1957, “Three body problem for short range forces. I. scattering of low energy neutrons by deuterons,” *Sov. Phys. JETP* **4**, 648–661 [*Zh. Eksp. Teor. Fiz.* **31**, 775–790 (1957)].
- Smirnov, Y. F., and K. V. Shitikova, 1977, “Method of K harmonics and the shell model,” *Sov. J. Part. Nucl.* **8**, 344–370 [*Fiz. Elem. Chastits At. Yadra* **8**, 847–910 (1977)].
- Smith, F. T., 1960, “Generalized angular momentum in many-body collisions,” *Phys. Rev.* **120**, 1058.
- Smith, F. T., 1962, “Three-body collision rates in atomic recombination reactions,” *Discuss. Faraday Soc.* **33**, 183.
- Snider, R. F., 1960, “Quantum-mechanical modified Boltzmann equation for degenerate internal states,” *J. Chem. Phys.* **32**, 1051.
- Söding, J., D. Guéry-Odelin, P. Desbiolles, F. Chevy, H. Inamori, and J. Dalibard, 1999, “Three-body decay of a rubidium Bose-Einstein condensate,” *Appl. Phys. B* **69**, 257–261.
- Sogo, T., O. Sorensen, A. S. Jensen, and D. V. Fedorov, 2005, “Semi-analytic solution to the N-boson problem with zero-range interactions,” *Europhys. Lett.* **69**, 732–738.
- Sorensen, O., D. V. Fedorov, and A. S. Jensen, 2004, “Structure of boson systems beyond the mean field,” *J. Phys. B* **37**, 93.
- Sørensen, P. K., D. V. Fedorov, A. S. Jensen, and N. T. Zinner, 2012, “Efimov physics and the three-body parameter within a two-channel framework,” *Phys. Rev. A* **86**, 052516.
- Spethmann, Nicolas, Farina Kindermann, Shincy John, Claudia Weber, Dieter Meschede, and Artur Widera, 2012, “Dynamics of Single Neutral Impurity Atoms Immersed in an Ultracold Gas,” *Phys. Rev. Lett.* **109**, 235301.
- Stephens, J. A., and U. Fano, 1988, “Slow electrons in condensed matter: The large polaron,” *Phys. Rev. A* **38**, 3372–3376.
- Stormer, Horst L., Daniel C. Tsui, and Arthur C. Gossard, 1999, “The fractional quantum hall effect,” *Rev. Mod. Phys.* **71**, S298–S305.

- Strauss, C., T. Takekoshi, K. Winker, R. Grimm, and J. H. Denschlag, 2010, “Hyperfine, rotational, and vibrational structure of the $a^3\sigma_u^+$ state of $^{87}\text{Rb}_2$,” *Phys. Rev. A* **82**, 052514.
- Strecker, K. E., G. B. Partridge, and R. G. Hulet, 2003, “Conversion of an atomic Fermi gas to a long-lived molecular Bose gas,” *Phys. Rev. Lett.* **91**, 080406.
- Suno, H., and B. D. Esry, 2008, “Adiabatic hyperspherical study of triatomic helium systems,” *Phys. Rev. A* **78**, 062701.
- Suno, H., B. D. Esry, and C. H. Greene, 2003a, “Recombination of three ultracold Fermionic atoms,” *Phys. Rev. Lett.* **90**, 053202.
- Suno, H., B. D. Esry, and C. H. Greene, 2003b, “Three-body recombination of cold Fermionic atoms,” *New J. Phys.* **5**, 53.
- Suno, H., B. D. Esry, C. H. Greene, and J. P. Burke, 2002, “Three-body recombination of cold helium atoms,” *Phys. Rev. A* **65**, 042725.
- Suno, H., Y. Suzuki, and P. Descouvemont, 2015, “Triple- α continuum structure and hoyle resonance of ^{12}C using the hyperspherical slow variable discretization,” *Phys. Rev. C* **91**, 014004.
- Suzuki, Y., and K. Varga, 1998, *Stochastic Variational Approach to Quantum-Mechanical Few-Body Problems* (Springer-Verlag, Berlin).
- Sykes, A. G., J. P. Corson, J. P. D’Incao, A. P. Koller, C. H. Greene, A. M. Rey, K. R. A. Hazzard, and J. L. Bohn, 2014, “Quenching to unitarity: Quantum dynamics in a three-dimensional Bose gas,” *Phys. Rev. A* **89**, 021601.
- Tan, S., 2008a, “Energetics of a strongly correlated Fermi gas,” *Ann. Phys. (N.Y.)* **323**, 2952–2970.
- Tan, S., 2008b, “Large momentum part of a strongly correlated Fermi gas,” *Ann. Phys. (N.Y.)* **323**, 2971–2986.
- Tan, S., 2008c, “Generalized virial theorem and pressure relation for a strongly correlated Fermi gas,” *Ann. Phys. (N.Y.)* **323**, 2987–2990.
- Tang, J. Z., S. Watanabe, M. Matsuzawa, and C. D. Lin, 1992, “Evidence of an excited angular-correlation mode in high-lying He,” *Phys. Rev. Lett.* **69**, 1633–1635.
- Tanihata, I., 1996, “Neutron halo nuclei,” *J. Phys. G* **22**, 157–198.
- Tanner, Gregor, Klaus Richter, and Jan-Michael Rost, 2000, “The theory of two-electron atoms: between ground state and complete fragmentation,” *Rev. Mod. Phys.* **72**, 497–544.
- Taylor, J. R., 1972, *Scattering theory* (John Wiley and Sons, Inc., New York).
- Tempere, J., W. Casteels, M. K. Oberthaler, S. Knoop, E. Timmermans, and J. T. Devreese, 2009, “Feynman path-integral treatment of the BEC-impurity polaron,” *Phys. Rev. B* **80**, 184504.
- Thomas, L. H., 1935, “The interaction between a neutron and a proton and the structure of ^3H ,” *Phys. Rev.* **47**, 903–909.
- Thouless, D. J., M. Kohmoto, M. P. Nightingale, and M. Denny, 1982, “Quantized Hall conductance in a two-dimensional periodic potential,” *Phys. Rev. Lett.* **49**, 405–408.
- Ticknor, C., C. A. Regal, D. S. Jin, and J. L. Bohn, 2004, “Multiplet structure of Feshbach resonances in nonzero partial waves,” *Phys. Rev. A* **69**, 042712.
- Tiecke, T. G., M. R. Goosen, J. T. M. Walraven, and S. J. J. M. F. Kokkelmans, 2010, “Asymptotic-bound-state model for Feshbach resonances,” *Phys. Rev. A* **82**, 042712.
- Tjon, J. A., 1975, “Bound states of ^4He with local interactions,” *Phys. Lett. B* **56**, 217.
- Tolra, B. Laburthe, K. M. O’Hara, J. H. Huckans, W. D. Phillips, S. L. Rolston, and J. V. Porto, 2004, “Observation of reduced three-body recombination in a correlated 1d degenerate Bose gas,” *Phys. Rev. Lett.* **92**, 190401.
- Tolstikhin, O. I., S. Watanabe, and M. Matsuzawa, 1996, “‘Slow’ variable discretization: A novel approach for Hamiltonians allowing adiabatic separation of variables,” *J. Phys. B* **29**, L389–L395.
- Tonks, L., 1936, “The complete equation of state of one, two and three-dimensional gases of hard elastic spheres,” *Phys. Rev.* **50**, 955–963.
- Truhlar, D. G., and J. T. Muckerman, 1975, “Reactive scattering cross sections: Quasiclassical and semiclassical methods,” in *Atom-Molecule Collision Theory: A Guide for the Experimentalist*, edited by R. B. Bernstein, Chap. 16 (Plenum Press, New York), pp. 505–566.
- Tscherbul, T. V., T. Calarco, I. Lesanovsky, R. V. Krems, A. Dalgarno, and J. Schmiedmayer, 2010, “rf-field-induced Feshbach resonances,” *Phys. Rev. A* **81**, 050701.
- Tung, S. K., K. Jiménez-García, J. Johansen, C. V. Parker, and C. Chin, 2014, “Geometric scaling of Efimov states in a $^6\text{Li} - ^{133}\text{Cs}$,” *Phys. Rev. Lett.* **113**, 240402.
- Ullrich, J., *et al.*, 2003, “Recoil-ion and electron momentum spectroscopy: Reaction-microscopes,” *Rep. Prog. Phys.* **66**, 1463–1545.
- Ulmanis, J., S. Häfner, R. Pires, E. D. Kuhnle, Y. Wang, C. H. Greene, and M. Weidemüller, 2016, “Heteronuclear Efimov scenario with positive intraspecies scattering length,” *Phys. Rev. Lett.* **117**, 153201.
- Ulmanis, J., S. Häfner, R. Pires, M. Weidemüller, and E. Timeann, 2015, “Universality of weakly bound dimers and Efimov trimers close to Li-Cs Feshbach resonances,” *New J. Phys.* **17**, 055009.
- Ulmanis, J., S. Häfner, R. Pires, F. Werner, D. S. Petrov, M. Weidemüller, and E. D. Kuhnle, 2016, “Universal three-body recombination and Efimov resonances in an ultracold Li-Cs mixture,” *Phys. Rev. A* **93**, 022707.
- Valliers, M., T. K. Das, and H. T. Coelho, 1976, “Generalized N-body harmonic oscillator basis functions for the hyperspherical approach,” *Nucl. Phys. A* **257**, 389.
- Van der Wiel, M. J., 1972, “Threshold behavior of double photoionisation in He,” *Phys. Lett. A* **41**, 389.
- Verma, S. P., and D. P. Sural, 1979, “Hyperspherical harmonics method for the hypertriton and ^9Be ,” *Phys. Rev. C* **20**, 781.
- Verma, S. P., and D. P. Sural, 1982, “Hyperspherical harmonics caluclaitons for ^3H with realistic n-p potential,” *J. Phys. G* **8**, 73–81.
- Vidaña, I., 2013, “Hyperons and neutrons stars,” *Nucl. Phys. A* **914**, 367–376.
- Volosniev, A. G., D. V. Fedorov, A. S. Jensen, and N. T. Zinner, 2014, “Borromean ground state of fermions in two dimensions,” *J. Phys. B* **47**, 185302.
- von Stecher, J., 2010, “Weakly bound cluster states of Efimov character,” *J. Phys. B* **43**, 101002.
- von Stecher, J., 2011, “Five- and six-body resonances tied to an Efimov trimer,” *Phys. Rev. Lett.* **107**, 200402.
- von Stecher, J., J. P. D’Incao, and C. H. Greene, 2009, “Signatures of universal four-body phenomena and their relation to the Efimov effect,” *Nat. Phys.* **5**, 417–421.
- von Stecher, J., and C. H. Greene, 2009, “Correlated Gaussian hyperspherical method for few-body systems,” *Phys. Rev. A* **80**, 022504.
- Wacker, L. J., N. B. Jørgensen, D. Birkmose, N. Winter, M. Mikkelsen, J. Sherson, N. Zinner, and J. J. Arlt, 2016, “Universal three-body physics in ultracold KRb mixtures,” *Phys. Rev. Lett.* **117**, 163201.
- Wang, F., X. Ye, M. Guo, D. Blume, and D. Wang, 2016, “Exploring Few-Body Processes with an Ultracold Light-Heavy Bose-Bose Mixture,” *arXiv:1611.03198*.
- Wang, J., J. P. D’Incao, B. D. Esry, and C. H. Greene, 2012, “Origin of the three-body parameter universality in Efimov physics,” *Phys. Rev. Lett.* **108**, 263001.

- Wang, J., J. P. D’Incao, and C. H. Greene, 2011, “Numerical study of three-body recombination for systems with many bound states,” *Phys. Rev. A* **84**, 052721.
- Wang, J., J. P. D’Incao, Y. Wang, and C. H. Greene, 2012, “Universal three-body recombination via resonant d -wave interactions,” *Phys. Rev. A* **86**, 062511.
- Wang, S.-J., and C. H. Greene, 2015, “General formalism for ultracold scattering with isotropic spin-orbit coupling,” *Phys. Rev. A* **91**, 022706.
- Wang, Y., J. P. D’Incao, and B. D. Esry, 2013, “Ultracold few-body systems,” *Adv. At. Mol. Opt. Phys.* **62**, 1–115.
- Wang, Y., J. P. D’Incao, and C. H. Greene, 2011a, “Efimov effect for three interacting bosonic dipoles,” *Phys. Rev. Lett.* **106**, 233201.
- Wang, Y., J. P. D’Incao, and C. H. Greene, 2011b, “Universal three-body physics for Fermionic dipoles,” *Phys. Rev. Lett.* **107**, 233201.
- Wang, Y., and B. D. Esry, 2009, “Efimov trimer formation via ultracold four-body recombination,” *Phys. Rev. Lett.* **102**, 133201.
- Wang, Y., and P. S. Julienne, 2014, “Universal van der Waals physics for three cold atoms near Feshbach resonances,” *Nat. Phys.* **10**, 768–773.
- Wang, Y., P. S. Julienne, and C. H. Greene, 2015, “Few-body physics of ultracold atoms and molecules with long-range interactions,” in *Annual Review of Cold Atoms and Molecules* (World Scientific, Singapore), Chap. 2, pp. 77–134.
- Wang, Y., W. B. Laing, J. von Stecher, and B. D. Esry, 2012, “Efimov physics in heteronuclear four-body systems,” *Phys. Rev. Lett.* **108**, 073201.
- Wang, Y., J. Wang, J. P. D’Incao, and C. H. Greene, 2012, “Universal three-body parameter in heteronuclear atomic systems,” *Phys. Rev. Lett.* **109**, 243201; **115**, 069901(E) (2015).
- Wang-Chang, C. S., G. E. Uhlenbeck, and J. deBoer, 1964, *Studies in Statistical Mechanics*, edited by J. deBoer and G. E. Uhlenbeck, Vol. 2 (North-Holland, Amsterdam).
- Wannier, G. H., 1953, “The threshold law for single ionization of atoms or ions by electrons,” *Phys. Rev.* **90**, 817–825.
- Watanabe, S., 1982, “Doubly excited states of the helium negative ion,” *Phys. Rev. A* **25**, 2074–2098.
- Watanabe, S., 1991, “The adiabatic expansion and Wannier’s ionization threshold law,” *J. Phys. B* **24**, L39–L44.
- Watanabe, S., and K. Komine, 1989, “Efimov states of the helium trimer using the hyperspherical method,” *Atomic Collision Research in Japan—Progress Report* **15**, 60–62.
- Watson, D. K., and B. A. McKinney, 1999, “Improved large- N limit for Bose-Einstein condensates from perturbation theory,” *Phys. Rev. A* **59**, 4091–4094.
- Weber, F., R. Negreiros, P. Rosenfield, and A. T. I. Cuadrado, 2007, “Neutron star interiors and the equation of state of ultradense matter,” *AIP Conf. Proc.* **892**, 515–517.
- Weber, T., J. Herbig, M. Mark, H.-C. Nägerl, and R. Grimm, 2003, “Three-body recombination at large scattering lengths in an ultracold atomic gas,” *Phys. Rev. Lett.* **91**, 123201.
- Weinberg, S., 1979, “Phenomenological Lagrangians,” *Physica A (Amsterdam)* **96**, 327.
- Weinberg, S., 1990, “Nuclear forces from chiral Lagrangians,” *Phys. Lett. B* **251**, 288.
- Weinberg, S., 1991, “Effective chiral Lagrangians for nucleon-pion interactions and nuclear forces,” *Nucl. Phys. B* **363**, 3.
- Wenz, A. N., T. Lompe, T. B. Ottenstein, F. Serwane, Zürn, and S. Jochim, 2009, “Universal trimer in a three-component Fermi gas,” *Phys. Rev. A* **80**, 040702.
- Werner, F., L. Tarruell, and Y. Castin, 2009, “Number of closed-channel molecules in the BEC-BCS crossover,” *Eur. Phys. J. B* **68**, 401–415.
- Werner, Félix, and Yvan Castin, 2006, “Unitary quantum three-body problem in a harmonic trap,” *Phys. Rev. Lett.* **97**, 150401.
- Whittaker, E. T., 1937, *A Treatise on the Analytical Dynamics of Particles and Rigid Bodies* (Cambridge University Press, Cambridge, England).
- Whitten, R. C., and F. T. Smith, 1968, “Symmetric representation for three-body problems. II. motion in space,” *J. Math. Phys. (N.Y.)* **9**, 1103–1113.
- Wigner, E. P., 1937, “Calculation of the rate of elementary association reactions,” *J. Chem. Phys.* **5**, 720.
- Wild, R. J., P. Makotyn, J. M. Pino, E. A. Cornell, and D. S. Jin, 2012, “Measurements of Tan’s contact in an atomic Bose-Einstein condensate,” *Phys. Rev. Lett.* **108**, 145305.
- Williams, J. R., E. L. Hazlett, J. H. Huckans, R. W. Stites, Y. Zhang, and K. M. O’Hara, 2009, “Evidence for and excited-state Efimov trimer in a three-component fermi gas,” *Phys. Rev. Lett.* **103**, 130404.
- Williams, R. A., L. J. LeBlanc, K. Jiménez-García, M. C. Beeler, A. R. Perry, W. D. Phillips, and I. B. Spielman, 2012, “Synthetic partial waves in ultracold atomic collisions,” *Science* **335**, 314–317.
- Willitsch, S., 2012, “Coulomb-crystallised molecular ions in traps: methods, applications, prospects,” *Int. Rev. Phys. Chem.* **31**, 175.
- Willitsch, S., M. Bell, A. Gingell, and T. P. Softley, 2008, “Chemical applications of laser- and sympathetically cooled ions in traps,” *Phys. Chem. Chem. Phys.* **10**, 7200.
- Wilson, K. G., 1971, “Renormalization group and strong interactions,” *Phys. Rev. D* **3**, 1818.
- Wilson, K. G., 1983, “The renormalization group and critical phenomena,” *Rev. Mod. Phys.* **55**, 583.
- Wilson, K. G., and J. Kogut, 1974, “The renormalization group and the ϵ expansion,” *Phys. Rep.* **12**, 75–200.
- Wódkiewicz, K., 1991, “Fermi pseudopotential in arbitrary dimensions,” *Phys. Rev. A* **43**, 68–76.
- Wong, Hin-Yiu, A. R. P. Rau, and C. H. Greene, 1988, “Negative-ion photodetachment in an electric field,” *Phys. Rev. A* **37**, 2393–2403.
- Wooten, R. E., K. M. Daily, and C. H. Greene, 2016, “Few-body, hyperspherical treatment of the quantum Hall effect,” *Eur. Phys. J. Web Conf.* **113**, 02006.
- Wooten, R. E., B. Yan, and C. H. Greene, 2017, “Few-body collective excitations beyond Kohn’s theorem in quantum Hall systems,” *Phys. Rev. B* **95**, 035150.
- Yamaguchi, Y., 1954, “Two-nucleon problem when the potential is nonlocal but separable. I,” *Phys. Rev.* **95**, 1628–1634.
- Yamashita, M. T., F. F. Bellotti, T. Frederico, D. V. Fedorov, A. S. Jensen, and N. T. Zinner, 2015, “Weakly bound states of two- and three-boson systems in the crossover from two to three dimensions,” *J. Phys. B* **48**, 025302.
- Yamashita, M. T., D. V. Fedorov, and A. S. Jensen, 2010, “Universality of brunnian (n -body borromean) four- and five-body systems,” *Phys. Rev. A* **81**, 063607.
- Yamashita, M. T., Lauro Tomio, A. Delfino, and T. Frederico, 2006, “Four-boson scale near a Feshbach resonance,” *Europhys. Lett.* **75**, 555–561.
- Yan, Y., and D. Blume, 2013, “Harmonically trapped Fermi gas: Temperature dependence of the Tan contact,” *Phys. Rev. A* **88**, 023616.
- Yan, Y., and D. Blume, 2015, “Energy and structural properties of N -boson clusters attached to three-body Efimov states: Two-body zero-range interactions and the role of the three-body regulator,” *Phys. Rev. A* **92**, 033626.
- Yan, Y., and D. Blume, 2016, “Path-integral Monte Carlo determination of the fourth-order Virial coefficient for a unitary two-component Fermi gas with zero-range interactions,” *Phys. Rev. Lett.* **116**, 230401.

- Yin, X., and L. Radzihovsky, 2016, “Postquench dynamics and prethermalization in a resonant Bose gas,” *Phys. Rev. A* **93**, 033653.
- Yin, X. Y., and D. Blume, 2015, “Trapped unitary two-component Fermi gases with up to ten particles,” *Phys. Rev. A* **92**, 013608.
- Yurovsky, V. A., 2005, “Feshbach resonance scattering under cylindrical harmonic confinement,” *Phys. Rev. A* **71**, 012709.
- Yurovsky, V. A., 2006, “Properties of quasi-one-dimensional molecules with Feshbach-resonance interaction,” *Phys. Rev. A* **73**, 052709.
- Yurovsky, V. A., M. Olshanii, and D. S. Weiss, 2008, “Collisions, correlations, and integrability in atom waveguides,” *Adv. At. Mol. Opt. Phys.* **55**, 61–138.
- Zaccanti, M., B. Deissler, C. D’Errico, M. Fattori, M. Jona-Lasinio, S. Mueller, G. Roati, M. Inguscio, and G. Modugno, 2009, “Observation of an Efimov spectrum in an atomic system,” *Nat. Phys.* **5**, 586–591.
- Zenesini, A., B. Huang, M. Berninger, S. Besler, H.-C. Nägerl, F. Ferlaino, R. Grimm, C. H. Greene, and J. von Stecher, 2013, “Resonant five-body recombination in an ultracold gas of bosonic atoms,” *New J. Phys.* **15**, 043040.
- Zhai, Hui, 2015, “Degenerate quantum gases with spin-orbit coupling: a review,” *Rep. Prog. Phys.* **78**, 026001.
- Zhang, C., and C. H. Greene, 2013, “Quasi-one-dimensional scattering with general transverse two-dimensional confinement,” *Phys. Rev. A* **88**, 012715.
- Zhang, P., L. Zhang, and W. Zhang, 2012, “Interatomic collisions in two-dimensional and quasi-two-dimensional confinements with spin-orbit coupling,” *Phys. Rev. A* **86**, 042707.
- Zhang, R., and W. Zhang, 2013, “Effective Hamiltonians for quasi-one-dimensional Fermi gases with spin-orbit coupling,” *Phys. Rev. A* **88**, 053605.
- Zhang, W., and P. Zhang, 2011, “Confinement-induced resonances in quasi-one-dimensional traps with transverse anisotropy,” *Phys. Rev. A* **83**, 053615.
- Zhang, Y.-C., S.-W. Song, and W.-M. Liu, 2014, “The confinement induced resonance in spin-orbit coupled cold atoms with Raman coupling,” *Sci. Rep.* **4**, 4992.
- Zhdanov, V. M., 2002, *Transport Processes in Multicomponent Plasma* (Taylor and Francis, London).
- Zhu, C. Y., Y. Teranishi, and H. Nakamura, 2001, “Nonadiabatic transitions due to curve crossings: Complete solutions of the Landau-Zener-Stückelberg problems and their applications,” *Adv. Chem. Phys.* **117**, 127–233.
- Zhu, Y., 2013, “Beam energy scan on hypertriton production and lifetime measurement at RHIC STAR,” *Nucl. Phys. A* **904–905**, 551c–554c.
- Zhukov, M. V., 1993, “Bound state properties of borromean halo nuclei: ${}^6\text{He}$ and ${}^{11}\text{Li}$,” *Phys. Rep.* **231**, 151.
- Zinner, N. T., 2012, “Universal two-body spectra of ultracold harmonically trapped atoms in two and three dimensions,” *J. Phys. A* **45**, 205302.
- Zinner, N. T., and A. S. Jensen, 2013, “Comparing and contrasting nuclei and cold atomic gases,” *J. Phys. G* **40**, 053101.
- Zinner, N. T., K. Mølmer, C. Özen, D. J. Dean, and K. Langanke, 2009, “Shell-model Monte Carlo simulations of the BCS-BEC crossover in few-fermion systems,” *Phys. Rev. A* **80**, 013613.
- Zucrow, M. J., and J. D. Hoffman, 1976, *Gas dynamics* (Wiley, New York).
- Zwierlein, M. W., A. Schirotzek, H. S. Christian, and W. Ketterle, 2006, “Fermionic superfluidity with imbalanced spin populations,” *Science* **311**, 492–496.
- Zwierlein, M. W., C. A. Stan, C. H. Schunck, S. M. F. Raupach, A. J. Kerman, and W. Ketterle, 2004, “Condensation of pairs of Fermionic atoms near a Feshbach resonance,” *Phys. Rev. Lett.* **92**, 120403.